

Ansökan om tillstånd enligt kärntekniklagen

Toppdokument	Ansökan om tillstånd enligt Kärntekniklagen för utbyggnad och fortsatt drift av SFR
Bilaga Begrepp och definitioner	Begrepp och definitioner för ansökan om utbyggnad och fortsatt drift av SFR
Bilaga F-PSAR SFR	Första preliminär säkerhetsredovisning för ett utbyggt SFR
Allmän del 1	Anläggningsutformning och drift
Allmän del 2	Säkerhet efter förslutning
Typbeskrivningar	<ul style="list-style-type: none">Preliminär typbeskrivning för hela BWR reaktortankar exklusive interndelar.Preliminär typbeskrivning för skrot i fyrkokillPreliminär typbeskrivning för hårdkomponenter i stältankar Utgått maj 2017
Bilaga AV PSU	Avvecklingsplan för ett utbyggt SFR Slutförvaret för kortlivat radioaktivt avfall
Bilaga VOLS-Ansökan PSU	Verksamhet, organisation, ledning och styrning för utbyggnad av SFR – Ansökans- och systemhandlingskede
Bilaga VOLS-Bygg PSU	Verksamhet, organisation, ledning och styrning för utbyggnad av SFR – Tillståndsprövnings- och detaljprojekteringskedet samt byggskedet.
Bilaga MKB PSU	Miljökonsekvensbeskrivning för utbyggnad och fortsatt drift av SFR
Bilaga BAT	Utbyggnad av SFR ur ett BAT-perspektiv

Kapitel 1	Inledning
Kapitel 2	Förläggningsplats
Kapitel 3	Konstruktionsregler <ul style="list-style-type: none">Tolkning och tillämpning av krav i SSMFSPrinciper och metodik för säkerhetsklassning – Projekt SFR utbyggnadSäkerhetsklassning för projekt SFR-utbyggnadAcceptanskriterier för avfall, PSU
Kapitel 4	Anläggningens drift
Kapitel 5	Anläggnings- och funktionsbeskrivning <ul style="list-style-type: none">Preliminär plan för fysiskt skydd för utbyggt SFRSFR FörslutningsplanMetod och strategi för informations- och IT-säkerhet, PSU
Kapitel 6	Radioaktiva ämnen <ul style="list-style-type: none">Radionuclide inventory for application of extension of the SFR repository - Treatment of uncertainties. (1) (2)Låg- och medelaktivt avfall i SFR. Referensinventarium för avfall 2013 (uppdaterad 2015-03)
Kapitel 7	Strålskydd <ul style="list-style-type: none">Dosprognos vid drift av utbyggt SFR
Kapitel 8	Säkerhetsanalys för driftskedet <ul style="list-style-type: none">SFR – Säkerhetsanalys för driftskedet
Kapitel 9	Mellanlagring av långlivat avfall Utgått maj 2017 <ul style="list-style-type: none">Ansökansinventarium för mellanlagring av långlivat avfall i SFR Utgått maj 2017
Huvudrapport	Redovisning av säkerhet efter förslutning för SFR Huvudrapport för säkerhetsanalysen SR-PSU (1) (3)
FHA report	Handling of future human actions in the safety assessment (2)
FEP report	FEP report for the safety assessment
Waste process report	Waste process report for the safety assessment
Geosphere process report	Geosphere process report for the safety assessment
Barrier process report	Engineered barrier process report for the safety assessment
Biosphere synthesis report	Biosphere synthesis report for the safety assessment
Climate report	Climate and climate related issues for the safety assessment
Model summary report	Model summary report for the safety assessment
Data report	Data report for the for the safety assessment (2)
Input data report	Input data report for the safety assessment (2) (3)
Initial state report	Initial state report for the safety assessment (2)
Radionuclide transport report	Radionuclide transport and dose calculations for the safety assessment (2)
SDM-PSU Forsmark	Site description of the SFR area at Forsmark on completion of the site investigation
Samrådsredogörelse	
Konsekvensbedömning av vattenmiljöer vid utbyggnad av SFR	
Ersatt juli 2016 av bilaga SFR-U K:2	
Naturmiljöutredning inför utbyggnad av SFR, Forsmark, Östhammar kommun.	

Kompletteringar

- (1) September 2015 – Svensk version av *Huvudrapport SR-PSU* i allmän del 2 samt ny version (3.0) av *Radionuclide inventory* i allmän del 1 kapitel 6
- (2) Oktober 2015 – Fem uppdaterade rapporter i allmän del 2 samt ny version (4.0) av *Radionuclide inventory* i allmän del 1 kapitel 6
- (3) Oktober 2017 – Uppdatering av *Huvudrapport SR-PSU* och *Input data report*

Technical Report

TR-14-10

Data report for the safety assessment SR-PSU

Svensk Kärnbränslehantering AB

November 2014

Svensk Kärnbränslehantering AB

Swedish Nuclear Fuel
and Waste Management Co

Box 250, SE-101 24 Stockholm
Phone +46 8 459 84 00



ISSN 1404-0344

SKB TR-14-10

ID 1385625

Updated 2015-10

Data report for the safety assessment SR-PSU

Svensk Kärnbränslehantering AB

November 2014

Update notice

The original report, dated November 2014, was found to contain factual errors which have been corrected in this updated version. The corrected factual errors are presented below.

Updated 2015-10

Location	Original text	Corrected text
Page 42, Section 4.4, first sentence	...inventory report (SKB 2013)...	...inventory report (SKB 2013, SKBdoc 1481419 (Mo-93))...
Page 42, Table 4-2, new reference		SKBdoc 1481419. Ny beräkning av Mo-93 i normkolli till PSU 2015-05
Page 43, first sentence	...inventory report (SKB 2013) and the calculated...	...inventory report (SKB 2013), except data sets for Mo-93 that are taken from SKBdoc 1481419, and the calculated...
Page 43, Table 4-3, new row inserted		SKBdoc 1481419
Page 44, Table 4-4, row Mo-93		This row is deleted
Page 44, Table 4-4, reference column, row Ni-59, Ni-63, Tc-99, I-129 and Cs-135	Cronstrand 2007	SKBdoc 1393443
Page 46, Figure 4-1		Figure updated
Page 46, figure text	KKV	NPP
Page 48, last paragraph	...each waste type (SKB 2013)...	...each waste type (SKB 2013, SKBdoc 1481419 (Mo-93))...
Page 49, Table 4-6	Wrong data in table	Table updated with correct data
Page 175, updated reference	1427105 ver 1.0	1427105 ver 4.0
Page 175, new reference		SKBdoc 1400742 ver 2.0. Kontroll av SFR-avfall. Delprojekt mätteknik. (In Swedish.) Gammadata mätteknik AB, 1990
Page 175, new reference		SKBdoc 1481419 ver 1.0. Ny beräkning av Mo-93 i normkolli till PSU 2015-05 (In Swedish.) SKB, 2015

Preface

This report provides data identified as essential for assessing the long-term radiation safety of the low-and intermediate level waste repository SFR. In addition, the process of qualifying the data for use in subsequent modelling is detailed. The report forms part of the SR-PSU safety assessment, which supports the application for a licence to extend SFR.

The report has been edited by Mikael Asperö, Kemakta konsult AB. Numerous of experts with responsibilities for specific scientific topics have contributed to the report.

The reviewers Russel Alexander, Bedrock Geosciences; Jordi Bruno, Amphos 21; Luc van Loon, PSI; Tommy Olsson, I&T Olsson AB; Kastriot Spahiu, SKB and M C Thorne, Mike Thorne and Associates Limited have reviewed specific topics in the report.

Stockholm, November 2014

Fredrik Vahlund

Project leader SR-PSU

Summary

This report presents, motivates and qualifies the data deemed as most important for the safety assessment SR-PSU. This is done using a quality assurance (QA) method created for assessing long term safety assessment data. Large amounts of data have been used in SR-PSU to calculate and assess the system. Therefore, the data presented here limits itself to being connected to the SR-PSU safety functions. All data used in the long term safety assessment is documented in the other data report, the **Input data report**.

The data presented in this report has to be qualified and motivated from several perspectives such as if there are conceptual uncertainties, spatial or temporal variabilities, or if the data differs drastically from data used for the same purpose in previous safety assessments. The general objective of this report is to present data that is fit to use in a long term safety assessment, with of all the possible uncertainties considered.

Sammanfattning

Denna rapport motiverar och kvalificerar de data som bedöms som viktigast för säkerhetsanalysen SR PSU. Detta görs med hjälp av en kvalitetssäkringsmetod (QA) som skapats för att bedöma data till långsiktiga säkerhetsanalyser. Stora mängder data har använts i SR-PSU för att beräkna och utvärdera systemet. Data som presenteras här begränsar sig till data som kopplar till säkerhetsfunktionerna för SR-PSU. Alla data som används i den långsiktigt säkerhetsanalysen dokumenteras i **Indata rapporten**.

De data som presenteras i denna rapport har kvalificerats och motiverats ur flera perspektiv såsom om det finns konceptuella osäkerheter, rumslig eller tidsmässig variabilitet, eller om uppgifterna skiljer sig avsevärt från data som används för samma ändamål i tidigare säkerhetsanalyser. Det övergripande målet med denna rapport är att presentera data som är lämpliga att användas i den långsiktiga säkerhetsanalysen med beaktade osäkerheter.

Contents

1	Introduction	11
1.1	Background	11
1.2	Report hierarchy in the SR-PSU safety assessment	12
1.3	This report	12
1.3.1	Compilation and qualification of essential input data	14
1.3.2	Identification of essential input data	14
1.4	Participating parties in this report	15
2	Methodology for identifying and qualifying data	17
2.1	Qualification of input data – instruction to supplier and customer	17
2.1.1	Modelling in SR-PSU	19
2.1.2	Experience from previous safety assessments	19
2.1.3	Supplier input on use of data in SR-PSU and previous safety assessments	21
2.1.4	Sources of information and documentation of data qualification	21
2.1.5	Conditions for which data are supplied	24
2.1.6	Conceptual uncertainty	24
2.1.7	Data uncertainty due to precision, bias, and representativity	25
2.1.8	Spatial and temporal variability	26
2.1.9	Correlations	27
2.1.10	Results of supplier’s data qualification	27
2.1.11	Judgements by the SR-PSU team	29
2.1.12	Data recommended for use in SR-PSU modelling	31
3	Radionuclide decay	33
3.1	Modelling in SR-PSU	33
3.2	Experience from previous safety assessments	33
3.3	Supplier input on use of data in SR-PSU and previous safety assessments	34
3.4	Sources of information and documentation of data qualification	34
3.5	Conditions for which data are supplied	35
3.6	Conceptual uncertainty	35
3.7	Data uncertainty due to precision, bias, and representativity	35
3.8	Spatial and temporal variability	37
3.9	Correlations	37
3.10	Result of supplier’s data qualification	37
3.11	Judgements by the SR-PSU team	37
3.12	Data recommended for use in SR-PSU modelling	38
4	Uncertainties in the radionuclide inventory	39
4.1	Modelling in SR-PSU	39
4.2	Experience from previous safety assessments	39
4.3	Supplier input on use of data in SR-PSU and previous safety assessments	42
4.4	Sources of information and documentation of data qualification	42
4.5	Conditions for which data are supplied	43
4.6	Conceptual and precision uncertainties	43
4.7	Spatial and temporal variability	47
4.8	Correlations	48
4.9	Result of supplier’s data qualification	48
4.10	Judgements by the SR-PSU team	48
4.11	Data recommended for use in SR-PSU modelling	48
5	Metallic corrosion	51
5.1	Modelling in SR-PSU	51
5.2	Experience from previous safety assessments	52
5.3	Supplier input on use of data in SR-PSU and previous safety assessments	53
5.4	Sources of information and documentation of data qualification	53

5.5	Conditions for which data are supplied	54
5.6	Conceptual uncertainty	54
5.7	Data uncertainty due to precision, bias, and representativity	54
5.8	Spatial and temporal variability	54
5.9	Correlations	55
5.10	Result of supplier's data qualification	55
5.11	Judgements by the SR-PSU team	56
5.12	Data recommended for use in SR-PSU modelling	56
6	Bitumen swelling pressure	57
6.1	Modelling in SR-PSU	57
6.2	Experience from previous safety assessments	57
6.3	Supplier input on use of data in SR-PSU and previous safety assessments	58
6.4	Sources of information and documentation of data qualification	59
6.5	Conditions for which data are supplied	68
6.6	Conceptual uncertainty	68
6.7	Data uncertainty due to precision, bias, and representativity	69
6.8	Spatial and temporal variability	69
6.9	Correlations	69
6.10	Result of supplier's data qualification	69
6.11	Judgements by the SR-PSU team	70
6.12	Data recommended for use in SR-PSU modelling	70
7	Bentonite and Concrete/Cement sorption data	71
7.1	Modelling in SR-PSU	72
7.2	Experience from previous safety assessments	73
7.3	Sources of information and documentation of data qualification	75
7.4	Conditions for which data are supplied	76
7.5	Conceptual uncertainty	80
7.6	Data uncertainty due to precision, bias, and representativity	81
7.7	Spatial and temporal variability	88
7.8	Correlations	88
7.9	Result of supplier's data qualification	89
7.10	Judgements by the SR-PSU team	111
7.11	Data recommended for use in SR-PSU modelling	111
8	Rock matrix and Crushed rock sorption data	113
8.1	Modelling in SR-PSU	113
8.2	Experience from previous safety assessments	113
8.3	Supplier input on use of data in SR-PSU and previous safety assessments	114
8.4	Sources of information and documentation of data qualification	114
8.5	Conditions for which data are supplied	116
8.6	Conceptual and bias uncertainties	118
8.7	Spatial and temporal variability	121
8.8	Correlations	122
8.9	Result of supplier's data qualification	122
8.10	Judgements by the SR-PSU team	123
8.11	Data recommended for use in SR-PSU modelling	124
9	Concrete/Cement diffusivity data	127
9.1	Modelling in SR-PSU	127
9.2	Experience from previous safety assessments	128
9.3	Supplier input on use of data in SR-PSU and previous safety assessments	129
9.4	Sources of information and documentation of data qualification	131
9.5	Conditions for which data are supplied	134
9.6	Conceptual uncertainty	134
9.7	Data uncertainty due to precision, bias, and representativity	134
9.8	Spatial and temporal variability	134
9.9	Correlations	135
9.10	Result of supplier's data qualification	135

9.11	Judgements by the SR-PSU team	137
9.12	Data recommended for use in SR-PSU modelling	137
10	Concrete/Cement hydraulic data	139
10.1	Modelling in SR-PSU	139
10.2	Experience from previous safety assessments	140
10.3	Supplier input on use of data in SR-PSU and previous safety assessments	141
10.4	Sources of information and documentation of data qualification	143
10.5	Conditions for which data are supplied	145
10.6	Conceptual uncertainty	145
10.7	Data uncertainty due to precision, bias, and representativity	146
10.8	Spatial and temporal variability	146
10.9	Correlations	147
10.10	Result of supplier's data qualification	147
10.11	Judgements by the SR-PSU team	149
10.12	Data recommended for use in SR-PSU modelling	149
11	Hydraulic pressure field in the SFR local domain	151
11.1	Modelling in SR-PSU	151
11.2	Experience from previous safety assessments	151
11.3	Supplier input on use of data in SR-PSU and previous safety assessments	154
11.4	Sources of information	154
11.5	Conditions for which data are supplied	155
11.6	Conceptual uncertainty	155
11.7	Data uncertainty due to precision, bias, and representativity	155
11.8	Spatial and temporal variability	155
11.9	Correlations	156
11.10	Result of supplier's data qualification	156
11.11	Judgements by the SR-PSU team	156
11.12	Data recommended for use in SR-PSU modelling	157
12	Shore-level evolution	159
12.1	Modelling in SR-PSU	159
12.2	Experience from previous safety assessments	160
12.3	Supplier input on use of data in SR-PSU and previous safety assessments	161
12.4	Sources of information and documentation of data qualification	161
12.5	Conditions for which data are supplied	161
12.6	Conceptual uncertainty	161
12.7	Data uncertainty due to precision, bias, and representativity	162
12.8	Spatial and temporal variability	162
12.9	Correlations	162
12.10	Result of supplier's data qualification	162
12.11	Judgements by the SR-PSU team	164
12.12	Data recommended for use in SR-PSU modelling	164
	References	165

1 Introduction

1.1 Background

The final repository for short-lived radioactive waste (SFR) located in Forsmark, Sweden is used for the final disposal of low- and intermediate-level operational waste from Swedish nuclear facilities. SKB plans to extend SFR to host waste from the decommissioning of the nuclear power plants and other nuclear facilities. Additional disposal capacity is needed also for operational waste from nuclear power units in operation since their operation life-times have been extended compared with what was originally planned.

The SFR repository includes waste vaults underground together with buildings above ground that include a number of technical installations. The underground part of the existing facility (SFR 1) is situated at 60 metres depth in the rock and is located below the Baltic Sea. SFR 1 comprises five waste vaults with a disposal capacity of approximately 63,000 m³. The extension (SFR 3)¹ will be built at 120 metres depth and will have a disposal capacity of 108,000 m³ in five new waste vaults plus one new vault for nine boiling water reactor pressure vessels, see Figure 1-1.

The long-term post closure safety of the whole SFR has been assessed and documented in the SR-PSU Main report with supporting documents, see Section 1.2. The Main report is part of SKB's licence application to extend and continue to operate SFR. This report is a main reference and presents, motivates and qualifies the data deemed as most important for the safety assessment SR-PSU. This is done using a quality assurance method created for assessing long term safety assessment data. Large amounts of data have been used in SR-PSU safety assessment to calculate and assess the system. Therefore, the data presented here is limited to information related to the SR-PSU safety functions, see Section 1.3.2.

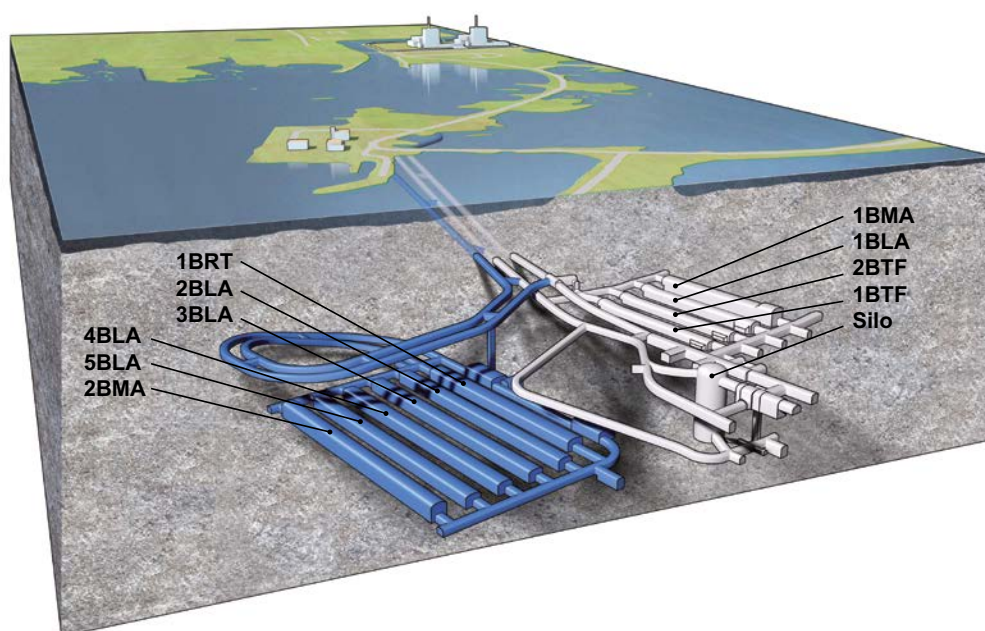


Figure 1-1. Schematic illustration of SFR. The grey part is the existing repository (SFR 1) and the blue part is the planned extension (SFR 3). The waste vaults in the figure are the silo for intermediate-level waste, 1-2BMA vaults for intermediate-level waste, 1-2BTF vaults for concrete tanks, 1-5BLA vaults for low-level waste and the BRT vault for reactor pressure vessels.

¹ The extension is called SFR 3 since the name SFR 2 was used in a previous plan to build vaults adjacent to SFR 1 for disposal of reactor core components and internal parts. The current plan is to dispose of this waste in a separate repository.

1.2 Report hierarchy in the SR-PSU safety assessment

The applied methodology for the long-term safety comprises ten steps and is described in Chapter 2 of the SR-PSU Main report. Several of the steps carried out in the safety assessment are described in more detail in supporting documents, so called main references that are of central importance for the conclusions and analyses in the **Main report**. The full titles of these reports together with the abbreviations by which they are identified in the following text (**abbreviated names in bold font**) together with short comments on the report contents are given in Table 1-1.

There are also a large number of additional references. The additional references include documents compiled within SR-PSU, but also documents compiled outside of the project, either by SKB or equivalent organisations as well as in the scientific literature. Additional publications and other documents are referenced in the usual manner.

A schematic illustration of the safety assessment documents is shown in Figure 1-2.

1.3 This report

This report documents and qualifies input data identified as essential for the long-term safety assessment (SR-PSU) of the SFR repository, and forms an important part of the reporting of the assessment. SR-PSU is performed according to a developed methodology including ten steps (see Chapter 2 in the **Main Report**). This report focuses on Step 6 – Compilation of input data.

The input data concern the data connected to the SR-PSU safety functions, as defined in assessment Step 5, and their longevity through the repository life time. Data are provided for a selection of relevant conditions and are qualified through traceable standardised procedures.

The **Data report** is complemented by the **Input data report**. The latter report documents all the data used in the safety assessment but does not qualify the data. Together these two reports form a data package which both qualifies and motivates important data as well as documents used input data in assessment Step 9 – Analysis of the selected scenarios.

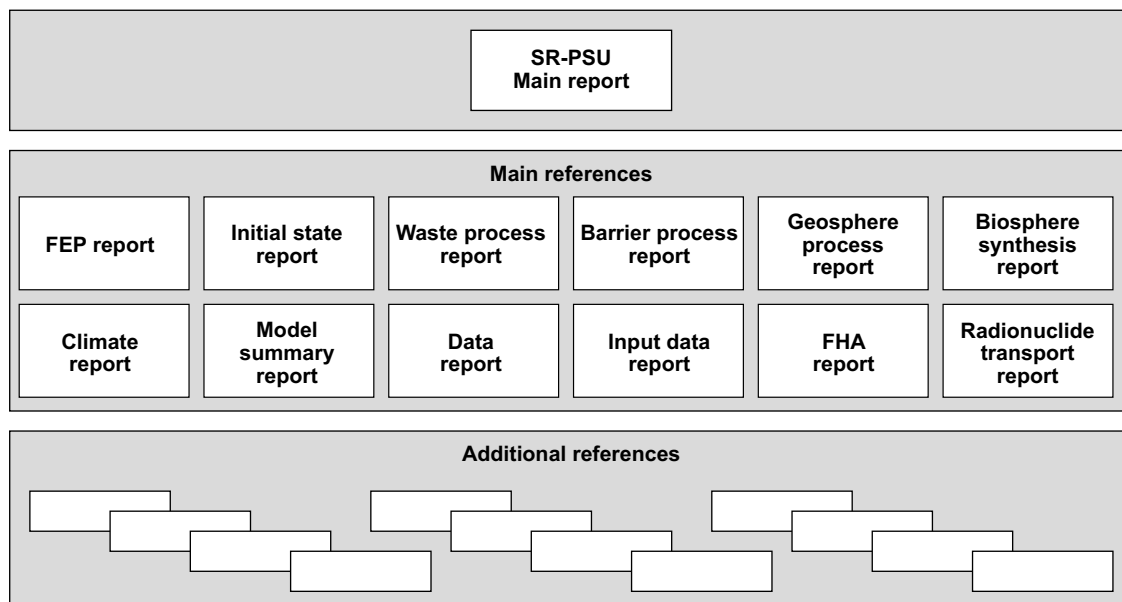


Figure 1-2. The hierarchy of the Main report, main references and additional references in the SR-PSU long-term safety assessment. The additional references either support the Main report or any of the main references.

Table 1-1. Main report and Main references in the SR-PSU long term safety assessment.
All reports are available at www.skb.se

Abbreviation used when referenced in this report	Full reference	Comment on content
Main report	Main report, 2014. Safety analysis for SFR. Long-term safety. Main report for the safety assessment SR-PSU. SKB TR-14-01, Svensk Kärnbränslehantering AB.	This document is the main report of the SR-PSU long-term post-closure safety assessment for SFR. The report is part of SKB's licence application to extend and continue to operate SFR.
Barriers process report	Engineered barriers process report, 2014. Engineered barrier process report for the safety assessment SR-PSU. SKB TR-14-04, Svensk Kärnbränslehantering AB.	Describes the current scientific understanding of the processes in the engineered barriers that have been identified in the FEP processing as potentially relevant for the long-term safety of the repository. Reasons are given in the process report as to why each process is handled a particular way in the safety assessment.
Biosphere synthesis report	Biosphere synthesis report, 2014. Biosphere synthesis report for the safety assessment SR-PSU. SKB TR-14-06, Svensk Kärnbränslehantering AB.	Describes the handling of the biosphere in the safety assessment. The report summarises site description and landscape evolution, FEP handling, exposure pathway analysis, the radionuclide model for the biosphere, included parameters, biosphere calculation cases and simulation results.
Climate report	Climate report, 2014. Climate and climate-related issues for the safety assessment SR-PSU. SKB TR-13-05, Svensk Kärnbränslehantering AB.	Describes the current scientific understanding of climate and climate-related processes that have been identified in the FEP processing as potentially relevant for the long-term safety of the repository. The report also describes the climate cases that are analysed in the safety assessment.
Data report	Data report, 2014. Data report for the safety assessment SR-PSU. SKB TR-14-10, Svensk Kärnbränslehantering AB.	Qualifies data and describes how data, including uncertainties, that are used in the safety assessment are quality assured.
FEP report	FEP report, 2014. FEP report for the safety assessment SR-PSU. SKB TR-14-07, Svensk Kärnbränslehantering AB.	Describes the establishment of a catalogue of features, events and processes (FEPs) that are of potential importance in assessing the long-term functioning of the repository.
FHA report	FHA report, 2014. Handling of future human actions in the safety assessment SR-PSU. SKB TR-14-08, Svensk Kärnbränslehantering AB.	Describes radiological consequences of future human actions (FHA) that are analysed separately from the main scenario, which is based on the reference evolution and less probable evolutions.
Geosphere process report	Geosphere process report, 2014. Geosphere process report for the safety assessment SR-PSU. SKB TR-14-05, Svensk Kärnbränslehantering AB.	Describes the current scientific understanding of the processes in the geosphere that have been identified in the FEP processing as potentially relevant for the long-term safety of the repository. Reasons are given in the process report as to why each process is handled a particular way in the safety assessment.
Initial state report	Initial state report, 2014. Initial state report for the safety assessment SR-PSU. SKB TR-14-02, Svensk Kärnbränslehantering AB.	Describes the conditions (state) prevailing in SFR after closure. The initial state is based on verified and documented properties of the repository and an assessment of the evolution during the period up to closure.
Input data report	Input data report, 2014. Input data report for the safety assessment SR-PSU. SKB TR-14-12, Svensk Kärnbränslehantering AB.	Describes the activities performed within the SR-PSU safety assessment and the input data used to perform these activities.
Model summary report	Model summary report, 2014. Model summary report for the safety assessment SR-PSU. SKB TR-14-11, Svensk Kärnbränslehantering AB.	Describes the calculation codes used in the assessment.
Radionuclide transport report	Radionuclide transport report, 2014. Radionuclide transport and dose calculations for the safety assessment SR-PSU. SKB TR-14-09, Svensk Kärnbränslehantering AB.	Describes the radionuclide transport calculations carried out for the purpose of demonstrating fulfilment of the criterion regarding radiological risk.
Waste process report	Waste process report, 2014. Waste form and packaging process report for the safety assessment SR-PSU. SKB TR-14-03, Svensk Kärnbränslehantering AB.	Describes the current scientific understanding of the processes in the waste and its packaging that have been identified in the FEP processing as potentially relevant for the long-term safety of the repository. Reasons are given in the process report as to why each process is handled in a particular way in the safety assessment.

1.3.1 Compilation and qualification of essential input data

In this **Data report**, essential input data are qualified and motivated for safety assessment use. These data are intended for use in subsequent SR-PSU safety assessment modelling. The data selection spans over different parts of the safety assessment.

The set of input parameters for the safety assessment is very large. Some “input data uncertainties” (including both data uncertainty and natural variability) will have a substantial influence on safety related output uncertainty, which ultimately leads to uncertainty in assessed radiological risk. Other data may range over orders of magnitude but still do not influence the assessed radiological risk.

It is therefore appropriate to identify input data to which safety related output is sensitive, and use these insights in allocating resources to the determination and, where feasible, reduction of input data uncertainties. It is also important to have a high degree of confidence in the data that are used to conclude that particular processes, radionuclides, etc will never contribute to radiological risk. The identification of essential input data is discussed in the next section, and in Chapter 2.

The data presented in this **Data report** are either compiled from supporting reports and documents, as part of previous tasks or as part of SR-PSU, or produced and justified in this **Data report**. The majority of data are compiled from background reports, such as the Site Description Model, the inventory report, SAR-08 and SAFE reports, etc and in those cases the justification of data is mainly done in the supporting documents. In such a case, the qualifying role of the **Data report** is to control that the suggested data are traceable and applicable for SR-PSU conditions, and to some extent to suggest their role in the safety assessment. For example, a set of data suggested in the site descriptions may only be valid for a certain climate domain of the glacial cycle, or at some other specified condition. Furthermore, estimates of uncertainties as well as of natural variability should be delivered by the **Data report**, so that the data can be properly used in the subsequent safety assessment modelling. It is part of the qualifying role to make sure that reasonable, quantitative, and usable uncertainty estimates are delivered.

The way of qualifying data is through traceable standardised procedures where extra effort is put into documenting the data qualification process, and to discuss uncertainty in data originating from conceptual uncertainty, data uncertainty, and natural variability. These standardised procedures are detailed in Chapter 2.

The qualified data recommended for use in the SR-PSU modelling are given in the last section in Chapters 3–12. In this section, clear referencing to tables in the preceding sections may substitute duplication of the data. Data that cannot be tabulated in this report, for example the coordinates of thousands of exit locations for groundwater flow paths, are stored in referenced databases.

1.3.2 Identification of essential input data

The overall post-closure safety principles *limitation of radioactive inventory* and *retention of radionuclides* may be broken down further to general safety functions for the repository. The identification of essential input data in SR-PSU have been performed using the safety functions described in the **Main report** (Chapter 5, Table 5-3).

SR-PSU safety functions

The overlying safety principles of the SFR repositories are based on a limited radionuclide inventory and on a slow transport of radionuclides from the waste packages present out through the technical barriers and through the geosphere.

The limited radionuclide inventory is controlled by with permits from the regulatory authority, SSM, and by the waste acceptance criteria which regulates each waste package and what the nuclear power plants can put in them. The slow transport of radionuclides from the waste packages is governed by a low flow of water through them, by a good sorption in the barriers the radionuclides pass, and by a low permeable geosphere. The overlying safety principles are broken down into safety functions which are directly connected to different the technical components present in the repositories. This is done to focus on the important parts in the safety assessment and to be able to make relevant scenario choices in the radionuclide transport calculations.

In this safety assessment the safety functions are also used to identify the essential input data which should be qualified and motivated in this report. By doing this the amount of data is limited down to a small but highly relevant list of data sets. The list of identified essential data is presented in Table 1-2.

It should be noted that the safety functions given in Table 1-2 are not valid for all the repository vaults. Since the BLA vaults do not have any engineered barriers defined for them the only safety function valid in them are Limited quantity of activity for example.

1.4 Participating parties in this report

The data recommended for use in SR-PSU are generally based on a mixture of measurements, modelling, and interpretation. Therefore, there is always a component of expert judgment involved in choosing the recommended data (as stated in Section 1.3, trivial data are not handled in this report). The work of producing much of the data, as well as of compiling the data and writing this report, has been done by experts working at, or on behalf of, SKB. Therefore, formally the expert should not be considered as independent. The experts could have their expertise in a narrow subject area, such as sorption of radionuclides in a bentonite matrix, or as generalists in the safety of radioactive waste (which indeed could also be considered as a narrow field of expertise).

The vocabulary used for separating the teams or persons supplying the data, the groups of persons within the SR-PSU team responsible for the data, and the SR-PSU team as a whole are:

- Supplier.
- Customer.
- The SR-PSU team.

This vocabulary is the same that was used in the latest KBS-3 safety assessments, SR-Site, Data report (SKB 2010a) where it was first implemented as a response to the authorities' request of a more transparent data assurance process.

Table 1-2. Data report chapters identified from SR-PSU safety function(s).

Ch	Data	Safety function(s)
3	Radionuclide decay	Limited quantity of activity
4	Uncertainties in the radionuclide inventory	Limited quantity of activity
5	Metallic corrosion	Good retention
6	Bitumen swelling pressure	Low water flow in waste vaults
7	Bentonite and Concrete/Cement sorption data	Good retention
8	Rock Matrix and Gravel sorption data	Good retention
9	Concrete/Cement diffusivity data	Good retention, Low water flow in waste vaults
10	Concrete/Cement hydraulic data	Low water flow in waste vaults
11	Hydraulic pressure field in the SFR local domain	Low water flow in bedrock, Low water flow to waste vaults
12	Shore-level evolution	Avoid wells in the direct vicinity of the repository

2 Methodology for identifying and qualifying data

2.1 Qualification of input data – instruction to supplier and customer

The final objective of the **Data report** is at performing data qualification including estimates of both conceptual and data uncertainty, as well as of natural variability, for various subject areas. In addition, the traceability of the data is examined. The qualified data are in later stages intended for use as input data in the SR-PSU safety assessment modelling.

The **Data report** does not concern all data used in the SR-PSU safety assessment, but those which are identified to be of particular significance for the SR-PSU safety functions (see Section 1.3.2 and Table 1-2). Data may concern both measured data from the laboratory and from the field, as well as output from detailed modelling where measured data are interpreted, depending on the subject area. Even though the data may represent both parameters and entities, in this instruction the word data is generally used.

It should be pointed out that in the process of qualifying and motivating data, the traceability that is the focus of many quality assurance systems is only one aspect. Perhaps the more important aspect is the scrutinising of the scientific adequacy of the data.

Each data supplied in this report is categorised into one of many different subject areas. For each subject area, the data qualification process comprises a sequence of stages resulting in a text of a standard outline. The sequence of stages and the standard outline are shown in Figure 2-1.

Below the parties involved in the **Data report** and the sequence of stages shown in Figure 2-1 are discussed. The standard outline is described in Section 2.1.1 to Section 2.1.12. For each subject area, the **Data report** team identifies the customer and supplier of data, and assigns a customer representative and a supplier representative that co-author the subject area section².

The customer is in broader terms the SR-PSU team that is responsible for performing the SR-PSU safety assessment. However, the entire team is generally not involved in each subject area but it is rather embodied by a group of persons with special knowledge and responsibility. The customer representative should represent the SR-PSU team, and not rely solely upon own opinions.

The suppliers are the teams originating the sources of data, for example the site-descriptive model reports, waste inventory reports, and other supporting documents. The supplier representative should represent the team, and not rely solely upon own opinions.

The intended chronology of the writing of a subject area section is the following.

- Stage A: The customer writes the first two sections defining what data are requested from the supplier, how the data will be used in SR-PSU modelling, and how similar data were used in previous assessment modelling.
- Stage B: The supplier writes the following eight sections that are the core of the data qualification. This is done according to a standard outline where a number of issues such as traceability, data uncertainty, and natural variability should be dealt with. This section should result in sets of qualified data that are the delivery to the customer.
- Stage C: The customer, representing the entire SR-PSU team, writes the last two sections making judgments upon the delivery and recommending data for use in SR-PSU modelling. The text is produced in close cooperation with the supplier and other persons within the SR-PSU team with expert knowledge in the subject area.

The text of each stage should be made available in good time to the person or persons responsible for writing the text of the subsequent stage. Upon the completion of the chapter, it will undergo a review process as part of Stage D.

Stage D: The report is reviewed according to standard procedures within the SKB quality framework.

In the following sections, the outline shown in the grey boxes in Figure 2-1 is described in detail.

² The terms customer and supplier come from standard quality assurance terminology.

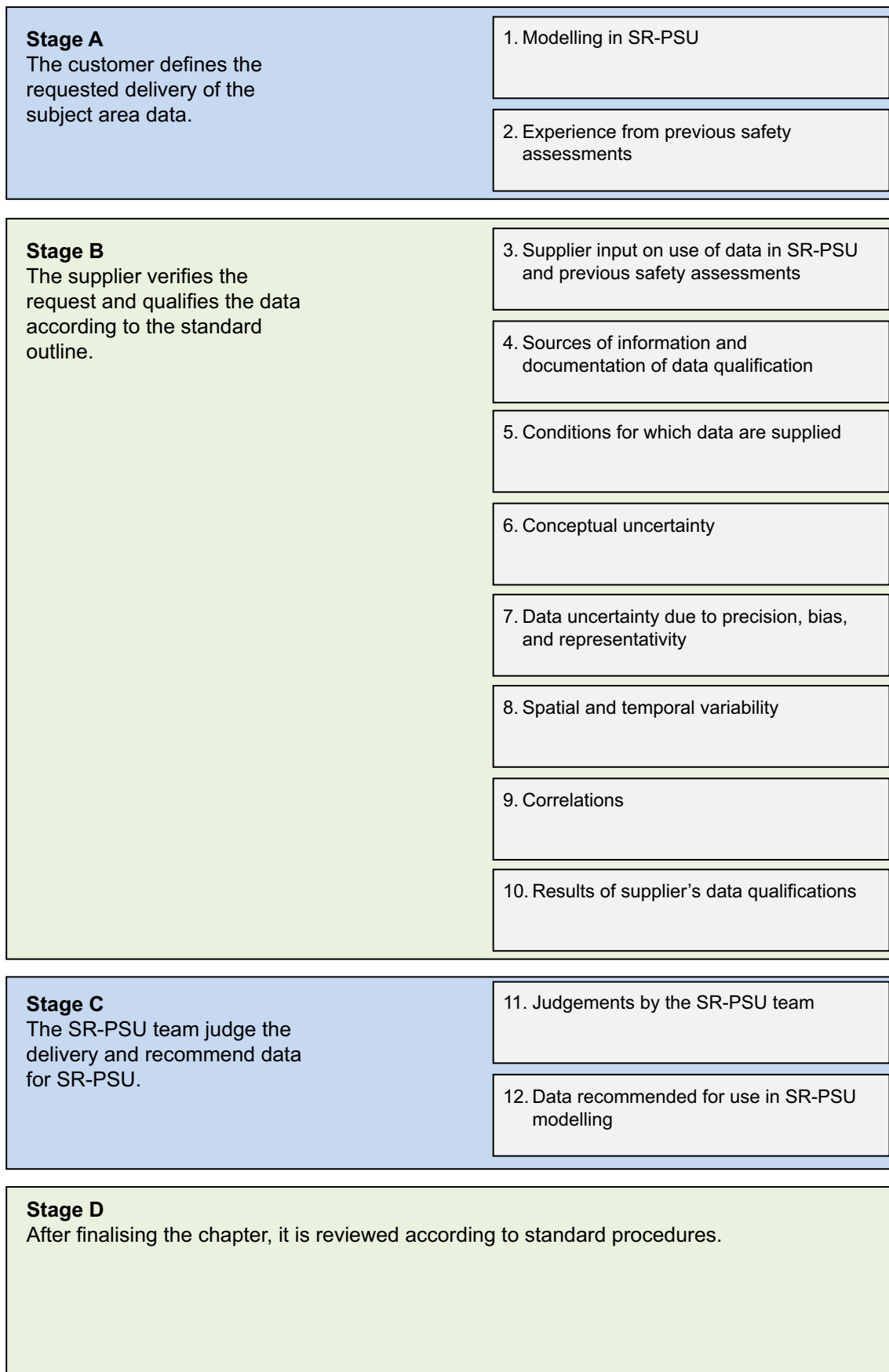


Figure 2-1. Stages of writing and reviewing the Data report. The standard outline of a subject area is shown in the grey boxes.

2.1.1 Modelling in SR-PSU

In this section, the customer should define what data are requested from the supplier, and give a brief explanation of how the data of the subject area are intended to be used in SR-PSU modelling activities.

Defining the data requested from the supplier

Here, the customer should define the data (parameters) that should be part of the supplier's delivery, in a bullet list. If applicable, the parameter symbol and unit should be provided in this list. If the supplier should focus on providing data of certain ranges, or for certain conditions, this should be specified. This text should not only facilitate the task of the supplier, but also assist the reader of the **Data report** in understanding the scope of the subject area section.

SR-PSU modelling activities in which data will be used

Here the customer representative should give a brief explanation of how the data are intended to be used in different SR-PSU modelling activities. This explanation should cover both how the data are used in specific models, and in the SR-PSU model chain. Differences from the use of this type of data in previous safety assessments should be highlighted. The justification for the use of these models in the assessment is provided in other SR-PSU documents, such as the **Main report** and process reports.

As a result of the extensive work that will be conducted up to near completion of the SR-PSU safety assessment, details of the models and the model chain may be modified. As a result, this text may have to be finalised in a late stage of the **Data report** project. Thus only a preliminary version is provided early on to the supplier representative.

2.1.2 Experience from previous safety assessments

In this section the customer should give a brief summary on how the data of the subject area were used in previous safety assessments. The experiences from these assessments should function as one of the bases for defining the input data required in SR-PSU modelling. The summary of how the data were used in previous safety assessments should conform to the following outline:

- Modelling in previous safety assessments.
- Conditions for which data were used in previous safety assessments.
- Sensitivity to assessment results in previous safety assessments.
- Alternative modelling in previous safety assessments.
- Correlations used in previous safety assessment modelling.
- Identified limitations of the data used in previous safety assessment modelling.

More detailed guidance regarding what should be included in the summary in relation to each of these bullets is given below.

Modelling in previous safety assessments

The use of the data in previous safety assessment models, as well as in previous safety assessments model chains, should be described. Repetitions from the section "Modelling in SR-PSU" should be avoided. If there is no difference between the previous safety assessments and SR-PSU modelling approaches, it is sufficient to state this. With "previous safety assessments", SAR-08 is generally referred to but in some case information from SAFE is more appropriate.

Conditions for which data were used in previous safety assessments

In this subsection, the relevant conditions to which the subject area data were subjected to in previous safety assessment modelling should be outlined. Relevant conditions are only those conditions that significantly influence the data, in the context of demonstrating repository safety. Different subject area data are affected by different conditions. For example, the sorption partition coefficient K_d may be strongly influenced by groundwater salinity. Thus, in characterising the conditions under which K_d values were used, it is likely to be appropriate to give the salinity range during repository evolution, for example as assessed in the previous safety assessments hydrogeochemical modelling. Other types of conditions may include gradients, boundary conditions, initial states, engineering circumstances, etc.

It is sufficient to state the relevant conditions used in previous safety assessment modelling (including those applied in sensitivity analyses, various initial states, different scenarios, and evolution within scenarios) and to refer to the previous safety assessments documents for background information. Justification as to why those conditions were studied is not required. Where appropriate, the relevant conditions should be tabulated. It should be noted that the stated conditions do not restrict qualification of data for use under other conditions, but merely underline the conditions considered appropriate within the modelling context of previous safety assessments.

Sensitivity to assessment results in previous safety assessments

Where appropriate, an account should be given of results from sensitivity analyses performed as part of the previous safety assessments. Such analyses were made in order to prioritise uncertainty assessments for those data and conditions judged to be potentially important for performance, both for overall end-points such as risk and for conditions affecting the state of the system. If such sensitivity analysis was performed, the following issues may be outlined:

- For what ranges of the data was the impact on the previous safety assessment significant and are there ranges where the impact was negligible? If sensitivity analyses show that only part of the range has an impact on repository safety, less effort may be given to quantifying parameter values outside this range.
- Was the impact monotonic, i.e. is there a unidirectional relationship between the data value and performance, is there an “optimal” value, or is the impact dependent in a complicated manner upon the values of other input data?
- What degree of variation in the data is needed to have an impact on safety assessment results (this answer may be different for different data ranges)?
- Were the results applicable to all conditions of interest – or only to some?

In discussing the above, the customer should consider if the cited sensitivity analyses were sufficiently general to provide definitive answers.

Alternative modelling in previous safety assessments

Whenever it applies, the customer representative should summarise alternative modelling approaches studied in previous assessments in which data of this type were used. The following issues may be reflected upon:

- What alternative models exist and what influence did they have on the safety assessment?
- Were conceptual uncertainties, related to the models in which the data were used, identified in previous safety assessments? In that case, what was the impact on assessment results?

Correlations used in previous safety assessment modelling

A correct treatment of probabilistic input data requires that any correlations between those data are identified and quantified. The correlations associated with the subject area data, as accounted for in previous safety assessments, should be briefly described. This includes internal correlations within the subject area and correlations with data of other subject areas. If the same correlations were used as will be used in SR-PSU, it is sufficient to state this.

Identified limitations of the data used in previous safety assessment modelling

If limitations or shortcomings of the data used in the previous safety assessments have been identified, which may significantly have affected the assessment, such should be accounted for. The limitations or shortcomings can be due to, for example, lack of site-specific data or lack of data obtained at conditions representative for the repository. The limitations and shortcomings may have been identified by the regulatory authorities, by SKB, or by other parties.

2.1.3 Supplier input on use of data in SR-PSU and previous safety assessments

In this section the supplier has the opportunity to comment on the two above sections. The focus for the supplier should be to help the SR-PSU team in choosing appropriate data and modelling approaches, and avoid repeating errors and propagating misconceptions from previous safety assessments or from other modelling activities. Even if a single individual has the roles as both supplier and customer representative, he or she may still make comment upon the use of data in SR-PSU and previous safety assessments.

2.1.4 Sources of information and documentation of data qualification

This section is devoted to presenting the most important sources of data, as well as categorising different data sets on the basis of their traceability and transparency. Sources of data may include SKB reports, SKB databases, and public domain material. Documents of importance for the data qualification may also consist of SKB internal documents. All underlying documents should be properly sited throughout the **Data report**.

Sources of information

The supplier is asked to tabulate the most prominent references used as sources of data. In addition, the reference of important documents describing the process of acquiring, interpreting, and refining data may be listed.

If the data qualification process is well documented in supporting documents, it is sufficient to reference these documents and to only briefly summarise the data qualification process. If not, the **Data report** gives the supplier a chance to appropriately document the data qualification process of the subject area data.

Concerning sources of information, the supplier representative should:

- Fully cite all sources of information throughout the text. It is necessary to keep in mind that the text may have readers with limited in-depth knowledge of the subject. Therefore, what normally would seem as trivial may deserve references for further reading. It is strongly recommended to make an extra effort to refer to the open literature where possible, and not only to SKB documents.
- In case of referring to a document of many pages, for example a site-descriptive model report, give detailed information on the section, figure, table, etc where the relevant information can be found.
- Properly cite databases, SKB internal documents, etc even though they may not be available to the general reader. In the case of referring to databases, the precise reference should be given to the individual data set used. For example, it is not sufficient to refer to the SKB database SICADA if not also giving detailed information, such as the activity id or data delivery note id. This is to ensure traceability within the SR-PSU project.
- Fully cite advanced modelling tools where the underlying code may have implications for data qualification.

Categorising data sets as qualified or supporting data

The supplier representative should categorise data as either qualified data or supporting data. Qualified data has been produced within, and/or in accordance with, the current framework of data qualification, whereas supporting data has been produced outside, and/or in divergence with, the framework. Data taken from peer-reviewed literature takes a special position in that they may be considered as qualified even though they are produced outside the SKB framework of data qualification. However, such data are not by necessity categorised as qualified, as they may be non-representative or lack in some other aspect.

Data recently produced by SKB, for example in the site investigations, should a priori be considered as qualified. However, before the data are formally categorised as qualified, a number of considerations need to be made as described below. Data produced outside the data qualification framework should a priori be considered as supporting data. This could for example be data produced by SKB prior to the implementation of its quality assurance system, or data produced by other organisations. Before formally categorise the data as supporting, a number of considerations need to be made as described below.

Data taken from widespread textbooks, engineering handbooks, etc which are considered to be established facts, need not to be scrutinised. Well-known data that should be excluded from the **Data report** need not to be categorised as qualified or supporting data, although their exclusion may need to be motivated.

It is outside the scope of the **Data report** to deal with individual data. Instead the supplier representative should characterise data sets as qualified or supporting. The supplier representative should decide to what extent various data can be included in a single data set for the specific case. The following examples of natural barrier data sets could be used for inspiration:

- Data or part of data, obtained by a specific method at a site, rock volume, borehole, etc.
- Data or part of data, obtained by various methods at certain conditions (e.g. saline water) at a site, rock volume, borehole, etc.
- Data or part of data, taken from an external publication.

Qualified data

The following considerations should be made for data that a priori are identified as qualified, before formally categorising them as qualified. Most of the data that is delivered to the **Data report** are refinements and interpretations of observed data. Such refinements and interpretations are performed both for engineered and natural barrier data. For example, the multitudes of data acquired within the site investigation are normally refined within the site-descriptive modelling by use of more or less complex models. The supplier should judge whether data acquisition and refinement, and associated documentation, are in accordance with the implemented data qualification framework. The following considerations may form the basis for the judgement.

Considerations concerning data acquisition:

- Is the acquisition of observed data performed in conformance with a widely adopted quality management system (e.g. the ISO 9000 series or equivalent)?
- Is it possible to trace relevant quality assurance documents (for example method descriptions, field notes, etc) for the measurements? It should be noted that even though the quality assurance documents may not be available for the general reader, they are accessible for the SR-PSU team.
- Is it possible to extract relevant information on the data quality, variability, and representativity from documents reporting the acquisition of data?
- Are concerns associated with the observed data and nonconformities of the measurements transparently described?
- Is the undertaken data acquisition programme sufficient to determine the full range of data uncertainty and natural variability, and do the acquired data appropriately characterise the intended aspect of the system (site, rock domain, concrete barrier, population, etc)?

Considerations concerning data refinement:

- Are concerns and nonconformities described in the supporting documents propagated to, and addressed in, the data refinement?
- In refining observed data by use of more or less complex modelling, is this done in accordance with documented methods?
- In case of more complex modelling, which may have implication for data qualification, is the details of the modelling described in either in a task description, planning document, or in the document reporting the modelling results? Furthermore, is the modelling tool developed in accordance with a widespread quality assurance system and/or is its quality tested in other ways?
- Has comparative/alternative modelling been performed to evaluate artefacts induced in the modelling, and to evaluate whether the modelled interpretation of the data is reasonable?

Going through these questions in detail for each data set may be a too extensive task, wherefore the sorting of data to some degree is based on expert judgement. However, in making this judgment, it may be helpful to revisit the above bullet lists.

If appropriate data qualification has been performed and documented in supporting documents, or can be performed and documented as part of the delivery, the data should be formally categorised as qualified data. If the documentation of the data qualification process is inadequate in supporting documents, and appropriate data qualification cannot be performed as part of the delivery, the data must be demoted to the category supporting data.

As mentioned before, data taken from peer-reviewed literature takes a special position in that they may be considered as qualified even though they are produced outside the SKB framework of data qualification. However, before formally categorising them, one needs to judge whether they are representative for the SFR repository system and the SFR site. A prerequisite for making such a judgement is often that the documents are transparently written. In case the data are non-representative for Swedish conditions, or their degree of representativity is difficult to evaluate, the data may be categorised as supporting data instead of as qualified data.

Supporting data

The following considerations should be made for data that a priori are identified as supporting, before formally categorising them as supporting data. Such data are produced by SKB outside the framework of data qualification, or by other organisations. The supplier representative should consider:

- How well is the method used to acquire the data described? The greater the transparency with which the method is described in the supporting document, the greater the value should be ascribed to the data.
- How well is the method used to interpret and refining the data described? The more transparently the interpretation and refinement is described in the supporting document, the greater the value should be ascribed to the data.
- Is it possible to identify and evaluate the data qualification process used in acquiring and refining the data? If it is shown that a sound data qualification process has been used, the data should be ascribed greater value.
- Judge, based on the above, whether the data can be used as part of the basis for recommending data to SR-PSU safety assessment modelling, as comparative data for other qualified data, or should not be used at all. In some cases the transparency of a document is so poor that crucial information concerning data qualification cannot be extracted. If this renders an assessment of the data's scientific adequacy and their representativity for Swedish conditions impossible, the supplier representative should recommend that the data are dismissed. This can be done even if the numerical values of the data are consistent with other, qualified data.

In case data that a priori are assumed to be supporting are acquired, interpreted, and refined according to a similar data qualification framework as implemented by SKB, and this is transparently described, the supplier representative can promote the data to the category qualified data.

It should be noted that data taken from peer-review literature can be categorised as supporting data. This can be done if, for example, data are only partially representative for the SFR repository concept and the SFR site.

Excluded data previously considered as important

Within the field of nuclear waste management, there are large quantities of data that are of little significance for the SR-PSU safety assessment, as they are less representative for the SFR site, the SFR repository concept, etc than other available data. In general, excluding such data from subsequent use in SR-PSU does not require justification. The exception is if the data constitutes a well-known part of the basis of previous safety assessments (or equivalent tasks), and/or have a significant impact on the perception of the appropriate choice of data value. If it could be seen as a significant inconsistency or omission not to use the data, their exclusion should be explicitly justified. Providing an appropriate justification is particularly important if the excluded data disagree with the presently used data.

2.1.5 Conditions for which data are supplied

The data of the different subject areas are likely affected by different conditions. Conditions refer to initial conditions, boundary conditions, barrier states, and other circumstances, which potentially may affect the data to be estimated. In the process of qualifying data for subsequent use in safety assessment, an important part is to account for the conditions for which data were acquired, and to compare these conditions with those of interest for the safety assessment.

In the section “Experience from previous safety assessments” it is stated for what conditions data were used in the previous safety assessments. These conditions should not limit the conditions for which data are examined, but merely point out conditions that are likely to be of importance for a safety assessment. The supplier may have been given instructions from the SR-PSU team, or may have opinions about important conditions, which lead to modifications of the previous safety assessments conditions.

In this section, the conditions for which the data have been obtained should be discussed and, as appropriate, justified as relevant to SR-PSU. Such a condition is often a single value (e.g. temperature), a range (e.g. salinity range), or a gradient (e.g. hydraulic gradient). Other factors of relevance for repository safety may be included as conditions, at the discretion of the supplier. Conditions that are deemed to be of particular importance for repository safety should be highlighted. Other conditions that do not significantly relate to repository safety, but may be of importance for data qualification, are also important to note. Such information is valuable when, for example, crosschecking data sets with those of other studies or evaluations. The supplier representative may list ranges of applied conditions during data acquisition, excluding conditions that are both general (such as the gravitational constant) and self-evident.

In many cases, it is expected that the conditions for which data are supplied will differ from those that apply in the SR-PSU safety assessment. For example, a set of supplied data may not represent the full temperature range required, or may have been obtained at a different pressure than expected in situ. The differences identified by the supplier representative should be outlined in this section. Furthermore, for each deviating condition of importance for the assessment results, the implications should be discussed.

2.1.6 Conceptual uncertainty

This section concerns conceptual uncertainty of the subject area data. Two types of conceptual uncertainty should be discussed. The first concerns how well the data, and the models wherein it is used, represent the physical reality, and the second concerns conceptual uncertainties introduced in the acquisition, interpretation, and refinement of the data. Generally data are included in models that represent an idealised reality, which to some degree differs from the physical reality. Therefore, one can expect that a degree of conceptual uncertainty is associated with all data compiled in this report.

To the extent possible, the supplier should describe such conceptual uncertainty. This should be done in the context of the models in which the data are used, intended to describe certain postulated processes. Also, it may be appropriate to discuss alternative conceptualisations in which the data may be used in different ways. If comprehensive discussions on the subject have already been documented, for example in the SR-PSU or SR-Site Process reports, such documents may be referred to and a short summary of the conceptual uncertainty will suffice. Aspects of the conceptual uncertainty that are obviously unrelated to repository safety may be disregarded.

Conceptual uncertainty may also be introduced in the acquisition, interpretation, and refinement of the data. For example the data may have been obtained by inverse modelling of experimental results, where conceptual uncertainty is introduced by the model. The data may also have been obtained by using some correlation relationship, where there is conceptual uncertainty in the correlation. Many other sources of conceptual uncertainty are conceivable and may be discussed at the discretion of the supplier. In doing this, the supplier representative should carefully differentiate between uncertainties introduced due to conceptual issues and data uncertainty introduced by measurement errors, etc. Data uncertainty should be discussed in the following section.

2.1.7 Data uncertainty due to precision, bias, and representativity

In this section data uncertainty should, if possible, be discussed in terms of precision, bias, and representativity, in the context of their application in SR-PSU. Such uncertainty is associated both with the acquisition of data, for example in the site investigations, and subsequent refinement of data, for example in the site-descriptive modelling. Data uncertainty includes neither conceptual uncertainty nor natural variability.

If comprehensive discussions on these matters are documented elsewhere, such documents should be referred to, and a short summary of the discussion will suffice. The supplier should begin with discussing the precision of the supplied data. To the extent possible, data spread due to the precision should be separated from data spread due to natural variability. Precision issues are both associated with the method used in acquiring the raw data and subsequent interpretation of data. Concerning acquiring raw data, limitations in precision are not only associated with the equipment and method used when performing the measurements, but also with the sampling procedure, sample preparation, etc. Precision issues associated with interpretation of the data depend to a large degree on the procedure used, and should be discussed at the discretion of the supplier. As an example, it may not be straightforward to estimate the precision of data that are a function of other acquired data, with their intrinsic limitations in precision.

Thereafter, the supplier representative should discuss the bias of the supplied data. Similar considerations apply as when discussing precision, both for bias associated with the acquisition of raw data and with their subsequent interpretation. Bias in observed data is often associated with the method used for acquiring data and its calibration, and with effects of sample preparation. Bias is also associated with the sampling procedure, sample size, and differences in conditions for example between those in the laboratory and in situ. Bias issues associated with data interpretation depend to a large degree on how the interpretation is made, and should be discussed at the discretion of the supplier representative.

Finally the supplier representative should discuss the representativity of the supplied data, both in terms of data acquisition, and data interpretation and refinement. Issues associated with the representativity of acquired data often concern the sampling procedure, the sample size relative to natural variability and correlation length, and differences in conditions between, for example, those in the laboratory and in situ.

An important issue is whether the data are generic or site and/or technique specific. In the case of access to generic data only, the supplier should discuss whether, and to what degree, the lack of site and/or technique specific data influences the data uncertainty. Representativity issues associated with data interpretation and refinement depend much on the specific interpretation and refinement process, and should be discussed at the discretion of the supplier representative.

As well known, the precision, bias, and degree of representativity often depend on a mixture of the above-suggested sources for data uncertainty, and may not be easily separated. However, the supplier representative is asked to reflect carefully on these issues, as an assessment of data uncertainty is crucial in data qualification. In case data uncertainty cannot be discussed in terms of precision, bias, and representativity, for example as the resolution in data does not allow for such separation, it will suffice to make a general data uncertainty discussion.

Comprehensible illustrations of different data sets are of high value. The objective of the illustrations is not necessarily to provide a detailed basis and description of the numerical values of the individual data. Sometimes the objective may be to give the reader an understanding of how much, and in what ways, the data varies and the data sets differ from each other. An example of presenting different data sets is given in Figure 2-2, where the reader can get an immediate perception about differences between the data sets. Examples of other illustrations of data sets are given in Figure 2-3 in Section 2.1.10.

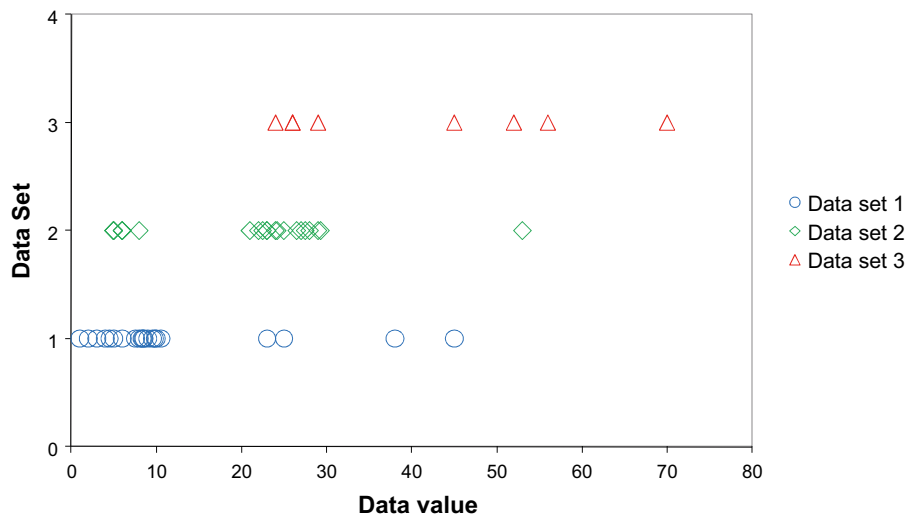


Figure 2-2. Example of presenting differences in data sets.

2.1.8 Spatial and temporal variability

In this section the supplier should discuss the spatial and temporal variability of the subject area parameters. The natural variability should as far as possible be separated from data uncertainty, discussed in the above section.

The supplier should describe what is known about the spatial variation, sometimes referred to as heterogeneity, of the subject area data. This may result in different data sets for different volumes or elements of the repository system, or for different time periods. If comprehensive discussions on the natural variability are documented elsewhere, such documents should be referred to and a short summary of the natural variability will suffice.

In the process of describing the spatial variability, it may be helpful to reflect on the following line of questions.

- Is there spatial variability of the data, and if so is it of consequence for the safety assessment?
- Is the spatial variability scale dependent? If so, can an appropriate approach of upscaling to safety assessment scale be recommended?
- What is known about correlation lengths from, for example, variograms?
- Can the spatial variability be represented statistically as a mean of data qualification and, if so, how is this done?
- Is there any information about the uncertainty in the spatial variability?

In the process of describing the temporal variability, it may be helpful to reflect on the following line of questions.

- Is there temporal variability of the data, and if so is it of consequence for the safety assessment?
- What processes affect the temporal variability of the data and how is the temporal variability correlated with these processes?
- Does the temporal variability follow any pattern, for example a cyclic pattern?
- Could the temporal variability be represented statistically as a mean of data qualification and if so, how is this done?
- Is there any information about the uncertainty in the temporal variability?

In addition, other relevant issues concerning the natural variability may be addresses at the discretion of the supplier. Comprehensible illustrations of different data sets from different volumes, elements, or time periods are of high value.

2.1.9 Correlations

An appropriate treatment of probabilistic input data requires that any correlations and functional dependencies between those data are identified and quantified. In the extensive work with the FEP database and the three process reports, many correlations and functional dependencies between parameters have been identified. Where appropriate, these correlations and functional dependencies should also be implemented in the safety assessment models. It should be an aim to aid those performing probabilistic modelling, by giving well defined and usable information on how to handle correlations between input data.

Correlations and functional dependencies may also have been used when acquiring, interpreting, and refining data. For example, concerning sorption partition coefficients, data have not been acquired for all relevant radionuclides. For species for which there is a lack in observations, the supplied sorption partition coefficient will have been estimated from data obtained for one or more analogue species. This has implications for how to correlate input data in stochastic safety assessment modelling.

In this section the supplier representative is requested to reflect on the following questions:

- For the subject area data, are there correlations or functional dependencies between parameters of the same or of different subject areas? If so, account for these and if possible also for the consequences for the safety assessment.
- If correlations have been used in acquiring, interpreting, and refining data, how is this done? Furthermore, is the outcome based solely upon correlations, or on both measurements and correlations?
- If the data varies in space and time – is anything known about its autocorrelation structure?
- Is there any other reason (apart from already cited correlations and functional dependencies) to suspect correlations between parameters considered as input to SR-PSU modelling?

2.1.10 Results of supplier's data qualification

In this section the supplier is requested to present data that are considered to be appropriate as a basis for suggesting input data for use in SR-PSU. Comprehensive information relating to each parameter requested in the bullet list under the heading “Defining the data requested from the supplier” (cf. Section 2.1.1) should be given. Only one set of data should be delivered for each specified condition, volume, element, time period, etc.

The general process of reducing and interpreting data, valuing different data sets, and finally selecting the recommended data for delivery to the SR-PSU team should be fully accounted for, if not already accounted for in the previous sections or in supporting documents. In the latter case, it is sufficient to briefly summarise the process of selecting the delivered data.

In case the data presented in supporting documents need reinterpretation and further refinement, in the light of this instruction and/or other information, this should be fully documented. In case the supporting documents give more than one data set for a specified condition, volume, element, time period, etc further data reduction is required. Such data reduction may include the merging of data sets, and there may be a need to give different weight to different data sets. Much weight should be given to peer-reviewed data judged as representative for the SFR site and repository system. Generally, more weight should be given to qualified data than to supporting data. The degree to which the data are representative in the context of their application in SR-PSU should also be a factor in the weighting. Exactly how much weight should be given to individual data sets must be decided upon by the supplier. The process of further reinterpretation, refinement, and data reduction should be fully documented. If it increases the readability of the text to also utilise other sections for such documentation, this is allowed. Also, if this requires much space, some information may be appended.

The data sets that the supplier recommends to the SR-PSU team should be in the form of single point values, probability distributions, mean or median values with standard deviations, percentiles, ranges, or as otherwise appropriate. If the data have significant variability and/or uncertainty, the spread in data could be described as a range. However, the meaning of the range has to be provided, e.g. does it represent all possible values, all “realistically possible” values or just the more likely values? The supplier may provide more than one range, representing different probabilities, as exemplified below:

- The range wherein the likelihood of finding the data is high.
- The range for which the likelihood of finding the data outside this range is very low.

All data should be recommended in the context of input data to safety assessment modelling, wherefore the final uncertainty estimate should encompass conceptual uncertainty, data uncertainty, and natural variability (cf. Section 2.1.6, Section 2.1.7 and Section 2.1.8). If the supplier representative has used some kind of mathematical expression to account for the uncertainty and natural variability, this expression should be provided and justified.

If the data are suggested to be described by a well-defined probability distribution, it should be justified on statistical grounds that the data indeed are (sufficiently well) distributed accordingly. The usage of standard deviation is often perceived to imply that the data are normally distributed; even though the definition of standard deviation is unrelated to specific probability distributions. Therefore, when giving the standard deviation, it should be remarked upon whether or not the normal distribution appropriately describes the data. If there are obvious differences between how the data set at hand is actually distributed, and the probability distribution (or range) finally recommended, the reasons for, and implications of, this should be discussed. Outliers should not be dismissed without justification.

It should be noted that in many cases, at some stage probability distributions must be assigned to numerical data being the input to probabilistic safety assessment modelling. If the supplier feels inadequate to deliver a defined distribution, but for example delivers a best estimate, an upper, and a lower limit for data, it may fall on the SR-PSU team to transform such information into probability distributions. This is justified as the SR-PSU team may have a better understanding of how the shape of the assigned distributions (especially in their tails) affects the assessment results. The SR-PSU team may also, in some cases, have a better understanding of the underlying statistics of the suggested distribution.

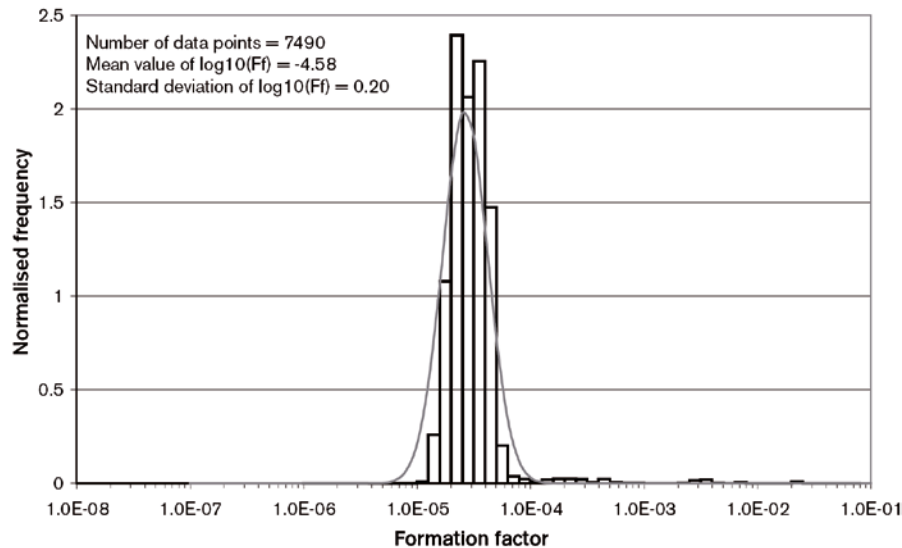
The above instructions are not applicable to all data, as all data are not necessarily in the form of numerical values. Examples are exit locations for groundwater flowpaths, given as co-ordinates, or information on solubility limiting phases, given as chemical species and reactions.

For a spatially varying function well described by a given stochastic process, e.g. through a variogram or as realised in a Discrete Fracture Network, a potential statement may be that all realisations of this spatially varying function are equally probable.

Finally, it may be impossible to express the uncertainty by other means than a selection of alternative data sets. There are a number of uncertainties that cannot be managed quantitatively in any other rigorous manner, from the point of view of demonstrating compliance, than by pessimistic assumptions. This is allowed, as long as the supplier clearly documents this together with the justification for adopting this approach.

Comprehensible illustrations and tables of the suggested data sets are of high value. In Figure 2-3 three examples (a,b and c) of representations of recommended data are given.

For data which are impractical to tabulate in the report (for example the co-ordinates of thousands of exit locations for groundwater flowpaths), it is sufficient to precisely refer to a SKB database or equivalent.



a

Nuclide/redox state		Non-saline K_d (m^3/kg)
Ni(II) ¹	best estimate	$1.2 \cdot 10^{-1}$
	$K_{d,25\%} - K_{d,75\%}$	$5.5 \cdot 10^{-2} - 3.0 \cdot 10^{-1}$
	$K_{d,low} - K_{d,high}$	$1.8 \cdot 10^{-2} - 5.4 \cdot 10^{-1}$
Sr(II) ¹	best estimate	$1.3 \cdot 10^{-2}$
	$K_{d,25\%} - K_{d,75\%}$	$6.5 \cdot 10^{-3} - 4.1 \cdot 10^{-2}$
	$K_{d,low} - K_{d,high}$	$1.0 \cdot 10^{-3} - 6.1 \cdot 10^{-1}$

b

	Limiting specie	Reaction
Ag(0)	Ag(s)	$Ag(s) + H^+ + 0.25O_2 = Ag^+ + 0.5H_2O$
Ag(I)	AgCl(cr)	$AgCl(cr) = Ag^+ + Cl^-$
Am(III)	Am(OH) ₃ (am)	$Am(OH)_3(am) + 3H^+ = Am^{+3} + 3H_2O$

c

Figure 2-3. Examples of representations of recommended data, taken from the SR-Can Data report (SKB 2006).

2.1.11 Judgements by the SR-PSU team

In this section, the customer representative, on behalfs of the SR-PSU team, should document the examination of the delivery provided by the supplier, and make judgment on the data qualification. This text should be produced in close cooperation with persons of the SR-PSU team with special knowledge and responsibility. In case of unresolved issues, the final phrasing should be decided upon by the SR-PSU team. Comments should be made on all the sections listed below:

- Sources of information and documentation of data qualification.
- Conditions for which data are supplied.
- Conceptual uncertainty.
- Data uncertainty due to precision, bias, and representativity.
- Spatial and temporal variability.
- Correlations.
- Results of supplier's data qualification.

Concerning the section “Sources of information and documentation of data qualification” the customer should judge if appropriate documents are referenced, and if the categorisation of data sets into qualified or supporting data is adequately performed and justified.

Concerning the section “Conditions for which data are supplied” the customer should focus upon whether the conditions given by the supplier are relevant for SR-PSU modelling. If not, it should be accounted for how this is handled in SR-PSU (for example by extrapolating data, using generic data, or assuming pessimistic values) and what degree of uncertainty such a procedure induces.

Concerning the section “Conceptual uncertainty” the customer should judge whether the discussion provided by the supplier is reasonable and sufficiently exhaustive. If the customer sees the need to include additional sources of conceptual uncertainty, such should be described and if possible quantified. Finally, where necessary the impact of the conceptual uncertainty on the assessment should be discussed, as well as how conceptual uncertainty is handled in SR-PSU modelling (for example by applying pessimistic corrections factors to the data).

Concerning the section “Data uncertainty due to precision, bias, and representativity”, the customer should make a judgment on the account provided by the supplier. Also, if the customer sees the need to include additional sources of data uncertainty, these should be described and if possible quantified. If necessary the impact of the data uncertainty on the assessment should be discussed, as well as how data uncertainty is handled in SR-PSU modelling (for example by applying data uncertainty distributions or using corrections factors for the data).

Concerning the section “Spatial and temporal variability” the customer should focus upon whether the spatial and temporal variability are adequately characterised and whether they are of relevance for SR-PSU modelling. Also, if the customer sees the need to include additional sources of spatial and temporal variability, such should be described and if possible quantified. In necessary, the impact of the spatial and temporal variability on the assessment should be discussed, as well as how this is handled in SR-PSU modelling (for example by applying data distributions or different data for different model times and volumes).

Concerning the section “Correlations” the customer should scrutinise the correlations and functional relationships suggested by the supplier. Also, if correlations other than those suggested by the supplier are identified in the SR-PSU programme (for example in Process reports) these should be briefly described where necessary. If appropriate, a summary could be provided concerning which correlations are of actual importance for safety assessment modelling and results.

Concerning the section “Result of data qualification” the customer should make judgement on the choice of data by the supplier, based on scientific adequacy, usefulness for the safety assessment, and the data qualification process. Comments should be made on the delivered estimates of data uncertainty and natural variability, as well as on the data reinterpretation/refinement/reduction process. Furthermore, the delivered distributions, data ranges, etc should be scrutinised from a statistical point of view. It should be judged whether the suggested way of representing data, for example by a log-normal distribution, is adequate for SR-PSU modelling. If the SR-PSU team chooses to promote other data than those suggested by the supplier, the choice should be fully documented.

For all the sections listed above, supplier statements or supplied data believed to be extra uncertain, dubious, or even erroneous should be highlighted by the customer. These matters should be raised with the supplier and, if possible, resolved and accounted for in this section.

2.1.12 Data recommended for use in SR-PSU modelling

The main delivery of the **Data report** to the SR-PSU modelling is recommendations of data that generally are numerically well defined. Such recommended data should be given in this section.

Based on all the available information, but also on the needs from SR-PSU modelling, the customer representative and SR-PSU team should make a final choice of data in form of single point values or well-defined probability distributions, encompassing natural variability, data uncertainty and other uncertainty. These data should be clearly tabulated (or otherwise presented) in this section. Alternatively, precise referencing to tables or equivalent in previous section can be made. For data which are impractical to tabulate in the report it is sufficient to precisely refer to a database or equivalent.

Also short guidelines for how to use the data in subsequent modelling should be given, as required. Justifications and guidelines should be kept short so that this section mainly contains tabulated data that are easily extractable for SR-PSU safety assessment modelling.

In the process of making the final choice of data, the supplier representative, and potentially also other members of the supplier team, will be consulted one more time in a data qualification meeting. Here the formal decision on the data recommended for use in SR-PSU modelling should be taken, and records of the meeting should be made as part of the SKB quality assurance system. The formal decision should be acknowledged by those representing the supplier team and those representing the SR-PSU team.

3 Radionuclide decay

The radionuclide inventory of the SFR repository consists of a great number of radionuclides. However, most of them do not have any significant consequences for the SR-PSU safety assessment, as they do not have a long enough half-life, large enough radiotoxicity, exist in large enough amounts, and/or produce decay products of the above standing attributes. Using the half-life values and basic screening calculations one can rule out a majority of the radionuclides which will have no significant effect and compile the radionuclides that will.

As the result of nuclear decay the inventory of radionuclides in the SFR repository will change over time. The nuclear decay will also influence which radionuclides that will result in any significant dose once released from the repository. The half-lives of the radionuclides are therefore needed in all the parts of the safety assessment.

3.1 Modelling in SR-PSU

This section describes what data are expected from the supplier, and in what SR-PSU modelling activities the data are to be used.

Defining the data requested from the supplier

- The half-lives, $t_{1/2}$ (yr), and the half-life uncertainties for the selected radionuclides.

SR-PSU modelling activities in which data will be used

The half-lives are used in the entire chain (near field, far field and biosphere) of the SR-PSU radionuclide transport modelling, as the inventory will constantly evolve due to the nuclear decay.

The half-lives will also be used for predicting the radionuclide inventory of the repository at closure (SKB 2013).

The evolution of the inventory by nuclear decay is calculated with standard methods using the Bateman equations (Bateman 1910).

3.2 Experience from previous safety assessments

This section briefly summarises experience from previous safety assessments, especially the SAFE and SAR-08 safety assessments, which may be of direct consequence for the data qualification in this report.

Modelling in previous safety assessments

In SAR-08, the half-lives were used in both inventory calculations (Almkvist and Gordon 2007), predicting the inventory of the selected radionuclides in the repository at the time of closure, in the radionuclide transport calculations; modelled in SAR-08 with the Amber software (SKB 2008), and in the biosphere dose calculations (Bergström et al. 2008).

Conditions for which data were used in previous safety assessments

No special conditions for half-life data were used in previous assessments.

Sensitivity to assessment results in previous safety assessments

No sensitivity analyses with regard to the half-lives were performed in previous safety assessments.

Alternative modelling in previous safety assessments

No alternative modelling with regard to the half-lives were performed in previous safety assessments.

Correlations used in previous safety assessment modelling

Many of the radionuclides are correlated through decay chains. No other correlation with regard to the half-lives is present.

Identified limitations of the data used in previous safety assessment modelling

Since SAR-08, results of new measurements of the half-lives of the radionuclides Ag-108m and Se-79 were published. These articles have reported decays time differing from the ones reported in Firestone et al. (1998) by one order of magnitude with regards to Se-79, and by around twenty years with regard to Ag-108m.

3.3 Supplier input on use of data in SR-PSU and previous safety assessments

The supplier agrees with the general approach of the previous safety assessments when considering conditions and uncertainties. However, the supplier recommends that the SR-PSU team use harmonised half-life data in all modelling activities. Therefore the recommended data below should be used in as many modelling activities as possible.

3.4 Sources of information and documentation of data qualification

Sources of information

The half-life data, for all the radionuclides except Ag-108m and Se-79, presented in this chapter are qualified in Firestone et al. (1998). For Ag-108m, the data is presented and qualified in Schrader (2004). For Se-79, the data is presented and qualified in Jörg et al. (2010). See Table 3-1 for the full references.

Categorising data sets as qualified or supporting data

Table 3-2 shows qualified and supporting data sets used in the qualification for this section.

Excluded data previously considered as important

As explained in this section, the half-life values from Firestone et al. (1998) for Ag-108m and Se-79 are considered obsolete. Instead values from Schrader (2004) and Jörg et al. (2010) were used in the data qualifying process.

Table 3-1. Main sources of information used in data qualification.

Sources of information
Firestone R B, Baglin C M (ed), Chu S Y F (ed), 1998. Table of isotopes: 1998 update. 8th ed. New York: Wiley.
Schrader H, 2004. Half-life measurements with ionization chambers – a study of systematic effects and results. Applied Radiation and Isotopes 60, 317–323.
Bienvenu P, Cassette P, Andreoletti G, Bé M-M, Comte J, Lépy M-C, 2007. A new determination of ⁷⁹ Se half-life. Applied Radiation and Isotopes 65, 355–364.
Jörg G, Bühnemann R, Hollas S, Kivel N, Kossert K, Van Winckel S, Gostomski C L, 2010. Preparation of radiochemically pure ⁷⁹ Se and highly precise determination of its half-life. Applied Radiation and Isotopes 68, 2339–2351.
A number of recent peer reviewed scientific publications from the open literature, as referred to in the present text.

Table 3-2. Qualified and supporting data sets.

Qualified data sets	Supporting data sets
Firestone et al. 1998, Table 1: Half-lives for all radionuclides except Ag-108m and Se-79.	A number of data taken from scientific publications as referred to in Table 3-3 for Se-79.
Schrader 2004: Half-life for Ag-108m.	
Jörg et al. 2010: Half-life for Se-79.	

3.5 Conditions for which data are supplied

The half-lives of radionuclides are not affected by external conditions such as temperature, pressure, chemical conditions and magnetic or electrical fields and therefore are valid under all conditions of the assessment.

3.6 Conceptual uncertainty

Radioactive decay has been thoroughly studied experimentally over a long period of time. The theoretical understanding of the process is good and sufficient for the needs of the safety assessment. No conceptual uncertainties are therefore reported.

3.7 Data uncertainty due to precision, bias, and representativity

When choosing the values, except for Ag-108m and Se-79, from Firestone et al. (1998), comparisons were made with other references to ensure that the half-lives of the selected radionuclides did not differ significantly. Compared with Chu et al. (1999) an average difference of 0.001% was found for the selected radionuclides. Compared with ENDF/B-VI (2001) a difference of around 0.7% was found for the selected radionuclides.

Even though the half-life of nearly all isotopes of radiological importance are known with an accuracy of 0.01% or better according to Håkansson (2000), some are still under debate. The two radionuclides, important for the SR-PSU safety assessment, for which the half-lives are still studied and updated, are discussed below:

Se-79

The half-life of the relatively stable isotope Se-79 is, even though several studies in radioactive waste context have been performed, still being debated in the scientific community. Later studies have been able to narrow the half-life to a range between $\sim 1\text{--}11 \cdot 10^5$ years, see Table 3-3. This rather large range is mainly due to difficulties obtaining adequately pure Se-79 samples, as it can currently only be obtained from spent nuclear fuel, in which it is a very minor component. Also the methods used to determine Se-79 contents in the wastes such as ICP-MS and radiometric methods, have difficulties giving reliable measurements. Detection of Se-79 by radiometric methods is difficult due to the low β -energy and the absence of γ -emission of the isotope, combined with the interference from Tc-99, Pm-147, Sm-151, Zr-93 and Pu-241 whose β -decay spectra are similar. The problem with the ICP-MS method is the high ionisation potential of selenium, which results in the ionisation of only $\sim 30\%$ of the Se atoms in the argon plasma, leading to poor sensitivity (Puranen 2010).

The half-life used for Se-79 in the latest safety assessment for spent fuel, SR-Site Data report (SKB 2010a), is the one reported in Bienvenu et al. (2007).

There is also the value on which the Decay data evaluation project (DDEP) working group base their recommendation (consult e.g. Helmer et al. (2002) for participants of DDEP). The recommended DDEP value for the Se-79 half-life ($3.56 \pm 0.40 \cdot 10^5$ years) is not a measured value but a weighted average of the two latest reported values available, at the time, in the open literature. The value recommended for use in SR-PSU is the latest from Jörg et al. (2010) which has a lower uncertainty margin than the DDEP value, see Table 3-3 and Figure 3-1.

In Figure 3-1 the values in Table 3-3 are plotted, showing the half-lives stabilising at a value around $2.80\text{--}3.80 \cdot 10^5$ years.

Table 3-3. Se-79 half-lives.

Half-life (years)	Source
$4.8 \pm 0.4 \cdot 10^5$	Yu et al. 1995
$1.1 \pm 0.2 \cdot 10^6$	Jiang et al. 1997
$1.24 \pm 0.19 \cdot 10^5$	He et al. 2000
$2.95 \pm 0.38 \cdot 10^5$	Jiang et al. 2001
$2.80 \pm 0.36 \cdot 10^5$	He et al. 2002
$3.77 \pm 0.19 \cdot 10^5$	Bienvenu et al. 2007
$3.27 \pm 0.08 \cdot 10^5$	Jörg et al. 2010

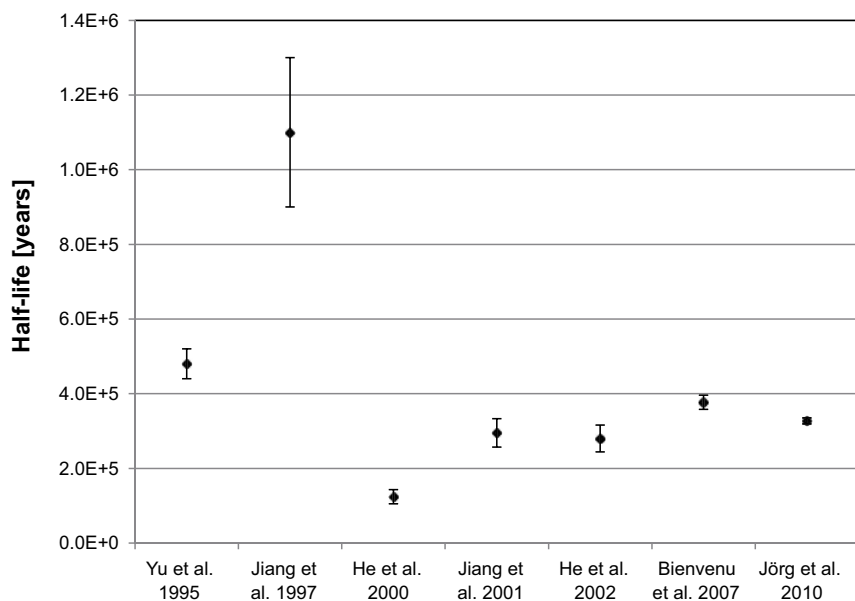


Figure 3-1. Measured half-life values of Se-79 with uncertainty margins.

Ag-108m

For the Ag-108m isotope the DDEP working group recommends the value taken from Schrader (2004) (438 ± 9 years) that reports results from measurements in which the decay was followed in an ionisation chamber for about 20 years.

3.8 Spatial and temporal variability

Spatial variability of data

Not relevant.

Temporal variability of data

Not relevant.

3.9 Correlations

Radionuclides as decay parents and daughters are correlated through decay chains. No other relevant correlations have been reported.

3.10 Result of supplier's data qualification

The half-lives and the uncertainty ranges, taken from Firestone et al. (1998), Schrader (2004) and Jörg et al. (2010), are reported in Table 3-4.

3.11 Judgements by the SR-PSU team

Sources of information

The same sources of information used in the data qualification, Section 3.4, are used in this judgment.

Conditions for which data is supplied

The SR-PSU team agrees with the supplier regarding the lack of special conditions for half-lives given in Section 3.5.

Conceptual Uncertainty

No conceptual uncertainties have been reported by the supplier. The SR-PSU team agrees with this.

Data uncertainty due to precision, bias, and representativity

The uncertainties reported by the supplier in Table 3-4 are considered too small to be significant in the safety assessment and will therefore not be used by the SR-PSU team. The SR-PSU team also agrees on using the references for Ag-108m and Se-79 provided by the supplier.

Spatial and temporal variability

No spatial or temporal variabilites have been reported by the supplier. The SR-PSU team agrees with this.

Table 3-4. Half-lives recommended for use in SR-PSU. All data taken from Firestone et al. (1998) except for a) Schrader (2004) and b) Jörg et al. (2010). All the supplied radionuclides will not necessarily be used in the SR-PSU safety assessment.

Nuclide	Half-life (years)		Nuclide	Half-life (years)			
	Min.	Max.		Min.	Max.		
Ag-108m ^{a)}	438	429	447	Ni-63	100.1	98.1	102.1
Am-241	432.2	431.5	432.9	Np-237	2.144E+06	2.137E+06	2.151E+06
Am-242m	141	139	143	Pd-107	6.5E+06	6.2E+06	6.8E+06
Am-243	7,370	7,330	7,410	Pm-147	2.6234	2.6232	2.6236
Ba-133	10.51	10.46	10.56	Pu-238	87.7	87.4	88.0
Be-10	1.51E+06	1.45E+06	1.57E+06	Pu-239	24,110	24,080	24,140
C-14inorg	5,730	5,690	5,770	Pu-240	6,563	6,556	6,570
Ca-41	1.03E+05	0.99E+05	1.07E+05	Pu-241	14.35	14.25	14.45
Cd-133m	14.1	13.6	14.6	Pu-242	3.733E+05	3.721E+05	3.745E+05
Cl-36	3.01E+05	2.99E+05	3.03E+05	Ru-106	373.59 days	373.44 d	373.74 d
Cm-243	29.1	29.0	29.2	Sb-125	2.7582	2.7571	2.7593
Cm-244	18.10	18.08	18.12	Se-79 ^{b)}	3.27E+05	3.19E+05	3.35E+05
Cm-245	8,500	8,400	8,600	Sm-151	90	82	98
Cm-246	4,730	4,630	4,830	Sn-126	~1E+05		
Co-60	5.2714	5.2709	5.2719	Sr-90	28.78	28.74	28.82
Cs-134	2.0648	2.0638	2.0658	Tc-99	2.111E+05	2.099E+05	2.123E+05
Cs-135	2.3E+06	2.0E+06	2.6E+06	U-232	68.9	68.5	69.3
Cs-137	30.07	30.04	30.10	U-234	2.455E+05	2.449E+05	2.461E+05
Eu-152	13.537	13.531	13.543	U-235	7.038E+08	7.033E+08	7.043E+08
Eu-154	8.593	5.589	8.597	U-236	2.342E+07	2.339E+07	2.345E+07
Eu-155	4.7611	4.7598	4.7624	U-238	4.468E+09	4.465E+09	4.471E+09
Fe-55	2.73	2.70	2.76	Zr-93	1.53E+06	1.43E+06	1.63E+06
H-3	12.33	12.26	12.39				
Ho-166m	1.20E+03	1.02E+03	1.38E+03				
I-129	1.57E+07	1.53E+07	1.61E+07				
Mo-93	4.0E+03	3.2E+03	4.8E+03				
Nb-93m	16.13	15.99	16.27				
Nb-94	2.03E+04	1.87E+04	2.19E+04				
Ni-59	7.6E+04	7.1E+04	8.1E+04				

Correlations

The supplier has identified correlations in data through the decay chains only. The SR-PSU team agrees.

Results of supplier's data qualification

The supplier has given data on half-lives and uncertainties in Table 3-4. The SR-PSU team accepts the data for all nuclides. The SR-PSU team consider the uncertainties reported in Table 3-4 to be too small to be significant in the SR-PSU context and will therefore not use them in the SR-PSU safety assessment.

3.12 Data recommended for use in SR-PSU modelling

The data presented in Table 3-4 are recommended for use in SR-PSU except for the uncertainties which are judged to be too small to make an impact on the safety assessment.

4 Uncertainties in the radionuclide inventory

Since the start of operations of SFR 1 in the Forsmark area in 1988, low and intermediate operational nuclear waste from the nuclear power plants, the Studsvik Research Site, and the Central Interim Storage for Spent Nuclear Fuel (CLAB) have been deposited in the repository. The waste is treated, stabilised and deposited in containers depending on the waste origin. Because the handling of radioactive waste has been going on since the start of the first commercial nuclear power plant (Oskarshamn 1) in the early 70's, and because the waste produced since then originates from several different facilities; the SFR repository contains several different types of containers with waste treated in different ways.

In order to keep some systematic classification of their origin, waste types have been defined depending on the container and the contained waste, and a code system for these types has been developed. The system is helpful for data transfer between the power plants and the SFR facility, and for making prognoses of the future SFR inventory. The code system shows where the waste originated, what sort of waste is contained and where in the SFR repository the waste should be placed. The code system is further described in the Reference inventory report (SKB 2013).

As an extension to earlier SFR safety assessments, in SR-PSU the inventory of the planned SFR 3 repository will be included in the inventory. The SFR 3 repository will contain one BMA type repository, four BLA type repositories, and a new type of repository called BRT which will contain decommissioned reactor pressure vessels from boiling water reactors.

In the Reference inventory report (SKB 2013) a best estimate of the radionuclide inventory in SFR is calculated. Several methods for estimating the amounts have been applied depending on the type and origin of waste. Each method is associated with uncertainties. Considering these uncertainties a high radionuclide inventory has been estimated (SKBdoc 1427105).

4.1 Modelling in SR-PSU

This section describes what data are expected from the supplier, and in what SR-PSU modelling activities the data are to be used.

Defining the data requested from the supplier

- A radionuclide inventory calculated from the best estimate inventory including uncertainties.

SR-PSU modelling activities in which data will be used

This high radionuclide inventory is used as input in the high inventory calculation case, CC20, for the radionuclide transport, described in the **Radionuclide transport report**. The radionuclide transport is modelled with the Ecolego software that is described in the **Model summary report**.

4.2 Experience from previous safety assessments

This section briefly summarises experience from previous safety assessments, especially the SAFE and SAR-08 safety assessments, which may be of direct consequence for the data qualification in this data report.

Modelling in previous safety assessments

The radionuclide transport in the SAFE assessment was modelled with the NUCFLOW software for the near-field transport and with the FARF31 software for the far-field transport (Lindgren et al. 2001). In the SAR-08 safety assessment, both the near-field and far-field transport were modelled with the AMBER software (SKB 2008).

In SAR-08 the Prosit tool used half-lives³ from Firestone et al. (1998) which, except for the half-lives for Ag-108m and Se-79, are the same half-lives recommended for the SR-PSU safety assessment. See Chapter 3 – Radionuclide decay – in this report.

Conditions for which data were used in previous safety assessments

In the SAR-08 safety assessment the delivered inventories were estimated using the Prosit tool which extracted the information from the Triumph database⁴. In the three different scenarios described in Almkvist and Gordon (2007), two of the scenario inventories varied depending on when the SFR 1 repository would close, either at year 2040 or year 2050.

In the third, “Full Inventory” scenario, the inventory was scaled up to the maximum allowed inventory limit; 10^{16} Bq, and to the full volumetric capacity of the repository. This scenario reflects the inventory presented in this chapter even though the method of scaling up is different.

Radionuclide estimations and prognoses

In the SAR-08 safety assessment inventory report “Low and Intermediate Waste in SFR 1” (Almkvist and Gordon 2007) wrote about measuring specific radionuclide activity in the following terms: “The most accurate method to estimate the radionuclides is almost always to make direct measurements on the waste. Unfortunately this is never feasible in reality due to a number of reasons, e.g. the waste is not produced yet, the geometry, the shielding of activity (high detection limit), the measurements are not correct etc. The solution is to make some kind of estimate.”

The prognosis tool used in SAR-08, Prosit, used several different methods to estimate inventories of the selected radionuclides, and where no other methods were available correlation factors were used. The methods and the correlation factors, taken from Almkvist and Gordon (2007), are described below.

C-14

The total inventory of C-14 was estimated in Magnusson et al. (2007) at the time of repository closure. The report also estimated an annual production of C-14 from each nuclear reactor. Almkvist and Gordon (2007) deducted the annual production from the total inventory. They used the correlation factor with Co-60 (Lindgren et al. 2007) to be able to distribute the C-14 inventory in the different waste packages present in the SFR repository. Almkvist and Gordon (2007) also wrote that the amount of C-14 will be correlated to the electric energy generated in the future.

Cl-36

The total amount of Cl-36 in produced waste up to 2005 was estimated in Almkvist and Gordon (2007). For the rest of the period, the correlation factor with Co-60 was used, which was also used for the distribution of Cl-36 in the different waste packages present in the SFR repository. Almkvist and Gordon (2007) also wrote that the amount of Cl-36 will be correlated to the electric energy produced in the future.

Mo-93

The total amount of Mo-93 in produced waste up to 2004 was estimated in Almkvist and Gordon (2007). For the rest of the period, the correlation factor with Co-60 was used, which was also used for the distribution of Mo-93 in the different waste packages present in the SFR repository.

Ni-59/Ni-63

For both nickel isotopes different correlation factors were used depending on if the waste originated from Boiling Water Reactors (BWR) or Pressurised Water Reactors (PWR), see Table 4-1.

³ Interface that extracts information from Triumph. Maintained by SKB [accessed in February 2007].

⁴ Database over radioactive operational waste in SFR 1. Maintained by SKB [accessed in February 2007].

Table 4-1. Nickel correlation factors used in SAR-08 (Almkvist and Gordon 2007).

Correlation factor (to Co-60 activity)	BWR	PWR
Ni-59	1E-3	3E-2
Ni-63	8E-2	4

Tc-99

The total amount of Tc-99 in produced waste up to 2004 was estimated in Almkvist and Gordon (2007). For the rest of the period, the correlation factors with Co-60 and Cs-137 were used. They were also used for the distribution of Tc-99 in the different waste packages present in the SFR repository.

I-129

The total amount of I-129 in produced waste up to 2004 was estimated in Almkvist and Gordon (2007). For the rest of the period, the correlation factor with Cs-137 was used, which was also used for the distribution of I-129 in the different waste packages present in the SFR repository.

Cs-135

The total amount of Cs-135 in produced waste up to 2004 was estimated in Almkvist and Gordon (2007). For the rest of the period, the correlation factor with Co-60 was used. This was also used for the distribution of Cs-135 in the different waste packages present in the SFR repository.

Pu-239/240

The mix of Pu-239/240 was used to estimate all transuranic nuclides relevant for the SAR-08 safety assessment. The method of estimating Pu-239/240 and the transuranic nuclides was based on measurements on the nuclear reactor water and water from the nuclear power plants fuel basins and from there calculating the correlated radionuclides using a method further described in Almkvist and Gordon (2007).

Correlation Factors

Where no other method was available, correlation factors were used to estimate the inventories of radionuclides for the whole repository lifetime. Actual measurements made on “key-nuclides”, Co-60, Cs-137 and Pu-239/240, and the radionuclide inventories were calculated from the correlation with these “key-nuclides” (Almkvist and Gordon 2007). The correlation factors that were used are described in “Correlation factors for C-14, Cl-36, Ni-59, Ni-63, Mo-93, Tc-99, I-129 and Cs-135 in operational waste for SFR 1” (Lindgren et al. 2007) and in “Low and Intermediate Level Waste in SFL 3-5: Reference Inventory” (SKBdoc 1416968).

Sensitivity to assessment results in previous safety assessments

In the above mentioned SAR-08 scenario “Alternative Inventory” the radionuclide inventory used was set at the by the authorities permitted activity limit, a factor seven larger than the radionuclide inventory used in the main scenario. The dose from the residual scenario was therefore a factor seven higher than the main scenario dose.

Alternative modelling in previous safety assessments

No alternative modelling was reported in SAFE and SAR-08.

Correlations used in previous safety assessment modelling

Except for the above discussed correlation factors used for estimating the inventories no correlations were reported in the previous safety assessments.

Identified limitations of the data used in previous safety assessment modelling

In the SAR-08 safety assessment Almkvist and Gordon (2007) identified the correlation factors used to quantify and estimate most of the radionuclides as the biggest uncertainty with the produced inventories. In Lindgren et al. (2007) this reasoning is expanded upon with several different examples: The correlation factors being based on measurements being done on several different material types, the measurements being done on reactor water when the reactor is still in operational mode, for instance. Also, they pointed out in the same report the measured correlation factors for a specific radionuclide can vary with several orders of magnitude.

Almkvist and Gordon (2007) wrote that the outcome of the SAR-08 safety assessment would show which radionuclides would need reduction of the uncertainties for the next safety assessment. Dose curves from the SAR-08 radionuclide transport showed that this focus should be set on C-14 primarily but also on I-129. For both of these radionuclides new estimation methods have been used in SR-PSU.

4.3 Supplier input on use of data in SR-PSU and previous safety assessments

The supplier considers the methods used in SAR-08 for estimating the inventory as sufficient for the requirements that were set at the time of that safety analysis. For the SR-PSU safety assessment the inventory has been updated with current prognoses for operational and decommissioning waste to the existing facility (SFR 1) and the planned extension (SFR 3). In addition, it was decided to include a radionuclide inventory considering the uncertainties in the estimates. Therefore the methodology presented below is used.

4.4 Sources of information and documentation of data qualification

Sources of information

The main source for this chapter is the Reference inventory report (SKB 2013, SKBdoc 1481419 (Mo-93)) which gives the average radionuclide inventories of each waste type, and discuss the uncertainties with measuring and estimating. The report also compiles the reported uncertainties, taken from various sources. All sources of information are given in Table 4-2.

A high inventory that would be valid if the considered uncertainties in the reference inventory are evaluated at a confidence level of 95% has been estimated (SKBdoc 1427105).

Table 4-2. Main sources of information used in data qualification.

Sources of information
ALARA Engineering, 2011. Mo-93, Tc-99 och Cs-135: Uppskattning av aktivitet i driftavfall från svenska LWR, Clab och Studsvik. SKBdoc 1393496, Svensk Kärnbränslehantering AB.
Anunti Å, Larsson H, Edelborg M, 2013. Decommissioning study of Forsmark NPP. SKB R-13-03, Svensk Kärnbränslehantering AB.
Carlsson J, 1994. PM Anläggningar 94/22 SFR1 – Kontroll av vissa ämnen i förvaret, SQ 662, Svensk Kärnbränslehantering AB.
Cronstrand P, 2005. Assessment of uncertainty to correlation factors. SKB R-05-76, Svensk Kärnbränslehantering AB.
Forsyth R, 1997. The SKB Spent Fuel Corrosion Programme. An evaluation of results from the experimental programme performed in the Studsvik Hot Cell Laboratory, SKB TR 97-25, Svensk Kärnbränslehantering AB.
Larsson H, Anunti Å, Edelborg M, 2013. Decommissioning study of Oskarshamn NPP. SKB R-13-04, Svensk Kärnbränslehantering AB.
Lindgren M, Petterson M, Wiborgh M, 2007. Correlation factors for C-14, Cl-36, Ni-59, Ni-63, Mo-93, Tc-99, I-129 and Cs-135. In operational waste for SFR 1. SKB R-07-05, Svensk Kärnbränslehantering AB.
SKB, 2013. Låg- och medelaktivt avfall i SFR. Referensinventarium för avfall 2013. SKB R-13-37, Svensk Kärnbränslehantering AB.
SKBdoc 1393443. Assessing uncertainty to correlation factors for ¹⁴ C, ³⁶ Cl, ⁵⁹ Ni, ⁶³ Ni, ⁹³ Mo, ⁹⁹ Tc, ¹²⁹ I, and ¹³⁵ Cs in operational waste for SFR 1. T-CKV 2007-030, Vattenfall Power Consultant AB.
SKBdoc 1427105. Radionuclide inventory for application of extension of the SFR repository – Treatment of uncertainties.
SKBdoc 1481419. Ny beräkning av Mo-93 i normkoli till PSU 2015-05.
Thierfeldt S, Deckert A, 1995. Radionuclides difficult to measure in waste packages. BS-Nr 9203-6, Brenk Systemplanung, Aachen, Germany.

Categorising data sets as qualified or supporting data

The qualified data sets are taken from the Reference inventory report (SKB 2013), except data sets for Mo-93 that are taken from SKBdoc 1481419, and the calculated radionuclide inventory considering uncertainties (SKBdoc 1427105), see Table 4-3.

Table 4-3. Qualified and supporting data sets.

Qualified data sets	Supporting data sets
SKB 2013, Appendix D Table D4-1	
SKB 2013, Appendix D Tables D5-2, D5-3 and D5-4	
SKBdoc 1427105, Table 3-9	
SKBdoc 1481419	

Excluded data previously considered as important

Since SAR-08 some radionuclide estimation methods have been updated to achieve lower uncertainties for important radionuclides:

For C-14 and Cl-36 a new method has been used (SKBdoc 1339709, 1393449), which correlates the activity from these two radionuclides with the power produced in the NPPs. Previously the activities were estimated using correlation factors which is described in Section 4.2 in this chapter. The Cl-36 activity originating from SNAB and SVAFO is still estimated using correlation factors though.

A new method has also been used for estimating Mo-93, Tc-99, I-129 and Cs-135 (SKBdoc 1341356). The new method estimates the mentioned radionuclide inventories from year 2007 and forward. Previously this was done with correlation factors also described in Section 4.2 in this chapter.

4.5 Conditions for which data are supplied

The radionuclide inventory supplied in this chapter is calculated from using a maximum from the 95 percentile value estimated for each radionuclide. Therefore it should be viewed as an extreme case which is highly unlikely to reflect the real SFR inventory. The supplied inventory should be used primarily to prove that the SFR repository can handle the inventory uncertainties without breaching the dose limit.

4.6 Conceptual and precision uncertainties

There are two types of uncertainties to mention here. The first regards the conceptual uncertainties that lay in the radionuclide estimation methods. These are too many to describe in detail here but are investigated further in the Reference inventory report (SKB 2013).

The largest conceptual uncertainties come from the use of correlation factors as an estimation method, radionuclides inventories estimated this way would have a numeric uncertainty up to a factor of 50, see Table 4-4.

Other radionuclides are estimated with methods such as for example correlation to generated power and fuel burn up. These methods produce results with less numerical uncertainties, see Figure 4-1.

The radionuclide inventory contained in the decommissioning waste is also estimated using correlation factors, called nuclide vectors, although these nuclide vectors differ from the ones used for estimating the operational waste. As these nuclide vectors differ both between NPPs as well as between different parts of each NPP they are far too many to give here. Examples of them can be found in Larsson et al. (2013) and Anunti et al. (2013). The uncertainties associated with the nuclide vectors have been summed together in SKB (2013) depending on where the waste packages are destined. See Table 4-5 for these decommissioning waste uncertainties.

The numerical uncertainties discussed above propagate to the calculations performed to estimate a high inventory (SKBdoc 1427105). When calculating a total uncertainty for a certain radionuclide in a waste type factors such as where the waste originated from and what and the type of waste package also become important. In Figure 4-1 the decision flow sheet to assess the uncertainty, is shown.

Table 4-4. Uncertainty factors for radionuclides correlated to key radionuclides with references (SKB 2013, Table D5-4).

Radionuclide	Correlates with ¹	Uncertainty factor	Reference
H-3	Co-60	50	Cronstrand 2005
Be-10	Co-60	50	Cronstrand 2005
Cl-36	Co-60	6	SKBdoc1393443
Fe-55	Co-60	5	Cronstrand 2005
Ni-59	Co-60	3	SKBdoc 1393443
Ni-63	Co-60	3	SKBdoc 1393443
Se-79	Cs-137	50	Cronstrand 2005
Sr-90	Cs-137	5	Cronstrand 2005
Zr-93	Co-60	50	Cronstrand 2005
Nb-93m	Co-60	20	Cronstrand 2005
Nb-94	Co-60	5	Cronstrand 2005
Tc-99	Co-60	5	SKBdoc 1393443
Pd-107	Cs-137	40	Cronstrand 2005
Pm-147	Cs-137	2	Forsyth 1997
Ag-108m	Co-60	50	Cronstrand 2005
Cd-113m	Cs-137	50	Cronstrand 2005
Sb-125	Co-60	10	Cronstrand 2005
Sn-126	Cs-137	40	Cronstrand 2005
I-129	Cs-137	5	SKBdoc 1393443
Ba-133	Co-60	2	Forsyth 1997
Cs-134	Cs-137	1.2	Forsyth 1997
Cs-135	Cs-137	3	SKBdoc 1393443
Sm-151	Cs-137	2	Forsyth 1997
Eu-152	Cs-137	2	Forsyth 1997
Eu-154	Cs-137	2	Forsyth 1997
Eu-155	Cs-137	2	Forsyth 1997
Ho-166m	Co-60	2	Forsyth 1997
U-232	Pu-239/240	2	Forsyth 1997
U-234	Pu-239/240	2	Forsyth 1997
U-235	Pu-239/240	2	Forsyth 1997
U-236	Pu-239/240	2	Forsyth 1997
Np-237	Pu-239/240	2	Forsyth 1997
Pu-238	Pu-239/240	2	Forsyth 1997
U-238	Pu-239/240	2	Forsyth 1997
Pu-241	Pu-239/240	2	Forsyth 1997
Am-241	Pu-239/240	10	Cronstrand 2005
Am-242m	Pu-239/240	2	Forsyth 1997
Pu-242	Pu-239/240	2	Forsyth 1997
Am-243	Pu-239/240	2	Forsyth 1997
Cm-243	Pu-239/240	2	Forsyth 1997
Cm-244	Pu-239/240	2	Forsyth 1997
Cm-245	Pu-239/240	2	Forsyth 1997
Cm-246	Pu-239/240	2	Forsyth 1997

¹Waste from SNAB and Svafo correlates actinides against Cs-137.

Table 4-5. Max uncertainty factors for decommissioning waste (SKB 2013, Table D5-2). Empty cells indicate no activity from that nuclide in the decommissioning waste in that particular rock vault.

Radionuclide	Max factor Silo	Max factor BRT	Max factor 1-2BMA	Max factor XBLA
H-3			7.19	3.17
Be-10			4.71	3.00
C-14	9.73	2.00	3.99	6.31
Cl-36	9.39	2.00	4.27	2.72
Ca-41			4.52	2.91
Fe-55	5.01	2.00	2.53	6.99
Co-60	5.16	2.00	2.20	7.81
Ni-59	4.18	2.00	2.32	7.37
Ni-63	4.20	2.00	2.31	7.42
Se-79	9.63		9.25	9.69
Sr-90	4.42	2.00	2.52	9.05
Zr-93	4.87	2.00	2.45	7.04
Nb-93m	4.65	2.00	2.10	7.65
Nb-94	4.59	2.00	2.17	7.38
Mo-93	4.68	2.00	2.17	6.23
Tc-99	8.07	2.00	3.21	9.17
Pd-107	9.79		2.00	8.16
Ag-108m	4.73	2.00	2.39	4.60
Cd-113m	9.78		3.30	9.06
In-115			3.00	
Sn-126	9.50	2.00	2.48	8.19
Sb-125	5.02	2.00	2.42	7.00
I-129	9.68		10.00	9.05
Cs-134	9.88		9.29	8.00
Cs-135	9.69		11.00	8.20
Cs-137	9.71		10.68	8.44
Ba-133	9.82		4.51	3.00
Pm-147	5.61	2.00	2.03	8.42
Sm-151	4.42	2.00	4.63	3.04
Eu-152	4.76	2.00	4.14	3.00
Eu-154	4.71	2.00	3.41	3.41
Eu-155	5.03	2.00	3.12	3.34
Ho-166m	4.85	2.00	5.27	3.00
U-232	5.19	2.00	2.01	8.47
U-235	4.33	2.00	2.35	7.68
U-236	4.98	2.00	1.98	8.36
Np-237	4.38	2.00	1.98	7.94
Pu-238	4.38	2.00	1.98	7.93
Pu-239	4.31	2.00	2.20	7.80
Pu-240	4.31	2.00	2.10	7.99
Pu-241	4.36	2.00	1.92	8.10
Pu-242	4.33	2.00	1.97	7.99
Am-241	4.37	2.00	2.03	7.96
Am-242m	4.21	2.00	1.96	7.84
Am-243	4.38	2.00	1.98	8.01
Cm-243	4.35	2.00	1.97	7.96
Cm-244	4.46	2.00	1.98	8.08
Cm-245	4.47	2.00	2.04	7.87
Cm-246	4.49	2.00	2.03	8.03

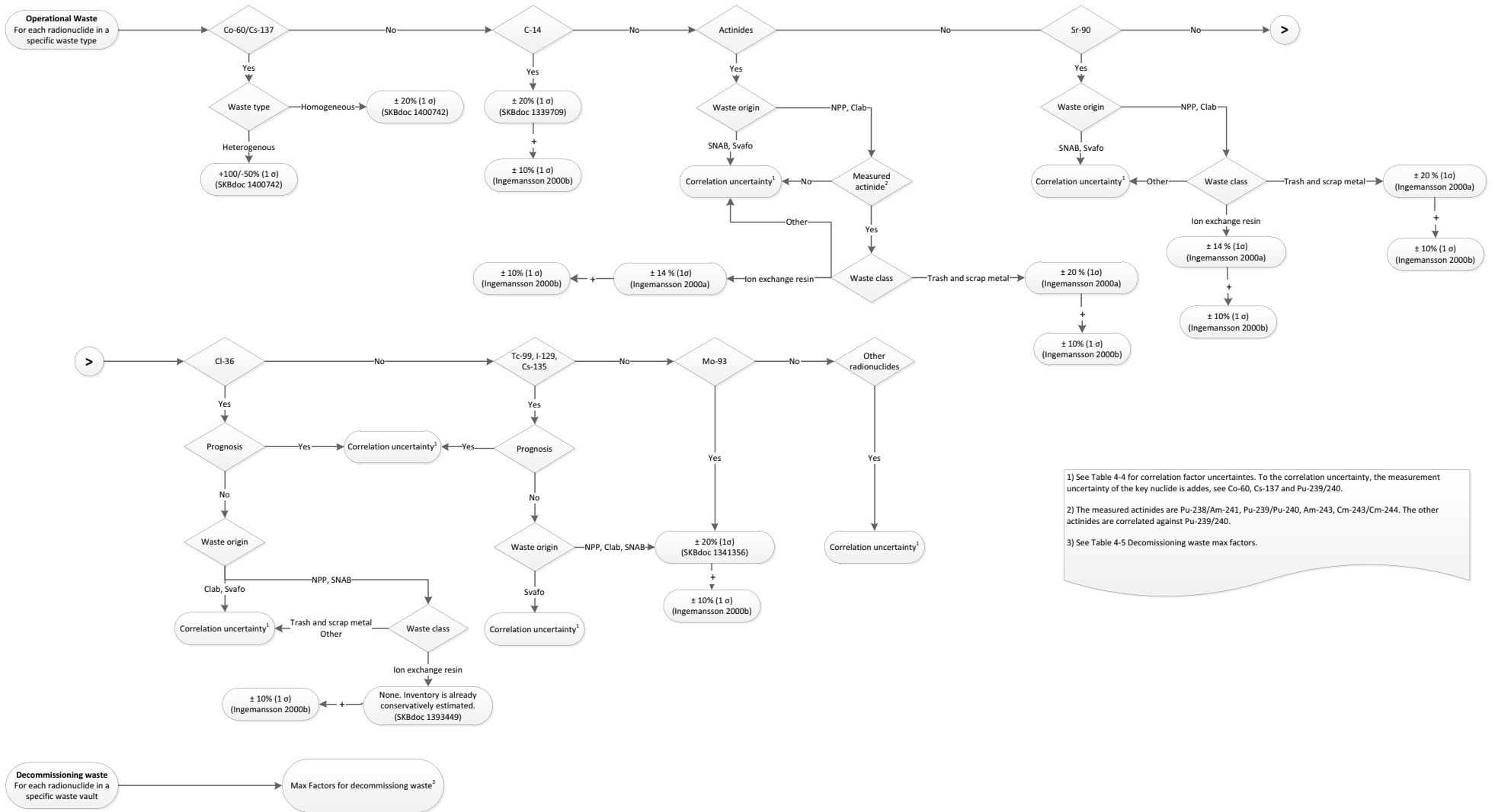


Figure 4-1. Radionuclide uncertainty flow sheet. NPP means the nuclear power plants. (SKBdoc 1427105).

Propagation of uncertainty from measurements to uncertainty factors

The measurement uncertainty of the nuclides Co-60, Cs-137 and Pu-239/240 are viewed as normally distributed when summed with other normally distributed uncertainties. The combined uncertainty factor is then calculated as in Equation 4-1.

$$k_z \frac{\Delta z}{z} \Big|_{95\%} = \sqrt{\left(k_x \frac{\Delta x}{x}\right)^2 / N + \left(k_y \frac{\Delta y}{y}\right)^2} \quad \text{Equation 4-1}$$

Where $k_x \frac{\Delta x}{x}$ and $k_y \frac{\Delta y}{y}$ = relative errors of two normally distributed random variables for a 95% confidence level.

N = the number of deposited packages of this particular waste type

$k_z \frac{\Delta z}{z} \Big|_{95\%}$ = sum of the relative errors of the two normally distributed random variables x and y .

The absolute error is then calculated using the reported mean value for the radionuclide times the total uncertainty calculated above. The sum of the mean value and the absolute error is used for the maximum inventory.

In case the measurement uncertainty is to be combined with a correlation uncertainty, the normal distribution of the measurement uncertainty is mapped on a log-normal distribution with the same $x_{50\%}$ (median) and $x_{95\%}$. A detailed description of this process is found in SKBdoc 1427105, Appendix B. The combined uncertainty is calculated as in Equation 4-2.

$$z + \Delta z \Big|_k = z \cdot e^{\sqrt{\left[\ln\left(1 + k \frac{\Delta x}{x} \Big|_{1\sigma} / \sqrt{N}\right)\right]^2 + \left[\ln\left(1 + k \frac{\Delta y}{y} \Big|_{1\sigma}\right)\right]^2}} \quad \text{Equation 4-2}$$

4.7 Spatial and temporal variability

Spatial variability of data

The spatial variability of the radionuclide inventory originates from the way the waste packages are packaged and conditioned. Much of these uncertainties are taken care of by using the waste acceptance criteria (SKB 2013), which among other things sets maximum allowed levels of metals and cellulose per waste type, and also makes sure that each waste package is conditioned according to requirements.

The uncertainty for the Co-60 and Cs-137 measurements has been estimated in SKBdoc 1400742 (unpublished document). The estimation of the uncertainty differs depending on if the waste in the package is assumed to be homogeneously or heterogeneously distributed.

Temporal variability of data

The main temporal process governing the radionuclide inventory is the decay of the radionuclides, further described in the **Waste process report**. The selected half lives for SR-PSU are presented and motivated in Chapter 3 in this report. As radionuclide decay is a very predictable process the variability is well reflected both when estimating the inventory and in the radionuclide transport calculations (**Radionuclide transport report**).

It is also worth mentioning that in the SR-PSU safety assessment the corrosion rates govern the release of radionuclides from the decommissioned Boiling water reactors (BWR) pressure vessels. The corrosion rates are presented and motivated in the Metallic corrosion chapter in this report.

4.8 Correlations

Identified correlations have been described previously in this chapter: Use of correlation factors and correlation to power generation when estimating some radionuclide inventories, described in Section 4.6.

4.9 Result of supplier's data qualification

The results given in Table 4-6 are reproduced from SKBdoc 1427105 where results on vault and package level are also given.

4.10 Judgements by the SR-PSU team

Sources of information

The SR-PSU team finds the sources of information used in Section 4.4 sufficient.

Conditions for which data is supplied

The SR-PSU team accepts the conditions for which data is supplied in Section 4.5.

Conceptual and precision uncertainties

The SR-PSU team accepts the methodology in Section 4.6 used to produce the maximum inventory and the conceptual uncertainties that are associated with it.

Spatial and temporal variability

The SR-PSU team finds the given variability in Section 4.7 to be handled in a satisfactory manner in this chapter.

Correlations

The SR-PSU team accepts the given correlations in Section 4.8.

Results of supplier's data qualification

The SR-PSU team finds the methodology presented in the this chapter to be sufficient for use in the high inventory calculation case CC20 in the radionuclide transport modelling.

4.11 Data recommended for use in SR-PSU modelling

The SR-PSU team agrees with the supplier regarding the handling of the uncertainties and recommends using the data given in Table 4-6. The inventory given in the column "High inventory" should be used in the less probable scenario with high radionuclide inventory calculation case CC20 and the inventory given in the column "Best estimate inventory" should be used for all other scenarios and calculation cases.

The best estimate radionuclide inventory, is calculated from the average radionuclide inventory in each waste type (SKB 2013, SKBdoc 1481419 (Mo-93)) and the number of packages of each waste type in the waste vaults given in the **Initial state report**. A high radionuclide inventory including uncertainties has been calculated from the best estimate inventory and uncertainties for different wastes, see Table 4-6.

Table 4-6. Best estimate radionuclide inventory and High radionuclide inventory at year 2075 (calculated from the best estimate inventory including uncertainties (95th percentile) (SKBdoc 1427105)).

Radionuclide	Best estimate inventory (Bq)	High inventory (Bq)	Ratio
H-3	3.52E+12	2.12E+13	6.04
Be-10	1.27E+06	6.38E+07	50.2
C-14 org*	9.22E+11	1.27E+12	1.38
C-14 inorg*	5.09E+12	7.00E+12	1.37
C-14 ind*	1.65E+10	4.26E+10	2.59
Cl-36	1.54E+09	5.62E+09	3.66
Ca-41	1.95E+10	7.08E+10	3.63
Fe-55	2.91E+12	1.59E+13	5.48
Co-60	1.55E+13	2.87E+13	1.85
Ni-59	1.02E+13	2.99E+13	2.95
Ni-63	8.06E+14	2.36E+15	2.93
Se-79	1.31E+09	6.56E+10	50.2
Sr-90	4.66E+12	7.16E+12	1.54
Zr-93	6.19E+09	1.26E+11	20.4
Nb-93m	2.36E+13	6.81E+13	2.88
Nb-94	1.91E+11	5.83E+11	3.05
Mo-93	2.92E+10	5.95E+10	2.03
Tc-99	6.33E+10	2.34E+11	3.71
Pd-107	2.89E+09	1.79E+10	6.19
Ag-108m	2.97E+11	6.44E+12	21.7
Cd-113m	1.06E+10	5.55E+11	52.2
In-115	3.13E+05	8.29E+05	2.65
Sn-126	2.61E+08	7.24E+09	27.7
Sb-125	1.32E+11	1.54E+12	11.6
I-129	1.17E+09	3.76E+09	3.20
Cs-134	2.20E+11	5.86E+11	2.66
Cs-135	5.67E+09	1.30E+10	2.30
Cs-137	7.06E+13	1.08E+14	1.53
Ba-133	8.31E+08	2.05E+09	2.47
Pm-147	3.59E+11	1.18E+12	3.28
Sm-151	6.00E+11	1.38E+12	2.29
Eu-152	1.52E+11	5.26E+11	3.47
Eu-154	5.58E+11	1.55E+12	2.78
Eu-155	1.01E+11	3.20E+11	3.17
Ho-166m	9.09E+09	1.98E+10	2.17
U-232	8.96E+05	2.22E+06	2.48
U-234	4.75E+07	1.14E+08	2.39
U-235	6.57E+08	1.82E+09	2.77
U-236	2.59E+07	6.25E+07	2.42
U-238	9.52E+08	2.09E+09	2.19
Np-237	5.75E+08	1.69E+09	2.94
Pu-238	1.32E+11	2.99E+11	2.27
Pu-239	2.80E+10	5.75E+10	2.06
Pu-240	3.87E+10	7.91E+10	2.04
Pu-241	5.23E+11	1.26E+12	2.42
Pu-242	2.03E+08	4.82E+08	2.38
Am-241	2.33E+13	2.82E+14	12.1
Am-242m	5.79E+08	1.37E+09	2.36
Am-243	2.57E+09	5.06E+09	1.97
Cm-243	3.25E+08	6.99E+08	2.15
Cm-244	2.19E+10	5.26E+10	2.40
Cm-245	2.84E+07	6.91E+07	2.44
Cm-246	8.58E+06	2.10E+07	2.45
Total	9.70E+14	2.95E+15	3.04

* C-14 has been divided into organic, inorganic and induced activity.

5 Metallic corrosion

This chapter deals with the corrosion rates used in the SR-PSU modelling activities. Large quantities of metals will be present in the SFR repository, mainly carbon steel, stainless steel, but aluminium and zinc as well. Carbon steel and stainless steel originates from various scrap metals, waste containers and reinforcement bars in concrete packaging and concrete constructions.

A number of parameters will affect the corrosion rate, especially metallurgical and environmental factors. Therefore, for the corrosion rate that will be used in the modelling the conditions chosen are of high importance. The period for aerobic corrosion will be followed by the period where the oxygen will be consumed and when the repository is oxygen-free the anaerobic corrosion will take place. From estimations of available metals and initial oxygen quantities trapped in the repository, it is assumed that all the available oxygen will be consumed rather shortly after the repository closes.

Corrosion of the metals in the repository will lead to property changes in both the metal packaging, reinforcement bars, metal waste (either non conditioned or stabilised in concrete). The anoxic corrosion with water will produce hydrogen gas which might cause volume changes as the pressure increases, leading to stresses generating cracks and causing changes to the waste hydrodynamic properties. Also, the generation of metal corrosion products, mainly oxides and hydroxides, is likely to affect the retention of radionuclides in the waste due to the normally high sorption capacity of hydroxides. These effects have to be considered in repository safety assessments.

Corrosion of metal waste will also govern the release of induced activity, for example from the BWR pressure vessels in the BRT vault.

A general description of the corrosion processes is found in the metal corrosion chapters in the **Waste process report**.

5.1 Modelling in SR-PSU

This section describes what data are expected from the supplier, and in what SR-PSU modelling activities the data are to be used.

Defining the data requested from the supplier:

- The corrosion rate of aluminium and zinc ($\mu\text{m}/\text{year}$).
- The corrosion rate of carbon steel ($\mu\text{m}/\text{year}$).
- The corrosion rate of stainless steel ($\mu\text{m}/\text{year}$).

The corrosion rates should reflect the conditions present in SFR repository, pre- and post closure of the repository, in terms of oxic and anoxic conditions.

SR-PSU modelling activities in which data will be used

The requested corrosion rates for carbon steel and stainless steel will be used in the redox-model due to the reducing capacity of Fe(II)-oxidation. Further, the corrosion rates will be used to quantify the theoretical gas generation in the SFR repository, and to evaluate the possible influence on the radionuclide release from the repository. The corrosion rates will also be used to determine the release of radionuclides from metal waste with induced activity, such as the BWR pressure vessels.

5.2 Experience from previous safety assessments

This section briefly summarises experience from previous safety assessments, especially the SAFE and SAR-08 safety assessments, which may be of direct consequence for the data qualification in this data report.

Modelling in previous safety assessments

In SAFE and SAR-08 safety assessments the corrosion rates were only used for gas formation calculations.

Conditions for which data were used in previous safety assessments

As the gas generating process was the focus in SAR-08, the following assumptions were used when modelling:

- The waste containing metals was completely saturated in water after the repository was sealed.
- Sufficient water was always available for the anoxic corrosion of the existing metals.
- Constant corrosion rates over time were assumed.
- No temperature influence was considered.
- Steel materials were considered of homogeneous composition and no difference between carbon and stainless steel rates was considered.
- The corrosion rate of zinc was assumed to be equal to the one of aluminium.
- Hyperalkaline conditions were assumed to prevail in all the repository system.
- Pitting corrosion was not considered to occur.

Sensitivity to assessment results in previous safety assessments

No sensitivity studies were performed in SAFE and SAR-08.

Alternative modelling in previous safety assessments

No alternative modelling was reported in SAFE and SAR-08.

Correlations used in previous safety assessment modelling

In the previous safety assessment modelling the corrosion rates was used for calculations of gas generation as well as in the discussion of reaching reducing conditions within the repository, due to oxygen consumption by the corrosion of metals.

Identified limitations of the data used in previous safety assessment modelling

In the metal corrosion chapters in the **Waste process report** the uncertainty of using corrosion rates from literature is discussed as these rates can span over more than four orders of magnitude depending on the type of material studied and the conditions imposed. The reason for this is explained with the methods used measuring metal corrosion rates in literature; in some cases the rates are obtained by measuring hydrogen generation, other cases by measuring metal loss, and sometimes by measuring the corrosion current. All of these methods have limitations due to assumptions in the stoichiometry of the processes involved, because of the non-stoichiometry of the surface film that forms on the metal-water interface, and because of other oxidation processes besides water reduction. A discussion on the adequacy of the different techniques for corrosion rate measurements is included in Kursten et al. (2003).

5.3 Supplier input on use of data in SR-PSU and previous safety assessments

Prior to supplying the corrosion rates there has been a literature survey, identifying corrosion rates from long term experimental work. The existing corrosion rate for aluminium and zinc of 1,000 $\mu\text{m}/\text{year}$ (Moreno et al. 2001) is suggested to be used in the future as well.

For steel the corrosion rates have been refined in terms of categorisation into carbon steel and stainless steel, since stainless steel is more corrosion resistant than carbon steel. The evolution of the repository environment will change, from oxic to anoxic and this will also affect the corrosion rates.

5.4 Sources of information and documentation of data qualification

Sources of information

The literature screening has used the work by Smart and Hoch (2010) as start. The supporting references in Table 5-2 are specific studies already listed in the exclusive report by Smart and Hoch (2010), see Table 5-1.

Categorising data sets as qualified or supporting data

As stated above, the main dataset is taken from Smart and Hoch (2010) which have compiled the data from the works given in the supporting data sets in Table 5-2.

Excluded data previously considered as important

Refined corrosion rates for steel, in terms of more specific use of different rates, are included for carbon steel and stainless steel. Therefore the corrosion rate of steel in the interval 0.1–10 $\mu\text{m}/\text{year}$ by Moreno et al. (2001) is excluded. This was the rates used in SAR-08.

Table 5-1. Main source of information used in data qualification.

Sources of information
Smart N R, Hoch A R, 2010. A survey of steel and zircaloy corrosion data for use in the SMOGG gas generation model. Report to the NDA RWMD. SA/ENV-0841, Issue 3, Serco, UK.

Table 5-2. Qualified and supporting data sets.

Qualified data sets	Supporting data sets
Smart and Hoch 2010	Blackwood et al. 2002 Smart et al. 2004 Kuron et al. 1985 Simpson and Weber 1988 Schenk 1988 Simpson et al. 1985 Treadaway et al. 1989 Mihara et al. 2002 Kritsky et al. 1987 Naish et al. 2001 Moreno et al. 2001

5.5 Conditions for which data are supplied

The same corrosion rate for aluminium and zinc will be used for the different stages identified for the SFR repository, for oxic as well as anoxic conditions. For stainless steel and carbon steel the rates are dependent of the pH, i.e. if the repository is alkaline or more neutral. Further, for stainless steel and carbon steel the presence of oxygen and the concentration of chloride are important as well.

5.6 Conceptual uncertainty

As previously mentioned the method used for determination of the corrosion rates are of high importance for the outcome. For the common methods used for corrosion rates determinations, a division into the categories instantaneous and integrated techniques can be done (Smart and Hoch 2010). Instantaneous techniques include electrochemical methods such as linear polarisation resistance, Tafel-slope extrapolation and passive current measurements, and the general similarity for these techniques are that they present a value for the corrosion rate at the time of measurement. Integrated techniques also includes dimensional change such as weight loss or hydrogen evolution and general for these techniques is that the total change over a period of time is used to derive the corrosion rates. Based on the difference in how the corrosion rates are derived, measurement from instantaneous techniques may give misleading high corrosion rates, especially in systems where a “steady state” corrosion rate is achieved after a long time.

Only the process general/uniform corrosion rates are included in the screening, the localised corrosion (pitting corrosion and intergranular attack) is excluded. The reason for excluding localised corrosion is made since it is unlikely that these processes contribute significantly to total metal loss or gas generation. However, localised corrosion may contribute in small areas but is really hard to distinguish to what extent.

The potential influence on corrosion of metals in the SFR repository by earth currents from the present Fenno-Skan cable has been investigated. The conclusion is that corrosion caused by earth currents is considerably slower than general corrosion of steel at repository conditions (SKBdoc 1434594).

5.7 Data uncertainty due to precision, bias, and representativity

The screening of the data selected is based on the conditions representative for the repository, meaning that corrosion rates determined at very low pH, for example pH 4, are excluded. Still, the corrosion rates under anoxic conditions for stainless steel are rather insensitive for pH adjustments in the interval 6.4 to 13 (Blackwood et al. 2002). Further, corrosion rates determined at high temperatures are excluded as well; the studies considered are those performed at ambient temperatures, 20–30°C.

Long term studies have shown that chloride concentration does not significantly affect the corrosion rate, under alkaline anaerobic conditions (Smart et al. 2004). For oxic and near neutral conditions the non-impact of the chloride concentration is not as clear. Some experiments (Kuron et al. 1985) have shown that the chloride concentration did not affect the corrosion rates while other results are more uncertain. The corrosion rates in Table 5-3 and Table 5-4 for non-alkaline, near neutral pH, oxic conditions are higher, taking this uncertainty into account.

Also, as motivated above, the suggested corrosion rates only correspond to general corrosion, where the various types of localised corrosions have been excluded.

5.8 Spatial and temporal variability

Spatial variability of data

One parameter that will vary between the different vaults in SFR is pH. In the Silo, BMA and BTF repositories a high pH (towards hyperalkaline) will be found. In the BLA repository the pH is assumed to follow the pH of the inflowing groundwater i.e. near neutral.

Temporal variability of data

The corrosion rate may decrease with increasing exposure time, due to the formation of oxide film. For experiments performed by Smart et al. (2004), higher initial corrosion rates lasting for several hundred hours were observed; they decline later towards a plateau, where the rates become steady. This reflects the expected conditions of the SFR repositories as the conditions there will be oxic during pre-closure time and a short time period after closing. As the available oxygen in the repositories is rapidly consumed and no new oxygen is able to enter, the corrosion rates will slow down.

In the vaults with an initial high pH of approximately 13.4 a decrease in pH to 12.5 may affect the corrosion rates but, the decrease in pH is an effect from the dissolution and washing out of KOH and NaOH. However, this decrease is disregarded since for stainless steel it is found that this pH drop does not effect the corrosion rate (Blackwood et al. 2002).

5.9 Correlations

This section supplies corrosion rates that will be used and included in gas formation calculations, oxygen consumption, and degree of corrosion of reinforcement bars i.e. the reducing capacity of the material within the waste and waste packaging as well as the transport of radionuclides from BWR.

5.10 Result of supplier's data qualification

The suggested corrosion rate for aluminium and zinc are the same as described in the SAR-08. The corrosion rates for steel are lower than the one previously used and are divided into carbon steel and stainless steel as well as for different conditions, see Table 5-3, Table 5-4 and Table 5-5.

Table 5-3. Corrosion rates for carbon steel.

Conditions within the repository	Corrosion rate ($\mu\text{m}/\text{year}$)	Reference
Alkaline oxic conditions	0.1	Blackwood et al. 2002
Alkaline anoxic conditions	0.05	Smart et al. 2004
Non-alkaline, near neutral pH, oxic	60	Kuron et al. 1985
Non-alkaline, near neutral pH, anoxic	2.8	Simpson and Weber 1988, Schenk 1988, Simpson et al. 1985

Table 5-4. Corrosion rates for stainless steel.

Conditions within the repository	Corrosion rate ($\mu\text{m}/\text{year}$)	Reference
Alkaline oxic conditions	0.02	Treadaway et al. 1989
Alkaline anoxic conditions	0.01	Mihara et al. 2002
Non-alkaline, near neutral pH, oxic	0.3	Kritsky et al. 1987
Non-alkaline, near neutral pH, anoxic	0.2	Naish et al. 2001

Table 5-5. Corrosion rates for Al and Zn.

Conditions within the repository	Corrosion rate ($\mu\text{m}/\text{year}$)	Reference
Alkaline anoxic conditions	1,000	Moreno et al. 2001

5.11 Judgements by the SR-PSU team

Sources of information

The SR-PSU team considers the references supplied in Section 5.4 valid for use in the SR-PSU assessment.

Conditions for which data is supplied

The conditions given in Section 5.5 describe the conditions in the SFR repository well according to the SR-PSU team.

Conceptual Uncertainty

The SR-PSU team agrees with the uncertainties given in Section 5.6.

Data uncertainty due to precision, bias, and representativity

The SR-PSU team agrees with the uncertainties given in Section 5.7.

Spatial and temporal variability

The SR-PSU team considers the given variabilities in Section 5.8 as sufficient and valid.

Correlations

The SR-PSU team agrees with the given correlations in Section 5.9 but adds that the supplied data will also be used to govern the release of radionuclides from the disposed BWR pressure vessels in the BRT vault.

Results of supplier's data qualification

The SR-PSU team agrees with the data delivered in Section 5.10.

5.12 Data recommended for use in SR-PSU modelling

The recommended data are presented in Table 5-3, Table 5-4 and Table 5-5.

6 Bitumen swelling pressure

The Silo and BMA vaults of the SFR 1 contain hygroscopic waste (ion exchange resins and evaporator salts) solidified in bitumen. Hygroscopic waste can cause swelling of the waste packages. The resulting pressure build-up can in turn affect the structural integrity of repository barriers. Providing expansion volume (void) around bituminised waste is an approach to reduce the swelling pressure around certain waste packages. Knowledge of the swelling pressure as a function of waste composition and expansion volume is important for a detailed structural mechanics analysis of the barriers in different waste storage configurations.

6.1 Modelling in SR-PSU

This section describes what data are expected from the supplier, and in what SR-PSU modelling activities the data are to be used.

Defining the data requested from the supplier

- The data required from the supplier are the swelling pressures as function of expansion volume for the waste types B05, B06, F05, F17, and F18. For each waste type, data is to be supplied for a reference waste package composition, according to Almkvist and Gordon (2007), as well as a waste package representing a worst case composition with respect to swelling pressure. The worst case composition for each waste type is to be reported and motivated.

SR-PSU modelling activities in which data will be used

The swelling pressures are used in a modelling activity to assess the possible impact of the bitumen swelling on the surrounding structures and barriers in the Silo and the 1BMA vaults. The modelling is performed in Comsol Multiphysics and is further described in the bitumen swelling report (von Schenck and Bultmark 2014).

6.2 Experience from previous safety assessments

This section briefly summarises experience from previous safety assessments, especially the SAFE and SAR-08 safety assessments, which may be of direct consequence for the data qualification in this data report.

Modelling in previous safety assessments

In SAR-08, the assessment of the risks associated with the swelling of bituminised waste was based on calculations of the maximum theoretical swelling volume, based on the swelling factor of the embedded waste (i.e. the ratio of resin volume after and before swelling). If the maximum swelling volume exceeded the available void the barriers could be affected.

In the previous assessment only the question of the total volume increase of the waste due to swelling was addressed (Pettersson and Elert 2001). The theoretical maximum volume increase due to water uptake of ion exchange and evaporate concentrates embedded in the waste was calculated for the bituminous waste types in SFR. The calculations were based on a maximum volume increase of a factor of 2 for ion-exchange resins (Nilsson et al. 1988) and a factor of 3.5 for evaporator concentrates containing NaNO_3 . The latter value is the volume increase when dry NaNO_3 is dissolved at 25°C and a saturated solution of sodium nitrate is formed (Pettersson and Elert 2001).

The volume of the various waste constituents was estimated using the densities of the materials given in Table 6-1.

Table 6-1. Material properties of bitumen used in Petterson and Elert (2001).

Material	Density (kg/m ³)	Range (kg/m ³)	Reference
Bitumen	1,030	–	Riggare and Johansson 2001
Ion-exchange resin (dry)	1,400	1,140–1,520 1,230–1,500	Nilsson et al. 1988 Berntsson 1992
Evaporator concentrates	2,680	–	Weast 1985

Conditions for which data were used in previous safety assessments

The available void space was assumed to consist of the void volume in the waste packages, between 10% and 20% of the total package volume. For the steel drums stored in the silo there is an additional void volume in the form of a metal box inserted in the middle of a plate with four drums.

Sensitivity to assessment results in previous safety assessments

The swelling factor was estimated from experimental results that show a large degree of variation. The uncertainty in swelling factor was discussed, but no full sensitivity analysis was performed for all variables (densities, waste content, swelling factors).

The effect of variations in waste content between different waste packages from the Barsebäck plant was studied. It was concluded that variation in waste mixing ratio had a large effect on maximum volume increase, particularly for the waste from Barsebäck produced before 1993.

The previous data only concerned the maximum theoretical swelling of the waste from water uptake without consideration of the effects of the bitumen matrix, the package, the metal box and surrounding barriers. No estimates were made of the pressures that could be developed as a result of the swelling. Furthermore, no assessment was made of the effect of radiolysis, microbial degradation and ageing upon water uptake.

Alternative modelling in previous safety assessments

No alternative modelling was reported in SAFE or SAR-08.

Correlations used in previous safety assessment modelling

No reported correlations were used in SAFE or SAR-08.

Identified limitations of the data used in previous safety assessment modelling

In its audit of the final safety reports for SFR (Dverstorp and Sundström 2003) the regulatory authorities pointed out that SKB's position on grouting around bitumen waste was not clearly stated. The authorities noted that grouting may have an important effect on the consequences of swelling of bitumen waste. The authorities concluded that the analysis of swelling was based on theoretical values and not results from tests from representative samples. Furthermore, they requested a better description of the coupling between various processes leading to degradation of waste and barriers, including the swelling of bitumen.

6.3 Supplier input on use of data in SR-PSU and previous safety assessments

Given the information in the section above and the need to assess the possible impact of swelling of bituminised waste it is recognised that there is a need for more experimental data on the potential swelling pressure, for use in the structural mechanics analysis. As all the processes that govern the bitumen swelling are not known or fully understood, experimental data from swelling tests performed under conditions similar to those of a closed SFR facility are preferred.

Given these uncertainties regarding the bitumen swelling, the supplier also recommends that further work should be done on the subject after the SR-PSU safety assessment. The suggestion is to consider a test program for swelling of conditioned bitumen within the next SKB RD&D programme..

6.4 Sources of information and documentation of data qualification

Bitumen has been used for solidification of ion-exchange resins only in a few countries, mainly Sweden and Finland. The data sources for water uptake and swelling of bituminised ion-exchange resins originate mainly from research performed in the 1980s and 1990s in Sweden, Finland, Norway and Denmark.

The experiments generating data can be divided into the following categories:

- Swelling of unconfined ion-exchange resins.
- Swelling of confined ion-exchange resins.
- Swelling and water uptake of bituminised ion-exchange resins in an unconfined space.
- Swelling and water uptake of bituminised ion-exchange resins in a confined space.

Furthermore, some relevant data from studies with bituminised evaporator concentrates have been included.

Swelling of unconfined and confined ion-exchange resins

The ion-exchange resins consist of polymer chains that are made stable by side chains (cross-linking) usually formed by adding divinylbenzene during the polymerisation. Different functional groups are added to the polymer structure in order to obtain the specific ion exchange properties of the resins. The cross-linking of the polymer chains reduces the swelling pressure of the resin, but will also reduce the exchange capacity.

Tests have been performed on swelling of samples of ion-exchange resins extracted from bituminised waste from Barsebäck. The initial water content of the resins was between 3% and 12%, The observed swelling factor for the resin after addition of water was between 1.8 and 2.4. The type of resin is not given. (Asea-Atom 1985).

Density measurements of cationic bead resin IR120 gave a swelling factor (i.e. the ratio of resin volume after and before swelling) for the resin of 2.43 (Brodersen et al. 1983). Experiments showed a faster and larger swelling in the case the resin was crushed. Tests on powdered resin showed a larger swelling than bead resin.

Aittola et al. (1982) studied the swelling properties of different ion-exchange materials. Swelling experiments were performed studying the effect of various types of heat treatment and treatment with Na_2SO_4 . The experiments were performed on unused granular anionic and cationic resins, spent powdered resin and spent mixed bed resin (premade mixtures of cationic and anionic resins). The granular anionic resin was degraded by heat treatment at temperatures higher than 140°C for a day resulting in a considerably reduced swelling. The swelling capacity of the cationic resin remained unchanged even after a long time treatment at 140°C (swelling factor 2.5–2.6). The experiments with the mixed bed resins indicated that the swelling behaviour of the cationic component was unaffected even after longer drying periods at 180°C . The powdered resin showed a higher swelling than the granular, explained to be caused by absorption of additional water between the resin grains. The powdered resins showed a somewhat reduced swelling capacity after long-term treatment at 180°C . Treatment with Na_2SO_4 caused some reduction of the swelling effect on the powdered resins, while the swelling of the granular resins was unaffected.

Valkiainen and Vuorinen (1985) studied the effect of heat treatment on the swelling properties of cationic and anionic resins. They came to the conclusions that thermal treatment did not affect the swelling properties of cationic resins. For anionic resins treatment at a temperature of at least 105°C reduced the swelling after a treatment lasting for 10 hours. At a temperature of at least 140°C the swelling tendency was strongly reduced after 3 hours. In this case the remaining swelling was 18%.

For the cationic resins a swelling of 155% was measured. The swelling for a mixture of heat treated anionic and cationic resins in volume ratio 2:1 was estimated to be 71%. The effect of irradiation on the swelling was studied by irradiating samples with a dose of 1.76 MGy and heat treating samples of resins. For cationic resins the swelling capacity increased by 8% after irradiation, whereas no effect was found for the anionic resins. Test performed on spent active resins (volume ratio anionic-cationic 2.3:1) showed a swelling capacity of 29% after heat treatment, which was lower than the estimated swelling capacity for the fresh resin.

Valkiainen and Vuorinen (1985) have also studied the swelling pressure of ion-exchange resins mixed with glass powder as well as that of bituminised resins. The measurements were performed in an oedometer for controlling volume and pressure. The ion-exchange resins were mixed with glass powder in a weight ratio 1:1.12 for the purpose of filling the void spaces of the resin particles and thus preventing the deformation of the resin grains. The ion-exchange resins (ARC351 cationic and ARA360 anionic resin in a volume ratio 1:2) were heat treated for 16 hours at 140°C before mixing with the glass powder. Experiments were also performed with spent, inactive granular mixed bed resins from Forsmark. When the samples were placed in the oedometer a preload pressure between 0.2 and 3 MPa was applied. After adding water to the resins the pressure increased during a couple of tens of minutes. After an equilibration period of a few days, during which a slow increase or decrease in pressure was observed, the available volume for swelling was increased in steps. The results of the tests are shown in Table 6-2.

The results of work on bitumen in a Nordic Study were compiled in Snellman and Valkiainen (1985) and Snellman et al. (1986). The report refers to Finnish and Swedish measurements of swelling pressures. The constrained swelling was simulated by mixing the ion-exchange resins with quartz powder, glass powder or glass beads. This approach does not completely eliminate the possibility of some volume increase. The results reported in Snellman and Valkiainen (1985) and Snellman et al. (1986) are summarised in Table 6-3. The first experiment was performed in Sweden (Jacobsson 1983, cited in Snellman and Valkiainen 1985), the second in Finland by Valkiainen and Vuorinen (1985).

Table 6-2. Measured swelling pressure of ion-exchange resins at different volume expansions (Valkiainen and Vuorinen 1985).

Sample	Test	Preload MPa	Swelling pressure (MPa)				Water content
			$\Delta V=0\%$	$\Delta V=10\%$	$\Delta V=20\%$	$\Delta V=30\%$	
Fresh resin	A1	0.5	5.8	0.60	0.15	–	59.3
	A2	1	5.9	0.65	0.15	–	49.2
	A3	1+0.2*	7.1	0.70	0.30	–	49.4
	A4	3	11.5	2.40	0.75	0.22	62.0
Spent resin	B1	0.5	3.3	0.22	0.12	–	52.7
	B2	1	4.0	0.26	0.16	–	47.6
	B3	1+0.2*	4.2	0.33	0.17	–	51.8
	B4	3	4.5	0.60	0.15	–	67.0
Cationic resin	C1**	3	26.8	15.4	10	8.5***	118

* Preloaded in compaction to 1 MPa, in the beginning of the test 0.2 MPa.

** Test C1 performed without glass beads as a mixing agent.

*** $\Delta V=25\%$

Table 6-3. Measured swelling pressure of ion-exchange resins at different volume expansions from Snellman and Valkiainen (1985) and Snellman et al. (1986).

Sample	Drying	Swelling pressure (MPa)		
		$\Delta V=0\%$	$\Delta V=10\%$	$\Delta V=20\%$
Anionic and cationic resin ARA 366 40%+ARC 351 60%, quartz powder 1:4	24 h, 105°C	31	2.5	0.3
Anionic and cationic resin ARA 366 67%+ARC 351 33%, quartz powder 1:09	16 h, 140°C	7.1	0.7	0.3

The Swedish Cement and Concrete Research Institute (CBI) has performed investigations of the swelling properties of radioactive ion-exchange resins from Forsmark (Ericsson and Klingstedt 1987). The swelling volume and pressure was measured in an apparatus consisting of a brass cylinder with a movable piston. Water was injected in the bottom of the cylinder. The pressure of the piston was kept at a constant value and the movement of the piston recorded. Tests were performed on powdered resin from the waste treatment plant before and after solidification in bitumen. The solidified samples were washed in xylene to remove the bitumen, rinsed with dichloromethane to remove the xylene and finally dried at 60°C. No specification is given on the type of resin or how the resin was treated before solidification. The samples extracted from the bituminised product had a water content of around 7%. The swelling of these samples resulted in a pressure of 15–17 MPa if no volume expansion was allowed. In the tests with a constant pressure of 2.5 MPa, the swelling of the resin was between 11 and 15% and at a constant pressure of 0.2 MPa, the swelling was 33–34%. If the volume expansion of the resin is converted to an equivalent swelling of the bituminised product, it would for a waste loading of 50% correspond to a volume expansion of 5–7% at a pressure of 2.5 MPa and a volume expansion of 15% at a pressure of 0.2 MPa. Except for the pressures observed at confined swelling this is within the range of the data reported by Valkiainen and Vuorinen (1985).

In Nilsson et al. (1988) the swelling behaviour of anionic and cationic ion-exchange resins was studied and a model was set up for the water uptake and the swelling pressures that the swelling causes. Experiments were performed with seven different resins in different chemical forms. For two of the resins the effect of heat treatment was also studied. For each resin the water uptake, density and volume was measured at different water activities. The internal swelling pressure was calculated for the resins. The swelling was measured at a temperature of 25°C, but estimates were also made for 0°C. The data provided in Nilsson et al. (1988) can be used to make estimates of the external swelling pressure exerted on waste packages and barriers at different degrees of volume expansion. However, it does not consider water that is present in pores and cracks of the bitumen matrix.

In a study by Matsuda et al. (1992) the swelling pressure developed in confined swelling of ion-exchange resins was measured. The study was focussed on solidification in cement, but as the experiments were performed on ion-exchange resin they are also applicable to bituminised waste. Masudo obtained the confined conditions by pelletising the resin under high pressure. Thereafter, the pressure was relieved and water was injected through a small opening in the experimental apparatus. The study included various types of cationic resins with different functional groups, degree of cross-linkage and different exchange capacity (a reduction in exchange capacity was obtained by thermal treatment). For a dry resin in H⁺-form with 8% cross-linkage and an exchange capacity of 4.8 meq/g, the pressure for confined swelling was measured to 51 MPa. For resin with Na⁺-form the confined swelling pressure was around 30 MPa. A reduction of the exchange capacity had a more than proportional effect on the confined swelling pressure. An increased initial water content of the resin had a strong reducing effect on the swelling pressure, since the elastic forces from the cross-linkage of the resins become more important for a resin that has taken up water and swelled. The experiment showed that for a resin with 8% cross-linkage, the swelling pressure was reduced by half at an initial water content of 30% by weight. A model based on osmosis was also developed that could simulate the experimental results based on ion-exchange capacity, functional group, ionic form, cross-linkage and initial water content.

Swelling and water uptake of bituminised ion-exchange resins in an unconfined space

In a Nordic study performed during 1978–1982 various types of mixtures of bitumen and ion-exchange resins were immersed in water for a period up to 1,500 days (Aittola and Kleveland 1982). A selection of samples was externally irradiated with Co-60 (0.1 to 1 MGy). The swelling was compared to the theoretical swelling calculated assuming that the ion-exchange resin had a swelling factor of 2.5. This was based on other investigations that had shown a swelling factor for the resin between 2.4 and 3.1 depending on the temperature and duration of the drying. The measured swelling of the samples ranged from about 10% to 100% of the theoretical maximum. The samples with irradiated resins had a faster water uptake and reached a swelling of 200% of the approximated theoretical maximum. However, the swelling factor of the irradiated resins was not measured. The reason for the increased water uptake in the irradiated samples was not discussed in the study. The water uptake and hence the swelling was generally found to be proportional to the square root of time, indicating that the water uptake is a diffusion controlled process. The results presented by Aittola and Kleveland (1982) correspond to a swelling rate from tenths of millimetres per year to a few mm per year.

The effect of temperature and waste-bitumen ratio on water uptake and swelling of ion-exchange resins solidified in bitumen (Mexphalt 40/50) immersed in water for up to 1 month was studied by Brodén and Wingefors (1992). For a matrix with 40% resin by weight almost no water uptake or swelling was observed at temperatures between 3°C and 30°C. At higher resin fractions (50%, 60% and 70%), the water uptake increased with increasing resin content, but no significant difference between a temperature of 20°C and 30°C was noticed. However, at 3°C the water uptake was considerably higher, with a weight increase of 24% after 20 days with a 50% waste loading, a weight increase of 127% after 28 days with a 60% waste loading and 149% weight increase after 27 days with a waste loading of 70%. At waste loadings of 60% or higher, the water uptake was so fast that a diffusion controlled mechanism could be excluded. The weight increase was higher than could be explained from measurements of water uptake by ion-exchange resins (Nilsson et al. 1988), indicating the formation of water-filled cracks and pores in the bitumen matrix.

Long-term water uptake experiments performed on small samples of bituminised mixed anionic and cationic resins have shown a weight increase after 5,000 days (nearly 14 years) of between 50% and 60% due to water uptake (Aalto and Valkiainen 1997). The weight increase did not show any signs of diminishing.

The behaviour of bituminised ion-exchange resins under repository conditions has been evaluated (Aalto and Valkiainen 2004). In this study water uptake and leaching were measured in samples placed in artificial concrete water at a temperature between 5 and 8°C. The low temperature was chosen since earlier studies had found that the rate of water uptake and swelling at lower temperatures was higher than at room temperature (Brodén and Wingefors 1992). The samples consisted of a 50:50 mixture of bitumen and dried ion-exchange resins cast at a temperature of 140°C. The samples had absorbed between 8% and 18% water after 1,250 days. The samples with the higher water uptake had been stored for 6 months before the experiment and it was estimated that they absorbed 5% water from the air during the storage. Microscopic examination of the wetting front showed that the range of the front was proportional to the square root of time for about 500 days, after which a decline in the front advancement was observed. The range of the front was around 11 mm in about 1,000 days.

Swelling and water uptake of bituminised ion-exchange resins in a confined space

Very few studies have been found on the swelling of bituminised ion-exchange resins in a confined space. Valkiainen and Vuorinen (1985, 1989) report experiments with bituminised resins performed on samples from a test drum with inactive resin from Olkiluoto Power Plant. Four samples were taken at different vertical positions in the drum and the swelling due to water uptake at constant pressure was measured. Initially a constant preload of 1 MPa was applied and the volume changes were monitored. During the course of the experiments the preloading was changed. The results corrected for escape of bitumen in the oedometer are published in Valkiainen and Vuorinen (1989). The samples taken from the middle and the top of the drum showed only a small volume increase (initially less than 5% and decreasing with time). After 200 days the preload was reduced to 0.5 MPa, which resulted in a small volume increase (less than 2%). The behavior was quite different for the sample from the bottom of the drum. In this case the volume increase with the initial preload of 1 MPa resulted in a swelling of 30% after 400 days. At that time the swelling was still increasing, but after the loading increased to 2 MPa, the swelling reduced to 26%. The examination of the resins in the samples showed that due to separation, the bottom sample only contained grains of cationic resin, while the upper two samples mainly contained grains of anionic resin. Also the resin content was higher in the bottom part of the drum (58%) compared to that in the middle and top of the drum (43–45%).

Swelling of evaporator concentrates

Bitumen is commonly used for stabilisation of evaporator concentrates. The swelling behaviour of bituminised evaporator concentrates has been extensively studied in Denmark, France, United Kingdom, Belgium and Germany. Although the processes for water uptake is similar to that of ion-exchange resins, there is a major difference in that the salts giving rise to osmotic pressure can leach out of the waste.

The osmosis-induced swelling, water uptake, pressure increase and NaNO₃ leaching of small cylindrical samples of Eurobitum (diameter 38 mm, height 10 mm) have been studied under constant total stress conditions and nearly constant volume conditions (Valcke et al. 2010, Mariën et al. 2013). The studied waste had a matrix of hard (blown and oxidised) bitumen (Mexphalte R85/40) with a waste loading of 40% out of which about 30% is NaNO₃. The theoretical osmotic pressure of a saturated NaNO₃-solution is 42.8 MPa. After four years of testing of water uptake under nearly confined conditions, pressures up to 20 MPa have been measured. Only the outer 1–2 mm of the sample was found to be hydrated and only about 10–20% of the initial content of NaNO₃ was released. The measurements under a constant total stress of 2.2 MPa resulted in a swelling after 900 days of around 8%. Higher total stress did not result in significantly smaller swelling. A counter pressure of 3.3 MPa gave around 10% swelling after 900 days and pressure of 4.4 MPa gave 7% swelling after 900 days and 16% swelling after 1,500 days. Examination of the samples with scanning electron microscopy after the tests showed that the high pressure recompresses the leached layer and that a low-permeable layer of recompressed bitumen was formed at the surface of the sample.

A coupled chemical-hydromechanical model has been set up (Mokni et al. 2011). A model prediction of the evolution of the osmosis-induced pressure in the nearly confined tests showed that the pressure would reach a maximal value of about 20 MPa after about 5.5 years, after which the pressure would start to decrease. After about 27 years, the pressure would have decreased to a value of ~2 MPa.

Data available

Limited data have been found for swelling pressures induced by bituminised ion-exchange resins. A number of studies have been performed on the confined swelling of samples containing ion-exchange resins only. These studies indicate very high swelling pressures, in the order of 30–60 MPa, for a completely confined ion-exchange resin. Thermal treatment of the anionic resins results in a reduced swelling, due to a reduction in ion-exchange capacity. Both experimental and theoretical studies indicate that the swelling pressure is drastically reduced if the ion-exchange resins are allowed to swell to a certain degree before being confined.

Presented below is a summary of experimental data of swelling pressure on waste with mixed anionic and cationic resins. Furthermore, theoretical calculations have been performed of the swelling based on the model and data for ion-exchange resins from Matsuda et al. (1992) and Nilsson et al. (1988).

Summary of experimental results

In Figure 6-1 a summary is presented of the available experimental results for mixed resins. It contains both experiments performed in Sweden and Finland with ion-exchange resins mixed with glass powder and as well as the Finnish experiments with samples from bituminised mixed anionic and cationic resins.

The measurements on bituminised waste indicate lower swelling from samples from the top and the middle of the waste drum (black squares) as compared to the swelling of resins with glass. The samples from the bottom of the drum (black diamonds) had a high swelling also at high pressure, which was explained as a result of the settling of the cationic resin at the bottom of the drum.

Theoretical approach based on experiments with ion-exchange resins

Using the model and data from Nilsson et al. (1988) and the model and data from Matsuda et al. (1992), the swelling pressure at different degrees of volume expansion has been calculated for various ion-exchange resins and waste loadings. Finally, calculations have been performed for conditions judged to be representative for the various bitumen waste types in SFR.

Figure 6-2 shows the swelling pressure as a function of the relative volume increase of the resin calculated using the model and data from Matsuda et al. (1992). Curves are given for cationic resins with different exchange capacity. The decrease in capacity was obtained by heating the resins at temperatures between 200 and 300°C. The figure shows that a rather drastic reduction of the exchange capacity is needed in order to reduce the swelling pressure.

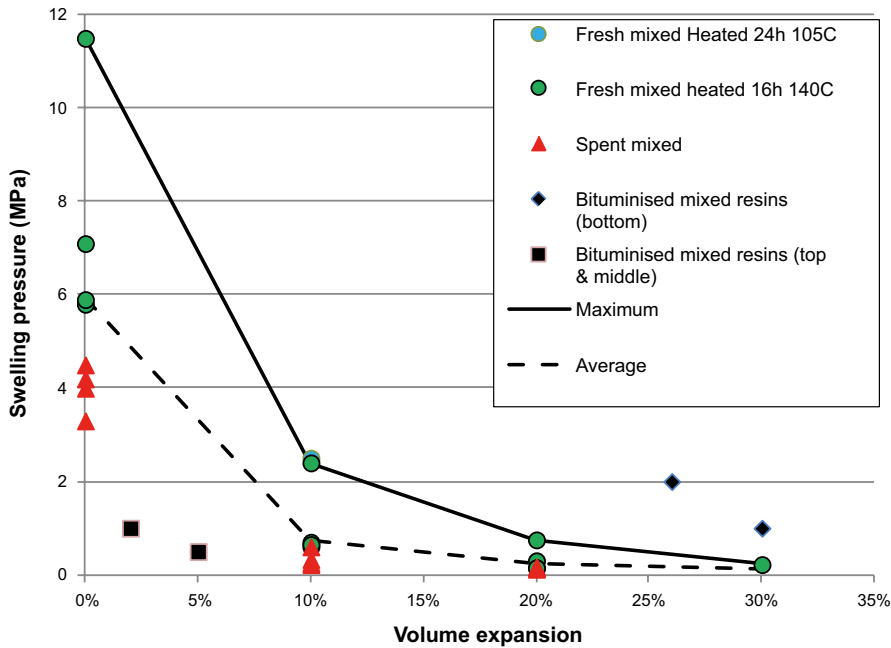


Figure 6-1. Swelling pressure as function of relative increase in volume of waste for mixed cationic and anionic resins including lines for maximum and average values. Data from Valkiainen and Vuorinen (1985, 1989).

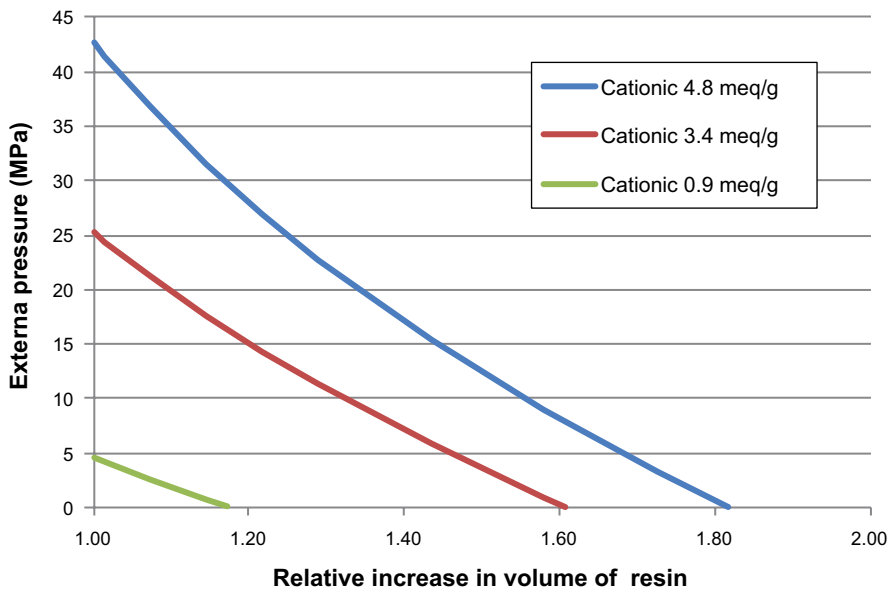


Figure 6-2. Swelling pressure as function of relative increase in volume of resin for cationic resins with different exchange capacity. Model and data from Matsuda et al. (1992).

In Figure 6-3 swelling pressures calculated according to the results of Matsuda et al. (1992) for different degrees of cross-linkage are presented together with results for the resins studied by Nilsson et al. (1988). Included are also results for the cationic resin ARC 351 heat treated for 1 hour at 150°C. The external pressure is very similar to that of the untreated resins, possibly due to the relative short treatment time. Figure 6-4 shows that water uptake in anionic resins results in a lower external pressure compared to that of the cationic resins, but also in this case, the effect of the heat treatment is small. However, there is an uncertainty in the calculation of the external pressure for the heat treated resins as the resin density is also changed.

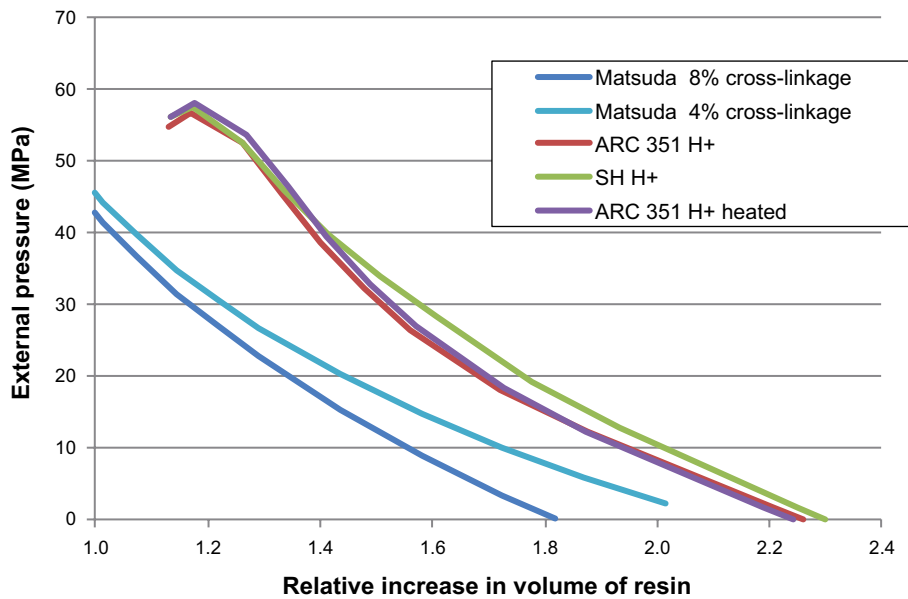


Figure 6-3. Swelling pressure as function of relative increase in volume of resin for cationic resins. Model and data from Matsuda et al. (1992) and calculated values based on model and data from Nilsson et al. (1998) for cationic resins (granulate ARC and powdered SH).

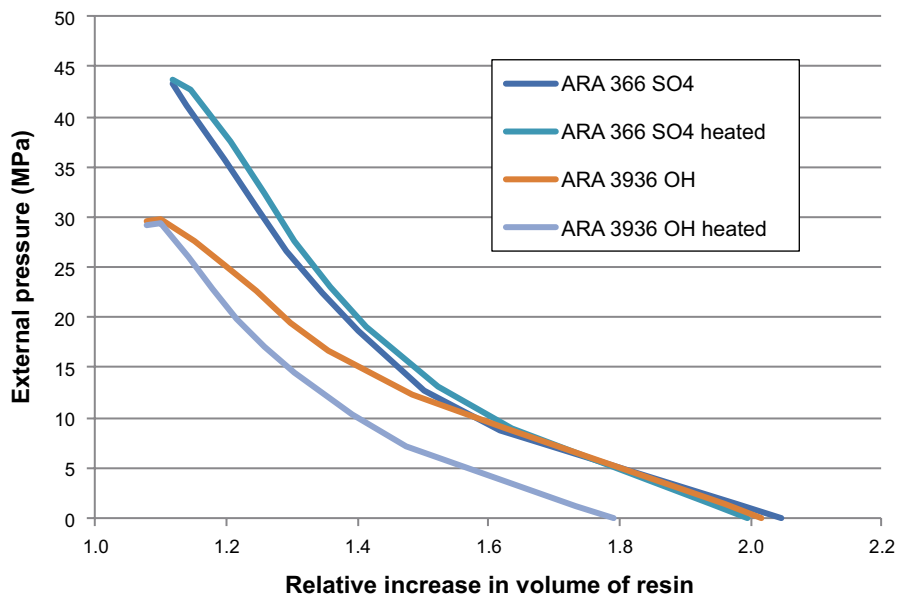


Figure 6-4. Swelling pressure as function of relative increase in volume of resin for anionic resins. Calculated values based on the model and data from Nilsson et al. (1988) for anionic resins (granulate ARC 366 and ARA 3936).

The results from the tests with ion-exchange resins have been extrapolated to waste packages taking into consideration the loading of resin in the bitumen matrix, see Table 6-4. No other effects such as elastic properties of the bitumen matrix have been taken into account. The properties of normal packages have been used. It is assumed that 35% of the resins are in cationic form (ARC 351 H⁺) and 65% in anionic form (ARA 9396 OH⁻ heat treated). When estimating the pressure of the mix of resins it is assumed that the water activity of the two types of resins is equal. The results of calculations are presented in Figure 6-5.

Table 6-4. Waste types placed in BMA and Silo parts of the SFR.

Waste type	Waste loading	Type of waste	Comment
B05, B06	25%	Powdered and ground bead resin. Anionic and cationic	Treated with Na ₂ SO ₄
F18	38%	Powdered resin (65% anionic 35% cationic) Bead resin (50% anionic 50% cationic). Filter aid.	Heat treated 150°C 15 hours.
F17	48%	Powdered resin (65–80% anionic and 20–35% cationic) Bead resin (50% anionic 50% cationic).	Heat treated 150°C 15 hours. May include up to 40% evaporator concentrates
F05	58%	Powdered resin (65–80% anionic and 20–35% cationic) Bead resin (50% anionic 50% cationic).	Heat treated 150°C 15 hours. Category F05:2 for shorter period.

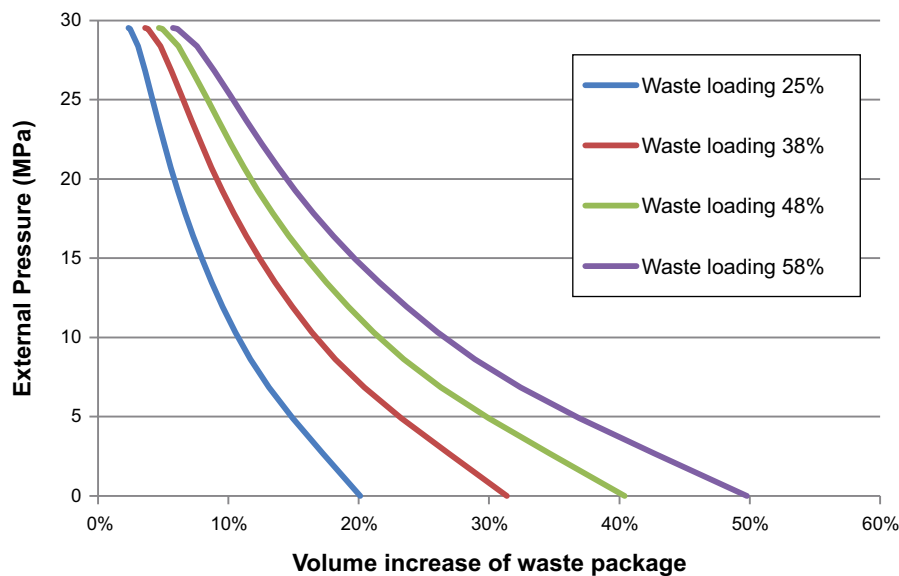


Figure 6-5. Estimated external pressure as a function of volume increase for different waste loadings corresponding to bituminised waste in Silo and BMA.

The results of the theoretical calculations indicate much higher pressures than obtained in the experiments reported by Valkiainen and Vuorinen (1985, 1989) and Snellman et al. (1986), see Figure 6-1. This large discrepancy between theoretical results and experimental measurements has been noted previously. One explanation is the deformation caused by the ion-exchange resins (Emrén 1983). The theoretical calculations of the swelling resins presented in Figure 6-5 also neglect the effect the bitumen matrix has on the water uptake and the related swelling pressure. Recent experiments performed in Belgium indicate that the bitumen matrix may reduce the swelling pressure of the solidified waste (Valcke et al. 2010). However, these experiments were performed on another type of waste (evaporator concentrates) and a harder type of bitumen (blown) than the distilled bitumen used in Sweden. Considering the effects neglected in the theoretical calculations, the emphasis in the evaluation is put on the experimental data presented in Figure 6-1.

Sources of information

The sources of information are given in Table 6-5.

Table 6-5. Main sources of information used in data qualification.

Sources of information
Aalto H, Valkiainen M, 1997. Simulated wetted bituminization product. In Vettyneen bitumointuotteen jatkokarakterisointi. Työraportti VLJ-6/97. VTT Chemical Technology.
Aalto H, Valkiainen M, 2004. Behaviour of bituminized ion-exchangers under repository conditions. In Long term behaviour of low and intermediate level waste packages under repository conditions. Results of a co-ordinated research project 1997–2002. IAEA-TECDOC-1397, International Atomic Energy Agency, 89–100.
Aittola J-P, Kleveland O, 1982. Swelling of bituminized ion exchange resins. NKA AVF (82) 215, Studsvik.
Aittola J-P, Chyssler J, Ringberg H, 1982. Thermal stability of ion-exchange resins. SKBF/KBS TR 81-13, Svensk Kärnbränsleämnings AB.
Almkvist L, Gordon A, 2007. Low and intermediate level waste in SFR 1. Reference waste inventory 2007. SKB R-07-17, Svensk Kärnbränslehantering AB.
Asea-Atom, 1985. B1 – Analys av bitumenprodukter: Svällningstester. Rapport KVC 85-204.
Berntsson J, 1992. Typbeskrivning av avfallskollin (B20) – Bitumensolidifierad jonbytarmassa och filterhjälpmedel i plåtfat förpackade i containrar, Beteckning B.20, PBD-9102-05, Sydkraft Barsebäcksverket. (In Swedish.)
Brodén K, Wingefors W, 1992. The effect of temperature on water uptake, swelling and void formation in a bitumen matrix with ion exchange resins. Waste Management 12, 23–27.
Brodersen K, Mose Pedersen B and Vinther A, 1983. Comparative study of test methods for bituminized and other low- and medium-level solidified waste materials. Final report (1981–1982) for contract WAS 235 DK(G). RISØ-M-2415, Risø National Laboratory, Roskilde, Denmark.
Dverstorp B, Sundström B, 2003. SSI:s och SKI:s granskning av SKB:s uppdaterade slutlig säkerhetsrapport för SFR 1. Granskningsrapport. SSI Rapport 2003:21, Statens strålskyddsinstitut (Swedish Radiation Protection Authority), SKI Rapport 2003:37, Statens kärnkraftinspektion (Swedish Nuclear Power Inspectorate). (In Swedish.)
Emrén , 1983. Theoretical calculation of swelling properties of ion-exchange resins. KEFYDA Konsult AB.
Ericsson K, Klingstedt G, 1987. Svällningsegenskaper hos radioaktiva jonbytarmassor från Forsmarksverket. Rapport 87041, The Swedish Cement and Concrete Research Institute (CBI). (In Swedish.)
Mariën A, Mokni N, Valcke E, Olivella S, Smets S, Li X, 2013. Osmosis-induced water uptake by Eurobitum bituminized radioactive waste and pressure development in constant volume conditions. Journal of Nuclear Materials 432, 348–365.
Matsuda M, Nishi T, Chino K, Kikuchi M, 1992. Solidification of spent ion exchange resin using new cementitious material, (I). Swelling pressure of ion exchange resin. Journal of Nuclear Science and Technology 29, 883–889.
Mokni N, Olivella S, Valcke E, Mariën A, Smets S, Li X, 2011. Deformation and flow driven by osmotic processes in porous materials: application to bituminised waste materials. Transport in Porous Media 86, 635–662.
Nilsson A-C, Högfeldt E, Muhammed M, Wingefors S, 1988. On the swelling of ion exchange resins used in the Swedish nuclear power plants. SKI TR 1988:1, Statens kärnkraftinspektion (Swedish Nuclear Power Inspectorate).
Pettersson M, Elert M, 2001. Characterisation of bituminised waste in SFR 1. SKB R-01-26, Svensk Kärnbränslehantering AB.
Riggare P, Johansson C, 2001. Project SAFE. Low and intermediate level waste in SFR-1. Reference Waste Inventory. SKB R-01-03, Svensk Kärnbränslehantering AB.
SKB, 2008. Safety analysis SFR 1. Long-term safety. SKB R-08-130, Svensk Kärnbränslehantering AB.
Snellman M, Valkiainen M (eds), 1985. Long-term properties of bituminised waste products. Nordic Liaison Committee for Atomic Energy (NKA).
Snellman M, Valkiainen M, Airola C, Bonnevie-Svendsen M, Brodersen K, Forsström H, Wingefors S, 1986. Long-term behavior of bituminized waste, Waste Management '86 Proceedings of the Symposium on Waste Management at Tuscon, Arizona, March 2-6, 1986. American Nuclear Society. Vol 3, 501–507.
Valcke E, Mariën A, Smets S, Li X, Mokni N, Olivella S, Sillen X, 2010. Osmosis-induced swelling by Eurobitum bituminized radioactive waste in constant total stress conditions. Journal of Nuclear Materials 406, 304–316.
Valkiainen M, Vuorinen U, 1985. Properties of bituminization product from Olkiluoto power plant. Report YJT-85-24, Nuclear Waste Commission of Finnish Power Companies.
Valkiainen M, Vuorinen U, 1989. Long-term properties of TVO's bituminized resins. Report YJT-89-06, Nuclear Waste Commission of Finnish Power Companies.
Weast R C, 1985. CRC Handbook of chemistry and physics : a ready-reference book of chemical and physical data. 65th ed. Cleveland, OH: CRC Press.

Categorising data sets as qualified or supporting data

No qualified data sets have been identified concerning the swelling pressure data for bituminised waste applicable to the waste forms in SFR. A number of supporting data sets have been identified, see Table 6-6. Data have been chosen for experiments with heat treated mixed anionic and cationic resins. Results from pure cationic resins have been excluded.

Table 6-6. Qualified and supporting data sets.

Qualified data sets	Supporting data sets
No peer reviewed sources of data have been found in the open literature. Information from technical reports have been found that contain relevant information applicable to the conditions in SFR.	Valkiainen and Vuorinen 1985, Table 5 Valkiainen and Vuorinen 1989, Figure 2-9

Excluded data previously considered as important

No previously considered data has been excluded.

6.5 Conditions for which data are supplied

The experiments have been conducted on mixed anionic and cationic granular resins with a waste loading corresponding to about 50% waste. The resins have been heat treated at 140°C for at least 10 hours. Other waste loadings, types of resins, treatments or additives may produce different results.

6.6 Conceptual uncertainty

A significant conceptual uncertainty relates to the behaviour of the bitumen matrix in the swelling waste. The mechanical properties of the bitumen (affected by temperature, ageing, radiation) are important for the possibility to form cracks or fissures that will generate an open porosity in the waste matrix. Furthermore, swelling will initiate at the surface and progressively affect parts of the interior of the waste package. The water uptake and the degree of swelling of waste particles (ion-exchange resin or salt) will be different in different parts of the waste packages. Salts may diffuse out of the package, and thus the potential for swelling is lost. As a consequence, the actual swelling only occurs in a limited zone. The pressure exerted on the leached zone may recompress the remaining bitumen matrix creating a bitumen layer with very low permeability as was observed in the Belgian experiments (Valcke et al. 2010, Mariën et al. 2013). Ion-exchange resins on the other hand will remain in the matrix, possibly forming a compressible zone in the outer parts of waste package. Since the long-term swelling of a bitumen matrix with ion-exchange resin has not been investigated it creates large uncertainties in the interpretation of how the swelling of the waste is propagated to the waste package.

Pressure build-up due to confined swelling is difficult to measure. Firstly, the equipment used must be able to ascertain the degree of confinement. It is somewhat uncertain whether confining conditions were maintained in the previous experiments with quartz powder (Snellman and Valkiainen 1985, Snellman et al. 1986). The oedometer type used by Valkiainen and Vuorinen (1985, 1989) and Valcke et al. (2010) to test the swelling of bituminised resins seems to be a usable experimental set up, although problems with bitumen “leakage” have been reported. However, measurements on bituminised resins have a very slow pressure build-up due to the slow diffusion of water into the waste. Another source of uncertainty is that most tests for practical and safety reasons have been performed on inactive samples. Radiation will influence both the resin and the bitumen. In some cases the effect of radiation has been simulated by external radiation (0.1–1 MGy). Radiolysis has been judged to have negligible effects for an absorbed energy less than 0.1 MGy (Eschrich 1980). The estimated energy absorbed in the bituminised waste placed in SFR is about 0.01 to 0.1 MGy, but a fraction of packages may obtain a dose exceeding 0.1 MGy (Pettersson and Elert 2001).

6.7 Data uncertainty due to precision, bias, and representativity

A limited amount of data is available on the swelling pressures that can develop due to water uptake of bituminised ion-exchange resins. The data selected here represent the part of the available data judged to best represent the bituminised wastes disposed of in SFR. However, the experimental data do not cover the full range of resin types, waste loadings or content of evaporator salts that is found in the bituminised SFR waste. Furthermore, the data show a variation that is not fully understood. There are uncertainties in how the experimental results can be explained by theoretical calculations of swelling pressure. This limits the possibility to extrapolate the data to other conditions.

6.8 Spatial and temporal variability

Spatial variability of data

Swelling tests performed on bituminised samples, for example Aittola and Kleveland (1982) show a large variance between samples. This is probably caused by difficulties in preparing homogenous samples. A variation can also be expected in the waste packages in SFR. The investigations performed in Finland show a large variation between samples taken from different parts of the drum due to the settling of the more dense cationic resin. The bituminised resins from Barsebäck are ground in order to decrease the effect of settling and produce a more homogeneous product.

Temporal variability of data

The water uptake process is very slow. The water uptake of small samples has been measured to be on the order of 10 g/m² and year as an average over 5 years (Aalto and Valkiainen 1997). The time for water uptake in the drum or a container will be very long. During that time changes in the properties of the bitumen and the ion-exchange resins that affect the pressure build-up may change.

6.9 Correlations

The bitumen swelling of a waste package is dependent on the amount of anionic or cationic resin deposited in the package. Therefore the delivered data have been assessed against the amounts of ion exchange resins present in the waste types B05, B06, F05, F17, and F18 asked for in Section 6.1. No other correlations have been identified within the SR-PSU safety assessment.

6.10 Result of supplier's data qualification

The supplier has requested the swelling pressure as function of expansion volume for the waste types B05, B06, F05, F17, and F18. The data is to be supplied for a reference waste package composition and a waste package representing a worst case composition with respect to swelling pressure.

The waste types B05, B06, F17, and F18 have similar or lower waste loading compared to what the data is developed for. The type of resins are similar, but not identical, where the data set was developed for granular mixed anionic and cationic resins, while the actual waste also contains powdered resins or ground granular resins. The actual waste packages have a varying ratio between the anionic and cationic resin, depending on the mix of powdered and granular resins.

The waste type F05 has a somewhat higher waste loading compared to what the data is developed for, a maximum of 60–65% compared to 50%.

The waste in F17 and F18 is heat treated in a similar way as in the experiments, while the waste in B05 and B06 is treated with Na₂SO₄ and only heated during the actual bituminisation process. No experimental data for swelling pressures from Na₂SO₄-treated waste has been found.

The waste type F17 may contain up to 40% evaporator concentrates that may cause swelling. Based on the investigations on the swelling of bituminised evaporates performed in Belgium (Valcke et al. 2010, Mariën et al. 2013), the swelling pressures of evaporator salts (or concentrates) are in the same order as the maximum values obtained due to swelling of ion-exchange resins.

The background material does not allow for confidently differentiating between the different waste types. Therefore it is recommended that the following data are used for all waste types with the average value representing the reference waste package and the maximum value as a more pessimistic case. Considering the uncertainties, the latter cannot be confidently referred to as a worst case. See Table 6-7 for the recommended data.

6.11 Judgements by the SR-PSU team

Sources of information

The sources of information summarised in Table 6-5 are used in this judgement.

Conditions for which data is supplied

The SR-PSU team accepts the conditions listed in Section 6.5.

Conceptual Uncertainty

The supplier notes significant conceptual uncertainties related to the behaviour of bitumen in the swelling waste. The SR-PSU team agrees that the swelling of bitumenised waste is a complex, coupled process and that the current understanding of the swelling process is incomplete.

Data uncertainty due to precision, bias, and representativity

The supplier notes that the amount of representative experimental data is limited and that theoretical models for swelling bitumenised waste are not comprehensive. The SR-PSU team agrees with the supplier that extrapolation of the data to conditions not represented by experiments should be performed with caution.

Spatial and temporal variability

The supplier notes that the water uptake process is very slow and that the properties of bitumen and ion exchange resin may change over time. The SR-PSU considers the stationary pressure exerted by swelling.

Correlations

The SR-PSU team agrees with the supplier on the correlations listed in Section 6.9.

Results of supplier's data qualification

The supplier concludes that the swelling behaviour of waste types B05, B06, F05, F17, and F18 cannot be confidently differentiated. In Table 6-7 the supplier suggests a swelling behaviour generic for all bitumenised waste forms in the SFR. The SR-PSU team accepts this conclusion.

6.12 Data recommended for use in SR-PSU modelling

The data presented in Table 6-7 is recommended for use in SR-PSU modelling.

Table 6-7. Data for swelling pressure at different volume increase of the waste.

	Swelling pressure (MPa) at different volume increase			
	0%	10%	20%	30%
Average	6	0.7	0.3	0.1
Maximum	12	2.5	0.75	0.22

7 Bentonite and Concrete/Cement sorption data

This section concerns sorption data for the different materials present in the SFR repository, or more specifically sorption partitioning coefficients for use in the radionuclide transport modelling, described in the **Radionuclide transport report** and the sorption reduction factors for the residual scenario calculation case “High concentrations of complexing agents”. The materials are the different bentonite materials present in the silo and the different concrete/cement mixtures present in the SFR repository both described in detail below:

Bentonite

The bentonite used has the trade name GEKO/QI and is a calcium montmorillonite based product transformed to the sodium form. The bentonite is used in the Silo repository part either in an unmixed form or mixed with 90% sand as a backfill surrounding the Silo.

In SKB (2008) the currently installed bentonite parts are described: The Silo rests on a 1.5 metre thick bed made of 90% sand and 10% bentonite. The total amount of bentonite used for the bed is 200 ton. The 0.85 metre wide room between the Silo and rock wall is filled with pure granulated bentonite which has been poured into the space. The top part, which will be installed when the repository closes, will also consist of a mixture of 90% sand and 10% bentonite GEKO/QI.

The design is mainly to prevent a high hydraulic flow through the Silo repository, but also to retard the diffusion of radionuclides through sorption to the bentonite minerals. The bentonite barrier also works as mechanical buffer between the rock and the Silo.

Concrete and cement

The cementitious materials that can be found in the SFR repository are mainly: structural concrete in buildings and waste packaging, concrete grout used as backfill around the waste packages in the Silo, BMA and BTF vaults and cement mortar and grout used as conditioning and solidification material for the waste. The mixing proportions of the different concrete types present in SFR are given in Table 7-1.

Structural Concrete

The structural concrete in the SFR repository is present in the Silo, BMA and BTF repositories as floors and lids. The Silo and BMA repositories also have inner and outer walls made of structural concrete. The BLA and BRT repositories both have structural concrete floors, but no lids. The concrete is also present as moulds and tanks in the BMA, BTF and Silo repositories, containing radioactive waste (Almkvist and Gordon 2007).

Table 7-1. Mixing proportions for concrete types in SFR taken from SKB (2001).

Component	Structural concrete	Silo grout	1BTF Grout bottom	1BTF Grout top
Cement (kg/m ³)	350	325	340	265
Water (kg/m ³)	164.5	366	252	141
Ballast (kg/m ³)	1,829	1,302	1,630	1,890
w/c ratio	0.47	1.125	0.74	0.53

Concrete Grout

The concrete grout is present as backfill, surrounding the waste packages in the BMA and Silo repositories. At the time of repository closure the BTF repositories will also be backfilled with concrete grout. The structural concrete and grout use Skövde SP and Degerhamn SP cement types (SKB 2001, **Initial state report**).

Conditioning and solidification of waste

Concrete and cement is also used as solidification and stabilisation of the waste, within the waste packages (Almkvist and Gordon 2007). The cement types used are Skövde SP, Degerhamn SP and Blast Furnace cement (SKB 2001, **Initial state report**).

7.1 Modelling in SR-PSU

This section describes what data are expected from the supplier, and in what SR-PSU modelling activities the data are to be used.

Defining the data requested from the supplier

- Sorption partitioning coefficients K_d (m³/kg) for the elements of the selected inventory in the concrete/cement and bentonite materials. As sorption partitioning coefficients are only valid for a particular set of conditions, values are supplied for an appropriate range of pore water compositions. For redox-sensitive elements, all relevant oxidation states are considered for data selection. The supplier should deliver data that reflects the sorption for different mechanical and chemical degradation states of the material, from the used condition of the materials present in current day SFR to a completely degraded condition.
- Sorption reduction factors for the elements of the selected inventory of radionuclides in the concrete – cement and bentonite materials. The supplier should give the lowest concentration for each complexing agent where effects of sorption can be expected. The complexing agents to include are ISA in both diastereomeric forms if available. NTA, EDTA, Gluconate, Citric acid and oxalate. The effects of cement additives should also be discussed and judged. If data is not available for all the radionuclides requested a discussion of general sorption reduction factor must be included and argued for. As a provisional example the sorption reduction of Ni²⁺ has been studied in the presence of ISA Co²⁺ has not the sorption reduction factor is set to be 10 for both RN based on arguments upon chemical similarities of Ni²⁺ and Co²⁺.
- Diffusion parameters (effective diffusivity, diffusion available porosity) for the bentonite barrier surrounding the Silo.

SR-PSU modelling activities in which data will be used

The radionuclide migration is modelled in Ecolego **Model summary report** as a diffusive and advective transport through the porous material, in combination with sorption of the radionuclides. The magnitude of these entities depends on physical properties of the concrete/cement and bentonite barriers, on the pore water composition and on the migrating species.

The sorption reduction factors are used for a residual scenario calculation case where a high amount of complexing agents are assumed to be present in the repository, causing a reduction in the sorption of the materials.

7.2 Experience from previous safety assessments

This section briefly summarises experience from previous safety assessments, especially the SAFE and SAR-08 safety assessments, which may be of direct consequence for the data qualification in this data report.

Modelling in previous safety assessments

The radionuclide transport in the SAFE safety assessment was modelled with the NUCFLOW software for the near-field transport and with the FARF31 software for the far-field transport (Lindgren et al. 2001). In the SAR-08 safety assessment, both the near-field and far-field transport was modelled with the AMBER software (Thomson et al. 2008). The modelling performed in SR-PSU modelling generally agrees with the latter SAR-08 modelling. No significant difference with bearing to the parameters of this section has been identified regarding to the sorption.

In both SAFE (Lindgren et al. 2001) and SAR-08 (Thomson et al. 2008), the complexing agents were handled in a residual scenario calculation case where the sorption reduction factors were used to simulate the reduced sorption. It was handled in a residual scenario because the amount of complexing agents in the SFR repository needed to affect the sorption was deemed very unlikely to occur according to Fanger et al. (2001).

Conditions for which data were used in previous safety assessments

In SAR-08, to be able to reflect the concrete/cement degradation in the repository during its life time, the sorption partitioning coefficients were gradually altered as a function of time, from values reflecting used materials to values reflecting completely degraded. This approach is also used in the SR-PSU safety assessment modelling to reflect the repository evolution.

Sensitivity to assessment results in previous safety assessments

Both in the SAFE and SAR-08 safety assessments the diffusion related parameters had a major influence on the time of release and dose of radionuclides from the SFR repository. Especially for the selected actinides such as for instance the Am isotopes and Np-237, as they were shown to have great sorption affinities to the materials present in the SFR repository (Cronstrand 2005).

In SAR-08, the result from the “High concentrations if complexing agents” scenario was a slightly lower dose in the coast period of the repository lifetime and a slightly higher dose, around a factor 2, in the beginning of the mire/forest period of the repository lifetime compared to the main scenarios Weichselian variant (SKB 2008). For the whole repository, the highest dose was not changed compared to the main scenarios Weichselian variant. This was because the maximum doses were dominated by organic C-14, which was not affected by the presence of complexing agents, see Figure 7-1.

Alternative modelling in previous safety assessments

No alternative modelling was reported in SAFE and SAR-08.

Correlations used in previous safety assessment modelling

No correlations were used in SAFE and SAR-08.

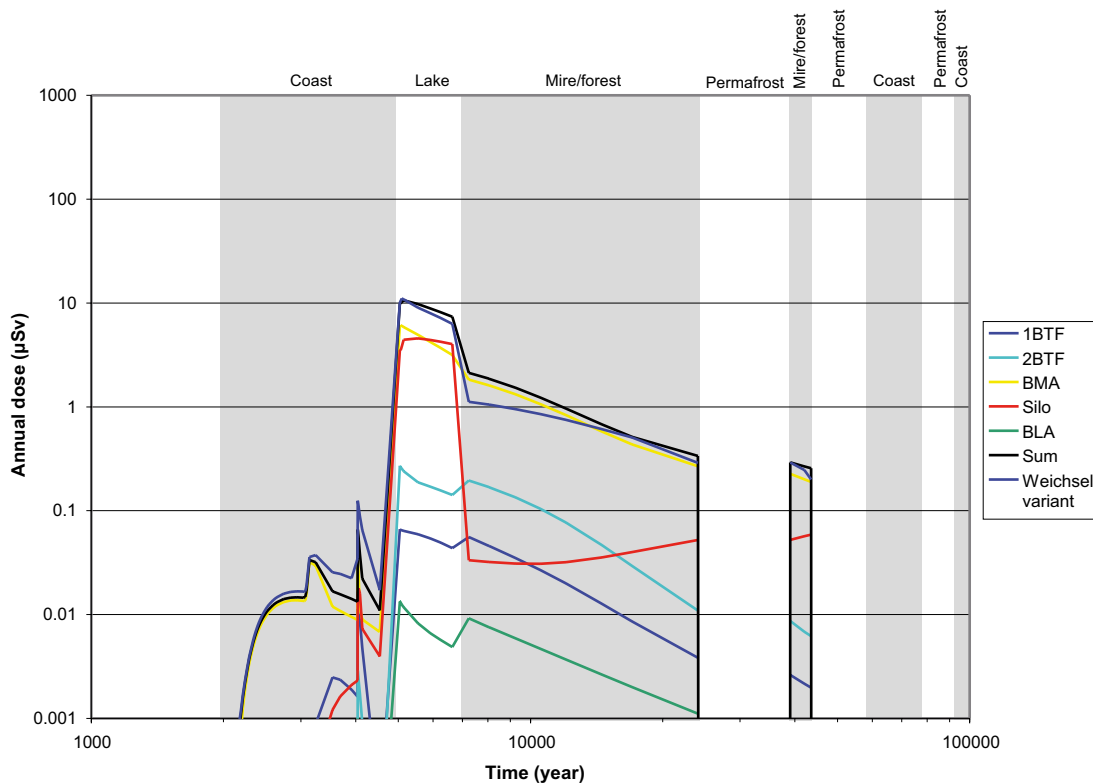


Figure 7-1. Annual individual dose for all of SFR 1 and contributions for the different repository parts to this dose according to the SAR-08 calculation case “High concentrations of complexing agents”. For comparison, the deterministic results for the main scenario’s Weichselian variant are also shown. From SKB (2008).

Identified limitations of the data used in previous safety assessment modelling

In its audit of the SAR-08 safety assessment the Swedish Radiation Safety Authority (Strålsäkerhetsmyndigheten, SSM) had the following concerns regarding on how the chemical properties of the materials was handled:

- Stronger arguments for that oxidative conditions will not occur after the redox buffering properties of the repository have been depleted was asked for.
- A discussion on how oxidative conditions would affect the sorption properties of the more redox sensitive nuclides such as Tc-99 was also wanted.
- A request for updated retention parameters for all the selected nuclides in the safety assessment regarding concrete/cement and bentonite, both from international literature as well as from SKB’s own publications. SSM wanted a special focus on the K_d values used for technetium(IV), neptunium(IV) and plutonium(IV).
- Further studies on how the bentonite barrier in the Silo is affected by diluted ground water. SSM wrote that the data used in SR-PSU should reflect the possibilities of infiltrating rain water and what the consequences of the changed ion strengths of this water could have on the bentonite mixtures.

7.3 Sources of information and documentation of data qualification

Sources of information

The main sources of information on sorption properties of concrete/cement and bentonite are given in Table 7-2. The main information sources in turn are based on an extensive evaluation of literature data. Among the references considered to be of major importance in Ochs and Talerico (2004) the following may be pointed out:

- A Nagra report on selected K_d values for MX-80 (Bradbury and Baeyens 2003), and original data sources cited therein.
- SKB reports on K_d , D_e , and D_a (Yu and Neretnieks 1997) and groundwater composition (Laaksoharju et al. 1998), and original data sources cited therein.

In the case of the reports by Wang et al. (2009) and Ochs et al. (2011) on sorption in cement systems, the following underlying key references are pointed out. Both describe the sorption processes of various RN in cementitious materials in different states of degradation and evaluate corresponding reference data:

- Wieland and Van Loon (2002).
- Andra (2005).

Table 7-2. Main sources of information used in data qualification.

Sources of information
Cronstrand P, 2007. Modelling the long-time stability of the engineered barriers of SFR with respect to climate changes. SKB R-07-51, Svensk Kärnbränslehantering AB.
Gaucher E, Tournassat C, Nowak C, 2005. Modelling the geochemical evolution of the multi-barrier system of the Silo of the SFR repository. Final report. SKB R-05-80, Svensk Kärnbränslehantering AB.
Ochs M, Talerico C, 2004. SR-Can. Data and uncertainty assessment. Migration parameters for the bentonite buffer in the KBS-3 concept. SKB TR-04-18, Svensk Kärnbränslehantering AB.
Ochs M, Vielle-Petit L, Wang L, Mallants D, Leterme B, 2011. Additional sorption parameters for the cementitious barriers of a near-surface repository. NIROND-TR 2010-06 E, ONDRAF/NIRAS, Belgium.
SKB, 2008. Safety analysis SFR 1. Long-term safety. SKB R-08-130, Svensk Kärnbränslehantering AB.
Wang L, Martens E, Jacques D, de Cannière P, Berry J, Mallants D, 2009. Review of sorption values for the cementitious near field of a near surface radioactive waste disposal facility. NIROND TR 2008-23E, ONDRAF/NIRAS, Belgium.
A very large number of peer reviewed scientific publications and technical reports from the open literature, as referred to in the above publications and in the present text.

Categorising data sets as qualified or supporting data

To the largest part, the recommended data are taken or directly evaluated from:

- Ochs and Talerico (2004), respectively SKB (2010a) for the bentonite barrier in the Silo.
- Wang et al. (2009) and Ochs et al. (2011) for the cement/concrete barriers in SFR.

All of these reports are dedicated data reports and the data therein are considered as qualified. As discussed in Section 7.4, Section 7.6 and Section 7.9 in more detail, it was verified that the conditions underlying these source data are sufficiently representative with regard to the conditions relevant for the different SFR reference periods. The conditions underlying the source data are based on various input data, such as groundwater and material composition, that fed into geochemical models. The conditions relevant for SFR are taken from SKB (2010a) and the results of various model calculations by Gaucher et al. (2005) and Cronstrand (2007).

Table 7-3. Qualified and supporting data sets.

Qualified data sets	Supporting data sets
1. Ochs and Talerico 2004, tables and text in Section 5.4. 2. SKB 2010a, Table 5-16 and Table 5-18. 3. SKB 2010a, Figure 5-5 to Figure 5-10. 4. Wang et al. 2009, overview plots and summary tables for Cl, I, Nb, Ni, Sr, Cs, Th, U, Pu, Np, Am, C and Tc in Chapter 4. 5. Ochs et al. 2011, overview plots and summary tables for Ag, Mo, Se, Sn and Zr in Chapter 3. 6. SKB 2010a, Table 4-12 and Table 4-13.	1. Ochs and Talerico 2004, tables in appendices A and B. 2. Wang et al. 2009, Figure 6. 3. Gaucher et al. 2005 and Cronstrand 2007, plots of model results in Chapter 5 and Appendix B, respectively.
1. & 2. Recommended K_d values on bentonite and upper/lower limits for reference conditions. 3. Overview plots of effective diffusion coefficients in bentonite as a function of clay dry density for Cs, HTO, anions. 4. & 5. Overview plots of experimental K_d values on hydrated cement phases as a function of degradation state and corresponding summary tables of K_d values and upper/lower limits. 6. Groundwater composition for SFR.	1. Assumed groundwater compositions and calculated porewater compositions for bentonite buffer (SR-Can). 2. Degradation states of cement containment and barriers. 3. Predicted evolution of bentonite and cement/concrete barriers in SFR for a large range of model assumptions.

Excluded data previously considered as important

The data that were previously considered as important for the qualification are also included in the present evaluation.

7.4 Conditions for which data are supplied

It is pointed out in several places of this report that especially sorption coefficients are significantly dependent on chemical conditions. The conditions under which the data are considered to be valid are discussed below for both bentonite as well as cement/concrete. It needs to be kept in mind in this context that the prevailing conditions are dependent on the evolution of the repository. Based on the reference periods defined in SKB (2008), Gaucher et al. (2005), and Cronstrand (2007) modelled the evolution of the various barrier systems in SFR.

While their results differ in detailed aspects, the following key aspects emerge from these studies:

- The evolution of the bentonite barrier in the Silo is largely determined by the adjacent cement barrier and shotcrete lining of the rock wall. The model calculations indicate that largely unperturbed bentonite can be expected for extended time periods. Within this timeframe, the largest portion of the bentonite barrier is predicted to be dominated by Na-smectite and non-alkaline porewater with a pH of about 8. When long time periods are considered, the bentonite barrier may be perturbed by the alkaline fluids; this is discussed further below.
- The various cement-based barriers are predicted to degrade to a different extent, depending on their composition and location. In the following, the states of degradation of hydrated cement paste (HCP) as outlined by Berner (1990) are considered for the evaluation of radionuclide retention. Even for the longest timeframes considered in SKB (2008), the models of Gaucher et al. (2005) and Cronstrand (2007) predict that degradation would not proceed further than state II (presence of portlandite, pH 12.5) in nearly all cases. In a few situations, degradation is predicted to proceed to the beginning of state III (absence of portlandite, pH 12). For the definition of sorption data, a wider range of degradation is considered, including fresh HCP up to nearly fully degraded material (end of state III, pH 10.5); see Section 7.9 for details.

Bentonite and porewater properties

The potential effect which the uncertainties in the porewater compositions may have will differ for the various migration parameters:

- K_d generally depends strongly on the aqueous composition. For alkaline and alkaline earth elements (Cs, Ra, Sr), sorption depends mainly on the concentration of other cations, and is therefore strongly influenced by salinity. On the other hand, the sorption of most other radionuclides is mainly governed by pH and the concentration of complexing ligands (especially carbonate).
- The diffusion parameters D_e and ϵ depend significantly less on the pore water composition, although extremely high or low ionic strength can have an influence on anion exclusion and enhanced cation diffusion effects.

Unperturbed bentonite

As described in Section 7.9, the sorption values for the bentonite barrier in the Silo of SFR are taken from Ochs and Talerico (2004). Due to the conditional nature of K_d , the difference in conditions between the SR-Can/SR-Site and the present case would require a re-calculation of K_d on formal grounds. However, a critical prerequisite for the derivation of K_d values is a careful calculation of porewater compositions. In this respect, it has to be admitted that the chemical boundary conditions regarding the bentonite barrier and contacting solutions are not sufficiently constrained to warrant such an approach. On the other hand, as further discussed below the conditions in the unperturbed bentonite barrier are viewed as similar enough to those considered by Ochs and Talerico (2004) (within the respective range of variations) for K_d to fall within the overall data range considered for the SR-Can/SR-Site case. The situation for altered bentonite is discussed separately below.

The reference materials for concrete/cement and bentonite barriers are given in the beginning of this chapter. The migration data for bentonite in Ochs and Talerico (2004) are supplied for MX-80 bentonite at a dry density of 1,590 kg/m³. The dry density of the bentonite buffer in the SFR Silo is expected to be 950–1,120 kg/m³. As pointed out in Ochs and Talerico (2004), K_d of a trace sorbate is independent of the solid/water ratio (for any given set of conditions). Therefore, no adjustment is needed for the difference in density.

The bentonite used for the Silo in SFR is GEKO/QI, which is a Na- montmorillonite type. The mineralogy and CEC are not known in detail. On the other hand, Ochs and Talerico (2004) only considered MX-80 bentonite (Na-form) in their data derivation. However, they considered the following variations in bentonite composition:

- bentonite converted completely to the Ca-form,
- bentonite completely depleted of soluble impurities and some accessory minerals (NaCl, KCl, gypsum, calcite).

The porewater composition in the bentonite will be affected by both the bentonite composition and density as well as by the composition of the infiltrating water. Further, it is not possible to measure the porewater composition in a straightforward fashion, and porewater composition has to be calculated with the help of a clay-water interaction model taking into account all aqueous reactions, mineral solubility, ion exchange and acid-base reactions at the clay edge surface. As a result, the calculated porewater composition is also dependent, to some degree, on the underlying porewater model and the related specific parameters used. This needs to be kept in mind when the influence of bentonite and properties of the infiltrating water on radionuclide migration parameters is discussed.

The reference groundwater used in Ochs and Talerico (2004) for pore water modelling was saline Beberg water (BFI01B). The main variations for detailed modelling included a non-saline and a highly saline groundwater; two saline groundwaters having alkaline to highly alkaline pH (up to pH 13.15) were considered in addition. In addition, two cases regarding exchange of gas (CO₂) with the host rock were further considered (a constant pCO₂ impost by the host rock vs. a closed buffer system).

A representative range of composition of the groundwater at the SFR site is given in SKB (2008), as well as the composition range of the overlying part of the Bothnian Sea (Öregrundsgrepen), which may be more representative for future groundwater compositions. In terms of pH and concentrations of major constituents, the two waters are very similar. Moreover, the indicated composition range, and in particular the expected salinity, is almost fully covered by the span of compositions represented by the reference groundwater and the two main variations considered by Ochs and Talerico (2004).

In all likelihood, the characteristics of the solution infiltrating the bentonite will be strongly influenced by the cement-based materials situated on both sides of the barrier (Silo wall, host rock wall lining). Ochs and Talerico (2004) give the calculated porewater composition for bentonite in contact with two hypothetical saline groundwaters, where the presence of sufficient alkalis was assumed to give a groundwater pH of 10.5 and 13.2. These solutions approximately represent saline groundwater in equilibrium with degraded and fresh hydrated cement. Due to the buffering effect of the bentonite, porewater pH remained at $\text{pH} \approx 7.5$, as long as the exchange of CO_2 with the surrounding host rock/groundwater system was considered.

As discussed in detail in SKB (2008) and Fanger et al. (2001), the Silo contains cement-based waste and barrier materials which can be expected to contain cellulose as well as some complexing agents. Their influence on radionuclide sorption directly in the various cementitious materials is discussed in Section 7.9 and the **Waste process report**. Based on the available information, it is difficult to evaluate whether the respective organic substances will also be present in the bentonite barrier, and if so, in which concentration range.

While the model results by Gaucher et al. (2005) for several simple ions do not allow to exclude the presence of organic ligands, it can be qualitatively estimated that the concentration of the organic substances will be clearly lower in the unperturbed bentonite than in the cement-based materials. Indeed, since the material in question is unperturbed, it can be assumed that no or only very few ions released from the cement have diffused into this portion of the bentonite and that the concentration of any organic molecules in this part will also be very low. On this basis, and considering the large uncertainty factors already introduced (Ochs and Talerico 2004), it is not considered meaningful to introduce any additional sorption reduction factors due to the possible presence of low levels of organic ligands in unperturbed bentonite, for several reasons. Primarily, the most important ligands in bentonite are the surface-bound silanol and aluminol groups, and a ligand needs to be present in sufficiently high concentrations to have a significant effect, while the presence of organics in the unperturbed bentonite is not relevant in view of the overall uncertainty. If organic ligands were to be considered, it should be done in the frame of a data derivation process as used for the recommended K_d values and not by reduction factors. As already pointed out above, the conditions in the bentonite barrier of SFR are not constrained well enough for such an approach. It is further not clear how differences in speciation should feed into K_d derivation in the absence of specifically developed sorption models, see Ochs and Talerico (2004), and it has to be admitted that the possible effect of minor solution constituents is difficult to capture in such a situation.

In view of the above-mentioned additional uncertainties in calculating porewater compositions, it is considered that the composition of the porewater in the unaltered parts of the bentonite barrier of the SFR Silo can be represented with the range of porewater compositions given in Ochs and Talerico (2004). In particular the reference porewater (RPW, corresponding to the saline Beberg groundwater) considered in Ochs and Talerico (2004) is expected to have a relatively similar composition.

Perturbed bentonite

Depending on the specific model used for assessing the evolution of the Silo barrier system, a strongly altered mineralogy and/or an elevated porewater pH may have to be expected for very long timeframes. Such conditions are obviously outside the range considered in Ochs and Talerico (2004). Accordingly, their values cannot be used for that period, and the conditions in the perturbed material are not defined well enough to warrant the derivation of new data. Note that the models of both Gaucher et al. (2005) and Cronstrand (2007) indicate a substantial portion of unperturbed material for all time periods in most scenarios.

At least for some of the relevant radionuclides, the minerals formed in the perturbed bentonite (e.g. zeolites) should be as good or better sorbents than the original bentonite minerals. However, the uncertainties in the modelling of the evolution of the mineral and solution composition do not allow a quantitative assessment. On the other hand, it is still reasonable to assume a certain level of sorption; and a K_d of zero (as essentially considered in the safety calculations) is very conservative. Further information is given in Section 7.9.

Concrete/cement and porewater properties

As a result of the interaction with groundwater addressed above, the concrete/cement barrier and other cement-based components in the Silo, as well as in all other relevant parts of SFR (mainly BMA), will also be degraded with time.

While there are differences regarding the details, the degradation of hydrated Portland cement follows the following scheme (Berner 1990, Taylor 1990). With respect to interaction with radionuclides (and other solution constituents) it is important to note that each state is characterised by a specific pH and mineralogy. Therefore, radionuclide sorption coefficients are recommended for each state.

- State I: This corresponds to fresh hydrated cement paste. High concentrations of alkalis are still present and are being leached. This leads to $\text{pH} \geq 13$ and elevated Na and K concentrations in the pore solution. Portlandite is present and the Ca/Si ratio of the CSH phases is high ($\text{C/S} \geq 1.5$).
- State II: When the alkali elements are largely removed, state I is followed by a relatively long and stable phase, which is characterised by equilibrium with portlandite and $\text{pH} \approx 12.5$. The C/S is about 1.5.
- State III: When most Ca has been leached from the system, portlandite disappears and the Ca/Si ratio of the CSH minerals starts to decrease continuously from about 1.5 to about 0.9 (when C/S reaches a value of about 0.8, roughly the C/S ratio of the mineral tobermorite, the CSH phases dissolve completely). In state III, the alumina-sulphate minerals, such as ettringite, also dissolve (at the end of state III, the actual cement matrix disappears and only residual minerals are left). Because state III is relatively heterogeneous, conditions for the beginning and end of this state are considered separately as follows:
 - State IIIa: CSH with a C/S ratio not much lower than 1.5, presence of Ca-aluminates, $\text{pH} 12$.
 - State IIIb: CSH with a lower C/S ratio (approaching $\text{C/S} \approx 1$), absence of Ca-aluminates, $\text{pH} 10.5$.

Many of the predicted details in the evolution of the cement-based materials (such as the exact C/S ratio of CSH) depend to some degree on the specific model used, and in particular on the underlying thermodynamic database. As there are very limited data from real systems, the models are typically parameterised on the basis of systematic data from simplified laboratory systems. Therefore, the predicted evolution and the compositional details are associated with a certain model uncertainty. On the other hand, independently of the composition of inflowing groundwater, some of the main constituents of porewaters in hydrated cement systems are controlled by the solid phases themselves:

- The pH (i.e. the concentration of OH^- ions) is very high. This is caused initially by the dissolution of alkalis in the cement, followed by the equilibrium with portlandite.
- The presence of portlandite also gives rise to fairly high concentrations of Ca and concurrent (calcite equilibrium) low concentrations of dissolved carbonate.

With regard to the sorption⁵ of most radionuclides in hydrated cement, it is widely agreed that the CSH minerals are the most important solid phase, and that generally strong sorption can be expected in their presence (Wieland and Van Loon 2002, Wang et al. 2009). As major parameters of the solution composition (in particular pH) are also directly related to the solid characteristics, it is reasonable to assume that data from literature sources are applicable for comparable C/S ratios. The influence of differences in the specific cement formulation and in minor solution constituents is expected to be negligible within the data uncertainty considered.

⁵ The term 'sorption' is used in the wider sense of uptake when applied to cement-based systems; it includes surface sorption (adsorption) as well as the formation of solid solutions and other incorporation processes.

Wang et al. (2009) and Ochs et al. (2011) derived their data for hydrated cement, based on a very extensive literature review. They report sorption data specifically for each relevant cement degradation stage, covering all phases from fresh hydrated cement (Phase I above) to the point where CSH disintegrate (end of Phase III above). Both Gaucher et al. (2005) and Cronstrand (2007) predicted in their modelling of SFR barrier evolution that CSH phases will be present up to 100,000 AD in the Silo wall and BMA. The only exception to this is the prediction of complete CSH loss at 50,000 AD in BMA for the case of extensive freeze-thaw cycles (Cronstrand 2007). However, Cronstrand (2007) considers the respective transport conditions as clearly exceeding the limits of the model used (i.e. the above prediction is not seen as realistic). Sorption values for the present purpose were selected to correspond to the predicted C/S ratios for the Silo wall and BMA, and are therefore considered to be well applicable. Conditions with elevated salinity or the presence of organic complexants are also considered.

7.5 Conceptual uncertainty

Bentonite

For the definition of K_d , the most significant conceptual uncertainties, in terms of representing reality, are related to the description of pore water composition in compacted clay as a function of conditions (cf. Ochs and Talerico 2004). In case of compacted bentonite, there are some fundamental conceptual uncertainties which are mainly related to scientific shortcomings regarding:

- The distribution of porosity and porewater types among one vs. different types of pores.
- The interpretation of the effects of the negative permanent electrostatic charge residing on the planar surfaces of clay platelets.

As the pore water composition of compacted bentonite cannot be determined experimentally with any certainty, it is calculated through thermodynamic surface chemical models. Several published models are available for this purpose (NEA 2012). While they are based on the same principles, they differ in a number of details regarding e.g. assumptions of single or multiple types of pores and porewaters as well as the treatment of electrostatic effects and of specific surface chemical equilibria. Because of the limited accessibility of the pore space of compacted bentonite, a direct comparison of pore water model and experimental results is extremely difficult. However, there are several comparisons of experimental and model-derived macroscopic migration parameters in compacted bentonite (NEA 2012); see also Ochs and Talerico (2004) which indicate that the available models are sufficiently robust for describing the effect of bentonite and groundwater properties on radionuclide migration within experimental uncertainties. These issues are discussed to some detail in the SR-Site Buffer, backfill and closure process report (SKB 2010b) and in the **Barrier process report** for the SR-PSU assessment..

In case of anions, it appears to be well established that an anion exclusion effect is operative. In case of the radionuclides sorbing exclusively via ion exchange (Cs, Ra, Sr), the situation is less clear. To date, there are several different models available (NEA 2012) that are all able to describe most of the observed effects. The degree to which the D_e and K_d for these ions have to be considered as correlated depends on the respective model concept used. This has implications regarding the selection of K_d values for compacted systems. Ochs and Talerico (2004) assigned D_e and K_d for these ions independently: first, K_d was calculated through sorption models calibrated on the basis of ion exchange observed in batch experiments, and D_e was subsequently estimated directly from experimental diffusion data.

Conceptual and numerical uncertainties are further introduced when transferring experimental data (especially K_d values) obtained at a specific set of conditions through models or estimation procedures to different conditions relevant for safety analyses. These are of two types:

- Because of the strong dependency of sorption on chemical conditions and surface properties, the experimental data need to be somehow converted to the safety analysis-specific conditions. This can be done through the use of thermodynamic sorption models, where available, or by the use of (semi-quantitative) conversion procedures. A particularly critical issue is the quantitative evaluation of the influence of differences in RN speciation. These types of uncertainty are largely included in the uncertainty factors applied by Ochs and Talerico (2004).

- Due to the difficulties in conducting systematic experiments (e.g. for a range of conditions) in compacted clay, most data are obtained in disperse batch systems. There are basic questions regarding the assumption that batch data are applicable to compacted systems. While this issue is not resolved yet on a fundamental scientific level (see the discussion on porespace characteristics above), all the available macroscopic evidence is compatible with this assumption (NEA 2012).

As discussed in Section 7.4, there are significant uncertainties associated with the application conditions themselves. It is therefore critical to take the conditional nature of the relevant migration parameters into account. In particular K_d values need to be derived for each specified set of (expected) conditions. In Ochs and Talerico (2004), the potential variability of geochemical conditions was addressed by deriving K_d values explicitly for several sets of possible geochemical conditions that covered a wide range.

Cement/concrete

For the cement-based barriers, only sorption data are selected here. As discussed in the SR-PSU **Waste and Barrier process reports**, the main uncertainty regarding the quantification of radionuclide sorption in these systems is related to the lack of clear evidence regarding the sorption processes. When the underlying processes are not identified, it becomes also more difficult to evaluate the influence of conditions on sorption and to assess the appropriateness of experimental procedures that form the basis of the available source data. Therefore, experimental sorption data for hydrated cement systems are possibly associated with larger uncertainties than comparable data for other solids. This becomes particularly relevant in cases where only limited data are available.

On the other hand, hydrated cement exerts a very strong influence on the porewater chemistry. Due to the properties of this material, solution chemistry is invariably dominated by a few constituents, whose concentration can be fairly well predicted. Therefore, the variability within cement systems is limited, and reliable data from laboratory systems can generally be viewed as representative. In a few cases, there is evidence that specific solid or solution constituents have a critical influence on sorption, these are addressed separately (Section 7.9). This may also include organic complexants, in cases where significant amounts are introduced with the waste or in the form of concrete admixtures.

It may be summarised that the scientific understanding of sorption in hydrated cement systems is associated with large uncertainties in many cases. However, the properties of the material lead to a comparatively small variability of conditions that needs to be considered in data derivation.

7.6 Data uncertainty due to precision, bias, and representativity

The uncertainty of the selected sorption and diffusion parameters is contributed to by experimental uncertainties in the underlying source data, but stems mainly from uncertainties that are introduced in the process of synthesising and scaling these data to the conditions specified for safety assessment. Where appropriate, data uncertainty is therefore discussed together with descriptions of the derivation of sorption and diffusion parameters, as well as the basic results of data derivation. The numerical results are summarised in Section 7.9.

Bentonite

Diffusion parameters

The data of concern are effective diffusion coefficients (D_e) and diffusion-available porosities (ϵ_{diff}) for the relevant radionuclides. Effective diffusivities are representative for steady-state conditions; i.e. retention processes and in particular sorption are not important. Accordingly, D_e values show little dependence on conditions, in contrast to K_d .

The conceptual uncertainties associated with diffusion parameters are briefly discussed in Section 7.5. With regard to data acquisition, D_e is measured in through-diffusion experiments which are more difficult to perform than sorption batch experiments due to the required experimental timeframe and the challenges in controlling chemical and other boundary conditions. This also puts limits on the existing database in terms of the radionuclide as well as in terms of the conditions treated. D_e values are largely available only for mobile but not for sorbing elements, and are only in a few cases available as a function of (limited) systematic variations of chemical conditions. Further, the extraction of D_e values from raw experimental data is not straightforward and requires the fitting of models that have to be chosen as a function of boundary conditions. This is an important issue especially in case of the diffusion of charged species.

On the other hand, diffusion experiments are very similar to the in situ conditions anticipated for a bentonite barrier in terms of clay density and pore characteristics. In combination with the relative insensitivity with respect to chemical conditions, this means that D_e values do typically not need to be recalculated (to the degree that this is required for K_d) to the chemical conditions expected for PA.

For the bentonite used in the SFR Silo barrier (GEKO/QI), no diffusion or porosity data are available. Following the above discussion, the recommended data for SFR were evaluated directly from the extensive compilation of D_e values for SR-Can (Ochs and Talerico 2004) which had been updated and extended for SR-Site (SKB 2010a). The data in these reports are presented in plots of reported D_e vs. clay dry density. Where available, diffusion data obtained as a function of conditions (e.g. ionic strength) were also plotted. Overall, these experimental data cover a very wide range of different conditions in terms of diffusion-relevant bentonite and solution characteristics (including type and ionic form of bentonite) which in turn influence pore size and characteristics. Since the selected D_e values for SR-Can/SR-Site take the overall spread of these data into account, it is assumed that uncertainties related to the influence of conditions are included in the uncertainties given for D_e in each case.

Following the approach of SR-Can (Ochs and Talerico 2004) and SR-Site (SKB 2010a), D_e was evaluated separately for neutral diffusants on the one hand, and anions and cations showing anion exclusion and enhanced diffusion effects, respectively, on the other hand. A review of the various model concepts that can be used to explain anion exclusion and enhanced cation diffusion is given in the **Barrier process report** and is not repeated here.

- The term neutral diffusants includes most elements of concern (hydrolysable cations, cations existing mainly as neutral ion pairs, neutral molecules). Many of these elements are moderately or strongly sorbing, and any element-specific D_e data, if available, typically represent isolated measurements. Therefore, it is preferred to base D_e data for this group on data for HTO, whose diffusion behaviour can be evaluated on the basis of a number of studies.
- Anions encompass only true, largely uncomplexed anions such as chloride or oxo-anions. On the other hand, negatively charged, labile complexes of hydrolysable metal ions are not included.
- Cs is the only element for which enhanced cation diffusion is considered. Other cations sorbing exclusively via ion exchange (Ra, Sr, Ba) may also be assigned to this group. Here the argumentation given in Ochs and Talerico (2004) is followed; i.e. it is assumed that these elements may exist in the form of ion-pairs (or possibly weak complexes) which are not positively charged. Also, the few available experimentally determined effective diffusion data (mainly for Sr^{2+} , see e.g. Muurinen et al. 1987, Choi and Oscarson 1996, Eriksen and Jansson 1996, Suzuki et al. 2004) show significant scatter and do not exhibit a clear trend as a function of dry density.

The recommended data given in Section 7.9 are directly evaluated from the plots of D_e vs. dry density given in SKB (2010a). Considering the lack of detailed information regarding the properties of the bentonite barrier in the Silo, it is not considered as meaningful to use a mathematical approach (e.g. a regression analysis as in SKB 2010a), because the apparent numerical accuracy would not be reflected in the data situation.

Assuming a clay dry density of 950 kg/m^3 to $1,120 \text{ kg/m}^3$ (top to bottom of Silo barrier, SKB 2008), the following value can be estimated from the plot given for neutral diffusants in SKB (2010a). Using the conservative assumption that the bentonites with a relatively low clay content (mainly

Kunigel-V1 with about 48% clay) are most representative for the Silo barrier, an average D_e of $4 \cdot 10^{-10}$ m²/s can be estimated for HTO, considering the density range indicated. Similarly, a lower and upper limit of $2 \cdot 10^{-10}$ m²/s and $9 \cdot 10^{-10}$ m²/s can be extracted. To our knowledge, no new data have become available, especially for the clay density of concern. Therefore, the source data used are considered to represent the present state of the art.

For anions, recommended values are also taken directly from the corresponding plot given in SKB (2010a). For the range of dry clay density considered, a best estimate value of $4 \cdot 10^{-11}$ m²/s is proposed, with lower and upper limits of $2 \cdot 10^{-11}$ m²/s and $2 \cdot 10^{-10}$ m²/s, respectively. These are to be used in combination with a reduced ϵ_{diff} value, see below. Again, the underlying source data are considered to represent the state of the art. The only additional datasets that are not given in SKB (2010a) are the D_e values for chloride measured by Glaus et al. (2010) in montmorillonite (obtained from Milos bentonite) and two values measured by Goutelard and Charles (2004) in MX-80. However, both datasets were measured at a much higher dry density than considered for the present case. Moreover, they are almost identical to the range of data already considered in SKB (2010a). Therefore, it can be concluded that these omitted data would have no influence on the present data selection.

In case of Cs, the recommended diffusion values given in Ochs and Talerico (2004) and SKB (2010a) are based on a single dataset determined by Sato (1998) for Kunigel-V1 over a wide range of dry density. The only comparable dataset that also extends to fairly low dry densities are the measurements by Molera and Eriksen (2002) in MX-80. However, they interpreted their experiments considering an additional surface diffusion coefficient. It is therefore not clear whether the resulting D_e values (which are always based on a model interpretation of raw diffusion data), are indeed representative. In either case, their data systematically indicate a lower diffusivity (by about factor 2.5 to 5) of Cs than the data by Sato (1998). Thus, the omission of these data would lead to a more conservative selection of recommended values. Due to the scarcity of experimental data at low dry clay density, recommended values are centred around the regression line given in SKB (2010a), which is based on the data by Sato (1998). This results in a best estimate D_e of $7.5 \cdot 10^{-10}$ m²/s for the density range of concern. Since upper/lower limits cannot be based on the data directly, they are somewhat arbitrarily set to $2 \cdot 10^{-9}$ m²/s and $2.5 \cdot 10^{-10}$ m²/s, respectively. This gives a slightly larger uncertainty range than considered in SKB (2010a) to acknowledge the additional uncertainty related to the lack of detailed knowledge on bentonite properties.

As diffusion-available porosity ϵ_{diff} of neutral diffusants and cations (Cs) the same value as for the physical porosity is assumed. For this, the value of 0.61 given in Höglund (2001) is accepted; this would also result from use of eq. 5-6 in Ochs and Talerico (2004) and a mean dry density of 1,050 kg/m³. For the ϵ_{diff} of anions, the same reduction factor of 2.5 in comparison to the physical porosity as in Ochs and Talerico (2004) and SKB (2010a) is applied, which results in $\epsilon_{\text{diff}}(\text{anions}) = 0.24$.

The selected diffusion parameters are valid for a temperature of 25°C. Following SKB (2010a), approximately a twofold increase or decrease of D_e can be expected for a 25°C-increase or -decrease of temperature, respectively. No effect on the diffusion-available porosity is expected (not considering processes like freezing, which change the hydrological parameters of the bentonite, see the **Barrier process report**).

Distribution coefficients

As discussed in Section 7.4 and Section 7.5, the K_d values selected in Ochs and Talerico (2004) and SKB (2010a) are considered to be applicable to the present conditions within the discussed uncertainties. Similarly, no new information has emerged in the pertinent literature published after Ochs and Talerico (2004) that would motivate a modification of the applied conversion procedures and uncertainty factors. While new thermodynamic sorption models addressing both ion exchange as well as surface complexation have been developed for several RN, many of these models are parameterised only for simple systems (e.g. pure montmorillonite in contact with an inert electrolyte solution) are therefore not directly applicable to more complex porewater compositions containing carbonate and other strong ligands (see discussions in NEA 2012). Ideally, the derivation of K_d values for safety analyses would be based on sorption models that are parameterised for similar conditions. While this situation is being clearly improved, the available experimental database is not sufficient yet to permit such an approach (NEA 2012).

The K_d values selected in Ochs and Talerico (2004) and SKB (2010a) are valid for 25°C. While the available data do not allow to assess the influence of temperature on sorption with sufficient certainty, it is not expected that temperature effects will be relevant in comparison to the geochemical uncertainties considered.

With regard to the underlying source data used for the derivation of K_d values, the selections made in Ochs and Talerico (2004) are generally still considered to be valid. For many radionuclides, no new relevant data have become available in the meantime, to our knowledge. The cases where new potentially relevant source data have been determined that were not considered in Ochs and Talerico (2004) and SKB (2010a) are discussed in the following

- In case of Ni, Tertre et al. (2005) measured sorption edges on montmorillonite (obtained from MX-80) in 0.025 M and 0.5 M NaClO₄ solution. Their data show approximately the same trend as the data on SWy-1 by Baeyens and Bradbury (1997) but indicate slightly lower sorption. Similarly, Ochs and Talerico (2004) also noted that the sorption isotherm by Bradbury and Baeyens (2003) on MX-80 gave a lower K_d for Ni than their SWy-1 data. Since Ochs and Talerico (2004) conservatively based the recommended K_d for Ni on the MX-80 source data, the additional data by Tertre et al. (2005) do not motivate any re-evaluation. Rather, they support the original, conservative choice of source data. More recently, Akafia et al. (2011) also measured Ni sorption on smectite (SWy-2). Their data fall within the range delineated by the data of Baeyens and Bradbury (1997) and Tertre et al. (2005).
- New experimental data have also become available in case of selenite, Se(IV). Missana et al. (2009) measured several pH edges of selenite on smectite in 0.001 M to 0.5 M background solutions. Their measured K_d values are higher by about factor 5 or more than the data by Bradbury and Baeyens (2003) considered by Ochs and Talerico (2004). Montavon et al. (2009) measured a sorption edge on MX-80 in 0.05 M background solution. At the relevant pH (7.8), these data agree very well with the sorption isotherm by Bradbury and Baeyens (2003). Ochs and Talerico (2004) also did not consider a number of K_d values measured by Shibusatani et al. (1994) and Tachi et al. (1999). These data show very large scatter, but their mean is also close to the source value used by Ochs and Talerico (2004). In summary, the mentioned additional data do not give a reason to revise the proposed sorption values. The other potentially relevant oxidation states Se(-II) and Se(VI) were assigned a K_d of zero. No new data were found that would motivate a revision in either case.
- For Mo, no K_d is given in Ochs and Talerico (2004). In SKB (2010a), a K_d of zero is assigned, based on an analogy between the molybdate anion (which is the only species of Mo occurring in normal aqueous solutions) and selenate. SKB (2010a) did not consider the study of Motta and Miranda (1989) and Goldberg et al. (1996). The two studies investigated the sorption of molybdate on montmorillonite, but do not give a clear picture. Motta and Miranda (1989) measured sorption isotherms at pH < 5 and saw low but significant sorption. On the other hand, Goldberg et al. (1996) observed a steep decrease of sorption with increasing pH and measured no appreciable sorption at pH > 7. On this basis, it is concluded that the K_d of zero selected in SKB (2010a) may be conservative, but that a re-evaluation of Mo sorption is not warranted.
- Andra (2005) report a sorption edge for Nb on smectite extracted from MX-80. These data became available after the publication of Ochs and Talerico (2004) and were not considered in SKB (2010a). At a similar pH value, this sorption edge gives a K_d similar to the value measured by Ikeda and Amaya (1998), which was considered in Ochs and Talerico (2004). However, their argument of using a conservative estimate due to the scarcity of data is still considered valid, and no re-evaluation to arrive at a higher value seems warranted.
- For Ag, Ochs and Talerico (2004) did not consider the study by Khan et al. (1995), who measured the sorption of Ag on bentonite. While their data are not conclusive, they indicate K_d values in the range of about 0.01–0.4 m³/kg. Considering further the potential effect of chloride on Ag sorption, it is proposed to revise the upper limit of 15 m³/kg given in Ochs and Talerico (2004) down to 1.0 m³/kg. As in Ochs and Talerico (2004), a lower limit of zero is proposed. Considering the uncertainties regarding Ag speciation in the porewater and its very high sensitivity with regard to complexation by chloride and sulphide, zero sorption is also proposed as best estimate.

- For Sn (specifically Sn(IV), Sn(II) is not relevant), Ochs and Talerico (2004) did not consider the study by Oda et al. (1999), who measured a sorption edge on untreated Kunigel-V1 bentonite in 0.01 M NaCl. Within the (relatively large) experimental scatter, their dataset is almost identical to the data by Bradbury and Baeyens (2003), which had been considered as potential source data but were not used in the end. Both studies indicate consistently high K_d values of $\approx 1,000 \text{ m}^3/\text{kg}$ for about pH 4–7, decreasing to $\sim 150 \text{ m}^3/\text{kg}$ at pH 10. Thus, the decision by Ochs and Talerico (2004) to base K_d for Sn on an analogy with Th can be viewed as conservative.
- In case of Pb, some new sorption data (Akafia et al. 2011) have become available after the publication of Ochs and Talerico (2004) and SKB (2010a). These data show generally a good agreement with the data by Ulrich and Degueldre (1993), which were selected as source data by Ochs and Talerico (2004). However, a part of the data by Akafia et al. (2011) indicate lower sorption than the data by Ulrich and Degueldre (1993). A comparison of the experimental conditions indicates that this can be attributed to the difference in initial Pb concentrations, which are significantly lower in case of Ulrich and Degueldre (1993). Assuming that trace concentrations are most representative for the migration of radionuclides in a bentonite barrier, the data by Ulrich and Degueldre (1993) are still regarded as the most representative. However, to acknowledge the data by Akafia et al. (2011), it is proposed to reduce the previously derived lower limit by a factor of five while retaining the best estimate and upper limit values given in Ochs and Talerico (2004).
- For Am, new sorption edge data by Bradbury and Baeyens (2006) on Na- and Ca-SWy-1 have become available. The data on Ca-SWy-1 agree well with the data by Gorgeon (1994), which are the source data for the K_d values recommended in Ochs and Talerico (2004) and SKB (2010a). In comparison, the data for Na-SWy-1 indicate higher sorption of Am. As the speciation of Am in the experiments by Bradbury and Baeyens (2006) is more straightforward than in case of Gorgeon (1994), it could be argued that the data recommendation should be re-evaluated, which could only lead to a higher recommended K_d . However, in view of the abovementioned difference between the Na- and Ca-forms, it is proposed to retain the more conservative value derived on the basis of the data by Gorgeon (1994).
- Ochs and Talerico (2004) and SKB (2010a) base the recommended K_d of Cm on an analogy with Am. Systematic sorption data of Cm have become available from Rabung et al. (2005) for Ca-SWy-1 in simple Ca-electrolyte solution and from Grambow et al. (2006) for MX-80 in synthetic porewaters. The data by Rabung et al. (2005) follow roughly the data by Bradbury and Baeyens (2006) for the Ca-system. The data by Grambow et al. (2006) show a much less pronounced sorption edge; they are similar to the data for Ca-smectite at pH ≈ 7 , but are by nearly an order of magnitude lower in the range of pH 8–10. Considering the established chemical similarity between Am and Cm and the good agreement between the data by Rabung et al. (2005) and the corresponding data by Bradbury and Baeyens (2006) for Am, the value proposed by Ochs and Talerico (2004) is still considered valid.
- In addition to the sorption edge of Th on SWy-1 determined in 0.1 M NaClO₄ (given originally in Bradbury and Baeyens 2003), Bradbury and Baeyens (2005) give a corresponding sorption edge in 1 M NaClO₄. The two datasets are nearly identical and show that Th sorption on montmorillonite is not influenced by ionic strength.
- New sorption data for U(VI) by Bradbury and Baeyens (2005) have become available. In comparison to the data by Pabalan and Turner (1997) these data would indicate higher sorption. Thus, the data derived in Ochs and Talerico (2004) may be somewhat conservative.
- For Pa, sorption edge measurements on Na-montmorillonite (SWy-1) by Bradbury and Baeyens (2006) became available after the publication of Ochs and Talerico (2004). These data were also not considered in SKB (2010a). They indicate a constant sorption value of about $90 \text{ m}^3/\text{kg}$ over a pH range from 4 to 10.5. This K_d value is more than an order of magnitude higher than the K_d values estimated previously by Ochs and Talerico (2004) on the basis of data for Pa presented in Yu and Neretnieks (1997). However, due to the lacking detail regarding the composition of the bentonite and porewater in the SFR Silo, and hence the speciation of Pa, no re-evaluation of Pa sorption is done and the values proposed in Ochs and Talerico (2004) are accepted as very conservative estimates.
- For all other radionuclides (C, Cl, Sr, Zr, Tc, I, Cs, Ho, Pd, Pu, Np, Cd, Eu, Sm), no new relevant sorption data have become available.

In the framework of a review of the safety assessment study SAR-08, Zhou et al. (2009) criticised the fact that the data recommended by Ochs and Talerico (2004) are based on a limited database. There are several reasons for this approach:

- The main reason is the strong dependency of K_d on chemical conditions. This means that K_d values can be directly applied only in case of very similar conditions. In all other cases, it is required to transfer the literature data to the PA-conditions (NEA 2005) by means of conversion procedures (or thermodynamic models, where available). The main uncertainty of recommended K_d stems from this transfer of sorption data to different conditions (NEA 2005). The respective uncertainties are considered explicitly in Ochs and Talerico (2004). The resulting overall uncertainties in K_d are significantly larger than the scatter of experimental data from different (reliable) sources.
- Because of the dependency of K_d on chemical conditions, it would be a misconception to assume that a compilation of experimental data from different sources would allow a better assessment of uncertainties in source data. This is because most of the apparent scatter observed in comparisons of experimental data is typically due to the variability of conditions rather than to actual uncertainty. When like is compared with like (i.e. data obtained under matching conditions), the scatter is often substantially reduced. Accordingly, Ochs and Talerico (2004) carried out a transparent, quantitative derivation on the basis of selected source data rather than a more qualitative expert estimation on the basis of large data compilation.
- The only datasets considered to be of highest quality are those that are obtained as a function of an important system variable, such as pH (sorption edges), radionuclide concentration (sorption isotherm), or other important solution constituents. The embedding in a series of related data lends additional confidence to the individual data points in terms of both representativeness and absence of bias. Single point measurements or data obtained under a narrow range of conditions are much less useful and more difficult to transfer to different conditions, because no clear trends can be assigned to such datasets. In the present context it is therefore not helpful to 'dilute' state of the art source data (as outlined above) with additional datasets of lesser quality.

Zhou et al. (2009) also comment on the rather high upper limits as well as the best estimate values given for several radionuclides in their tetravalent oxidation state (Tc, Sn, Np, Pu) in Ochs and Talerico (2004) and SKB (2010a). In particular, it is pointed out that such high values have not been recommended for earlier safety assessments. Regarding the recommended values given in Section 7.9 as well as those in the previous assessments of Ochs and Talerico (2004) and SKB (2010a), the following is pointed out:

- From a fundamental point of view, it needs to be made clear that the very strong sorption of tetravalent elements is experimentally confirmed, which is consistent with their pronounced tendency towards hydrolysis. Indeed, the mentioned best estimates are well within the range of experimentally measured K_d values for e.g. Sn(IV) and Th. Thus, they are not unusual according to the present state of the art.
- The values for the abovementioned radionuclides in their tetravalent oxidation state are based on analogy with Th. In turn, the recommended values for Th were selected by Ochs and Talerico (2004) on the basis of high-quality and well-established experimental sorption data (Bradbury and Baeyens 2003).
- The high upper limits are simply the result of the applied uncertainty factors. As already pointed out in Ochs and Talerico (2004), it has to be admitted that it is not clearly established whether errors should be distributed around derived K_d values in a linearly or logarithmically symmetrical way. In choosing the latter option, Ochs and Talerico (2004) followed the approach of Bradbury and Baeyens (2003). In any case, when the recommended parameter space is sampled stochastically, the bounding upper/lower values will feed into safety assessment calculations as part of the entire data range.
- As discussed in Section 7.9, the present use of Th data as analogue for tetravalent elements is handled in a simplified way in comparison to the approach used in Ochs and Talerico (2004) and SKB (2010a). Conservatively, the increased uncertainty is not considered to be log-symmetrical with respect to the selected values but is only applied to the lower limit. Thus, some of the high upper limits are avoided.

Hydrated cement/concrete

Unlike as in the case for bentonite, no underlying dedicated data report is available. Cronstrand (2005) reviewed sorption values on both bentonite and cement-based materials, but did not perform a quantitative data derivation based on original experimental data. Therefore, the sorption values for the Silo wall and BMA are based on the very recent and comprehensive reviews of Wang et al. (2009) and Ochs et al. (2011). Both of these reviews are directed at defining recommended K_d values as well as upper and lower limits for a cement-based near-surface repository for Belgian category A radioactive waste. To this end, the degradation of the cementitious material was modelled in detail. Subsequently, a comprehensive review of the available literature was conducted and the available data for each radionuclide were analysed in order to allow their assignment to a specific degradation state. To the degree possible, trends of sorption values as a function of degradation were tied in with the concurrent known or modelled changes in solid composition and speciation.

The processes of radionuclide sorption on hydrated cement are reviewed in the **Waste process report**. This is done for each radionuclide in an element-specific fashion. The values proposed in the following are selected to be consistent with the respective sorption process.

A general overview of cement degradation is given in Section 7.4 as well as in the **Barrier process report**. Section 7.4 also discusses how the data recommended by Wang et al. (2009) and Ochs et al. (2011) can be applied to the situation at SFR by considering the C/S ratio as master variable. For a few elements with specific sorption behaviour, such as Se, the presence of specific host minerals, such as ettringite, also needs to be taken into account.

It follows that the assignment of K_d values hinges on the modelling of the cementitious system evolution, and in particular the change in C/S ratio and other mineralogical properties of the hydrated cement material. With respect to the scenarios in SKB (2008), the models by Gaucher et al. (2005) and Cronstrand (2007) predict the presence of CSH phases for all periods, with C/S ratios decreasing from 1.8 to 1.1. As outlined in Section 7.4, a somewhat wider range of conditions is considered for the present purpose:

Wang et al. (2009) and Ochs et al. (2011) also evaluated the influence of elevated chloride concentration on sorption. They considered typical saline solutions such as sea water, but did not consider extreme cases such as concentrated brines. It was concluded in both studies that the lack of systematic sorption data obtained under different salinity conditions does not allow a quantitative evaluation.

Moreover, high salinity can affect the pH (release of OH^- due to addition of Na) as well as the mineralogy (uptake of chloride in hydrated cement minerals) of concrete/cement systems. This is often not taken into account in experimental studies. For the present case, it is assumed that such effects are already contained in the modelling by Gaucher et al. (2005) and Cronstrand (2007); i.e. the effect of salinity is assessed only with regard to the actual sorption process.

Based on the available, sketchy evidence from sorption experiments and on thermodynamic considerations (influence of chloride on speciation and especially on solubility limits), Wang et al. (2009) and Ochs et al. (2011) made a qualitative assessment of the effect of salinity on sorption of different groups of radionuclides. With respect to the radionuclide of concern in the present case, the following effects are likely:

- High impact: Cs, Sr and Ba will sorb less due to the competition effect by the increased Na concentration. Soft metal cations (Ag, Cd, Pd) due to their tendency to form very strong chloride complexes.
- Medium impact: Radioactive iodide and chloride will be affected by competition with the stable chloride. The same is assumed for molybdate, selenate and Tc(VII).
- Low impact: ^{14}C assuming isotope exchange, Se(IV), and Zr, Nb, Sn, Ho, U, Pu, Am, Np, Cm, Eu in their relevant oxidation states. Ni assuming isotope exchange and no impact of salinity on the stability of LDH phases (in case of actual sorption, a medium effect would have to be assumed due to the relative stability of Ni-chloride complexes). For Tc(IV), medium impact is assumed by Wang et al. (2009) based on expert opinion. Here it is assumed that hydrolysis will be dominating at high pH (as in case of actinides) and that impact will be low.

7.7 Spatial and temporal variability

Spatial variability of data

Within SFR, there is of course spatial variability in the sense that each system component contains a different combination of waste, structural and barrier materials. While this is of relevance for the safety analysis modelling, it is not taken into account here because the data are recommended in a generic fashion for the barrier materials and the specified geochemical conditions.

There is no spatial variability of the type typically encountered in geological media. In principle, both the bentonite as well as the cement/concrete barriers can be considered as completely homogeneous within the scale of radionuclide transport distances, at least in the initial repository period. With progressed evolution of the repository (see below), zones of degraded material will develop in both types of materials. In case of bentonite, the altered portion is not addressed explicitly in the data derivation (and is not considered to contribute to sorption in the safety calculations). Some pertaining qualitative information is given in Section 7.9. In case of cement/concrete, the difference between degraded and fresh material is much more gradual. The values selected for the main degradation states (see below) are deemed valid for the entire barrier within the uncertainty of the modelling of the cement evolution.

Temporal variability of data

The data themselves and the underlying processes are not subject to temporal variability. However, the temporal evolution of the repository gives rise to concurrent changes in geochemical conditions which influence the magnitude of sorption. The evolution of the bentonite and cement/concrete barriers is addressed in Gaucher et al. (2005) and Cronstrand (2007). In case of cement/concrete, the temporal evolution of the material properties is addressed directly in the data selection. In case of bentonite, the data are essentially selected for unperturbed bentonite, a significant portion of which is presumed to be present in most scenarios for all periods. See also Section 7.9.

7.8 Correlations

The supplied migration parameters for a number of radionuclides are based on analogies with similar elements for which a better data basis is available. This is described for each radionuclide in Section 7.4 and Section 7.9. Similarly, as pointed out in Section 7.4, the magnitude of sorption correlates with chemical parameters (pH, solids composition, etc) which are the results of initial repository conditions and the subsequent evolution.

Based on their chemical characteristics (which fed into analogy considerations used in data selection), the radionuclides considered can be organised into correlating groups of elements and oxidation states whose migration behaviour will generally show a similar response to variations in chemical conditions. Overall, the following grouping results:

- Alkaline and alkaline earth elements: Cs, Ba, Sr.
- Tri-valent actinides and lanthanides: Am, Cm, Pu(III), Ho, Eu.
- Tetra-valent actinides: U(IV), Pu(IV), Np(IV). Data for these are largely based on Th, which is not included as a relevant RN for SFR. For some data, Zr and Sn(IV) were also evaluated on the basis of data for Th.
- Penta-valent actinide elements: Np(V), Pu(V).
- Hexa-valent actinide elements: U(VI), Pu(VI).
- In terms of diffusion data in bentonite, the three groups defined correlate:
 - Anions.
 - Cs.
 - HTO and all non-anionic RN.

7.9 Result of supplier's data qualification

Bentonite barrier in the SFR Silo

With regard to radionuclide migration parameters for a bentonite buffer, the principal work was done in a dedicated SR-Can report (Ochs and Talerico 2004). The present report largely relies on that work, without reproducing the data derivation procedures. This is motivated by the expected similarity in conditions, cf. Section 7.4. Only in a few cases (diffusion data to account for the lower clay density, Ag to take into account literature information previously not considered) have the supplied data been changed from those recommended in SR-Can.

Diffusion parameters

As pointed out in Section 7.6, the diffusion-available porosity for neutral diffusants and Cs is taken as the physical porosity. As best estimate, the value of 0.61 given in Höglund (2001) is accepted. Considering the density range of 950 kg/m³ to 1120 kg/m³ analogously gives a porosity range of 0.65 to 0.59. For the diffusion-available porosity of anions, the reduction factors (best estimate 2.5, upper limit 1.8 and lower limit 3.5) given in Ochs and Talerico (2004) are accepted. The derivation of the D_e values summarised below is discussed in Section 7.6.

With regard to the probability distributions that should be applied to the data, the approach taken in SKB (2010a) is generally followed:

- The porosity values are given as best estimates with upper and lower limits. As these are approximately symmetric in the linear space, double triangular distributions (with the best estimate as mode) are recommended.
- Diffusion coefficients and associated uncertainties are evaluated directly from various plots of experimental data given in SKB (2010a), see Section 7.6. The evaluation was done on the basis of data in the log-space, and accordingly, a distribution in the log-space is recommended. Following the argumentation in SKB (2010a), a log-double triangular distribution is proposed.

Table 7-4. Diffusion-available porosity ϵ_{diff} .

element	ϵ_{diff} (-)		
	lower limit	best estimate	upper limit
neutral diffusants	0.59	0.61	0.65
anions	0.17	0.24	0.36
Cs	0.59	0.61	0.65

Table 7-5. Effective diffusion coefficients D_e .

element	D_e (m ² /s)		
	lower limit	best estimate	upper limit
neutral diffusants	$2.0 \cdot 10^{-10}$	$4.0 \cdot 10^{-10}$	$9.0 \cdot 10^{-10}$
anions	$2.0 \cdot 10^{-11}$	$4.0 \cdot 10^{-11}$	$2.0 \cdot 10^{-10}$
Cs	$2.5 \cdot 10^{-10}$	$7.5 \cdot 10^{-10}$	$2.0 \cdot 10^{-9}$

Sorption distribution coefficients (K_d)

The recommended K_d values are given in Table 7-6. As discussed in Section 7.4, the values for saline groundwater are taken from Ochs and Talerico (2004). While Ochs and Talerico (2004) report no K_d values that explicitly correspond to a non-saline groundwater, the bentonite pore water composition was also calculated using a non-saline groundwater as well. The calculated ionic strength in this pore water is almost identical as in case of the saline groundwater, because the pore water in compacted bentonite is to a large degree controlled by the soluble constituents of the bentonite itself. Thus, it can be expected that K_d for a non-saline groundwater will lie well within the range given for the saline groundwater.

Table 7-6. Distribution coefficients (K_d) for unperturbed bentonite and reference pore water, corresponding to saline and non-saline groundwaters.

Radionuclide (oxidation state)	K_d (m ³ /kg)	Upper K_d limit (m ³ /kg)	Lower K_d limit (m ³ /kg)
Ac(III)	8	233	0.3
Ag(I)	0	1	0
Am(III)	61	378	10
Ba(II)	0.005	0.031	0.0009
¹⁴ C, carbonate species	9.0E-05	1.8E-04	1.8E-05
¹⁴ C, CH ₄ , organic acids	0	0	0
Ca(II)	0.005	0.031	0.0009
Cd(II)	0.30	13.3	0.007
Cl(-)	0	0	0
Cm(III)	61	378	10
Cs(I)	0.11	0.60	0.018
Eu(III)	8	93	0.8
Ho(III)	8	93	0.8
I(-)	0	0	0
Mo(VI)	0	0	0
Nb(V)	3	45	0.2
Ni(II)	0.30	3.3	0.03
Np(IV)	63	700	4
Np(V)	0.02	0.2	0.004
Pa(IV, V)	3	45	0.2
Pd(II)	5	75	0.3
Pb(II)	74	457	2.4
Po(IV)	0.04	0.4	0.003
Pu(III)	61	378	10
Pu(IV)	63	700	4
Pu(V)	0.02	0.2	0.002
Pu(VI)	3	18	0.3
Ra(II)	0.005	0.031	0.0009
Se(-II)	0	0	0
Se(IV)	0.04	0.4	0.003
Se(VI)	0	0	0
Sm(III)	8	93	0.8
Sn(IV)	63	700	2.3
Sr(II)	0.005	0.031	0.0009
Tc(IV)	63	700	2.3
Tc(VII)	0	0	0
Th(IV)	63	700	6
U(IV)	63	700	3.6
U(VI)	3	18	0.5
Zr(IV)	4	103	0.1

Most values derived in Ochs and Talerico (2004) are directly accepted, but some of the values based on analogy considerations are re-evaluated:

- Ochs and Talerico (2004) made direct use of analogue values (e.g., accepting the values for Am directly for Cm) only in those cases where it was felt that the speciation of the two radioelements is sufficiently similar. Such values are accepted also directly for the present report.
- In all other cases, only the experimental data for an analogue element (e.g. Am) had been used by Ochs and Talerico (2004), and the whole data derivation process had been applied again to these experimental data, taking into account the different speciation of the target element (e.g. Pu(III)). For the present case, the bentonite porewater composition is not deemed to be sufficiently well defined to warrant a distinction of the speciation of similar elements.

- In such cases, the K_d values for the analogue element were accepted directly for the present purpose instead of using the recalculated value for the target element. Accordingly, some of the K_d values for these cases differ between the present report and Ochs and Talerico (2004), as follows:
 - all values (best estimate and upper/lower limit) differ in case of Pu(III) and take on a lower value;
 - the upper limits of Np(IV), Pu(IV), Pu(VI), Sn(IV), Tc(IV) and U(IV) are lower,
 - the lower limits of the above RN(IV) oxidation states would slightly increase by using the direct analogy approach: to be conservative, the lower values of Ochs and Talerico (2004) have been retained;
 - for Zr, the conservative values by Ochs and Talerico (2004) have been kept instead of using the direct analogy with Th.

The elements barium (Ba), calcium (Ca), polonium (Po), actinium (Ac), and cobalt (Co) were not considered in SR-Can (Ochs and Talerico 2004). In case of inorganic ^{14}C (carbonate), isotopic exchange is indicated in Ochs and Talerico (2004), but no K_d value is given. In SKB (2010a), zero sorption is assumed in lack of further information. Arguments for the proposed K_d values and uncertainties are summarised in the following:

- Ba and Ca were not considered by Ochs and Talerico (2004) and SKB (2010a). It is proposed to treat both elements analogously to Sr and Ra.
- Some experimental data for Po sorption on montmorillonite are available from Ulrich and Degueldre (1993). However, a complete K_d derivation as in SR-Can (Ochs and Talerico 2004) is not deemed reasonable for the bentonite in SFR, based on the lacking detailed information regarding bentonite and porewater composition (see Section 7.4). Bradbury and Baeyens (2003) proposed to use Se(IV) as analogue for Po, due to the lack of sorption data for Po. In view of the tendency of dissolved Po to easily oxidise to the +IV state (due to self-irradiation) and the similarity between Se(IV) and Po(IV) (Bradbury and Baeyens 2003, Yui et al. 1999), this analogy is also adopted here. A comparison of the limited number of Po sorption data by Ulrich and Degueldre (1993) with data for selenite (see above) indicate that Po sorption is about an order of magnitude higher than Se(IV) sorption. Therefore, the analogy is considered sufficiently conservative to directly use the data proposed for Se(IV) in SR-Can.
- No values for Ac are recommended in Ochs and Talerico (2004). SKB (2010a) gives a K_d and the corresponding uncertainties. These are based on analogy with the lanthanide elements Eu, Ho and Sm, since Ac exists only in the +III form in normal aqueous solutions. SKB (2010a) considers this analogy as conservative, since Ac bears also some similarity to trivalent actinide elements. To be consistent with the data derivation in Ochs and Talerico (2004), increased uncertainties were assumed. The values recommended in SKB (2010a) are also deemed to be valid for the conditions relevant to SFR.
- No values for cobalt are given in either Ochs and Talerico (2004) or SKB (2010a). Co can be expected to exist only in the +II-valent oxidation state in the bentonite porewaters. The aqueous chemistry of Co(II) is generally very similar to that of Ni(II), see e.g. Baes and Mesmer (1976). Relevant experimental data comprise sorption edges on smectite (Akafia et al. 2011) and a sorption edge on Na-illite (Bradbury and Baeyens 2009). Molera and Eriksen (2002) also measured Co sorption edge on MX-80. Some of their datapoints are derived from diffusion experiments and agree well with the corresponding batch-type data, as well as with the data by Akafia et al. (2011). Tiller and Hodgson (1960) measured Co sorption on a Ca-montmorillonite in 0.1 M CaCl_2 in the pH range 4 to 8. Grütter et al. (1994) measured an isotherm at pH 7.9 in synthetic porewater on Na-montmorillonite (SWy-1) as well as on an illite sample. They observed nearly identical sorption of Ni and Co on illite, but significantly higher sorption of Co on montmorillonite. On the other hand, the sorption edge on illite by Bradbury and Baeyens (2009) agrees with the corresponding data for Ni from the same study only up to $\text{pH} \approx 8$, whereas at higher pH values, the sorption of Co increases more strongly with pH. The datasets for Ni and Co by Akafia et al. (2011) are consistent with this observation. These results indicate some unresolved inconsistencies in the sorption behaviour of Ni and Co, but show that the magnitude of Co sorption is equal to or higher than the sorption of Ni. On this basis, it is proposed to base the data for Co on a direct analogy with Ni.

- For ^{14}C in inorganic form, isotopic exchange of radioactive carbonate species with stable C isotopes in bentonite solids, particularly calcite, can be expected as most relevant uptake mechanism. To define a corresponding, nominal K_d value, the dissolved total concentration of carbonate species in the bentonite porewater and the amount of calcite accessible to isotopic exchange per unit mass of bentonite need to be known.
 - For GEKO/QI bentonite, Pusch and Cederström (1987) report less than 2% carbonate. No further details are available, to our knowledge. For the calculation of a nominal K_d value, a solid carbonate content of 0.5% is assumed as best estimate, with 1% and 0.1% as upper and lower limit, respectively.
 - Regarding the accessibility of solid carbonate with respect to isotopic exchange, Bradbury and Baeyens (1997) estimated a very conservative accessibility of 0.27% of the total calcite in MX-80. This value is accepted for the present purpose, no further uncertainties are considered.
 - The porewater composition and therefore the dissolved carbonate concentration in the bentonite barrier of SFR is not known. As discussed in Section 7.4, it is assumed that the reference porewater (RPW) considered in Ochs and Talerico (2004) represents a good approximation. The respective total dissolved carbonate concentration of $1.48\text{E}-03\text{ M}$ is a fairly typical value for bentonite-groundwater equilibria (it corresponds to an elevated $p\text{CO}_2$ and leads to a more conservative K_d than e.g. atmospheric $p\text{CO}_2$).
- In case of ^{14}C in organic form, isotopic exchange is conservatively neglected. The forms of organic ^{14}C are expected to include CH_4 and small organic acids that do not sorb appreciably.

With regard to transferring the best estimates and the corresponding uncertainty limits to probabilistic distributions for safety calculations, the approach documented in SKB (2010a) is generally followed. As a direct result of the calculation of uncertainties, the best estimates and the upper and lower limits are in most cases symmetric in the \log_{10} -space. Therefore, triangular distributions in the log-space are generally recommended. For inorganic ^{14}C (carbonate species), uncertainties of sorption are related to uncertainties in the calcite content. As this does not result in upper and lower limits which are symmetric in the \log_{10} -space, a continuous triangular distribution in the linear space is recommended. In case of Ag , a skewed triangular distribution in the linear space is recommended, with $K_d = 0$ as minimum as well as modal value and with $1.0\text{ m}^3/\text{kg}$ as maximum value.

The effect of alkaline solutions on sorption is not quantitatively assessed, because there are considerable uncertainties regarding the detailed conditions. Sorption in the perturbed portion of the bentonite is not taken into account in the transport calculations for safety analyses. This is seen as a very conservative approach, since the change in mineralogy should not result in a dramatic decrease of sorption, as at least some of the new minerals to be expected are very good sorbents (possibly better than bentonite, e.g. zeolites, see Gaucher et al. 2005), see also Section 7.4.

For the unperturbed bentonite, the following qualitative assessment can be given for sorption at elevated pH, based on Ochs and Talerico (2004) and some newer literature (for some elements, no relevant information is available):

- III-valent actinides, lanthanides and Ac: In the absence of carbonate, sorption may increase up to pH 11 or so. In the presence of significant carbonate concentrations, sorption may decrease at pH 8–9 due to increased carbonate complexation. In the presence of atmospheric CO_2 levels, Marques Fernandes et al. (2008) measured a K_d for Eu of about $0.1\text{ m}^3/\text{kg}$ at $\text{pH} \approx 10.5$. No reliable data are available for higher pH values.
- IV-valent actinides: Available data indicate no decrease of Th sorption up to $\text{pH} \approx 11.5$, which is consistent with Th hydrolysis behaviour. Information on the influence of carbonate on Th sorption is limited. Bradbury and Baeyens (2003) report on measured Th sorption isotherms on MX-80 in synthetic porewater including carbonate and sorption edges in carbonate free solutions. The good agreement of the K_d values obtained in both cases indicates that sorption of ternary Th-hydroxo-carbonato surface complexes is contributing to the overall Th sorption.
- V-valent actinides: The data by Turner et al. (1998) show that Np(V) sorption increases up to $\text{pH} \approx 11$ in the absence of carbonate. In the presence of atmospheric CO_2 levels, sorption starts to decrease above $\text{pH} \approx 8.5$; at $\text{pH} 9.5$ Turner et al. (1998) report a K_d of about $0.05\text{ m}^3/\text{kg}$. No reliable data are available for higher pH values. The data by Bradbury and Baeyens (2006) indicate constant sorption of Pa(V) on montmorillonite between $\text{pH} 4$ and $\text{pH} 11$. Data for higher pH and for the presence of carbonate are not available.

- Cs, Sr, Ra, Ba: The main effect by highly alkaline solutions would be the competition by Na- and K-ions. This influence is expected to be within the limits given in Table 7-6, based on the range of porewater compositions predicted by Gaucher et al. (2005).
- Ni and Co: The data by Bradbury and Baeyens (1999, 2005) on Na- and Ca-montmorillonite show that Ni sorption starts to decrease at $\text{pH} \approx 9$, but that sorption is still substantial ($K_d \approx 1 \text{ m}^3/\text{kg}$) at $\text{pH} 12$. The Co sorption data by Akafia et al. (2011) and Molera and Eriksen (2002) indicate increasing sorption up to $\text{pH} \approx 10$, but no data for higher pH are available.
- Pb: The data by Akafia et al. (2011) indicate increasing sorption of Pb on smectite up to $\text{pH} 10$. No systematic data for higher pH values were found for either clay minerals or oxides. A very approximate analogy with cementitious materials suggests that Pb sorption may decrease again at pH values above $\text{pH} \approx 10$ (Ochs et al. 2011). It appears that both increase and decrease in the magnitude of sorption amounts to about an order of magnitude for each pH-unit, with a sorption maximum near $\text{pH} \approx 10$. This would be consistent with the hydrolysis of Pb (Baes and Mesmer 1976).
- Se(IV) and Po(IV): Despite the considerable scatter, the trend in the data by Missana et al. (2009), Shibutani et al. (1994) and Tachi et al. (1999) indicates that sorption at $\text{pH} 12$ may be about an order of magnitude lower than at $\text{pH} 7$. However, this probably applies only to a system where calcite is present, which seems to be partly responsible for Se(IV) sorption at high pH (Goldberg and Glaubig 1988). In a calcite-free system, sorption would presumably tend towards zero. No additional information for Po is available.
- Tc(IV): Based on the hydrolysis behaviour of Tc(IV), it can be expected that sorption may decrease above $\text{pH} 10$. However, no corresponding sorption data are available.
- Sn: Sorption at $\text{pH} \approx 11.5$ is about $5\text{--}10 \text{ m}^3/\text{kg}$ according to the data by Oda et al. (1999). No reliable data are available for higher pH values.
- U(VI): The data by Bradbury and Baeyens (2005) suggest that in the absence of carbonate, sorption at $\text{pH} 11$ may be about two orders of magnitude lower than the peak sorption of U(VI) occurring around $\text{pH} 6\text{--}7$. The data obtained by Pabalan and Turner (1997) in the presence of atmospheric CO_2 levels indicate that sorption in the presence of elevated carbonate concentrations may be close to zero at $\text{pH} > 10$.

Cement/concrete barriers: sorption parameters

Recommended values

The recommended K_d values are given in Table 7-7 to Table 7-10. As described in Section 7.6, the principal work was done in recent project on data derivation in cementitious systems (Wang et al. 2009, Ochs et al. 2011). The present report largely relies on that work, without reproducing the data derivation procedures. This is motivated by the expected similarity in conditions, cf. Section 7.4. It is noted that in contrast to the present handling of sorption as a function of degradation, the above reports do not divide state III into two parts. Cases where the values of Wang et al. (2009) and Ochs et al. (2011) are not considered clearly valid for the entire state III (i.e. from $\text{pH} \approx 10\text{--}12.5$) are discussed separately below. Similarly, all situations where there may be significant differences in the conditions assumed in these studies in comparison to SR-PSU are discussed below and alternative values are being proposed in some cases.

Following the discussion in Section 7.6, K_d values are provided for the different degradation states of hydrated cement as outlined in Section 7.4 (states I, II, IIIa, IIIb). These can be linked to reference periods in the repository evolution via pH value and mineralogical characteristics (C/S ratio, presence or absence of portlandite and Ca-aluminates).

These tables give values corresponding to non-saline conditions. For those radionuclides where the effect of salinity is deemed significant, an additional discussion is provided further below. The effect of organic complexants on sorption is evaluated in the **Waste process report**, the corresponding no-effect levels of organics or reductions factors, where appropriate, are also given in a separate table further below.

Where values given in Table 7-7 to Table 7-9 are not taken directly from Wang et al. (2009) or Ochs et al. (2011), additional comments are provided below. This applies especially to values recommended for state III, because these authors do not explicitly distinguish between the different parts of state III.

Note also that the values given in Table 7-7 to Table 7-9 correspond to sorption on pure hydrated cement paste (HCP). Values for the various cement-based materials listed in Table 7-1 are given in the appendix. For the calculation of the values in the appendix, it is assumed that only HCP will be involved in the uptake of radionuclides, which may be conservative in the case of some elements (e.g., Cs could sorb stronger on some aggregate materials than on HCP). K_d values for the cement-based materials are calculated using the composition given in Table 7-1.

- Actinium: No data are given in Wang et al. (2009) and Ochs et al. (2011), and no other sorption data were found. As pointed out above in the section on bentonite, lanthanide elements are considered as a reasonable chemical analogue for Ac. This analogy had also been used by Wieland and Van Loon (2002). For the present purpose, the values selected for lanthanides and trivalent actinides are applied directly. Considering the consistently high sorption observed for these elements, no additional conservatism is introduced for Ac.
- Silver: No sorption data on cement/concrete are available, to our knowledge. Ochs et al. (2011) give a best estimate on the basis of an experimental sorption value for Ag on calcite; they give no upper limit and propose zero sorption as lower limit. However, they were specifically considering a concrete with calcareous aggregate. For the present purpose, the value for calcite is accepted as upper limit for states I & II. As lower limit, zero sorption is assumed, and no best estimate is given. Depending on the type of simulation (see Gaucher et al. 2005, Cronstrand 2007), calcite may have disappeared in state III. Thus, no sorption of Ag is assumed for either part of state III (pH 12 and 10.5).
- Americium: The values from Wang et al. (2009) are directly accepted. Based on the available experimental data, no distinction between the different parts of state III is warranted.
- Barium: No values are given in Wang et al. (2009) or Ochs et al. (2011). The behaviour of Ba can be expected to be intermediate between Sr and Ra. Conservatively, the lower values given for Sr are recommended.
- Carbon (^{14}C): Sorption of carbon depends strongly on the form in which it is present (inorganic carbonate species and organic forms). Further, different types of uptake processes need to be considered in case of carbonate.

The uptake of inorganic forms of carbon (carbonate species) by hydrated cement can occur through various sorption reactions or by isotopic exchange. Isotopic exchange is mainly important in the presence of solid carbonates (mainly calcite), while sorption can take place on hydrated cement paste (CSH-phases) (Wang et al. 2009).

Several critical uncertainties need to be considered for the calculation of K_d based on isotopic exchange with solid carbonate (calcite). While the total carbonate content can be measured in fresh concrete or mortar, it only can be estimated for material degraded under in situ conditions. Ideally, such estimations should be based on a good geochemical model for the development of solid and dissolved carbonate concentrations in the concrete as a function of degradation, taking into account initial composition and groundwater chemistry. Second, an estimate is needed regarding the actual availability of solid carbonates for isotope exchange. Bradbury and Sarott (1995) assumed 10% of all calcite in the cement system to be available for this process, while Pointeau et al. (2002) used a much smaller value of about 0.5% for calcite fines, based on more systematic measurements.

For the concrete used in SFR, a solid carbonate concentration of 0.65 moles CO_3/kg concrete can be calculated from the measurements of Ecke and Hansson (2012). Assuming this value also for State II in combination with a dissolved carbonate concentration of $6 \cdot 10^{-6}$ M (SKB 2001) would result in a K_d of about $11 \text{ m}^3/\text{kg}$ using the approach of Bradbury and Sarott (1995) (10% availability of calcite). Using the availability estimate of Pointeau et al. (2002) would give a K_d of about $0.6 \text{ m}^3/\text{kg}$.

On the other hand, the extent of sorption can only be assessed on the basis of experimental data from systems where no solid carbonates are present. Such sorption data for the sorption of $^{14}\text{CO}_3$ on CSH are available from Noshita et al. (2001) and indicate a K_d of about 2–4 m^3/kg . In terms of chemical conditions, these data correspond to degradation state II.

Wang et al. (2009) further list selected sorption data from HCP systems where the dissolved carbonate concentration was below the solubility limit of calcite. While isotope exchange may play a role in these systems, they are conservative in the sense that $^{14}\text{CO}_3$ can only interact with CSH and relatively small amounts of (pre-existing) calcite, but cannot co-precipitate with calcite.

Based on the evidence discussed above, K_d values for $^{14}\text{CO}_3$ are proposed as follows:

- Largely, the general approach and recommended values of Wang et al. (2009) are accepted. It needs to be pointed out that all underlying experimental data represent sorption on CSH and HCP. K_d values recommended on this basis are considered to be more reliable and more conservative than values calculated on the basis of isotopic exchange, in view of the uncertainties regarding the detailed ratio of dissolved/solid carbonate in phase II/III and especially regarding the accessibility of the calcite present.
 - The lower limit is based on the assumption that only sorption of $^{14}\text{CO}_3$ on CSH will take place; i.e. that no calcite will be present. The recommended K_d value of 2 m^3/kg corresponds directly to the data for CSH by Noshita et al. (2001), which are directly applicable to state II. No experimental data on CSH are available for states I and III; therefore, the recommended values are based on the value for state II and the trend of $^{14}\text{CO}_3$ sorption on HCP illustrated in Wang et al. (2009) (considering in particular the data by Pointeau et al. 2008).
 - The best estimate takes into account the range of values measured for CSH as well as further data on HCP. The data given in Wang et al. (2009) span a range of about 2–10 m^3/kg for state II, the proposed best estimate of 5 m^3/kg corresponds to the centre of that range. Considering that in addition to sorption on CSH, isotope exchange with calcite will take place to some degree, this is a reasonable value.
 - The upper limit of 20 m^3/kg for state II can be based on taking into account isotope exchange with calcite and considering some uncertainty in the predicted ratio of dissolved/solid carbonate concentration. Wang et al. (2009) give no upper/lower limit for the sorption of carbonate in state III, due to the lack of data especially for the 2nd half of state III. For the first part of state III (pH 12), the bounding values are estimated directly from the data by Pointeau et al. (2008) and Bayliss et al. (1988) (given in Wang et al. 2009). For the second part of state III (pH 10.5), the trend indicated by the data of Pointeau et al. (2008) is again used as reference.
 - For simple organic compounds, Wang et al. (2009) conservatively propose a value of zero, although it is acknowledged that sorption is very low but not zero. However, they felt that there is not enough information available to establish a non-zero value. For the cement-based barriers in SFR, the conservative choice of $K_d = 0$ is adopted for ^{14}C in organic form.
- Cadmium: Only very few data are available for Cd (see also the **Waste process report**. Wang et al. (2009) and Ochs et al. (2011), as well as earlier reports on the derivation of sorption values for cement systems (Wieland and Van Loon 2002, Andra 2005) give no value for Cd. The studies of Pomiès et al. (2001) and Poletti et al. (2002) indicate appreciable sorption of Cd to CSH and hydrated cement, most likely by exchanging against Ca in the CSH and portlandite structure. but do not allow to extract actual sorption data due to experimental limitations (**Waste process report**). Based on the aqueous chemistry of Cd, reasonable analogues would be divalent B-type metal ions, such as Ni or Pb, for which sorption data are available. Due to the particular uptake mechanism of Ni, this element is not useful, however. Therefore, it is proposed to base the data for Cd on the values selected for Pb by Ochs et al. (2011). The available data shown there and in Ochs et al. (2003) indicate a strong increase of Pb sorption with increasing degradation (i.e. with decreasing pH from state I to III). To remain on the conservative side, and to acknowledge the additional uncertainty due to the analogy use, the Pb data selected for state I by Ochs et al. (2011) are being used conservatively for all degradation states, and an additional reduction factor of 5 is applied.
 - Calcium: Ca is a main component of various minerals that make up the HCP matrix. HCP pore solutions are saturated with respect to dissolved (stable) Ca. Therefore, it can be expected that the solid/solution partitioning of radioactive Ca will take place by isotopic exchange with stable Ca (Wieland and Van Loon 2002, Ochs et al. 2011). To define a corresponding, nominal K_d value, the concentration of stable Ca in the cement/concrete and the accessibility of this stable Ca pool need to be known, as well as the dissolved Ca concentration in the corresponding equilibrium solutions.

In states I and II of cement degradation, total Ca solubility is controlled by portlandite, whereas in state III it is controlled by CSH, under normal conditions. Accordingly, for both portlandite and CSH, their contribution to the total Ca content of HCP plus the corresponding accessibility factors have to be estimated. However, these relations are not well established for the cement/concrete components of SFR. To estimate a nominal K_d value corresponding to isotopic exchange, the following approach was taken:

- The concentration of stable Ca in HCP can be estimated from the amount of relevant solid phases (portlandite, CSH, etc) present during the various degradation states. To a first approximation, this information could be taken from the models of Gaucher et al. (2005) and Cronstrand (2007). However, the two models predict different amounts of relevant mineral phases (with variable Ca-content) for states I to III. Further, both studies consider different scenarios that lead to different conditions in the various compartments of SFR. The large spread of conditions and results makes it extremely difficult to select a set of reference data for deriving a nominal K_d .
- A comparison of the model results in Gaucher et al. (2005) and Cronstrand (2007) shows that the results by Cronstrand (2007) are more conservative in the sense that Ca-containing minerals are being degraded faster. Most relevant are the results for the outer concrete part of BMA, because there degradation is predicted to proceed into state III. Cronstrand (2007) further shows that the different scenarios considered give very similar results for BMA.
- Based on these considerations, scenario A for the concrete of BMA was selected as reference. Conservatively, only the Ca contained in portlandite and CSH phases was considered, Ca contained in further minerals (including calcite) was neglected. The amount of portlandite and CSH present was estimated from the composition predicted for 0–1,000 years for state I (pH > 13), 10,000–50,000 years for state II (pH 12.5), and 100,000 years for state IIIa (pH ≈ 12). For state IIIb (pH ≈ 10.5), no data are available in Cronstrand (2007) (or Gaucher et al. 2005), as such a pronounced degradation is not considered. The Ca content was estimated by considering the same amount of CSH present as in state IIIa, but with a C/S of 0.83 instead of 1.1. The total concentration of Ca in the solid phase was calculated from the molar volume of the mineral phases and their stoichiometry; results were normalised to pure HCP assuming 22% HCP in the concrete (see Table 7-1).
- The dissolved concentration of Ca corresponding to each pH value was taken from the model calculations of Wang et al. (2009).
- As experimentally determined accessibility factors are not available, the required values were evaluated as follows: Best estimate and upper limit were defined in analogy to the accessibility of Ni in LDH, where Wieland et al. (2006) determined values in the range of 2.8–4.5%. For the present case, 2.0% and 5.0% were used as best estimate and upper limit, respectively. For the lower limit, the lowest accessibility factor considered by Ochs et al. (2011), 0.08% for Ca in calcite, was used.

The resulting K_d values appear to be conservative in comparison with the values calculated by Ochs et al. (2011) for the exchange of radioactive Ca with stable Ca in calcite and also in comparison with the values calculated by Wieland and Van Loon (2002) for whole HCP.

- Chloride and iodide: Values for all degradation states are taken directly from Wang et al. (2009); their value for state III is considered applicable to pH 10.5 and pH 12. The selected values refer to total chloride concentrations larger than about 1 mM (but not to saline conditions). For lower chloride concentrations, much higher sorption can be expected (see Wang et al. (2009) and the **Waste process report**), however, such low chloride concentrations are viewed as not representative for the present case. The best estimate value for iodide is close to the lower end of the data range, because Wang et al. (2009) placed more weight on diffusion-derived sorption values than on values from batch experiments. This had been done to account for uncertainties in the effect of the solid/liquid ratio on sorption.
- Curium: Wang et al. (2009) and Ochs et al. (2011) give no data for Cm, and no systematic data are available, to our knowledge. Based on the very similar chemistry of Am and Cm, the values selected for Am are also proposed for Cm.
- Cobalt: Wang et al. (2009) and Ochs et al. (2011) give no data for Co. Some uptake data are available, but these are likely to include precipitation (e.g. Kaplan et al. 2008). On the other hand, based on some literature as well as in-house data, Wieland and Van Loon (2002) argue that Co is not taken up by a sorption process, but is showing a solubility-limited behaviour similar to Ni.

In lack of any better evidence, this is accepted for the present purpose. As a cautious approach, the values estimated for Ni are reduced by a factor of five.

- Caesium: For state I, Wang et al. (2009) indicate only a range of values (with a conservative lower limit), but give no best estimate. Based on the best estimate for state II and considering the data shown in Figure 38 of Wang et al. (2009) as well as the increased competition by alkali ions in state I, a best estimate of $1 \cdot 10^{-3} \text{ m}^3/\text{kg}$ is proposed here. All other values are taken directly from Wang et al. (2009). As very few data are available for the second part of state III, the values selected for pH 12 are also proposed for pH 10.5. Considering the trend of increasing sorption with decreasing pH shown by Cs, this is viewed as a cautious approach. Note that a few additional studies (e.g. Volchek et al. 2011) have become available since the publication of Wang et al. (2009); these concern states I or II and do not provide new information in the light of the large number of studies evaluated by Wang et al. (2009). Accordingly, the carefully evaluated values from Wang et al. (2009) are still considered to give the best representation of the state of the art.
- Europium, samarium and holmium: Wang et al. (2009) and Ochs et al. (2011) give no recommended data for Eu, but Wang et al. (2009) use experimental data of both Am and Eu in their evaluation of Am uptake. The available data indicate a higher sorption for Eu than for Am in state I. No reliable and systematic data are available for Eu sorption in the other states, to our knowledge. For the present purpose, a conservative approach is followed and the data for Eu are based on analogy with Am. The same approach is followed for the other lanthanide elements of concern, Sm and Ho.
- Molybdenum: The sorption of molybdate is strongly related to the presence of ettringite, see the **Waste process report**. Accordingly, Ochs et al. (2011) give values for state III considering the presence and absence of ettringite. As pointed out above, ettringite is assumed to be present during states I, II and the first part of state III, and the values selected by Ochs et al. (2011) for the presence of ettringite are accepted in these cases. On the other hand, the presence of ettringite is not clearly established for the second part of state III, and it is also not likely that a large amount of calcite will be present. Therefore, zero sorption of molybdate has to be assumed.
- Niobium: Wang et al. (2009) give the same K_d values for all degradation states. Their recommended values are accepted for states I and II and the first part of state III. However, they do not consider explicitly the second part of state III, and the underlying experimental data could indicate a downward trend of sorption in this region. Therefore, it is proposed to reduce the values for the second part of state III by an order of magnitude.
- Nickel: Based on a review of the relevant literature, Wang et al. (2009) conclude that the uptake of radioactive Ni by hydrated cement is due to isotopic exchange with stable Ni and not to sorption. Earlier reviews by Andra (2005) and Wieland and Van Loon (2002) arrived also at this conclusion. The solubility of Ni in hydrated cement systems is very low, with a Ni-substituted Al-layered double hydroxide (LDH) controlling the solubility in all likelihood. As a result, the low concentration of stable Ni that is typically present in any cement/concrete is sufficient to reach the corresponding solubility limit in the porewater. The partitioning of introduced radioactive Ni is then controlled by isotope dilution rather than by a chemical process. In order to define an apparent K_d value, the concentration of stable Ni in the cement/concrete as well as the accessibility of this stable Ni pool need to be known. As this is not the case for the present system, recommended values are based on the abovementioned literature:
 - Wang et al. (2009) used site-specific Ni concentrations in the cement and porewater and accessibility factors of 0.028 and 0.045, based on Wieland et al. (2006). Together with uncertainties in total Ni content and Ni solubility, this resulted in a total range of K_d values of about 0.02 to $4.5 \text{ m}^3/\text{kg}$.
 - Using a measured total Ni content of $5.6 \cdot 10^{-4} \text{ moles/kg}$ for a CEM-V cement, measured Ni solubilities in porewaters as a function of degradation and accessibility factors of 0.02–1.0, Andra (2005) estimated K_d values of about 0.05– $2.4 \text{ m}^3/\text{kg}$ for states I–III. Based on a similar approach, Wieland and Van Loon (2002) estimated K_d values of about 0.04 to $2.0 \text{ m}^3/\text{kg}$ (presumably, their values apply mainly to state II).

It appears that relatively similar values are derived, despite differences in the system-specific data. Therefore, recommended values for SFR are based on the above literature values (even though site-specific data should be used in a strict sense). Specifically, the values calculated by Wang et al. (2009)

are considered, as they address the different states in the most transparent fashion (their value for state III is considered valid for pH 10.5 and pH 12). To take into account the lack of site-specific data, these values are further reduced by factor 2 (rounded).

- Neptunium: For the different oxidation states, the following approach is taken:
 - For Np(IV), Wang et al. (2009) recommend the same values as for Th. These data are directly accepted, as the few available Np(IV) data are consistent with the much broader database for Th. Both experimental sorption data as well as expected speciation of Th indicate constant sorption over all degradation states.
 - For Np(V), Wang et al. (2009) give only lower limits, which are taken from Wieland and Van Loon (2002). Due to the lack of experimental data, they had conservatively estimated K_d values for Np(V) on the basis of sorption data for divalent metal ions, as these have an effective charge similar to those of pentavalent actinide oxo-cations. Their assessment is accepted for the present case as well. No distinction between degradation states is made.
- Protactinium: Recommended values for Pa are given in Wang et al. (2009), but the underlying database is very limited:
 - As best estimate for Pa(IV), Wang et al. (2009) use the analogy with Th. This is directly accepted for all degradation states. Wang et al. (2009) give no upper or lower limits, however. We propose to use the same upper limit as for Th and to reduce the lower limit by a factor of 5.
 - For Pa(V), Wang et al. (2009) give recommended values, based on a single literature study and circumstantial evidence from Pa(V) sorption on geological materials. As there is also no good chemical analogue for Pa(V), their values are directly accepted. Based on the fairly constant Pa(V) sorption as a function of pH observed on bentonite (see above), the same value are proposed for both parts of state III.
- Lead: The values proposed by Ochs et al. (2011) are directly accepted. Their value given for state III is considered to be valid at pH 12. The underlying data from Andra (2005) and Pointeau (2000) as well as the model analysis by Ochs et al. (2003) indicate that sorption should be greater at pH 10.5 than at pH 12. Conservatively, the respective value of Ochs et al. (2011) is proposed here for both parts of state III.
- Palladium: In the absence of relevant data, the approach of Ochs et al. (2011) was followed and Pb was used as analogue. The best estimate and upper limit selected for Pb are directly accepted. For the lower limit, the corresponding values for Pb were reduced by an order of magnitude. Both the trend observed for Pb (see above) as well as the speciation of Pd (formation of negatively charged hydrolytic species above $\text{pH} \approx 10$, cf. Ochs et al. 2011) indicate potentially stronger sorption at pH 10.5 than at pH 12. Therefore, the value selected for State IIIa is also proposed for state IIIb.
- Polonium: No values for Po are given in Wang et al. (2009) and Ochs et al. (2011). No other sorption data are available, to our knowledge. In the section addressing data for sorption on bentonite above, it is argued that selenite may be an appropriate chemical analogue. Considering that sorption on HCP is more complex in comparison to bentonite, this analogy is adopted conservatively as follows: the values selected for Se(IV) are reduced by an order of magnitude; the lower limit is set to zero.
- Plutonium: Wang et al. (2009) give best estimate and the corresponding upper/lower limits for Pu(IV), which are directly accepted. The compiled experimental data are consistent with the Th data and do not indicate a decrease of sorption with progressing degradation. For the other oxidation states, no or no complete set of data is proposed and the following approach is taken:
 - No values are given for Pu(III) or Pu(V), because no reliable experimental data are available for these oxidation states. Therefore, we are proposing the same values as for Am(III) and Np(V), respectively.
 - For Pu(VI), only a best estimate is given by Wang et al. (2009), based on analogy with U(VI). For the present purpose, this analogy is extended to the upper/lower limits.
- Radium: The values given in Wang et al. (2009) for states I and II are directly accepted. In contrast to Sr, the available experimental data do not extend to pH values below ≈ 11.5 . The values recommended by Wang et al. (2009) for state III are therefore considered valid for pH 12. Taking into account the general trend of sorption vs. pH shown for both Sr and Ra in Wang et al. (2009), higher sorption should be expected for pH 10.5. Considering the lack of direct confirmation through experimental sorption data, it is proposed to conservatively use the values for pH 12 also for the second part of state III.

- Selenium: Sorption behaviour and data situation is dependent on the respective oxidation state. Values for Se(IV) and Se(VI) are directly taken from Ochs et al. (2011). The values for Se(VI) in the first part of state III (IIIa) are based on the presence of ettringite; see Gaucher et al. (2005) and Cronstrand (2007)), those for the second part of state III (IIIb) are based on the absence of ettringite. As discussed for molybdate above, zero sorption has to be assumed in this case. On the other hand, Se(IV) appears to sorb on a variety of HCP minerals, and the available data indicate fairly constant sorption across states II–III. For selenide (Se(–II)), no data are available, to our knowledge. Ochs et al. (2011) conservatively propose a value of zero throughout, although they expect that Se(–II) may be immobilised by hydrated cement. Their recommendation is accepted, considering that zero sorption is also proposed for bentonite (see above). Se(0) is not treated, as it is considered to be practically insoluble (this is likely to hold also for selenide).
- Tin: Selected values for states I & II are taken directly from Ochs et al. (2011). For state III, no directly applicable experimental data are available, and Ochs et al. (2011) give a very conservative estimate of 0.003 m³/kg. This is based on the assumption that HCP minerals (especially CSH and ettringite) have disappeared and that calcite is the only remaining sorbing phase. Moreover, it is stated in Ochs et al. (2011) that sorption values in state III with CSH and ettringite present would be close to values in state II. This is corroborated by the sorption data of Sn(IV) on various CSH phases given in Andra (2005), which show approximately constant sorption within a range of C/S from 1.65 to 0.83. These data were all measured at pH ≈ 12.5, but the hydrolysis behaviour of Sn(IV) suggests that sorption should increase when pH is lowered from pH 12.5 towards pH 9, as the negatively charged and highly hydrolysed species become less important. Therefore, the following approach is taken for state III:
 - The upper limit for the first part of state III is directly taken from state II. Best estimate and lower limit are taken as 0.5 × the value for state II, to acknowledge the slightly greater uncertainty.
 - In the second part of state III, ettringite may have disappeared, which may have some influence on sorption. CSH still will be present, however. To acknowledge the greater uncertainty in comparison to state II, best estimate and lower limit are reduced by a factor of 5, while the upper limit is directly accepted. This is viewed as sufficiently conservative, since the sorption of other elements with approximately similar behaviour shows either constant (Th) or increasing (Pb, Zr) sorption with increasing degradation, as long as CSH are present.
- Technetium: For Tc(IV), the experimental data given in Wang et al. (2009) indicate constant sorption over all degradation states, and their recommended values are directly accepted. For Tc(VII), Wang et al. (2009) provide a best estimate on the basis of very few available experimental data, but give no bounding values. Considering the data situation, upper and lower limits are arbitrarily set an order of magnitude higher and lower, respectively. For the second part of state III, zero sorption has to be assumed, following the argumentation for other oxo-anions above.
- Strontium: The values given in Wang et al. (2009) for states I and II are directly accepted. Taking into account the trend of sorption vs. pH shown for both Sr and Ra in Wang et al. (2009), we consider their value given for state III as justified for pH 10.5. On the other hand, it is proposed to reduce the best estimate and lower limit for pH 12 by one order of magnitude in comparison to the values for pH 10.5.
- Thorium: The values given in Wang et al. (2009) are directly accepted. The underlying data indicate constant sorption over all degradation states.
- Uranium: The data proposed by Wang et al. (2009) for U(VI) are directly accepted. The underlying experimental data indicate constant sorption within state III. For U(IV), Wang et al. (2009) give the same values for as for Th in case of states II and III, whereas a lower value is proposed for state I. The underlying experimental data as well the speciation of U(IV) indicate constant sorption over state III. Wang et al. (2009) give no upper and lower limits for U(IV). In these cases, the values given for Th in the same reference are proposed.
- Zirconium: Recommended values for states II & III are taken directly from Ochs et al. (2011). The underlying experimental data indicate constant sorption across state III. No experimental data are available that correspond directly to state I, however. Based on the hypothesis that the observed trend in Zr sorption is mainly related to the mineralogy of hydrated cement (rather than the aqueous Zr speciation), Ochs et al. (2011) propose the same upper and lower limit as for state II, but give no best estimate. To take into account the additional uncertainty, we propose as best estimate half the corresponding value for state II. It can be seen that the resulting values are conservative in comparison to the values for +IV-valent actinides or Sn, which may be considered as reasonable analogues.

Table 7-7. Distribution coefficients (K_d) for hydrated cement paste, corresponding to degradation state I. The listed values correspond to non-saline conditions and absence of organic complexants.

Radionuclide (oxidation state)	K_d (m ³ /kg)	Upper K_d limit (m ³ /kg)	Lower K_d limit (m ³ /kg)
Ac(III)	1.00E+01	5.00E+03	1.00E-01
Ag(I)	0	1E-03	0
Am(III)	1.00E+01	5.00E+03	1.00E-01
Ba(II)	1.00E-01	3.00E-01	3.00E-02
¹⁴ C, carbonate species	2.00E+00	3.00E+00	7.00E-01
¹⁴ C, CH ₄ , organic acids	0	0	0
Ca(II)	3.54E-02	8.86E-02	1.42E-03
Cd(II)	6.00E-02	2.00E-01	2.00E-02
Cl(-I)	1.00E-03	1.00E-02	2.00E-04
Cm(III)	1.00E+01	5.00E+03	1.00E-01
Co(II)	6.00E-03	8.00E-02	4.00E-03
Cs(I)	1.00E-03	1.00E-02	1.00E-04
Eu(III)	1.00E+01	5.00E+03	1.00E-01
Ho(III)	1.00E+01	5.00E+03	1.00E-01
I(-I)	1.00E-03	1.00E-02	0
Mo(VI)	3.00E-03	3.30E-02	3.00E-04
Nb(V)	5.00E+01	1.00E+03	1.00E+00
Ni(II)	3.00E-02	4.00E-01	2.00E-02
Np(IV)	3.00E+01	1.00E+03	1.00E+00
Np(V)	1.00E-01	1.40E-01	7.10E-02
Pa(IV)	3.00E+01	1.00E+03	2.00E-01
Pa(V)	1.00E+01	1.00E+03	5.00E-01
Pb(II)	3.00E-01	1.00E+00	1.00E-01
Pd(II)	3.00E-01	1.00E+00	1.00E-02
Po(IV)	2.00E-02	6.00E-01	0
Pu(III)	1.00E+01	5.00E+03	1.00E-01
Pu(IV)	5.00E+00	1.00E+03	1.00E+00
Pu(V)	1.00E-01	1.40E-01	7.10E-02
Pu(VI)	2.00E+00	1.00E+01	4.00E-01
Ra(II)	3.00E-01	1.00E+00	1.00E-01
Se(-II)	0	0	0
Se(IV)	2.00E-01	6.00E+00	1.00E-02
Se(VI)	3.00E-03	2.00E-02	1.00E-03
Sm(III)	1.00E+01	5.00E+03	1.00E-01
Sn(IV)	2.00E+01	2.00E+02	1.00E+01
Sr(II)	1.00E-01	3.00E-01	3.00E-02
Tc(IV)	3.00E+00	2.00E+01	7.00E-01
Tc(VII)	1.00E-03	1.00E-02	1.00E-04
Th(IV)	3.00E+01	1.00E+03	1.00E+00
U(IV)	3.00E+01	1.00E+03	1.00E+00
U(VI)	2.00E+00	1.00E+01	4.00E-01
Zr(IV)	5.00E+00	1.00E+02	1.00E-01

Table 7-8. Distribution coefficients (K_d) for hydrated cement paste, corresponding to degradation state II. The listed values correspond to non-saline conditions and absence of organic complexants.

Radionuclide (oxidation state)	K_d (m ³ /kg)	Upper K_d limit (m ³ /kg)	Lower K_d limit (m ³ /kg)
Ac(III)	1.00E+01	5.00E+03	1.00E+00
Ag(I)	0	1E-03	0
Am(III)	1.00E+01	5.00E+03	1.00E+00
Ba(II)	3.00E-02	1.00E-01	5.00E-03
¹⁴ C, carbonate species	5.00E+00	2.00E+01	2.00E+00
¹⁴ C, CH ₄ , organic acids	0	0	0
Ca(II)	3.09E-03	7.72E-03	1.23E-04
Cd(II)	6.00E-02	2.00E-01	2.00E-02
Cl(-I)	1.00E-03	1.00E-02	2.00E-04
Cm(III)	1.00E+01	5.00E+03	1.00E+00
Co(II)	4.00E-02	4.00E-01	1.60E-02
Cs(I)	2.00E-03	5.00E-02	1.00E-04
Eu(III)	1.00E+01	5.00E+03	1.00E+00
Ho(III)	1.00E+01	5.00E+03	1.00E+00
I(-I)	1.00E-03	1.00E-02	0
Mo(VI)	3.00E-03	3.30E-02	3.00E-04
Nb(V)	5.00E+01	1.00E+03	1.00E+00
Ni(II)	2.00E-01	2.00E+00	8.00E-02
Np(IV)	3.00E+01	1.00E+03	1.00E+00
Np(V)	1.00E-01	1.40E-01	7.10E-02
Pa(IV)	3.00E+01	1.00E+03	2.00E-01
Pa(V)	1.00E+01	1.00E+03	5.00E-01
Pb(II)	3.00E+00	1.00E+01	1.00E+00
Pd(II)	3.00E+00	1.00E+01	1.00E-01
Po(IV)	2.00E-02	6.00E-01	0
Pu(III)	1.00E+01	5.00E+03	1.00E+00
Pu(IV)	3.00E+01	1.00E+03	1.00E+00
Pu(V)	1.00E-01	1.40E-01	7.10E-02
Pu(VI)	3.00E+01	3.00E+02	3.00E+00
Ra(II)	1.00E-01	1.00E+00	1.00E-03
Se(-II)	0	0	0
Se(IV)	2.00E-01	6.00E+00	1.00E-02
Se(VI)	3.00E-03	1.00E-02	1.00E-03
Sm(III)	1.00E+01	5.00E+03	1.00E+00
Sn(IV)	2.00E+01	2.00E+02	1.00E+01
Sr(II)	3.00E-02	1.00E-01	5.00E-03
Tc(IV)	3.00E+00	2.00E+01	7.00E-01
Tc(VII)	1.00E-03	1.00E-02	1.00E-04
Th(IV)	3.00E+01	1.00E+03	1.00E+00
U(IV)	3.00E+01	1.00E+03	1.00E+00
U(VI)	3.00E+01	3.00E+02	3.00E+00
Zr(IV)	1.00E+01	1.00E+02	1.00E-01

Table 7-9. Distribution coefficients (K_d) for hydrated cement paste, corresponding to the first part of degradation state III (state IIIa, pH 12). The listed values correspond to non-saline conditions and absence of organic complexants.

Radionuclide (oxidation state)	K_d (m ³ /kg)	Upper K_d limit (m ³ /kg)	Lower K_d limit (m ³ /kg)
Ac(III)	1.00E+01	5.00E+03	3.00E+00
Ag(I)	0	0	0
Am(III)	1.00E+01	5.00E+03	3.00E+00
Ba(II)	1.00E-02	3.00E+00	1.00E-03
¹⁴ C, carbonate species	2.00E+00	5.00E+00	5.00E-01
¹⁴ C, CH ₄ , organic acids	0	0	0
Ca(II)	3.09E-03	7.73E-03	1.24E-04
Cd(II)	6.00E-02	2.00E-01	2.00E-02
Cl(-I)	1.00E-03	1.00E-02	2.00E-04
Cm(III)	1.00E+01	5.00E+03	3.00E+00
Co(II)	4.00E-02	4.00E-01	1.60E-02
Cs(I)	2.00E-02	3.00E-01	1.00E-03
Eu(III)	1.00E+01	5.00E+03	3.00E+00
Ho(III)	1.00E+01	5.00E+03	3.00E+00
I(-I)	1.00E-03	1.00E-02	0
Mo(VI)	3.00E-03	3.30E-02	3.00E-04
Nb(V)	5.00E+01	1.00E+03	1.00E+00
Ni(II)	2.00E-01	2.00E+00	8.00E-02
Np(IV)	3.00E+01	1.00E+03	1.00E+00
Np(V)	1.00E-01	1.40E-01	7.10E-02
Pa(IV)	3.00E+01	1.00E+03	2.00E-01
Pa(V)	1.00E+01	1.00E+03	5.00E-01
Pb(II)	3.00E+01	1.00E+02	1.00E+00
Pd(II)	3.00E+01	1.00E+02	1.00E-01
Po(IV)	2.00E-02	6.00E-01	0
Pu(III)	1.00E+01	5.00E+03	3.00E+00
Pu(IV)	3.00E+01	1.00E+03	1.00E+00
Pu(V)	1.00E-01	1.40E-01	7.10E-02
Pu(VI)	3.00E+01	3.00E+02	1.00E+01
Ra(II)	8.00E-01	8.00E+00	8.00E-02
Se(-II)	0	0	0
Se(IV)	2.00E-01	6.00E+00	1.00E-02
Se(VI)	3.00E-03	1.00E-02	1.00E-03
Sm(III)	1.00E+01	5.00E+03	3.00E+00
Sn(IV)	1.00E+01	2.00E+02	5.00E+00
Sr(II)	1.00E-02	3.00E+00	1.00E-03
Tc(IV)	3.00E+00	2.00E+01	7.00E-01
Tc(VII)	1.00E-03	1.00E-02	1.00E-04
Th(IV)	3.00E+01	1.00E+03	1.00E+00
U(IV)	3.00E+01	1.00E+03	1.00E+00
U(VI)	3.00E+01	3.00E+02	1.00E+01
Zr(IV)	1.00E+02	5.00E+02	1.00E+00

Table 7-10. Distribution coefficients (K_d) for hydrated cement paste, corresponding to the second part of degradation state III (state IIIb, pH 10.5). The listed values correspond to non-saline conditions and absence of organic complexants.

Radionuclide (oxidation state)	K_d (m ³ /kg)	Upper K_d limit (m ³ /kg)	Lower K_d limit (m ³ /kg)
Ac(III)	1.00E+01	5.00E+03	3.00E+00
Ag(I)	0	0	0
Am(III)	1.00E+01	5.00E+03	3.00E+00
Ba(II)	1.00E-01	3.00E+00	1.00E-02
¹⁴ C, carbonate species	7.00E-01	2.00E+00	1.00E-01
¹⁴ C, CH ₄ , organic acids	0	0	0
Ca(II)	4.67E-02	1.17E-01	1.87E-03
Cd(II)	6.00E-02	2.00E-01	2.00E-02
Cl(-)	1.00E-03	1.00E-02	2.00E-04
Cm(III)	1.00E+01	5.00E+03	3.00E+00
Co(II)	4.00E-02	4.00E-01	1.60E-02
Cs(I)	2.00E-02	3.00E-01	1.00E-03
Eu(III)	1.00E+01	5.00E+03	3.00E+00
Ho(III)	1.00E+01	5.00E+03	3.00E+00
I(-)	1.00E-03	1.00E-02	0
Mo(VI)	0	0	0
Nb(V)	5.00E+00	1.00E+02	1.00E-01
Ni(II)	2.00E-01	2.00E+00	8.00E-02
Np(IV)	3.00E+01	1.00E+03	1.00E+00
Np(V)	1.00E-01	1.40E-01	7.10E-02
Pa(IV)	3.00E+01	1.00E+03	2.00E-01
Pa(V)	1.00E+01	1.00E+03	5.00E-01
Pb(II)	3.00E+01	1.00E+02	1.00E+00
Pd(II)	3.00E+01	1.00E+02	1.00E-01
Po(IV)	2.00E-02	6.00E-01	0
Pu(III)	1.00E+01	5.00E+03	3.00E+00
Pu(IV)	3.00E+01	1.00E+03	1.00E+00
Pu(V)	1.00E-01	1.40E-01	7.10E-02
Pu(VI)	3.00E+01	3.00E+02	1.00E+01
Ra(II)	8.00E-01	8.00E+00	8.00E-02
Se(-II)	0	0	0
Se(IV)	2.00E-01	6.00E+00	1.00E-02
Se(VI)	0	0	0
Sm(III)	1.00E+01	5.00E+03	3.00E+00
Sn(IV)	4.00E+00	2.00E+02	2.00E+00
Sr(II)	1.00E-01	3.00E+00	1.00E-02
Tc(IV)	3.00E+00	2.00E+01	7.00E-01
Tc(VII)	1.00E-03	1.00E-02	1.00E-04
Th(IV)	3.00E+01	1.00E+03	1.00E+00
U(IV)	3.00E+01	1.00E+03	1.00E+00
U(VI)	3.00E+01	3.00E+02	1.00E+01
Zr(IV)	1.00E+02	5.00E+02	1.00E+00

In contrast to the data for bentonite (Table 7-6), no explicit conversion to different conditions is required in case of cement systems, and no formal error calculations were carried out, therefore. The best estimates as well as the upper and lower limits are based directly on the available and reliable experimental data. Based on the experimental data, the resulting best estimates and limiting values for many of the radionuclides of concern are approximately symmetrical in the logarithmic space. Therefore, a continuous triangular probability distribution in the logarithmic space is generally recommended, with the best estimate as mode. For some radionuclides, this distribution will be somewhat skewed.

In some cases, it is not possible to use a log-triangular distribution. Despite their skewedness, the proposed linear triangular distributions are preferred over uniform distributions, which would also be possible but do not have a unique modal value.

- Silver: for states I and II, a skewed triangular distribution in the linear space is recommended, with $K_d = 0$ as minimum as well as modal value and with $1 \cdot 10^{-3} \text{ m}^3/\text{kg}$ as maximum value.
- Iodine: Again, a skewed triangular distribution in the linear space is recommended, with the best estimate K_d as mode.

Influence of saline conditions

The influence of saline water on sorption is difficult to quantify, as there are almost no systematic sorption data available that were measured as a function of salinity. A grouping of radionuclides according to the expected impact based on the reviews of Wang et al. (2009) and Ochs et al. (2011) is given in Section 7.6. Cronstrand (2005) indicates that reduction factors would be in the range of 5–10 for a number of radionuclides, but up to 100 for some like Sr. It is also not reported how these factors are derived, nor is any underlying information provided.

An approximate evaluation is given in Wang et al. (2009). They used a model developed by Wieland et al. (2008) and Tits et al. (2004) to calculate the effect of salinity on the K_d of Sr. Note that according to the grouping given in Section 7.6, Sr is one of the elements that should be most affected. For an increase in salinity from dilute solutions (less than 0.1 M) to a salinity of about 0.8 M, the calculated K_d decreases only by factor ≈ 2 . Considering the data range already considered by Wang et al. (2009) and Ochs et al. (2011) in defining the recommended values, it is concluded that no additional values need to be developed as long as salinity in the porewater does not exceed $\approx 0.8 \text{ M}$.

Influence of organic complexants

As pointed out in the **Waste process report**, the waste and in some cases the cement/concrete can introduce a range of soluble organic substances into the porewater. These substances may stem from the waste, but may also be part of the cementitious materials, e.g. in the form of organic concrete admixtures. Depending on their concentrations, these substances may have a significant effect on sorption. Previous work (Fanger et al. 2001) indicates that relevant organics include primarily the following classes of compounds (see the **Waste process report** for a more detailed discussion and underlying references):

- A number of well-defined complexing agents containing carboxylate functional groups, which stem mainly from decontamination processes at nuclear power plants (EDTA, NTA, as well as citric, gluconic and oxalic acid).
- Degradation products of cellulose (isosaccharinic acid, ISA).
- Concrete admixtures and their degradation products.

Considering the typical concentrations of Ca ions in cement/concrete systems, the approximate concentration limits given below can be expected. While these concentration ranges are considered in the derivation of sorption reduction factors, it has to be pointed out that assuming elevated concentrations of organics over long timeframes or in all states of degradation is a pessimistic approach. The organics of concern all sorb to HCP components: while the effect of sorption in the presence of radionuclides is taken into account in investigations of sorption reduction, and is therefore implicitly contained in the reduction factors, the effect of sorption of organic molecules is

also likely to lower their dissolved concentrations. Cellulose degradation to ISA is most important at very high pH (state I), and lower ISA concentrations should be expected as HCP degrades further (Wang et al. 2009). Further, in the presence of O₂, ISA is converted to simple organic acids with lower radionuclide complexation strength (Glaus and Van Loon 2009). For the present purpose, the following concentrations are considered:

- ISA: Bradbury and Van Loon (1998) measured a solubility of ≈ 10 mM (pH 12.5) to ≈ 40 mM (pH 13.3).
- EDTA, NTA, citrate, gluconate: No relevant limit expected.
- Oxalate: A concentration limit in the range of about 0.5–20 μ M can be expected, based on the range of commonly available solubility products and expected Ca-concentrations (not taking into account further reactions with other cations present in cement solutions).

The various processes of relevance regarding an influence of these organic substances on radionuclides sorption are discussed in the **Waste process report**; this discussion is not repeated here. Briefly, the complexation of organic substances with RN is important, but also the competition of these reactions by Ca-ions as well as the sorption behaviour of the organic substances themselves.

In view of these different interactions, it is admitted that the definition of reduction factors for radionuclide sorption is difficult, because these factors would depend not only on the concentration of organic substances but also on Ca concentration. Therefore, the potential impact of organic complexants is assessed as far as possible by defining limiting concentrations of organics below which no effects are expected. This is based on the experimental data and information discussed in the **Waste process report**. As discussed there, the available literature information does not nearly cover all the elements of concern, and is not conclusive for many of those cases where data are available.

As much as possible, the limiting concentrations and reduction factors summarised in Table 7-11 are directly based on experimental observations. To fill gaps in the experimental database, some analogies and approximations are used, as explained in the additional comments below. Similarly, it is pointed out where interpretations made in pertinent literature (e.g., Wang et al. 2009) are directly accepted.

In many cases, evidence regarding no-effect concentration and reduction factors is available only for ISA. As a first approximation, the respective values can be expected to be relevant for the other organic ligands as well, based on the complexation behaviour of ISA and some sketchy evidence for other ligands (see the **Waste process report** and the discussion for each element below). While this may lead to generally conservative values, the available evidence is not seen as complete enough to warrant the definition of separate reduction factors for each complexant.

To take this situation into account and for better transparency, Table 7-11 is divided into three parts:

- Values recommended on the basis of experimental evidence obtained for ISA are given in Table 7-11a.
- Values based on limited evidence for other ligands and/or analogy with ISA are given in Table 7-11b.
- Additional conservative values are given in Table 7-11c.

For the indicated no-effect concentrations and sorption reduction factors, the assessments by Wang et al. (2009), Ochs et al. (2011), Thomson et al. (2008) and Bradbury and Van Loon (1998) were considered in addition to the original literature quoted below and in the **Waste process report**. The reasoning regarding each proposed value is summarised below.

Regarding use of the values given in Table 7-11, it should be noted that the values in Table 7-11 are derived as generic values, independently of any expected inventory of organic substances. Further, as pointed out in several sections below, the best estimate values are in many cases cautious estimates, due to lacking specific information. Thus, additional conservative estimates are given for a few RN only.

- Effect of EDTA and NTA: Because of the strong competition of Ca for complexation by these compounds, it appears as a first approximation that their effect on radionuclide sorption is only relevant when their concentration exceeds the dissolved concentration of Ca (Dario et al. 2004). In detail, the effect will depend on the stabilities of all relevant species in the RN-EDTA-Ca-HCP system. The dissolved Ca concentration in equilibrium with portlandite and other HCP minerals can be estimated as approximately 1 mM (states I and III) to 10 mM (state II), depending on conditions (see e.g. Wang et al. 2009).
- Concrete admixtures and their degradation products are not considered explicitly. As pointed out in the **Waste process report**, none of these compounds contains functional groups with a higher affinity towards metal ions than the compounds already considered. Therefore, it can be assumed that any potential effects are within the ranges indicated.
- Ag: No quantitative information is available, and no realistic sorption reduction factor can be derived. Therefore, no realistic value is proposed. However, an arbitrary, conservative reduction factor of 100 is recommended for N-containing ligands (EDTA, NTA). As the complexation of Ag by EDTA is approximately comparable to the complexation of Ca, this is only applied to ligand concentrations above the dissolved Ca concentration. No effect is expected for organic O-ligands (hydroxo-carboxylic acids, see the **Waste process report**). To acknowledge the lack of information, an conservative factor of 10 is assigned arbitrarily for organic ligand concentrations > 10 mM.
- ¹⁴C: It can be expected that the presence of organic ligands will not influence the isotopic exchange process of ¹⁴CO₃ with calcite.
- Ca: It is not expected that the organic ligands will influence the isotopic exchange process of radioactive vs. stable Ca.
- Cd: The estimation given in Table 7-11 is based on analogy with Co and Ni on Ni-free model minerals (i.e. in a situation where Ni is taken up by sorption rather than by isotopic exchange), see the section on the effect of ISA on Ni-uptake in the **Waste process report**. Values for the other ligands are based on analogy with ISA due to lacking specific information.
- Cl and I: Following the **Waste process report**, no effects are expected.
- Cs: Based on the arguments provided and experimental data cited in the **Waste process report**, no effects are expected.
- Lanthanides, trivalent actinides, Ac: Van Loon and Glaus (1998) and Wieland and Van Loon (2002) observed no effect of ISA on Eu sorption at concentrations < 1 mM. This is consistent with observations by Dario et al. (2004) for EDTA/NTA, ISA, citrate and material from UP2 filter aid. Dario et al. (2004) observed a decrease of Eu sorption at gluconate levels around 10 µM. This is in disagreement with Bradbury and Van Loon (1998) who report on several studies where no effect was observed up to 0.3–250 mM of gluconate, indicating substantial uncertainty. In view of the limited data, it is proposed to base the recommended values for EDTA/NTA, citrate, oxalate and gluconate on the estimates for ISA. The no-effect value observed by Dario et al. (2004) is reflected in an additional conservative estimate for gluconate.
- The available evidence for all IV-valent elements as well as Tc(IV) and Sn(IV) is focused on studies carried out with Th and ISA. These data are roughly consistent with data for Pu(IV), which are less well defined, however. Based on sketchy evidence presented in Wang et al. (2009), and following their argumentation, an additional conservative reduction factor of 1,000 is given for Pu(IV). For all other tetravalent radionuclides, it is proposed to use the values for Th. On the basis of the available data, it is not possible to define a no-effect concentration for all organic ligands. Therefore, a cautious limit for ISA is selected that can be assumed to also cover the effect of the other organic substances. The extension to the other organic ligands takes into account the strong complexing ability of ISA as well as the conservative nature of the selected value. As the measured no-effect concentrations show some scatter (see the **Waste process report**), the lowest value (rather than an average) was chosen. The selected reduction factor is also largely based on data for Th (see the **Waste process report**). It is conservative in the sense that it is also valid for [ISA] ≥ 1 mM (for the restricted concentration range of 0.1–1 mM, a reduction factor of 10 may be more appropriate).

- No information is available for the V-valent actinides. The approach taken in the derivation of K_d would suggest an analogy with Sr. As a conservative approach we propose the same effect for Np(V) and Pu(V) as for trivalent actinides and the same effect for Pa(V) as for tetravalent actinides, respectively.
- Hexavalent U/Pu: the proposed values are based on the assessment given in Wang et al. (2009) for the effect of ISA on U(VI).
- The values for Nb are based on Th, which is very conservative.
- Ni, Co: Based on the discussion given in the **Waste process report**, no effects of organics are expected for Ni and by analogy for Co. As an additional conservative value, a constant, arbitrary reduction factor of 10 is assigned for organic ligand concentrations above 1 mM.
- Pb: Ochs et al. (2011) estimated sorption reduction factors for ISA based on a study by Brownsword et al. (2002) carried out with cellulose degradation products. In lack of any other evidence, their recommendation is directly accepted. The concentration of organics in the underlying experiments was not low enough to observe a no-effect level, however. A constant reduction of sorption was observed at estimated ISA levels (calculated from cellulose loading according to Wang et al. (2009)) from 0.01 mM to 1 mM.; i.e. higher ISA concentration did not lead to a higher reduction in sorption. A no-effect level of 0.02 mM is proposed here, based on the observation that the lowest no-effect levels directly observed for any element considered is 0.1 mM. In view of the uncertainties in the cellulose-loading to ISA conversion, and considering the effect of organic ligands on other elements, the present assessment may be conservative.
- Pd: In lack of any other evidence, the assessment for Pb is also accepted for Pd.
- Po: No information is available. Se(IV) is taken as analogue.
- In case of the oxo-anions (selenate, molybdate, pertechnetate), no pertinent data are available, but it is estimated that organics have no influence on the relevant sorption process (solid solution formation with ettringite).
- Se(IV): the available experimental data do not allow a clear conclusion. Depending on the experimental setup, a range of very little to strong effects can be observed at 2mM ISA or EDTA, see the discussion in the **Waste process report**. Pointeau et al. (2006) propose that sorption of the organic anions competes with the sorption of the selenite anion, see also the **Waste process report**. Due to this uncertainty, the lowest no-effect concentration observed for any radionuclide listed in Table 7-11 is adopted conservatively. Similarly, a reduction factor of 10 is proposed.
- Sr: The limiting concentration given in Table 7-11 is based on information for ISA (**Waste process report**). Due to the simple chemistry of Sr in terms of complexation reactions, this is deemed valid for the other organic ligands as well. No reduction factors have been measured at elevated ligand concentrations, to our knowledge. A reduction factor of 10 is assigned arbitrarily. These estimates are used for Ba and Ra as well.
- Zr: Based on the experiments by Brownsword et al. (2002) (see Pb above), reduction factors between ≈ 30 –125 were estimated (Ochs et al. 2011). However, considering the strong similarity between Zr and tetravalent actinides (Baes and Mesmer 1976), we consider the analogy with Th as more reliable.

Table 7-11a. Limiting no-effect concentrations and sorption reduction factors for ISA concentrations exceeding these values (see text for explanations on each radionuclide). Radionuclides are grouped where appropriate, those radionuclides where information only applies by analogy are indicated in italics. A realistic (cautious best estimate) value is given for all radionuclides, conservative values are additionally given in some cases (Table 7-11c). Reduction factors apply to all radionuclide sorption values (i.e. best estimate and upper/lower limits).

Radionuclide (oxidation state)	no-effect concentration & comments	reduction factor for ISA*
Ag(I)	no effect expected for ISA (see Table 7-11c for conservative values)	–
¹⁴ C, carbonate species	isotope exchange, no effects expected	1
¹⁴ C, CH ₄ , organic acids	not relevant: K _d = 0 assumed	1
Ca (radioactive isotopes)	no effects expected	1
Cd(II)	no effects expected for [ISA] < 10 mM	10
Cl(–I), I(–I)	no effects expected	1
Cs(I)	no effects expected	1
<i>Ac(III), Eu(III), Am(III), Cm(III), Ho(III), Pu(III), Sm(III)</i>	no effects expected for [ISA] < 1 mM	10
Mo(VI), Se(VI), Tc(VII)	no effects expected	1
Nb(V)	no realistic value proposed, (see Table 7-11c for conservative values)	–
Ni(II), <i>Co(II)</i>	isotope exchange, no effects expected	1
Pb(II), <i>Pd(II)</i>	no reduction of sorption at [ISA] < 0.02 mM	100, constant
Th, <i>Np(IV), Pu(IV), U(IV), Pa(IV), Tc(IV), Zr(IV), Sn(IV)</i>	no reduction of sorption at [ISA] < 0.1 mM	100
Np(V), Pu(V), Pa(V)	no realistic value proposed, (see Table 7-11c for conservative values)	–
Se(–II)	not relevant: K _d = 0 assumed	–
Se(IV), <i>Po(IV)</i>	no reduction of sorption at [ISA] < 0.1 mM	10
Sr(II), <i>Ba(II), Ra(II)</i>	no reduction of sorption at [ISA] < 10 mM	10
U(VI), <i>Pu(VI)</i>	no reduction of sorption at [ISA] < 0.5 mM	10

* The proposed reduction factors will increase by a factor of 10 with each 10-fold increase of [ISA] above the indicated no-effect level, except for Pb/Pd. I.e. with an indicated no-effect of 1 mM [ISA] and a reduction factor of 10, sorption values are expected to be reduced by a factor of 10 between >1 mM to 10 mM [ISA], and by a factor of 100 between >10 mM to 100 mM [org], etc.

Table 7-11b. Limiting no-effect concentrations and sorption reduction factors for organic complexants other than ISA exceeding these concentrations (see text for explanations for each radionuclide). Radionuclides are grouped where appropriate, those radionuclides where information only applies by analogy are indicated in italics, [org] stands for any of the compounds indicated above (other than ISA). A realistic (cautious best estimate) value is given for all radionuclides, conservative values are additionally given in some cases (Table 7-11c). Reduction factors apply to all radionuclide sorption values (i.e. best estimate and upper/lower limits).

Radionuclide (oxidation state)	no-effect concentration & comments	reduction factor for other organics*
Ag(I)	no effect expected (see Table 7-11c for conservative values)	–
¹⁴ C, carbonate species	isotope exchange, no effects expected	1
¹⁴ C, CH ₄ , organic acids	not relevant: K _d = 0 assumed	1
Ca (radioactive isotopes)	no effects expected	1
Cd(II)	no effects expected for [Iorg] < 10 mM (analogy with ISA)	10
Cl(–I), I(–I)	no effects expected	1
Cs(I)	no effects expected	1
<i>Ac(III), Eu(III), Am(III), Cm(III), Ho(III), Pu(III), Sm(III)</i>	no effects expected for [Iorg] < 1 mM (analogy with ISA)	10
Mo(VI), Se(VI), Tc(VII)	no effects expected	1
Nb(V)	no realistic value proposed, (see Table 7-11c for conservative values)	–
Ni(II), <i>Co(II)</i>	isotope exchange, no effects expected	1
Pb(II), <i>Pd(II)</i>	no effects expected for [Iorg] < 0.02 mM (analogy with ISA)	100 (constant)
<i>Th, Np(IV), Pu(IV), U(IV), Pa(IV), Tc(IV), Zr(IV), Sn(IV)</i>	no effects expected for [Iorg] < 0.1 mM (analogy with ISA)	100
Np(V), Pu(V), Pa(V)	no realistic value proposed, (see Table 7-11c for conservative values)	–
Np(V), Pu(V), Pa(V)	no direct evidence available, see Table 7-11c	see Table 7-11c
Se(–II)	not relevant: K _d = 0 assumed	–
Se(IV), <i>Po(IV)</i>	no effects expected for [Iorg] < 0.1 mM (analogy with ISA)	10
Sr(II), <i>Ba(II), Ra(II)</i>	no effects expected for [Iorg] < 10 mM (analogy with ISA)	10
U(VI), <i>Pu(VI)</i>	no effects expected for [Iorg] < 0.5 mM (analogy with ISA)	10

* Except for Pb/Pd, reduction factors will increase by a factor of 10 with each 10-fold increase of [org] above the indicated no-effect level. I.e. with an indicated no-effect of 1 mM [org] and a reduction factor of 10, sorption values are expected to be reduced by a factor of 10 between >1 mM to 10 mM [org], and by a factor of 100 between >10 mM to 100 mM [org], etc.

Table 7-11c. Conservative limiting no-effect concentrations and sorption reduction factors for organic complexants exceeding these concentrations (see text for explanations for each radionuclide). Radionuclides are grouped where appropriate, those radionuclides where information only applies by analogy are indicated in italics, [org] stands for any of the compounds indicated above. See tables 7-11a and 7-11b for realistic (cautious best estimate) values (see text). Reduction factors apply to all radionuclide sorption values (i.e. best estimate and upper/lower limits).

Radionuclide (oxidation state)	no-effect concentration & comments	reduction factor conservative*
Ag(I)	no effects for [EDTA, NTA] < [Ca] no effects for other ligands < 10 mM	100 (constant) 10 (constant)
¹⁴ C, carbonate species	not applicable	–
¹⁴ C, CH ₄ , organic acids	not applicable	–
Ca (radioactive isotopes)	not applicable	–
Cd(II)	not applicable	–
Cl(–I), I(–I)	not applicable	–
Cs(I)	not applicable	–
<i>Ac(III), Eu(III), Am(III), Cm(III), Ho(III), Pu(III), Sm(III)</i>	no effect for [gluconate] < 10 μM	10
Mo(VI), Se(VI), Tc(VII)	not applicable	–
Nb(V)	no effects expected for [Iorg] < 0.1 mM	100
Ni(II), Co(II)	no effects expected for [org] < 1 mM	10 (constant)
Pb(II), Pd(II)	not applicable	–
Th, <i>Np(IV), Pu(IV), U(IV), Pa(IV), Tc(IV), Zr(IV), Sn(IV)</i>	no effects expected for [Iorg] < 0.1 mM (analogy with ISA)	1,000, only for Pu(IV)
Np(V), Pu(V)	no effects expected for [org] < 1 mM	10
Pa(V)	no effects expected for [org] < 0.1 mM	100
Se(–II)		–
Se(IV), Po(IV)	not applicable	–
Sr(II), Ba(II), Ra(II)	not applicable	–
U(VI), Pu(VI)	not applicable	–

* Except for Pb/Pd and Ag, reduction factors will increase by a factor of 10 with each 10-fold increase of [org] above the indicated no-effect level. I.e. with an indicated no-effect of 1 mM [org] and a reduction factor of 10, sorption values are expected to be reduced by a factor of 10 between >1 mM to 10 mM [org], and by a factor of 100 between >10 mM to 100 mM [org], etc.

7.10 Judgements by the SR-PSU team

Sources of information

The SR-PSU team find the sources given in given in Section 7.3 sufficient for safety assessment use.

Conditions for which data is supplied

The SR-PSU team find that the conditions given in Section 7.4 reflect the conditions assumed in the repository during the safety assessment lifetime.

Conceptual Uncertainty

The SR-PSU team has considers the given uncertainties in Section 7.5 sufficient to describe the uncertainties of the K_d concept.

Data uncertainty due to precision, bias, and representativity

The uncertainties given in Section 7.6 are considered sufficient according to the SR-PSU team.

Spatial and temporal variability

The SR-PSU team accepts the variabilites considered in Section 7.7.

Correlations

The SR-PSU team finds the approach used in Section 7.8 acceptable.

Results of supplier's data qualification

The SR-PSU team considers the suppliers data qualification to be sufficient and the data will therefore be used in the radionuclide transport calculations.

7.11 Data recommended for use in SR-PSU modelling

Bentonite

The recommended K_d data for bentonite are given in Table 7-6. The diffusion available porosities are given in Table 7-4 and the effective diffusivities are given in Table 7-5.

Bentonite/Sand

For the 90% Sand and 10% Bentonite mixture on the bottom and on the top of the Silo the K_d values are calculated by weighing using 90% of the value from the Rock Matrix and gravel chapter, Table 8-6 and 10 % from the bentonite Table 7-6.

Concrete

The recommended K_d data is produced using the values from Table 7-7, Table 7-8 and Table 7-9. These values are then multiplied by the hydrated cement paste (HCP) content (%) of the different concrete/cement types present in SFR. The HCP content for each type is given in Table 7-12.

Sorption reduction factors

The recommended sorption reduction factors given in Table 7-11a to Table 7-11c.

These factors together with the concentrations of complexing agents anticipated in SFR (Keith Roach et al. 2014) are recommended to be used in the high concentration of complexing agents scenario.

Table 7-12. Hydrated cement paste content (%) for different SFR parts.

SFR Concrete/Cement type	HCP (%) content
Structural concrete	21.9
Silo grout	34.7
1BMA grout	17.7
2BMA grout	34.7
BTF grout – bottom	26.6
BTF grout – top	17.7

8 Rock matrix and Crushed rock sorption data

This section concerns the retardation of radionuclides, by sorption mechanisms, in both the geosphere rock matrix and the repository backfill. The sorption partition coefficients presented in this report is used in the radionuclide transport calculations described in the **Radionuclide transport report** to model the release of radionuclides from the gravel, present in the repository, and from the geosphere rock matrix.

Rock matrix

Since the rock surrounding the SFR repository is geochemically similar to the one surrounding the planned KBS-3 repository the data presented in this chapter is based on the same geologic assumptions made in the SR-Site geosphere K_d report (Crawford 2010) e.g. based on a reference granite to granodiorite, metamorphic medium grained rock type (SKB rock code 101057). This rock type is selected as it is dominant within the domains of both the planned KBS-3 repository and the current and planned SFR repository.

Repository backfill

At final closure of the SFR repository the 1-2BMA, 1-2BTF and BRT vaults and repository tunnels will be backfilled with macadam/crushed rock. The primary function of the backfill is to prevent rock fallout in the vaults when the repository is filled with inflowing groundwater, but the backfill will also function as an engineered sorption barrier, retarding radionuclides on their way out of the repository.

The crushed rock to be used is macadam in the size range 16–32 mm. The hydraulic conductivity in the macadam is high, initially higher than 10^{-2} m/s (SKBdoc 1358612).

8.1 Modelling in SR-PSU

This section describes what data are expected from the supplier, and in what SR-PSU modelling activities the data are to be used.

Defining the data requested from the supplier

- The rock matrix and crushed rock sorption partition coefficients, K_d , (m^3/kg) for the selected radionuclides in relevant pH and redox conditions. The conditions deemed relevant are described further in Crawford (2013).

SR-PSU modelling activities in which data will be used

The K_d values are used in the radionuclide transport calculations to model retardation of the radionuclides flowing out from the SFR repository (**Radionuclide transport report**). The radionuclide transport is modelled using the Ecolego software (**Modell summary report**).

8.2 Experience from previous safety assessments

This section briefly summarises experience from previous safety assessments, especially the SAFE and SAR-08 safety assessments, which may be of direct consequence for the data qualification in this data report.

Modelling in previous safety assessments

In SAR-08, the backfill K_d values were presented and qualified in Cronstrand (2005). The rock matrix K_d values used were taken from the SR-Can safety assessment, and are presented and qualified in the SR-Can Data report (SKB 2006).

The SAR-08 radionuclide transport calculations were performed with the Amber Software (Thomson et al. 2008). This modelling approach does not differ significantly from the near field modelling performed in SR-PSU, only main difference being that the vaults discretisation differs between safety assessments, and the addition of the SFR 3.

Conditions for which data were used in previous safety assessments

SAR-08 data conditions for both the crushed rock and the rock matrix K_d were similar to the approach used in SR-PSU. The main difference is the inclusion of a possible pH plume in the geosphere, possibly affecting the rock matrix sorption, in SR-PSU.

Sensitivity to assessment results in previous safety assessments

As the conductivity of the backfill was relatively high comparing to the conductivities in the concrete and bentonite the radionuclides were not retarded for long in the backfill. Therefore the crushed rock K_d values were not of major importance to retarding the output to the geosphere.

As the travel times from the repository to the surface has always been relatively short in SFR safety assessments the rock matrix K_d values have had a limited impact on the dose curves. This was highlighted in the SAR-08 radionuclide transport report (Thomson et al. 2008) where a calculation case (CC13) compared the effect of using geosphere retardation to not considering the geosphere as a barrier at all.

Alternative modelling in previous safety assessments

No alternative modelling was reported for SAR-08.

Correlations used in previous safety assessment modelling

No correlations were reported in SAR-08.

Identified limitations of the data used in previous safety assessment modelling

No known limitations have been reported with the SAR-08 rock sorption data.

8.3 Supplier input on use of data in SR-PSU and previous safety assessments

The supplier considers the data used in SAR-08 to be acceptable but out of date since a lot of new research has been performed regarding geosphere sorption since 2008, especially in the SR-Site safety assessment for the KBS-3 repository. Also, the inclusion of the possibility of a pH plume from the repository is something which the SAR-08/SR-Can data did not account for.

8.4 Sources of information and documentation of data qualification

Sources of information

The main source of information for this section is Crawford (2013). In Table 8-1 some of the supporting sources cited in the report are listed.

Table 8-1. Main sources of information used in data qualification.

Sources of information
Main source:
Crawford J, 2013. Quantification of rock matrix K_d data and uncertainties for SR-PSU. SKB R-13-38, Svensk Kärnbränslehantering AB.
Supporting sources:
Banwart S A, 1999. Reduction of iron(III) minerals by natural organic matter in groundwater. <i>Geochimica et Cosmochimica Acta</i> 63, 2919–2928.
Bernhard G, Geipel G, Reich T, Brendler V, Amayri S, Nitsche H, 2001. Uranyl(VI) carbonate complex formation: validation of the $\text{Ca}_2\text{UO}_2(\text{CO}_3)_3(\text{aq.})$ species. <i>Radiochimica Acta</i> 89, 511–518.
Bertetti F, Pabalan R, Almendarez M G, 1998. Studies of neptunium ^V sorption on quartz, clinoptilolite, montmorillonite, and α -alumina. In Jenne E A (ed). <i>Adsorption of metals by geomedial: variables, mechanisms, and model applications</i> . San Diego, CA: Academic Press, 131–148.
Bradbury M H, Baeyens B, 2005. Experimental measurements and modeling of sorption competition on montmorillonite. <i>Geochimica et Cosmochimica Acta</i> 69, 4187–4197.
Bradbury M H, Baeyens B, 2009. Sorption modelling on illite. Part I: Titration measurements and the sorption of Ni, Co, Eu and Sn. <i>Geochimica et Cosmochimica Acta</i> 73, 990–1003.
Bradbury M H, Baeyens B, 2009. Sorption modelling on illite. Part II: Actinide sorption and linear free energy relationships. <i>Geochimica et Cosmochimica Acta</i> 73, 1004–1013.
Bradbury M H, Baeyens B, 2011. Predictive sorption modelling of Ni(II), Co(II), Eu(III), Th(IV) and U(VI) on MX-80 bentonite and Opalinus Clay: a “bottom-up” approach. <i>Applied Clay Science</i> 52, 27–33.
Byegård J, Skarnemark G, Skålberg M, 1995. The use of some ion-exchange sorbing tracer cations in in situ experiments in high saline groundwaters. In Murakami T, Ewing R C (eds). <i>Scientific basis for nuclear waste management XVIII: symposium held in Kyoto, Japan, 23–27 October 1994</i> . Pittsburgh, PA: Materials Research Society. (Materials Research Society Symposium Proceedings 353) 1077–1084.
Byegård J, Johansson H, Skålberg M, Tullborg E-L, 1998. The interaction of sorbing and non-sorbing tracers with different Äspö rock types. Sorption and diffusion experiments in the laboratory scale. SKB TR-98-18, Svensk Kärnbränslehantering AB.
Crawford J, 2010. Bedrock K_d data and uncertainty assessment for application in SR-Site geosphere transport calculations. SKB R-10-48, Svensk Kärnbränslehantering AB.
Duro L, Grivé M, Cera E, Domènech C, Bruno J, 2006. Update of a thermodynamic database for radionuclides to assist solubility limits calculation for performance assessment. SKB TR-06-17, Svensk Kärnbränslehantering AB.
Goldberg S, Forster H S, Godfrey C L, 1996. Molybdenum adsorption on oxides, clay minerals, and soils. <i>Soil Science Society of America Journal</i> 60, 425–432.
Goldberg S, Johnston C T, Suarez D L, Lesch S M, 2007. Mechanism of molybdenum adsorption on soils and soil minerals evaluated using vibrational spectroscopy and surface complexation modeling. In Barnett M, Kent D (eds). <i>Adsorption of metals by geomedial II: variables, mechanisms, and model applications</i> . Amsterdam: Elsevier. (Developments in Earth & Environmental Sciences 7), 235–266.
Hummel W, Berner U, Curti E, Pearson F J, Thoenen T, 2002. Nagra/PSI chemical thermodynamic data base 01/01. Boca Raton: Universal Publishers.
Jensen M P, Choppin G R, 1998. Complexation of uranyl(VI) by aqueous orthosilicic acid. <i>Radiochimica Acta</i> 82, 83–88.
Kulmala S, Hakanen M, 1993. The solubility of Zr, Nb and Ni in groundwater and concrete water, and sorption on crushed rock and cement. YJT-93-21, Nuclear Waste Commission of Finnish Power Companies.
Marques Fernandes M, Baeyens B, Bradbury M H, 2008. The influence of carbonate complexation on lanthanide/actinide sorption on montmorillonite. <i>Radiochimica Acta</i> 96, 691–697.
Marques Fernandes M, Stumpf T, Baeyens B, Walther C, Bradbury M H, 2010. Spectroscopic identification of ternary Cm-carbonate surface complexes. <i>Environmental Science & Technology</i> 44, 921–927.
Pabalan R, Turner D, Bertetti F, Prikryl J, 1998. Uranium ^{VI} sorption onto selected mineral surfaces: key geochemical parameters. In Jenne E A (ed). <i>Adsorption of metals by geomedial: variables, mechanisms, and model applications</i> . San Diego, CA: Academic Press, 99–130.
Panak P J, Kim M A, Klenze R, Kim J-I, Fanghänel T, 2005. Complexation of Cm(III) with aqueous silicic acid. <i>Radiochimica Acta</i> 93, 133–139.
Papelis C, 2001. Cation and anion sorption on granite from the Project Shoal Test Area, near Fallon, Nevada, USA. <i>Advances in Environmental Research</i> 5, 151–166.
Salas J, Gimeno M J, Molinero J, Auqué L F, Gómez J, Juárez I, 2010. SR-Site – Hydrogeochemical evolution of the Forsmark site. SKB TR-10-58, Svensk Kärnbränslehantering AB.
Seiler R L, 2011. ²¹⁰ Po in Nevada groundwater and its relation to gross alpha radioactivity. <i>Ground Water</i> 49, 160–171.
Seiler R L, Stillings L L, Cutler N, Salonen L, Outola I, 2011. Biogeochemical factors affecting the presence of ²¹⁰ Po in groundwater. <i>Applied Geochemistry</i> 26, 526–539.

Categorising data sets as qualified or supporting data

The data set presented in Table 8-2 concerns all the radionuclides presented in Crawford (2013).

Table 8-2. Qualified and supporting data sets.

Qualified data sets

Crawford (2013) Table 2 and Table 3

Excluded data previously considered as important

Not applicable.

8.5 Conditions for which data are supplied

As written in the introduction the rock types assumed are the same as for the SR-Site safety assessment as the sites of the SFR repository and the KBS-3 is within a rock domain dominated by the same rock type (Crawford 2010, 2013).

Regarding groundwater the following K_d values are based on new speciation calculations performed with the SFR groundwater compositions reported by Auqué et al. (2013). The different compositions are shown in Table 8-3, Table 8-4 and Table 8-5.

The aforementioned work also includes the possibility of a high pH plume from the repository given its content of cement and concrete materials. In Crawford (2013) a method is presented to scale the rock matrix K_d values depending on the amount of influence from the repository Ordinary Portland Cement (OPC) water. For the crushed rock data presented below the assumption is made that the influence is high enough (e.g. repository water around the backfill at a pH > 10). This is supported by modelling performed in Crawford (2013) showing that mixing even smaller fractions (< 20%) of OPC-water with the SR-PSU groundwaters results in large jumps in both pH and eH, see Figure 8-1.

Table 8-3. Proposed composition and concentration ranges for penetrating brackish saline groundwater when the repository location is submerged under the sea. Data reproduced from Auqué et al. (2013, Table 5-1).

	Composition	Range
pH	7.3	6.6–8.0
Eh (mV)	–225	–100 to –350
Cl (mg/L)	3,500	2,590–5,380
SO ₄ ²⁻ (mg/L)	350	74–557.2
HCO ₃ ⁻ (mg/L)	90	40–157
Na (mg/L)	1,500	850–1,920
K (mg/L)	20	3.8–60
Ca (mg/L)	600	87–1,220
Mg (mg/L)	150	79–290
SiO ₂ (mg/L)	11	2.6–17.2

Table 8-4. Proposed composition of the fresh groundwater around the repository during temperate and periglacial climate domains when the repository is not covered by the sea. Data reproduced from Auqué et al. (2013, Table 5-2).

	Reference composition	Range	Reference composition	Range
	Not extending for more than approximately 40,000 years		Extending for more than 40,000 years	
pH	7.4	6.6–8.3	7.6	6.6–8.3
Eh (mV)	-210	-135 to -300	-250	-135 to -300
Cl (mg/L)	190	16–503	90	5–357
SO ₄ ²⁻ (mg/L)	50	25–163	40	17–110
HCO ₃ ⁻ (mg/L)	300	300–500	200	120–324
Na (mg/L)	180	65–400	110	38–250
K (mg/L)	5	5–15	3	2–5.3
Ca (mg/L)	50	24–105	30	7–48
Mg (mg/L)	12	7–24	6	2–13
SiO ₂ (mg/L)	12	2–21	10	12–31

Table 8-5. Proposed composition and concentration ranges for the glacial-derived groundwater expected to reach the repository during a glacial climate domain. Data reproduced from Auqué et al. (2013, Table 5-3).

	Composition	Range
pH	9.3	9.0 – 9.6
Eh (mV)	+400	+900 to -290
Cl (mg/L)	0.5	0.5–178.0
SO ₄ ²⁻ (mg/L)	0.5	0.1–5.8
HCO ₃ ⁻ (mg/L)	22.7	17.0–150.0
Na (mg/L)	0.17	0.17–130.0
K (mg/L)	0.4	0.14–3.6
Ca (mg/L)	6.8	6.6–21.0
Mg (mg/L)	0.1	0.05–2.0
SiO ₂ (mg/L)	12.8	7.9–14.5

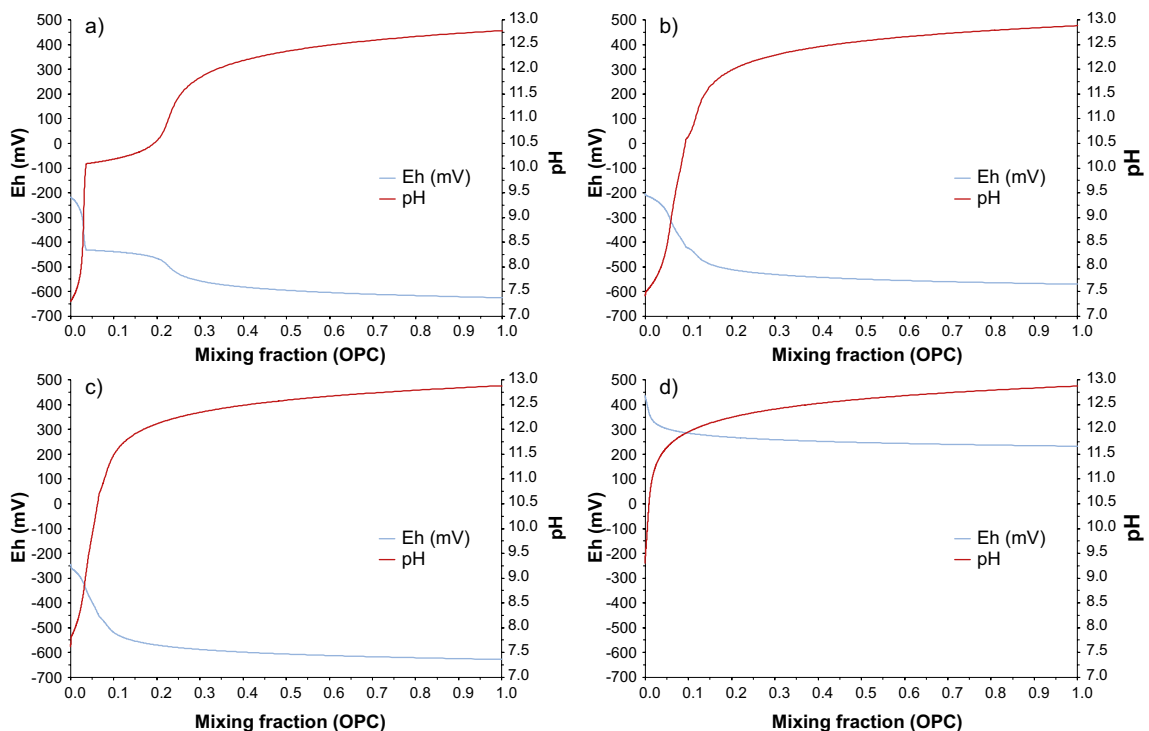


Figure 8-1. Trends in groundwater composition (Eh and pH) as a function of mixing fraction for mixing of Portlandite equilibrated groundwater with un-affected groundwater. Plots are shown for a) Temperate saline, b) Early Periglacial, c) Late Periglacial, and d) Glacial derived groundwater. Reproduced from Crawford (2013).

8.6 Conceptual and bias uncertainties

Methods of estimating K_d values differ between radionuclides. The following text is focused on the radionuclides which sorption estimation methods and underlying data are considered to have the largest uncertainties. A more in depth discussion of all the selected radionuclides is found in Crawford (2013), which this chapter is based on.

Carbon-14 (^{14}C)

^{14}C is expected to migrate from the repository both as inorganic and organic compounds. The inorganic forms are expected to be either gaseous CO_2 or dissolved HCO_3^- (Carbonate). Organic forms expected are gaseous or dissolved CH_4 as well as dissolved organic acids. All the organic forms of ^{14}C are deemed as non-sorbing given their either non-polarity (methane) or their negative charge as conjugate bases.

Inorganic ^{14}C , in the form of dissolved carbonate, has rock matrix sorption mechanisms dependent on the available calcite precipitates (Albinsson 1991). Unfortunately calcite data is lacking in the site-specific investigations of the Forsmark bedrock and an estimate of the impact of this mechanism cannot be performed. Therefore, for SR-PSU, the inorganic form of ^{14}C is also deemed as non-sorbing for both the rock matrix and the repository gravel, which can be seen as a conservative estimate.

Molybdenum (Mo)

Molybdenum's only relevant form in geosphere and repository conditions is the molybdate ion MoO_4^{2-} . Being negatively charged it is not expected to sorb significantly on matrix minerals. There has been studies performed which shows sorption on granitic rocks, clay minerals and soils (Goldberg et al. 1996, 2007). Though, for this to have any effect an abundance of minerals (such as goethite, hematite, or magnetite) that have a point of zero charge around groundwater pH levels must be accounted for. Instead, for SR-PSU, molybdenum is deemed as non-sorbing, for both the repository gravel and the rock matrix, which can be seen as a somewhat conservative assumption.

Neptunium (Np)

As neptunium is a redox sensitive radionuclide it can exist both in its (IV) and (V) forms in normal groundwater compositions and Eh ranges. The highly sorbing pentavalent state is predominant in reducing conditions, whereas the more weakly sorbing is predominant in occurs in weakly oxidising conditions. In SR-Site (Crawford 2010) SDM-site experiments showed that sufficiently reducing conditions for a dominance of Np(IV) could not be certain and therefore the K_d range for neptunium in that safety assessment was selected assuming a dominance of Np(V).

In Crawford (2010) the suggested K_d difference factor between the two oxidation states were at around 130. However, new calculations performed in Crawford (2013) with groundwaters influenced by OPC-water implies an even higher difference at around a factor of 10^4 – 10^5 . To avoid data consistency problems Crawford (2013) therefore suggests using the Np(IV) K_d value from SR-Site for reducing saline Temperate and Periglacial groundwater types with a pH below 10. For oxidising conditions, and for repository gravel, a new K_d value is taken from the Crawford (2013) calculations.

Niobium (Nb)

Niobium is present in the oxidation state (V) in groundwater conditions where the NbO_3^- oxyanion and the $\text{Nb}(\text{OH})_5$ hydrocomplex is the dominant species. In a study by Kulmala and Hakanen (1993) sorption tests were performed both using Finnish native groundwaters as well as groundwaters equilibrated with cement. In this study significant increases in measured Nb K_d values were detected in the latter. The former K_d values, with only fresh groundwater, was used as the basis for the SR-Site recommendations.

However, calculations performed in Crawford (2013) shows that the less sorbing NbO_3^- oxyanion should increase in dominance with increasing pH. This suggests that increased surface complexation outweighs the oxyanion increase but is hard to prove. In order to be conservative in this case the recommended Nb K_d value is the same as was used in SR-Site and does not increase for a pH over 10.

Plutonium (Pu)

Plutonium is dominantly present in oxidation state Pu(III) for temperate saline groundwater up until around pH 8.75, after which Pu(IV) becomes more abundant. The apparent K_d value follow a similar trend where it increases up to a maximum around pH 8.5, after which it starts to decrease. At around pH 12 the K_d reaches a minimum which is calculated to around one order of magnitude less than the non-leachate affected groundwater. Similar reactions occur in Periglacial groundwater types, though the Pu(IV) dominance and K_d decrease starts around pH 10, the latter having a minimum around pH 12 which is about two order of magnitude lower than then unaffected groundwater.

As the degree of influence of the leachate water on the groundwater is an uncertainty the question of which of the oxidation states will dominate in the geosphere. This uncertainty can be avoided for the repository gravel by conservatively assuming a constant high pH from the concrete/cement porewater.

Polonium (Po)

Polonium is a part of the ^{238}U decay chain where ^{210}Pb beta decays to ^{210}Bi which in turn beta decays in to ^{210}Po . Due to uncertain redox chemistry and being a very difficult radionuclide to measure it is difficult to recommend K_d values for the safety analysis. Although the broad qualitative chemical properties of Po and its various redox states has been described in detail in some early works (e.g. Bagnall 1962, Figgins 1961), thermodynamic data suitable for modelling of speciation under normal environmental conditions is relatively sparse. Where such data exists it is very inconsistent and frequently contradictory. The only possible relevant oxidation state, given the available thermodynamic data, where any sorption should occur is the tetravalent Po(IV) where its speciation would be dominated by the PoO_3^{2-} oxyanion and only sorb on minerals that have an non negligible positive surface charge at normal groundwater pH levels. An increase in pH suggests reduced sorption. The other possible oxidation state, according to the thermodynamic data, is the nonsorbing Po(-II).

The only experimental data that has been found for Po sorption on relevant geological materials is that reported by Baston et al. (1998), where a K_d range of 0.1–0.23 m^3/kg was estimated (duplicate measurement) for crushed Japanese granodiorite in contact with a semi-synthetic groundwater (rock-equilibrated deionised water). Reducing conditions ($E_h \leq -200$ mV) were initially achieved by addition of Na-dithionite, although α -radiolysis may have altered this during the four month contact time. K_d values about an order of magnitude higher than the range cited above were obtained when phase separation was performed by filtration ($< 0.45\mu\text{m}$ and $< 10,000$ MWCO, respectively) rather than centrifugation which suggests possible colloid formation. No information was given concerning the particle size of the crushed rock.

As the thermodynamics of polonium is uncertain and the existing data suggests a low K_d even at neutral pH conditions the recommendation is to set polonium as a non-sorbing Po(-II) radionuclide in the rock matrix for Saline, Early- and Late-Periglacial groundwaters. The same recommendation is made for the OPC-affected groundwater, e.g. in the repository gravel. For the glacial-derived groundwater the speciation will likely be Po(IV) and a K_d value can be set, although with a high uncertainty.

An approach to consider is the possibility of assuming that polonium is in secular equilibrium with the parent ^{210}Pb . Using this assumption the need for specific polonium calculations can be avoided and therefore also the uncertainties in the above K_d value. The assumption of a $^{210}\text{Pb}/^{210}\text{Po}$ equilibrium can be described as an conservative approach as a compilation of well data from geographically dispersed sites shows that the ratio is more slumped towards the less dose affecting ^{210}Pb .

A longer discussion regarding polonium chemistry and its uncertainties can be found in Crawford (2013, Appendix C).

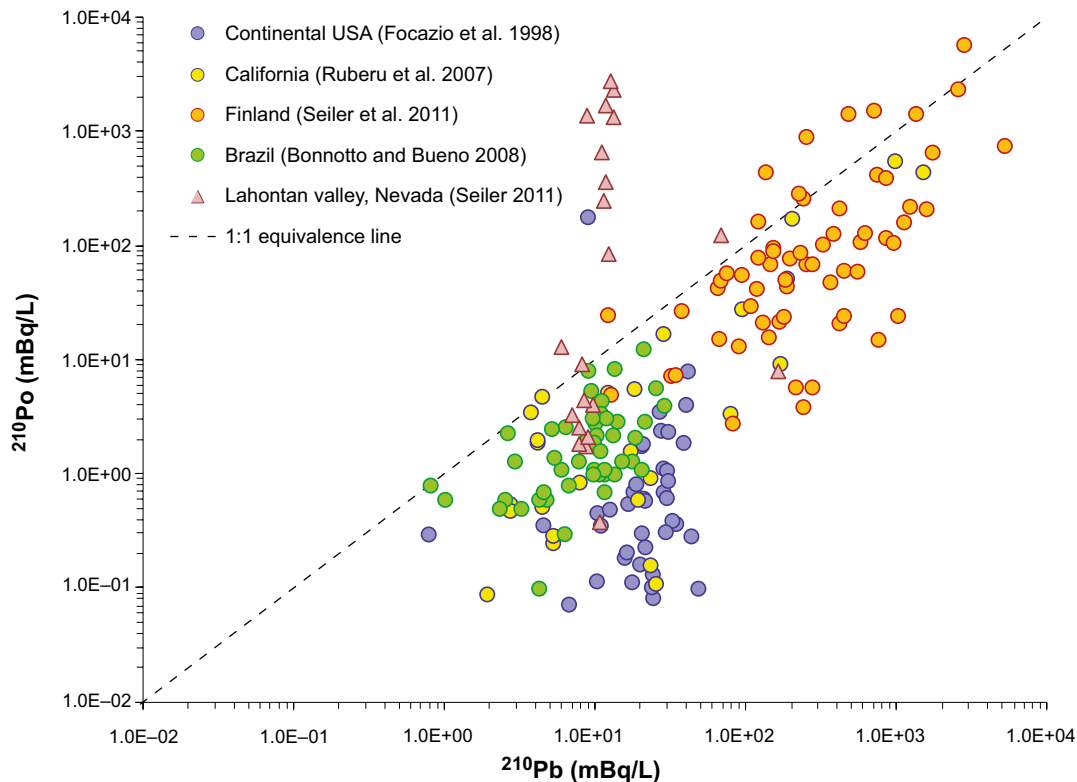


Figure 8-2. Cross plot of groundwater well ^{210}Po and ^{210}Pb activities reported by various authors in the open literature for geographically dispersed sites. Reproduced from Crawford (2013).

Silver (Ag)

Even though silver normally exists as monovalent Ag^+ in relevant redox ranges the sorption of the specie has been problematic to quantify. Previously Cs(I) has been used as an analogue but Crawford (2013) finds many problems with this method as the sorption chemistry differs a lot between the radionuclides. In Bradbury and Baeyens (2005) cation exchange modelling was performed on montmorillonite, and the results showed very small K_d values which led to an recommendation of $^{108\text{m}}\text{Ag}$ as a non-sorbing radionuclide in MX-80 bentonite used in the SR-Site safety assessment.

Another issue is that the Ag^+ ions strongly complexes to chloride in both fresh and saline groundwaters to form AgCl and AgCl_2^- . Therefore the free Ag^+ concentration only consists of a fraction of the total Ag(I) concentration, adding more uncertainty to any set K_d for silver. Given these uncertainties Crawford (2013) recommends setting $^{108\text{m}}\text{Ag}$ as a non-sorbing radionuclide both in the repository gravel and in the geosphere rock matrix.

Technetium (Tc)

^{99}Tc occurs in the relevant groundwater types in two states; as tetravalent Tc(IV) $\text{TcO}(\text{OH})_2$, $\text{TcO}(\text{OH})_3^-$ and $\text{TcO}(\text{OH})_3\text{CO}_3^-$ complexes, and as highly oxidised Tc(VII) state with the oxyanion TcO_4^- dominating.

Uncertainties occur with a lack of suitable analogues for the former, less oxidised state. In this state, which is valid for all non-glacial (e.g. anoxic) groundwater type, the K_d value used in SR-Site (Crawford 2010) is recommended which is low and has a large uncertainty margin. For the glacial groundwater types the uncertainty is much lower due to the much higher redox from which one can safely assume the non-sorbing TcO_4^- as a dominating specie.

Crawford (2013) writes that an extra level of conservatism can be applied to technetium sorption by assuming it as a non-sorbing radionuclide both in the OPC-affected water surrounding the repository gravel, as well as in the geosphere where the mixing of waters adds to the uncertainty.

Uranium (U)

The uranium isotopes of interest for SR-PSU are all present in the SR-Site safety assessment for the KBS-3 repository. Therefore a lot of work has been done regarding the sorption of uranium in rock matrix, for a longer discussion see Crawford (2010, 2013).

Even though a lot of work has been performed regarding uranium sorption there are still some uncertainties with suggesting K_d values for the radionuclides. This is because indications of a very complex redox interactions system that cannot be fully explained just by speciation. For example U(VI) is calculated to be the dominant aqueous redox state for Temperate saline and both periglacial type groundwaters (i.e. non-OPC affected) while U(IV) is also found but in sorbed form in the same conditions. The presence of different species in aqueous and sorbed phases during these phases makes estimating K_d values harder. For more oxidising conditions found in Glacial-derived groundwaters the estimation is easier due to U(VI) being dominant in both aqueous and sorbed phases.

To avoid data inconsistency the recommended K_d value for Temperate saline and peri-Glacial groundwaters not affected by the OPC-water is the same one that is used for U(IV) in SR-Site. A similar recommendation is done regarding the U(VI) K_d value valid for the more oxidising Glacial groundwaters, e.g. the SR-Site value.

For the repository gravel the SR-Site U(VI) K_d value is recommended. This can be seen as a conservative assumption due to the possibility of non oxidising conditions in the repository and that the U(VI) K_d value is almost a factor 500 lower.

Zirconium (Zr)

The only relevant oxidation state for zirconium in the given groundwaters is Zr(IV) as zirconium is not considered a redox sensitive radionuclide. Zr(IV) is present as strongly hydrolysed $Zr(OH)_4$ which is expected to sorb by a surface complexation mechanism sensitive to the groundwater pH.

The SR-Site zirconium K_d recommendations were based on the study performed by Kulmala and Hakanen (1993), where test were made on finnish granite and groundwaters. In the study sorption measurements were also made using cement equilibrated groundwater, and significant increases in K_d values were noted. However, since the underlying mechanisms for these pH increases are uncertain as well as uncertainties in the underlying data, this increase in pH is not accounted for in the SR-PSU K_d recommendation. Therefore the K_d values recommended are the same that used was used in SR-Site, both for the rock matrix and for the repository gravel.

8.7 Spatial and temporal variability

Spatial and temporal variabilites become important when considering the different groundwaters the radionuclides come in contact with. Groundwater chemical properties such as pH, redox and different naturally occurring ion concentrations are critical when assessing the sorption of the selected radionuclides.

The groundwater compositions, presented in Table 8-3 to Table 8-5, have been produced to account for all possible variations that might occur both in the spatial and in the temporal domain. The K_d values presented in this chapter are differentiated using the same compositions.

8.8 Correlations

Except for the groundwater compositions from Auqué et al. (2013), presented in Table 8-3 to Table 8-5, the presented rock matrix K_d values have not been correlated with any other data set produced within the SR-PSU safety assessment.

In Crawford (2013) a method is presented for the estimation of effective K_d values for crushed rock based on consideration of diffusive disequilibrium on the timescale of radionuclide transport. In the calculations presented in the **Radionuclide transport report** the crushed rock used as backfill is considered to be fully equilibrated owing to the long water residence time and K_d values for rock can therefore be used directly without modification.

8.9 Result of supplier's data qualification

The rock matrix K_d values for the different groundwater compositions are given in Table 8-6. To be noted is that K_d values less than 10^{-5} (m^3/kg) may be considered to be effectively zero owing to the dominance of dissolved storage in the matrix porosity in such cases.

Table 8-6. Proposed rock matrix K_d values given the groundwater compositions in Table 8-3 to Table 8-5. Separate values are given for high pH conditions where deemed feasible to do so. Reproduced from Crawford (2013, Table 2 H to Cm and Table 3 Ac to Po).

Radionuclide (Redox State)	GW Type	Best estimate K_d (m^3/kg)	μ	σ	Lower K_d (m^3/kg)	Upper K_d (m^3/kg)
H(I)	all	0.0	–	–	0.0	0.0
C, HCO_3^-	all	0.0	–	–	0.0	0.0
C, CH_4	all	0.0	–	–	0.0	0.0
C, $-CO_2H$	all	0.0	–	–	0.0	0.0
Cl(–I)	all	0.0	–	–	0.0	0.0
Ca(II)	all	0.0	–	–	0.0	0.0
Co(II)	all	$7.4 \cdot 10^{-4}$	–3.13	0.79	$2.1 \cdot 10^{-5}$	$2.7 \cdot 10^{-2}$
Ni(II)	all	$7.4 \cdot 10^{-4}$	–3.13	0.79	$2.1 \cdot 10^{-5}$	$2.7 \cdot 10^{-2}$
Se(–II, IV, VI)	all	0.0	–	–	0.0	0.0
Sr(II)	T-Sal	$1.5 \cdot 10^{-5}$	–4.83	0.6	$9.7 \cdot 10^{-7}$	$2.2 \cdot 10^{-4}$
	Per	$2.0 \cdot 10^{-4}$	–3.69	0.6	$1.3 \cdot 10^{-5}$	$3.1 \cdot 10^{-3}$
	L-Per	$3.5 \cdot 10^{-4}$	–3.46	0.6	$2.3 \cdot 10^{-5}$	$5.3 \cdot 10^{-3}$
	Glac	$1.6 \cdot 10^{-3}$	–2.79	0.6	$1.1 \cdot 10^{-4}$	$2.5 \cdot 10^{-2}$
	all, pH > 10	$1.5 \cdot 10^{-5}$	–4.83	0.6	$9.7 \cdot 10^{-7}$	$2.2 \cdot 10^{-4}$
Mo(VI)	all	0.0	–	–	0.0	0.0
Nb(V)	all	$2.0 \cdot 10^{-2}$	–1.70	0.64	$1.1 \cdot 10^{-3}$	$3.5 \cdot 10^{-1}$
Zr(IV)	all	$2.1 \cdot 10^{-2}$	–1.67	0.35	$4.5 \cdot 10^{-3}$	$1.0 \cdot 10^{-1}$
Tc(IV)	non-Glac	$5.3 \cdot 10^{-2}$	–1.28	0.65	$2.8 \cdot 10^{-3}$	$9.8 \cdot 10^{-1}$
Tc(VII)	Glac	0.0	–	–	0.0	0.0
Ag(I)	all	0.0	–	–	0.0	0.0
Cd(II)	all	$7.4 \cdot 10^{-4}$	–3.13	0.79	$2.1 \cdot 10^{-5}$	$2.7 \cdot 10^{-2}$
Sn(IV)	all, pH < 10	$1.6 \cdot 10^{-1}$	–0.80	0.28	$4.5 \cdot 10^{-2}$	$5.6 \cdot 10^{-1}$
	all, pH > 10	$1.6 \cdot 10^{-4}$	–3.80	0.28	$4.5 \cdot 10^{-5}$	$5.6 \cdot 10^{-4}$
I(–I)	all	0.0	–	–	0.0	0.0
Ba(II)	T-Sal	$1.0 \cdot 10^{-3}$	–3.00	0.46	$1.3 \cdot 10^{-4}$	$8.0 \cdot 10^{-3}$
	Per	$1.4 \cdot 10^{-2}$	–1.86	0.46	$1.7 \cdot 10^{-3}$	$1.1 \cdot 10^{-1}$
	L-Per	$2.4 \cdot 10^{-2}$	–1.62	0.46	$3.0 \cdot 10^{-3}$	$1.9 \cdot 10^{-1}$
	Glac	$1.1 \cdot 10^{-1}$	–0.96	0.46	$1.4 \cdot 10^{-2}$	$8.9 \cdot 10^{-1}$
	all, pH > 10	$1.0 \cdot 10^{-3}$	–3.00	0.46	$1.3 \cdot 10^{-4}$	$8.0 \cdot 10^{-3}$
Cs(I)	T-Sal	$8.8 \cdot 10^{-4}$	–3.05	0.58	$6.6 \cdot 10^{-5}$	$1.2 \cdot 10^{-2}$
	Per	$3.0 \cdot 10^{-3}$	–2.52	0.58	$2.2 \cdot 10^{-4}$	$4.0 \cdot 10^{-2}$
	L-Per	$3.8 \cdot 10^{-3}$	–2.42	0.58	$2.8 \cdot 10^{-4}$	$5.1 \cdot 10^{-2}$
	Glac	$7.7 \cdot 10^{-3}$	–2.12	0.58	$5.7 \cdot 10^{-4}$	$1.0 \cdot 10^{-1}$
	all, pH > 10	$8.8 \cdot 10^{-4}$	–3.05	0.58	$6.6 \cdot 10^{-5}$	$1.2 \cdot 10^{-2}$

Radionuclide (Redox State)	GW Type	Best estimate K_d (m ³ /kg)	μ	σ	Lower K_d (m ³ /kg)	Upper K_d (m ³ /kg)
Sm(III)	all	$1.5 \cdot 10^{-2}$	-1.83	0.72	$5.7 \cdot 10^{-4}$	$3.8 \cdot 10^{-1}$
Eu(III)	all	$1.5 \cdot 10^{-2}$	-1.83	0.72	$5.7 \cdot 10^{-4}$	$3.8 \cdot 10^{-1}$
Ho(III)	all	$1.5 \cdot 10^{-2}$	-1.83	0.72	$5.7 \cdot 10^{-4}$	$3.8 \cdot 10^{-1}$
U(IV)	non-Glac, pH < 10	$5.3 \cdot 10^{-2}$	-1.28	0.65	$2.8 \cdot 10^{-3}$	$9.8 \cdot 10^{-1}$
	non-Glac, pH > 10	$1.1 \cdot 10^{-4}$	-3.97	0.66	$5.5 \cdot 10^{-6}$	$2.1 \cdot 10^{-3}$
U(VI)	Glac	$1.1 \cdot 10^{-4}$	-3.97	0.66	$5.5 \cdot 10^{-6}$	$2.1 \cdot 10^{-3}$
Np(IV)	non-Glac, pH < 10	$5.3 \cdot 10^{-2}$	-1.28	0.65	$2.8 \cdot 10^{-3}$	$9.8 \cdot 10^{-1}$
	non-Glac, pH > 10	$4.1 \cdot 10^{-4}$	-3.38	0.74	$1.5 \cdot 10^{-5}$	$1.2 \cdot 10^{-2}$
Np(V)	Glac	$4.1 \cdot 10^{-4}$	-3.38	0.74	$1.5 \cdot 10^{-5}$	$1.2 \cdot 10^{-2}$
Pu(III/IV)	all, pH < 10	$1.5 \cdot 10^{-2}$	-1.83	0.72	$5.7 \cdot 10^{-4}$	$3.8 \cdot 10^{-1}$
	all, pH > 10	$1.5 \cdot 10^{-5}$	-4.83	0.72	$5.7 \cdot 10^{-7}$	$3.8 \cdot 10^{-4}$
Am(III)	all	$1.5 \cdot 10^{-2}$	-1.83	0.72	$5.7 \cdot 10^{-4}$	$3.8 \cdot 10^{-1}$
Cm(III)	all	$1.5 \cdot 10^{-2}$	-1.83	0.72	$5.7 \cdot 10^{-4}$	$3.8 \cdot 10^{-1}$
Ac(III)	all	$1.5 \cdot 10^{-2}$	-1.83	0.72	$5.7 \cdot 10^{-4}$	$3.8 \cdot 10^{-1}$
Pa(V)	all	$5.9 \cdot 10^{-2}$	-1.23	0.48	$6.8 \cdot 10^{-3}$	$5.1 \cdot 10^{-1}$
Th(IV)	all	$5.3 \cdot 10^{-2}$	-1.28	0.65	$2.8 \cdot 10^{-3}$	$9.8 \cdot 10^{-1}$
Ra(II)	T-Sal	$1.0 \cdot 10^{-3}$	-3.00	0.46	$1.3 \cdot 10^{-4}$	$8.0 \cdot 10^{-3}$
	Per	$1.4 \cdot 10^{-2}$	-1.86	0.46	$1.7 \cdot 10^{-3}$	$1.1 \cdot 10^{-1}$
	L-Per	$2.4 \cdot 10^{-2}$	-1.62	0.46	$3.0 \cdot 10^{-3}$	$1.9 \cdot 10^{-1}$
	Glac	$1.1 \cdot 10^{-1}$	-0.96	0.46	$1.4 \cdot 10^{-2}$	$8.9 \cdot 10^{-1}$
	all, pH > 10	$1.0 \cdot 10^{-3}$	-3.00	0.46	$1.3 \cdot 10^{-4}$	$8.0 \cdot 10^{-3}$
Pb(II)	all	$2.5 \cdot 10^{-2}$	-1.60	0.56	$2.0 \cdot 10^{-3}$	$3.1 \cdot 10^{-1}$
Po(IV)/PoO ₃ ²⁻	all	$\sim 1.0 \cdot 10^{-3}$	-	-	$3.0 \cdot 10^{-4}$	$1.0 \cdot 10^{-2}$
	all, pH > 10	0	-	-	0	0
Po(-II, II, VI)	all	0	-	-	0	0

8.10 Judgements by the SR-PSU team

Sources of information

The SR-PSU team considers the sources of information used by the supplier as sufficient.

Conditions for which data is supplied

The SR-PSU team agrees with the conditions stated by the supplier and find these relevant within the SR-PSU safety assessment.

Conceptual and bias uncertainties

The SR-PSU team agrees with the K_d recommendations given by the supplier for all radionuclides except polonium.

The reasoning the supplier has given regarding the polonium is deemed valid for the all the groundwater types presented in Table 8-3 to Table 8-5, but as the supplier self writes the uncertainties associated with the glacial groundwater polonium K_d -value are large. This groundwater type is the one reflecting the uppermost part of the geosphere, e.g. closest to the surface where mixing with other more oxygen rich waters affects the redox conditions. Due to the half life of ²¹⁰Po and its parent radionuclides, the uncertain Po(IV) K_d value might have a concentrating effect of polonium in the upper parts of the geosphere which in turn can lead to dose consequences in Radionuclide transport well scenarios.

Instead, the SR-PSU team instead chooses to consider polonium in secular equilibrium with its parent ²¹⁰Pb, given as a suggestion in Section 8.6. The well data given in Figure 8-2 gives support to this approach as a conservative one.

Spatial and temporal variability

The SR-PSU team agrees with the handling of variabilites by the supplier and considers them sufficient to describe the groundwater evolution in an around the repository.

Correlations

The SR-PSU team agrees with the given correlations. The suggestion to use equation 1 to estimate the gravel K_d values is accepted, however, without any addition of the porosity and density terms, simplifying the equation.

Results of supplier's data qualification

The SR-PSU team considers the data supplied in this chapter to be sufficient for usage in the safety assessment.

8.11 Data recommended for use in SR-PSU modelling

The K_d values that will be used in the SR-PSU safety assessment is given in Table 8-7 for the rock matrix. As stated above the polonium uncertainties will be not handled in the radionuclide transport. Instead the dose from polonium will be calculated as a fraction of the ^{210}Pb release, assuming secular equilibrium.

The K_d values for macadam/crushed rock will be taken from the rock matrix table, choosing speciation from the assumption of a high pH and redox for the duration of the safety assessment.

Table 8-7. Rock matrix K_d values given the groundwater compositions in Table 8-3 to Table 8-5 as recommended by the SR-PSU team.

Radionuclide (Redox State)	GW Type	Best estimate K_d (m ³ /kg)	μ	σ	Lower K_d (m ³ /kg)	Upper K_d (m ³ /kg)
Ac(III)	all	$1.5 \cdot 10^{-2}$	-1.83	0.72	$5.7 \cdot 10^{-4}$	$3.8 \cdot 10^{-1}$
Ag(I)	all	0.0	-	-	0.0	0.0
Am(III)	all	$1.5 \cdot 10^{-2}$	-1.83	0.72	$5.7 \cdot 10^{-4}$	$3.8 \cdot 10^{-1}$
Ba(II)	T-Sal	$1.0 \cdot 10^{-3}$	-3.00	0.46	$1.3 \cdot 10^{-4}$	$8.0 \cdot 10^{-3}$
	Per	$1.4 \cdot 10^{-2}$	-1.86	0.46	$1.7 \cdot 10^{-3}$	$1.1 \cdot 10^{-1}$
	L-Per	$2.4 \cdot 10^{-2}$	-1.62	0.46	$3.0 \cdot 10^{-3}$	$1.9 \cdot 10^{-1}$
	Glac	$1.1 \cdot 10^{-1}$	-0.96	0.46	$1.4 \cdot 10^{-2}$	$8.9 \cdot 10^{-1}$
	all, pH > 10	$1.0 \cdot 10^{-3}$	-3.00	0.46	$1.3 \cdot 10^{-4}$	$8.0 \cdot 10^{-3}$
C, HCO ₃ ⁻	all	0.0	-	-	0.0	0.0
C, CH ₄	all	0.0	-	-	0.0	0.0
C, -CO ₂ H	all	0.0	-	-	0.0	0.0
Ca(II)	all	0.0	-	-	0.0	0.0
Cd(II)	all	$7.4 \cdot 10^{-4}$	-3.13	0.79	$2.1 \cdot 10^{-5}$	$2.7 \cdot 10^{-2}$
Cl(-)	all	0.0	-	-	0.0	0.0
Cm(III)	all	$1.5 \cdot 10^{-2}$	-1.83	0.72	$5.7 \cdot 10^{-4}$	$3.8 \cdot 10^{-1}$
Co(II)	all	$7.4 \cdot 10^{-4}$	-3.13	0.79	$2.1 \cdot 10^{-5}$	$2.7 \cdot 10^{-2}$
Cs(I)	T-Sal	$8.8 \cdot 10^{-4}$	-3.05	0.58	$6.6 \cdot 10^{-5}$	$1.2 \cdot 10^{-2}$
	Per	$3.0 \cdot 10^{-3}$	-2.52	0.58	$2.2 \cdot 10^{-4}$	$4.0 \cdot 10^{-2}$
	L-Per	$3.8 \cdot 10^{-3}$	-2.42	0.58	$2.8 \cdot 10^{-4}$	$5.1 \cdot 10^{-2}$
	Glac	$7.7 \cdot 10^{-3}$	-2.12	0.58	$5.7 \cdot 10^{-4}$	$1.0 \cdot 10^{-1}$
	all, pH > 10	$8.8 \cdot 10^{-4}$	-3.05	0.58	$6.6 \cdot 10^{-5}$	$1.2 \cdot 10^{-2}$
Eu(III)	all	$1.5 \cdot 10^{-2}$	-1.83	0.72	$5.7 \cdot 10^{-4}$	$3.8 \cdot 10^{-1}$
H(I)	all	0.0	-	-	0.0	0.0
Ho(III)	all	$1.5 \cdot 10^{-2}$	-1.83	0.72	$5.7 \cdot 10^{-4}$	$3.8 \cdot 10^{-1}$
I(-)	all	0.0	-	-	0.0	0.0
Mo(VI)	all	0.0	-	-	0.0	0.0
Nb(V)	all	$2.0 \cdot 10^{-2}$	-1.70	0.64	$1.1 \cdot 10^{-3}$	$3.5 \cdot 10^{-1}$
Ni(II)	all	$7.4 \cdot 10^{-4}$	-3.13	0.79	$2.1 \cdot 10^{-5}$	$2.7 \cdot 10^{-2}$
Np(IV)	non-Glac, pH < 10	$5.3 \cdot 10^{-2}$	-1.28	0.65	$2.8 \cdot 10^{-3}$	$9.8 \cdot 10^{-1}$
	non-Glac, pH > 10	$4.1 \cdot 10^{-4}$	-3.38	0.74	$1.5 \cdot 10^{-5}$	$1.2 \cdot 10^{-2}$
Np(V)	Glac	$4.1 \cdot 10^{-4}$	-3.38	0.74	$1.5 \cdot 10^{-5}$	$1.2 \cdot 10^{-2}$
Pa(V)	all	$5.9 \cdot 10^{-2}$	-1.23	0.48	$6.8 \cdot 10^{-3}$	$5.1 \cdot 10^{-1}$
Ra(II)	T-Sal	$1.0 \cdot 10^{-3}$	-3.00	0.46	$1.3 \cdot 10^{-4}$	$8.0 \cdot 10^{-3}$
	Per	$1.4 \cdot 10^{-2}$	-1.86	0.46	$1.7 \cdot 10^{-3}$	$1.1 \cdot 10^{-1}$
	L-Per	$2.4 \cdot 10^{-2}$	-1.62	0.46	$3.0 \cdot 10^{-3}$	$1.9 \cdot 10^{-1}$
	Glac	$1.1 \cdot 10^{-1}$	-0.96	0.46	$1.4 \cdot 10^{-2}$	$8.9 \cdot 10^{-1}$
	all, pH > 10	$1.0 \cdot 10^{-3}$	-3.00	0.46	$1.3 \cdot 10^{-4}$	$8.0 \cdot 10^{-3}$
Se(-II, IV, VI)	all	0.0	-	-	0.0	0.0
Sm(III)	all	$1.5 \cdot 10^{-2}$	-1.83	0.72	$5.7 \cdot 10^{-4}$	$3.8 \cdot 10^{-1}$
Sn(IV)	all, pH < 10	$1.6 \cdot 10^{-1}$	-0.80	0.28	$4.5 \cdot 10^{-2}$	$5.6 \cdot 10^{-1}$
	all, pH > 10	$1.6 \cdot 10^{-4}$	-3.80	0.28	$4.5 \cdot 10^{-5}$	$5.6 \cdot 10^{-4}$
Sr(II)	T-Sal	$1.5 \cdot 10^{-5}$	-4.83	0.6	$9.7 \cdot 10^{-7}$	$2.2 \cdot 10^{-4}$
	Per	$2.0 \cdot 10^{-4}$	-3.69	0.6	$1.3 \cdot 10^{-5}$	$3.1 \cdot 10^{-3}$
	L-Per	$3.5 \cdot 10^{-4}$	-3.46	0.6	$2.3 \cdot 10^{-5}$	$5.3 \cdot 10^{-3}$
	Glac	$1.6 \cdot 10^{-3}$	-2.79	0.6	$1.1 \cdot 10^{-4}$	$2.5 \cdot 10^{-2}$
	all, pH > 10	$1.5 \cdot 10^{-5}$	-4.83	0.6	$9.7 \cdot 10^{-7}$	$2.2 \cdot 10^{-4}$
Tc(IV)	non-Glac	$5.3 \cdot 10^{-2}$	-1.28	0.65	$2.8 \cdot 10^{-3}$	$9.8 \cdot 10^{-1}$
Tc(VII)	Glac	0.0	-	-	0.0	0.0
Th(IV)	all	$5.3 \cdot 10^{-2}$	-1.28	0.65	$2.8 \cdot 10^{-3}$	$9.8 \cdot 10^{-1}$
U(IV)	non-Glac, pH < 10	$5.3 \cdot 10^{-2}$	-1.28	0.65	$2.8 \cdot 10^{-3}$	$9.8 \cdot 10^{-1}$
	non-Glac, pH > 10	$1.1 \cdot 10^{-4}$	-3.97	0.66	$5.5 \cdot 10^{-6}$	$2.1 \cdot 10^{-3}$
U(VI)	Glac	$1.1 \cdot 10^{-4}$	-3.97	0.66	$5.5 \cdot 10^{-6}$	$2.1 \cdot 10^{-3}$
Pb(II)	all	$2.5 \cdot 10^{-2}$	-1.60	0.56	$2.0 \cdot 10^{-3}$	$3.1 \cdot 10^{-1}$
Pu(III/IV)	all, pH < 10	$1.5 \cdot 10^{-2}$	-1.83	0.72	$5.7 \cdot 10^{-4}$	$3.8 \cdot 10^{-1}$
	all, pH > 10	$1.5 \cdot 10^{-5}$	-4.83	0.72	$5.5 \cdot 10^{-6}$	$3.8 \cdot 10^{-4}$
Zr(IV)	all	$2.1 \cdot 10^{-2}$	-1.67	0.35	$4.5 \cdot 10^{-3}$	$1.0 \cdot 10^{-1}$

9 Concrete/Cement diffusivity data

This section concerns the effective diffusivity of the concrete/cement types used in the SFR repository. The cementitious materials that can be found in the SFR repository are mainly: structural concrete in buildings and waste packaging, concrete grout used as backfill around the waste packages in the Silo, BMA and BTF vaults and cement mortar and grout used as conditioning material for the waste (SKB 2001).

The different cements used for the concrete are standard Portland types: Skövde SP, Degerhamn SP and Blast furnace cement. The chemical compositions of these are given in SKB (2001) and the **Initial state report**.

Barriers

The concrete barriers comprise the concrete structures in the different repository parts, i.e. the bottom, lid and outer and inner walls of the Silo and BMA, the concrete floor and lid in the BTF vaults and the concrete floor in BLA. They also include shotcrete and rock bolts in the rock walls in all repository parts, the concrete backfill surrounding the waste packages in the Silo and parts of BMA, and the concrete that will fill the void between the concrete tanks and the vault walls in the BTF vaults and in between the ash drums in 1BTF.

Waste

Concrete moulds are used in the Silo, BMA and 1BTF repository parts and concrete tanks are used in the 1BTF and 2BTF repository parts, as waste containers. Cement is used both for solidification of ion exchange resins and sludge, and for stabilisation of scrap metal and refuse within many of the different waste packages present in the repository (Almkvist and Gordon 2007).

The mixing proportions of the different concrete types present in SFR are given in Table 9-1.

Table 9-1. Mixing proportions for concrete types in SFR taken from SKB (2001) and Höglund (2001).

Component	Structural concrete	Silo grout	1BTF Grout bottom	1BTF Grout top	Conditioning cement
Cement (kg/m ³)	350	325	340	265	1,180
Water (kg/m ³)	164.5	366	252	141	437*
Ballast (kg/m ³)	1,829	1,302	1,630	1,890	–
w/c ratio	0.47(0.46–0.49)	1.125	0.74	0.53(0.75)**	0.37

* The added water may be insufficient to allow for full hydration of the cement, estimates show a maximum of 96% hydration.

** Value including specified maximum humidity in ballast material.

9.1 Modelling in SR-PSU

This section describes what data are expected from the supplier, and in what SR-PSU modelling activities the data are to be used.

Defining the data requested from the supplier

The supplier should deliver the following data:

- The effective diffusivity D_e (m²/s) of the installed concrete/cement types present in SFR. The data should be given for different chemical and mechanical degradation states: from the concrete currently present in the SFR repository to a completely degraded state.

When considering degradation, the supplier should prioritise mechanical degradation as chemical degradation probably is negligible, unless the supplier considers otherwise.

SR-PSU modelling activities in which data will be used

The effective diffusivity of the concrete/cement will be used as input to the radionuclide transport calculations for the near field.

9.2 Experience from previous safety assessments

This section briefly summarises experience from the previous safety assessments, SAFE and SAR-08, which may be of direct consequence for the data qualification in this data report.

Modelling in previous safety assessments

Calculation of radionuclide release including transport by diffusion has been an important part of all previous safety assessments for the SFR repository.

Conditions for which data were used in previous safety assessments

In the SAFE safety assessment, a general assumption for the Base Scenario was that the state of barriers at repository closure is in accordance with their design criteria (SKB 2001). Since Höglund (2001) calculated that the concrete barriers would only become completely depleted of CSH phases to a depth of 0.2 m in the 10,000 year period considered in SAFE, the effective diffusivity was considered to be constant over time. The value for the effective diffusivity was representative of Stage II (SKB 2001) of concrete degradation. Concrete grout has a higher porosity than structural concrete, thus the effective diffusivity was considered to be ten times higher. The SAFE analysis gave the same value to the cement grout in the Silo (30% porosity) and the BTF (20% porosity) although the diffusivity in BTF grout would be expected to be lower. The scenario analysis that addressed the possibility of initial defects in the technical barriers focussed on increased water flow, thus the diffusivity was not altered in the calculations.

In the SAR-08 safety assessment (Thomson et al. 2008), the diffusivity assigned to the structural concrete was lower than used in SAFE and was a typical value for Stage I of concrete degradation. However, since radionuclide transport was calculated over a longer time period in this assessment, the diffusion coefficient was increased by a factor of ten for the period from 66,000 years post closure onwards. Again, since concrete grout has a higher porosity than structural concrete, it was assigned an initial diffusivity 10 times higher than for concrete after 66,000 years. This diffusivity was used throughout the time period considered. The project included assessments of the effects of early barrier failure but, as with SAFE, this did not account for any changes in diffusivity.

Sensitivity to assessment results in previous safety assessments

The use of a lower initial effective diffusivity for structural concrete in the SAR-08 assessment reduced the calculated release of radionuclides relative to the SAFE assessment. The sudden increase in the diffusivity of the structural concrete assumed in the SAR-08 safety assessment model is caused by the failure of the barriers, thus is accompanied by a sudden increase in the water flow. It was calculated in Holmén and Stigsson (2001a) and Holmén (2005, 2007) that failed barriers in sections of the tunnels would lead to a two to three times higher flow in the BLA and BMA tunnels, and a somewhat smaller flow in the BTF tunnel as result of the changed flow direction in the tunnels. These changes make it difficult to assess the sensitivity of the analyses to the change in the diffusivity of the concrete barriers alone.

Alternative modelling in previous safety assessments

No alternative modelling was reported in SAFE or SAR-08.

Correlations used in previous safety assessment modelling

Correlations between the degradation, the effective diffusivities and the radionuclide migration from the repository parts were used both in SAFE and SAR-08.

Identified limitations of the data used in previous safety assessment modelling

The diffusion coefficient used in SAR-08 for the first 66,000 years post closure is representative of fresh concrete, and thus is likely to underestimate diffusion in this period. The 10-fold increase in the diffusion coefficient after 66,000 years only takes the value into the range for intact concrete in the portlandite leaching stage, whereas the concrete would be expected to be significantly degraded by this point.

9.3 Supplier input on use of data in SR-PSU and previous safety assessments

When selecting representative data for the effective diffusivity of the concrete barriers it is essential to reflect the anticipated physical status of the actual materials used in the SFR repository. In the SAFE safety assessment, a general assumption for the Base Scenario is that the state of barriers at repository closure is in accordance with design criteria (SKB 2001). The concrete used for construction is a high quality concrete with the purpose of providing high mechanical strength, which also means that the effective diffusion coefficient may be very low. The mixing proportions used for the concrete will give a low porosity with a low degree of connectivity of the conductive pores. At full hydration of the cement minerals, the major part of the porosity will be gel pores and contraction pores, both of which would present a high degree of tortuosity and thus low effective diffusivity, whereas the capillary porosity is low. Capillary pores enable greater diffusive transport through the cement phase. The diffusivities encountered in assessments of SFR concrete only range over three orders of magnitude; species have a fairly low diffusivity in water ($2 \cdot 10^{-9}$ m²/s), and it is reasonable to expect that the effective diffusivity of a fresh, fully hydrated concrete, produced according to the mixing proportions used for construction concretes in the SFR repository, would be on the order of $3 \cdot 10^{-12}$ m²/s or less. The occurrence of fractures in the initial concrete structures may affect the expected initial overall effective diffusivity.

In concrete constructions, steel reinforcement bars are used to minimise the width and penetration of fractures caused by mechanical loads and volume changes as cement hydrates and dries. The amount of reinforcement in some of the concrete constructions currently in the SFR repository does not meet present day standards for restricting the width of fractures (cf. Boverket 2004); the Silo bottom and the lower part of the Silo wall contain only about 30% and 70% of the prescribed minimum amount of reinforcement, respectively; for the BMA vault, the concrete bottom contains about 50% of the minimum amount of reinforcement to restrict fracture width (Vattenfall 2011). It therefore seems reasonable to expect that fractures will occur in these structures, although it is difficult to predict the time when this will happen.

Inspection of a 40 m section of the 1BMA vault showed that concrete barriers are already fractured to an extent that will significantly affect the hydraulic conductivity (SKBdoc 1430853). The fractures have been attributed to early thermal phenomena during the hydration of the concrete and shrinkage as the concrete dries during the operational period. The fracturing in the concrete is significantly more extensive than previously known and the fractures observed have also been found to be fully penetrating (SKBdoc 1430853). It should be pointed out that only one quarter of the 1BMA vault has been inspected which means that extrapolation of the results to the entire concrete structure would introduce some uncertainty. Likewise, extrapolation of the observations from the 1BMA concrete barriers to the other parts of the SFR repository would introduce further uncertainty.

During inspection of the 1BMA barrier, the steel reinforcement in the concrete was also seen to have been affected by corrosion, in some areas causing the concrete covering the reinforcement bars to fracture. As a result of this, the surface layer of the concrete has spalled locally. From this, it may be inferred that fracturing will also occur over time as a result of corrosion of the steel form ties that run through the concrete walls in the 1BMA vault.

The mechanisms leading to fracture formation in concrete are discussed briefly in Höglund (2014) and in more detail in US DOE (2009) and Vattenfall (2011). The types of fractures that form due to shrinkage and heating during early hydration processes are expected to be fully penetrating (US DOE 2009), as observed in the 1BMA vault (Vattenfall 2011). Hence, these fractures will be present from the start and would also be possible to observe in many cases. Cooling of the concrete structures as a result of groundwater filling the vaults after closure will result in thermal contraction that is likely to cause fractures. Such fractures can be expected to occur within a few years after closure.

Corrosion of reinforcement bars and other steel components, such as form rods, in the concrete barriers may gradually cause fractures to form and increase in size as the corrosion progresses. Initially, the alkaline conditions may protect the steel from corrosion by passivation, but the ingress of chloride ions from the saline groundwater will initiate corrosion. Once corrosion has started, the formation of corrosion products, which have larger volume than the corroded steel, will create a mechanical pressure that will eventually initiate fracture formation in the concrete surrounding the steel components. Estimates show that corrosion induced fractures may form within a few decades of the onset of corrosion (Höglund 2014). Other types of fractures, e.g. due to chemical processes leading to the formation of minerals with large molar volumes such as ettringite and thaumasite, may appear at much later stages, although it is highly uncertain when they will occur. Model calculations of such chemical processes are presented in Höglund (2014). However, further research is necessary to improve the predictions of the temporal evolution of these fractures.

As a consequence of these observations, it is judged necessary that the selection of effective diffusivities should reflect the observed and likely occurrence of fractures. This means that the overall effective diffusivities of the corresponding concrete barriers must be assumed to be higher than in intact concrete.

Therefore, the data selection to represent the effective diffusivity of different concrete structures in the SFR repository in the SAFE and SAR-08 studies need to be updated. The implications of a more fractured concrete at an early stage are an increased overall porosity of the barriers (and the waste) after closure, and as a result, an increased effective diffusivity and an increased rate of chemical degradation due to faster diffusion exchange of dissolved components. Hence, significant early fracturing would change the basis for the assessment of the chemical degradation of the concrete barriers, and this has not been considered in previous assessments. The presence of fractures enhances the risk for advective flow through the concrete barriers and will also mean that the flow will be preferential, hence concentrated to a few locations of the cross-sectional area. Preferential flow also means an increased risk that chemical leaching will be preferential, thus over time further increasing the local damage to the concrete barriers. Quantitative estimates of their importance for the barrier integrity have been made and are presented in Höglund (2014). The processes are however complex and the results and interpretation are subject to uncertainty. Since fracturing causes sudden changes of the effective diffusivity (although to a lesser degree compared with the hydraulic conductivity), the assumption of sudden changes of the effective diffusivity of the concrete barriers may be motivated for the safety assessment. This is another area where further studies are necessary. The impact of the results have been considered in the radionuclide release calculations (SKB 2014b)

A modified barrier system has been designed for the new 2BMA vault. The concrete barriers consist of 14 detached caissons of non-reinforced concrete. The floor and walls are cast in one step to minimise joints in the constructions. During filling, a temporary pre-fabricated concrete cover may be used as a radiation shield over the waste, which will be removed when filling is completed. After filling of the caissons with waste packages, a 0.5 m thick lid will be constructed using cast concrete. The concrete constructions will be supported from the inside by the waste packages and concrete grout backfill and on the outside by crushed rock/gravel/macadam. The grouting will be carried out in steps to minimise the mechanical stress on the non-reinforced concrete walls. The concrete floor rests on a bed of gravel (grain size 6–20 mm) which also acts as part of a hydraulic cage around the caissons.

The concrete walls, floor and lid consists of construction concrete. The composition of the concrete (cement quality, w/c-ratio, ballast quality and content) is assumed to be the same as in 1BMA. The concrete will experience temperature and moisture variations during construction that will cause dimensional changes and may result in mechanical stresses. Such stresses may cause small fractures in the concrete. In the evaluation of 2BMA it is assumed that thin fractures, with a dimensioning aperture width of 10 μm with an average fracture spacing of 1 m, are present in the concrete at closure. Occasional appearance of fractures with a maximum aperture width of 100 μm is possible.

Due to the absence of reinforcement bars and other steel components in the concrete barriers the impact of steel corrosion on the barrier function does not need to be considered for the 2BMA vault. However, thermal shrinkage of the concrete structures as a result of groundwater filling the 2BMA vault after closure is likely to cause fractures. Such fractures can be expected to occur within a few years after closure (Höglund 2014).

9.4 Sources of information and documentation of data qualification

Sources of information

In general, specific data for the concrete barriers in the SFR repository are not available, in particular and for obvious reasons, no data exists for concrete in aged and degraded stages. The safety assessments have therefore been based on judgements of reasonable data sets from typical structural concretes and different modelling approaches to estimate the diffusivity. In Table 9-2 some data from different sources have been compiled. Previous safety assessments for SFR presented values for effective diffusivity in fresh, aged and degraded SFR concrete; the values were selected using relevant literature data as a guide. For SFR, diffusion coefficients have not been assessed specifically in terms of concrete fracture size or density (as opposed to degradation), and the impact of fractures has been assessed with a focus on increased flow. Although Cronstrand (2007) included freeze-fracture scenarios in a performance assessment model, it was stated that they "...should merely be considered as a tentative approach with the aim to illustrate that fractures and freezing effects could be dramatic, not that they actually will be. Substantial amount of experimental work are required in order to parameterise models including fractures."

However, there have been a number of studies and modelling exercises that have examined the impact of fracture width and frequency on effective diffusivity of dissolved species and Rn gas through concrete, and these are included in Table 9-2. Additionally, experiments have identified that chloride ion diffusion in cracks $< \sim 55 \mu\text{m}$ is restricted by a combination of mechanical interactions between the fractured surfaces and self-healing reactions in the concrete (Gagné et al. 2001, Ismail et al. 2004). Therefore, Ismail et al. (2004) suggested that cracks have a diffusion threshold of approximately $50 \mu\text{m}$. The data of Yoon (2012) presented in Table 9-2 showed a lower possible threshold value, of less than $\sim 20 \mu\text{m}$. The difference may be due to the cracking methods employed or the material used, but the data suggest that very narrow cracks should not affect the diffusivity of the bulk material.

For reference, the stages of concrete degradation were defined as follows:

- Stage I: Corresponds to fresh hydrated concrete. Alkali metal hydroxides leach out causing the porewater pH to be above 12.5
- State II: The concrete porewater is controlled by the dissolution of portlandite ($\text{Ca}(\text{OH})_2$) to a pH of 12.5
- State III: Portlandite is exhausted and the pH is buffered by the incongruent dissolution of CSH phases. The pH of the porewater gradually decreases from 12.5 to about 10.5 as CSH phases lose Ca.

Table 9-2. Some data on effective diffusivities of concrete from safety assessments, literature and model estimates. Included are also measurements of the diffusivity increase factor when comparing fractured and unfractured concretes.

Material	Effective diffusivity (m^2/s)	Diffusivity increase factor due to ageing or cracking*	Type of data	Source
SFR Structural concrete				
Fresh structural concrete (porosity 15%)	$3 \cdot 10^{-12}$	10 (aged); 300 (degraded)	Data report	SKB 2001
Structural concrete in the Silo, stage I of concrete degradation	$3 \cdot 10^{-12}$	10 (stage II); 300 (stage III)	Performance assessment	Höglund and Bengtsson 1991
Structural concrete in BMA (equivalent to stage II of concrete degradation)	$3 \cdot 10^{-11}$	30 (after 1,000 years)	Performance assessment	Höglund and Bengtsson 1991
Structural concrete (porosity 15%)	$1 \cdot 10^{-11}$	None, this represents Stage II	Performance assessment	Höglund 2001
Unfractured structural concrete (porosity 15%)	$1 \cdot 10^{-11}$	None, this represents Stage II	Safety assessment.	SKB 2001
Construction concrete (Silo, BMA and BTF) stage I of concrete degradation	$2.5 \cdot 10^{-12}$	10 (stage II); 200 (stage III)	SKI data report	Savage and Stenhouse 2002
Structural concrete (Silo, BMA and BTF)	$3 \cdot 10^{-12}$	10 (after 66,000 years)	Safety assessment	Thomson et al. 2008

Material	Effective diffusivity (m ² /s)	Diffusivity increase factor due to ageing or cracking*	Type of data	Source
Structural concrete (Silo and BMA)	1 · 10 ⁻¹¹	2–5 every freeze-thaw cycle	Performance assessment	Cronstrand 2007
Structural concrete in the Silo	1.5 · 10 ⁻¹¹	Diffusivity of all materials was related to porosity using a pore diffusivity of 1 · 10 ⁻¹⁰		Gaucher et al. 2005
SFR backfill grout				
Porous concrete (porosity 20%)	3 · 10 ⁻¹⁰	–	Data report	SKB 2001
Porous backfill concrete in SFR	3 · 10 ⁻¹⁰	–	Performance assessment	Höglund and Bengtsson 1991
Porous concrete (Silo and BTF) stage I of concrete degradation	6.3 · 10 ⁻¹⁰	No change with degradation	SKI data report	Savage and Stenhouse 2002
Concrete backfill (porosity 20–30%)	1 · 10 ⁻¹⁰	–	Safety assessment	SKB 2001
Backfill concrete in SFR (porosity 36%)	1.2 · 10 ⁻¹⁰	–	Literature review and adjustment for porosity	Luna et al. 2006
Concrete cement conditioning and waste package concrete in Silo, BMA and BTF)	3 · 10 ⁻¹⁰	–	Safety assessment	Thomson et al. 2008
Other concretes				
Self-compacting concrete based on Portlandite cement, calcite and river sand and gravel; water:cement ratio = 0.46	2.4 · 10 ⁻¹²	~10 with 3–5 cracks of 390 ± 70 µm width per 100 mm	Experimental data of chloride penetration into artificially cracked concrete	Mu et al. 2013
Concrete prepared with water:cement = 0.51, cement:sand:pea gravel = 1:2:4.	–	10 (concrete with a 1.3 mm fracture in a 8.9 cm diameter sample vs intact concrete)	Laboratory measurements of Rn gas diffusion through artificially cracked concrete	Daoud and Renken 1999
Construction concrete	10 ⁻¹²	10	Sensitivity analysis	Zhang and Lounis 2006
Modified Portlandite cement (Type I and II) prepared with a water:cement ratio of 0.4 and using a fine aggregate	2 · 10 ⁻¹³	–	Determined in Tc and I diffusion experiments using soil-concrete half cells	Mattigod et al. 2009
Structural concrete	~10 ⁻¹²	1,000 (to the diffusivity in free water) due to damage	Coupled diffusion-damage modelling	Gerard et al. 1998
Ordinary Portland cement concrete; water:cement ratio = 0.5	–	2 (crack of ~47 µm width at the concrete surface)		Yoon 2012
High performance concrete; water:cement ratio = 0.2	–	8 (crack of ~20 µm width at the concrete surface)		Yoon 2012
High performance concrete; water:cement ratio = 0.2	–	18 (crack of ~47 µm width at the concrete surface)		Yoon 2012
High performance concrete reinforced with steel fibre (to introduce complex cracks); water:cement ratio = 0.33	–	4 (crack of ~20 µm width at the concrete surface)		Yoon 2012
High performance concrete reinforced with steel fibre (to introduce complex cracks); water:cement ratio = 0.33	–	10 (crack of ~36 µm width at the concrete surface)		Yoon 2012
High performance concrete reinforced with steel fibre (to introduce complex cracks); water:cement ratio = 0.33	–	4–6 (crack of ~43–47 µm width at the concrete surface)		Yoon 2012
Bulk mortar; porosity = 18%	6 · 10 ⁻¹¹	300 (to diffusivity in free water within a crack)	COMSOL Multiphysics simulation validated by µXFR measurement	Lu et al. 2012

*Note that when two factors are given, both are relative to the diffusivity given in the second column.

Table 9-3. Sources of data on diffusivities of concrete from safety assessments, model estimates and literature.

Sources of information

- Boverket, 2004.** Boverkets handbok om betongkonstruktioner: BBK 04. 3rd ed. Karlskrona: Boverket. (In Swedish.)
- Cronstrand P, 2007.** Modelling the long-time stability of the engineered barriers of SFR with respect to climate changes. SKB R-07-51, Svensk Kärnbränslehantering AB.
- Daoud W Z, Renken K J, 1999.** Laboratory measurements of the radon gas diffusion coefficient for a fractured concrete sample and radon gas barrier systems. Proceedings of the International Radon Symposium (AARST), 1999, 14.0–14.12.
- Gagné R, François R, Masse P, 2001.** Chloride penetration testing of cracked mortar samples. In Banthia N, Sakai K, GjØrv E E (eds). Concrete under severe conditions: environment and loading: proceedings of the Third International Conference on Concrete under Severe Conditions, CONSEC'01, Vancouver, Canada, 18–20 June 2001. Vol 1. Vancouver: University of British Columbia, 198–205.
- Gaucher E, Tournassat C, Nowak C, 2005.** Modelling the geochemical evolution of the multi-barrier system of the Silo of the SFR repository. Final report. SKB R-05-80, Svensk Kärnbränslehantering AB.
- Gerard B, Pijaudier-Cabot G, Laborderie C, 1998.** Coupled diffusion-damage modelling and the implications on failure due to strain localisation. International Journal of Solids and Structures 35, 4107–4120.
- Höglund L O, 2001.** Project SAFE. Modelling of long-term concrete degradation processes in the Swedish SFR repository. SKB R-01-08, Svensk Kärnbränslehantering AB.
- Höglund L O, 2014.** The impact of concrete degradation on the BMA barrier functions. SKB R-13-40, Svensk Kärnbränslehantering AB.
- Höglund L O, Bengtsson A, 1991.** Some chemical and physical processes related to the long-term performance of the SFR repository. SKB SFR 91-06, Svensk Kärnbränslehantering AB.
- Ismail M, Toumi A, François R, Gagné R, 2004.** Effect of crack opening on the local diffusion of chloride in inert materials. Cement and Concrete Research 34, 711–716.
- Lu Y, Garboczi E, Bentz D, Davis J, 2012.** Modeling chloride transport in cracked concrete: a 3-D image-based microstructure simulation. In Proceedings of COMSOL Conference 2012, Boston, MA, 3–5 October 2012. Available at: http://www.nist.gov/customcf/get_pdf.cfm?pub_id=912153.
- Luna M, Arcos D, Duro L, 2006.** Effects of grouting, shotcreting and concrete leachates on backfill geochemistry. SKB R-06-107, Svensk Kärnbränslehantering AB.
- Mattigod S V, Bovaird C C, Wellman D M, Skinner D J, Cordova E A, Wood M I, 2009.** Effect of concrete waste form properties on radionuclide migration. PNNL-18745, Pacific Northwest National Laboratory, Richland, Washington.
- Mu S, De Schutter G, Ma B-G, 2013.** Non-steady state chloride diffusion in concrete with different crack densities. Materials and Structures 46, 123–133.
- Savage D, Stenhouse, M, 2002.** SFR 1 vault database. SKI Report 02:53, Statens kärnkraftinspektion (Swedish Nuclear Power Inspectorate).
- SKB, 2001.** Project SAFE. Compilation of data for radionuclide transport analysis. SKB R-01-14, Svensk Kärnbränslehantering AB.
- SKBdoc 1430853.** Sprickor i BMA:s betongbarriär – Inspektion och orsak. AE-NCC 12-004, Vattenfall Power Consultant.
- Thomson G, Miller A, Smith G, Jackson D, 2008.** Radionuclide release calculations for SAR-08. SKB R-08-14, Svensk Kärnbränslehantering AB.
- US DOE, 2009.** Review of mechanistic understanding and modeling and uncertainty analysis methods for predicting cementitious barrier performance. Cementitious Barriers Partnership. CBP-TR-2009-002, Rev.0, U.S. Department of Energy.
- Yoon I-S, 2012.** Chloride penetration through cracks in high performance concrete and surface treatment system for crack healing. Advances in Materials Science and Engineering 2012, 294571. doi:10.1155/2012/294571.
- Zhang J, Lounis Z, 2006.** Sensitivity analysis of simplified diffusion-based corrosion initiation model of concrete structures exposed to chlorides. Cement and Concrete Research 36, 1312–1323.
-

Categorising data sets as qualified or supporting data

Qualified data is presented in Höglund (2014) and other references stated in Table 9-3. Supporting data is various references used in the derivation of the data in Höglund (2014) (see reference list of this report).

Excluded data previously considered as important

Data selection may need reconsideration.

9.5 Conditions for which data are supplied

The recent information regarding the status of concrete barriers in SFR suggest the previous basis for safety assessments need reconsideration. Some implications are stated in Section 9.3.

The observations of cracks in BMA and the insufficient reinforcement in parts of the BMA and Silo discussed in Section 9.3 demonstrate that the selection of data for the effective diffusivities of concrete structures in the SFR repository need to be revised. A more fractured concrete at an early stage of the repository lifetime means that shorter diffusion paths through the barriers will exist, which may also potentially enhance radionuclide release. Additionally, there will be more rapid localised degradation in the fracture, with the higher diffusivity enhancing Ca leaching and lowering the barrier performance. Quantitative estimates of their importance for the barrier integrity have been made and are presented in Höglund (2014).

It should be noted that diffusion out of the Silo repository (as well as groundwater flow) is likely to be controlled by the sand/bentonite and bentonite barriers, thus may not be affected by fractures to the same extent as diffusion in the BMA and BTF. However, consideration should also be given to the possible effect on the diffusive properties of the bentonite if fractures form in the Silo wall or bottom. Bentonite may tend to fill the fractures in the concrete, a process that may lead to a locally decreased bentonite concentration outside the concrete wall. The possible impact on the local diffusive properties of bentonite in response to such fractures needs to be addressed but has been judged to be beyond the scope of the present investigation.

9.6 Conceptual uncertainty

In general, the conceptual uncertainties related to the diffusivity of concrete are small. Diffusion processes are well known and intact concretes are known to have low diffusivity and be of high durability. However, the status of the concrete barriers in the SFR repository according to recent information (SKBdoc 1430853) introduces significant uncertainty and suggests that the previously used data are not representative of the real system. A thorough revision of the basis for diffusivity data for the concrete barriers is therefore necessary.

The progression of physical degradation processes with time, including different processes leading to fracture formation in the concrete, is difficult to predict with present day knowledge (US DOE 2009) and is an area that would require further research.

9.7 Data uncertainty due to precision, bias, and representativity

Previously used data sets need reconsideration due to recent observations of the BMA barrier status. Fractures may be widespread throughout the concrete structures of the BMA, Silo and BTF, but as yet, only part of the BMA has been inspected. The observed crack frequency in this part of the BMA has been applied to the remainder of the BMA, and the Silo and BTF. However, the lack of knowledge of the current status of these repository parts introduces significant uncertainty.

9.8 Spatial and temporal variability

Spatial variability of data

There will be considerable spatial variability in the diffusive properties of concrete. In particular the occurrences of fractures and other heterogeneities in concrete barriers constitute very significant discontinuities in the diffusive properties of the concrete barriers. Examples of model applications to demonstrate the impact of such defects in concrete barriers are presented in Höglund (2014). For the safety assessment, the spatial variability can be averaged by means of calculating equivalent diffusion resistances. However, it is not currently possible to use a statistical approach to qualify the data. There is more or less a complete lack of site specific data on the diffusion properties and the presence of fractures for all parts of the SFR repository. Only one part of the 1BMA vault has been inspected and the results show few but large fractures. Fractures less than about 100 µm wide were not recorded.

The expected progression of different degradation processes, both chemical and physical, may also cause the spatial variability to evolve over time. It is also likely that fractures will not be equally distributed in the different concrete structures.

Temporal variability of data

The diffusivity of concrete materials in the SFR repository will change over time due to ongoing chemical and physical degradation. The chemical degradation processes are governed by diffusion or the flow of groundwater in different parts of the repository. The groundwater flow is in turn variable in time due to external factors such as land rise, glaciation periods etc. The diffusivity of different components in the repository will in turn be affected by the different degradation processes, hence creating a coupled system. Despite the inherent difficulties in assessing the properties of such systems over time in detail, the evolution of the processes would be possible to quantify with reasonable accuracy using existing model tools for alternative scenarios. Results of such model exercises are presented for the BMA vaults in Höglund (2014). Available data on the long-term chemical degradation of concrete are scarce and would not allow for statistical approaches to study temporal variability.

The progression of physical degradation processes with time, including different processes leading to fracture formation in the concrete, is difficult to predict with present day knowledge (US DOE 2009) and is an area that would require further research. Further studies would be required for full coverage of the physical degradation processes. Some aspects of the physical degradation in the BMA vault have been modelled in Höglund (2014). Systematic and well defined observations on the physical degradation of the barriers over time are scarce and would not allow for statistical approaches to study temporal variability.

9.9 Correlations

Correlations exist between fracture formation, overall barrier degradation, diffusivity, hydraulic conductivities, porosity and radionuclide migration from the repository parts since the processes are coupled. Correlations need to be considered in the SR-PSU evaluations through the use of relevant models.

9.10 Result of supplier's data qualification

The results of the inspection of the physical status of the concrete barriers of a part of the 1BMA vault and the insights gained from the models developed to study the impact of fractures on the hydraulic conductivity suggest significant and possibly serious deviations from the desired barrier functions in 1BMA. Investigations also showed that the concrete constructions of the 1BMA vault and the Silo are not in compliance with present day standards with respect to the amount of reinforcement required to restrict the width of fractures formed due to dry-shrinkage and thermal dimensional changes. This could mean an increased risk for large fractures. Such fractures have also been observed in the inspected part of the 1BMA vault, whereas no information is available for the Silo and the BTF vaults.

Since the results of the inspection (SKBdoc 1430853) and subsequent model evaluations (Höglund 2014) represent significant deviations from the design requirements of 1BMA, the state of the concrete structures have recently been investigated in more detail by SKB and a plan has been developed for repairing and reinforcing the barrier extensively, to achieve the desired properties at closure. The closure plan for SFR (SKBdoc 1358612) describes the planned measures for closure of 1BMA. Therefore, in the PSU safety assessment, it is reasonable to assume that these concrete barriers will be in a good condition at closure.

For the BMA vaults, data have been selected based on the new design of the 2BMA concrete caissons. As in previous assessment (SAR-08) the effective diffusivity of intact concrete has been assumed to $3 \cdot 10^{-12} \text{ m}^2/\text{s}$, further it was assumed to contain 1 fracture per metre with an aperture of $10 \text{ }\mu\text{m}$. This equals an overall effective diffusivity of the intact but slightly fractured concrete of $3.5 \cdot 10^{-12} \text{ m}^2/\text{s}$. This is suggested as an initial value for the concrete barriers of the BMA vaults in the PSU safety assessment.

The anticipated progression of different degradation processes in the 2BMA concrete caissons and in the concrete walls of the silo is described in Höglund (2014). Values of the effective diffusivity suggested for the safety assessment calculations are presented in Table 9-4 for different steps of the degradation. As far as possible the suggested values are based on interpretations of the results of modelling of the chemical degradation of the 2BMA concrete barriers in combination with estimates using simple models to assess different physical degradation processes (Höglund 2014). The time scales for the different steps of the degradation are indicative and need to be considered uncertain. Due to spatial and temporal variability the effective diffusivity different values may be representative for different parts of the barriers and may evolve over time.

Table 9-4. Suggested data on effective diffusivities in concrete materials to be used in the SR-PSU for different time periods and for different parts of SFR.

Part of SFR Material	Time period (years after closure)	Effective diffusivity (m ² /s)
Silo		
Construction concrete in bottom, inner and outer walls and lid	0–100	$3,5 \cdot 10^{-12}$
Concrete moulds	0–100	$3,5 \cdot 10^{-12}$
Concrete grout	0–100	$3,5 \cdot 10^{-10}$
Construction concrete in bottom, inner and outer walls and lid	100–10,000	$1 \cdot 10^{-11}$
Concrete moulds	100–10,000	$2 \cdot 10^{-11}$
Concrete grout	100–10,000	$3,5 \cdot 10^{-10}$
Construction concrete in bottom, inner and outer walls and lid	10,000–20,000	$5 \cdot 10^{-11}$
Concrete moulds	10,000–20,000	$1 \cdot 10^{-10}$
Concrete grout	10,000–20,000	$5 \cdot 10^{-10}$
Construction concrete in bottom, inner and outer walls and lid	20,000–100,000	$1 \cdot 10^{-10}$
Concrete moulds	20,000–100,000	$1 \cdot 10^{-10}$
Concrete grout	20,000–100,000	$1 \cdot 10^{-9}$
BMA		
Construction concrete in bottom, walls and lid	0–100	$3,5 \cdot 10^{-12}$
Concrete moulds	0–100	$3,5 \cdot 10^{-12}$
Concrete grout	0–100	$3,5 \cdot 10^{-10}$
Construction concrete in bottom, walls and lid	100–10,000	$5 \cdot 10^{-12}$
Concrete moulds	100–10,000	$2 \cdot 10^{-11}$
Concrete grout	100–10,000	$4 \cdot 10^{-10}$
Construction concrete in bottom, walls and lid	10,000–20,000	$5 \cdot 10^{-12}$
Concrete moulds	10,000–20,000	$5 \cdot 10^{-11}$
Concrete grout	10,000–20,000	$4 \cdot 10^{-10}$
Construction concrete in bottom, walls and lid	20,000–50,000	$1 \cdot 10^{-11}$
Concrete moulds	20,000–50,000	$1 \cdot 10^{-10}$
Concrete grout	20,000–50,000	$5 \cdot 10^{-10}$
Construction concrete in bottom, walls and lid	50,000–100,000	$2 \cdot 10^{-10}$
Concrete moulds	50,000–100,000	$5 \cdot 10^{-10}$
Concrete grout	50,000–100,000	$1 \cdot 10^{-9}$
BTF		
Concrete floor and lid	0–100	$3,5 \cdot 10^{-12}$
Concrete tanks	0–100	$3,5 \cdot 10^{-12}$
Concrete grout	0–100	$3,5 \cdot 10^{-10}$
Concrete floor and lid	100–10,000	$2 \cdot 10^{-11}$
Concrete tanks	100–10,000	$5 \cdot 10^{-11}$
Concrete grout	100–10,000	$3,5 \cdot 10^{-10}$
Concrete floor and lid	10,000–20,000	$1 \cdot 10^{-10}$
Concrete tanks	10,000–20,000	$2 \cdot 10^{-10}$
Concrete grout	10,000–20,000	$5 \cdot 10^{-10}$
Concrete floor and lid	20,000–100,000	$5 \cdot 10^{-10}$
Concrete tanks	20,000–100,000	$8 \cdot 10^{-10}$
Concrete grout	20,000–100,000	$1 \cdot 10^{-9}$

9.11 Judgements by the SR-PSU team

In this final section the SR-PSU team should judge the data qualification made by the supplier to make sure it is sufficient for the SR-PSU safety assessment.

Sources of information

The SR-PSU team agrees with the sources of information used in Section 9.4.

Conditions for which data is supplied

The SR-PSU team finds the conditions given in Section 9.5 valid and reflecting the conditions assumed in the repository.

Conceptual Uncertainty

The SR-PSU team agrees with the statements regarding the need to revisit conceptual uncertainties, given in Section 9.6.

Data uncertainty due to precision, bias, and representativity

The SR-PSU team agrees with the given uncertainties in Section 9.7. The lack of fracture information mentioned is rectified by a pessimistic (high value) data selection in Table 9-4.

Spatial and temporal variability

The SR-PSU team agrees with the given variabilites given in Section 9.8.

Correlations

The correlations mentioned in Section 9.9 are valid in the SR-PSU safety assessment.

Results of supplier's data qualification

The SR-PSU team agrees with the data given in Table 9-4 and considers it sufficient for usage in the safety assessment.

9.12 Data recommended for use in SR-PSU modelling

The SR-PSU team considers the data supplied in this chapter to be sufficient for SR-PSU and recommend that it is used in the radionuclide transport modelling. The recommended data is therefore given in Table 9-4.

Except for the effective diffusivity of the concrete moulds in the silo during the time period between 10,000–20,000 after closure where the corresponding value for BMA is chosen instead, since it seems unlikely that the concrete moulds in the silo would degrade quicker than the concrete moulds in BMA.

The results of the modelling of the chemical degradation of the 2BMA concrete barriers is shown in Höglund (2014, Figure 9-2). A min and max overall effective diffusivity during a certain time period can be obtained by considering the min and max value of the three curves during the time period. The result is shown in Table 9-5. The min, max and best estimate values can be associated with a log-triangular distribution of effective diffusivities.

The results of the modelling of the chemical degradation of the 2BMA concrete barriers is interpreted in terms of effective diffusivity of the silo concrete barriers in Höglund (2014, Figure B-7). A min and max overall effective diffusivity of the silo barrier can be obtained by taking the min and max values of the silo interpretation and the 2BMA interpretation. The result is shown in Table 9-5. The min and max values can be associated with a log-triangular distribution of effective diffusivities.

Table 9-5. Effective diffusivities used in SR-PSU radionuclide transport modelling.

Time AD	BMA1-2 Construction concrete in bottom, walls and lid D_e (m ² /s)			Silo Construction concrete in bottom, inner and outer walls and lid D_e (m ² /s)			BTF1-2 Concrete floor and lid, Concrete tanks D_e (m ² /s)		
	Best estimate	Min	Max	Best estimate	Min	Max	Best estimate	Min	Max
2000 – 2100	$3.5 \cdot 10^{-12}$	–	–	$4.0 \cdot 10^{-12}$	–	–	$3.0 \cdot 10^{-12}$	–	–
2100 – 2500	$5.0 \cdot 10^{-12}$	–	–	$4.0 \cdot 10^{-12}$	–	–	$4.0 \cdot 10^{-12}$	–	–
2500 – 3000	$5.0 \cdot 10^{-12}$	–	–	$6.0 \cdot 10^{-12}$	$5.0 \cdot 10^{-12}$	$6.0 \cdot 10^{-12}$	$4.0 \cdot 10^{-12}$	–	–
3000 – 22,000	$5.0 \cdot 10^{-12}$	–	–	$1.0 \cdot 10^{-11}$	$5.0 \cdot 10^{-12}$	$1.0 \cdot 10^{-11}$	$1.0 \cdot 10^{-11}$	–	–
22,000 – 34,000	$2.0 \cdot 10^{-11}$	$8.0 \cdot 10^{-12}$	$2.0 \cdot 10^{-11}$	$5.0 \cdot 10^{-11}$	$8.0 \cdot 10^{-12}$	$1.0 \cdot 10^{-10}$	$1.0 \cdot 10^{-11}$	–	–
34,000 – 54,000	$2.0 \cdot 10^{-11}$	$8.0 \cdot 10^{-12}$	$2.0 \cdot 10^{-11}$	$5.0 \cdot 10^{-11}$	$8.0 \cdot 10^{-12}$	$1.0 \cdot 10^{-10}$	$1.0 \cdot 10^{-11}$	–	–
52,000 – 58,000	$2.0 \cdot 10^{-10}$	$2.0 \cdot 10^{-11}$	$2.0 \cdot 10^{-10}$	$5.0 \cdot 10^{-11}$	$2.0 \cdot 10^{-11}$	$1.0 \cdot 10^{-10}$	$1.0 \cdot 10^{-11}$	–	–
58,000 – 102,000	$2.0 \cdot 10^{-10}$	$2.0 \cdot 10^{-11}$	$2.0 \cdot 10^{-10}$	$5.0 \cdot 10^{-11}$	$2.0 \cdot 10^{-11}$	$1.0 \cdot 10^{-10}$	$1.0 \cdot 10^{-11}$	–	–

10 Concrete/Cement hydraulic data

This section concerns the hydraulic conductivity and physical porosity of the concrete/cement types used in the SFR repository. The cementitious materials that can be found in the SFR repository are mainly: structural concrete in buildings and waste packaging, concrete grout used as backfill around the waste packages in the Silo, BMA and BTF vaults and cement mortar and concrete grout used as conditioning material for the waste (SKB 2001).

The different cements used for the concrete are standard Portland types: Skövde SP, Degerhamn SP and Blast furnace cement. The chemical compositions of these are given in SKB (2001) and the **Initial state report**.

Barriers

The concrete barriers comprise the concrete structures in the different repository parts, i.e. the bottom, lid and outer and inner walls of the Silo and BMA, the concrete floor and lid in the BTF vaults and the concrete floor in BLA. They also include shotcrete and rock bolts in the rock walls in all repository parts, the concrete backfill surrounding the waste packages in the Silo and parts of BMA, and the concrete grout that will fill the void between the concrete tanks and the vault walls in the BTF vaults and in between the ash drums in 1BTF.

Waste

Concrete moulds are used in the Silo, BMA and 1BTF repository parts and concrete tanks are used in the 1BTF and 2BTF repository parts, as waste containers. Cement is used both for solidification of ion exchange resins and sludge, and for stabilisation of scrap metal and refuse within many of the different waste packages present in the repository (Almkvist and Gordon 2007).

The mixing proportions of the different concrete types present in SFR are given in Table 10-1.

Table 10-1. Mixing proportions for concrete types in SFR taken from SKB (2001) and Höglund (2001).

Component	Structural concrete	Silo grout	1BTF Grout bottom	1BTF Grout top	Conditioning cement
Cement (kg/m³)	350	325	340	265	1,180
Water (kg/m³)	164.5	366	252	141	437*
Ballast (kg/m³)	1,829	1,302	1,630	1,890	–
w/c ratio	0.47(0.46–0.49)	1.125	0.74	0.53(0.75)**	0.37

* The added water may be insufficient to allow for full hydration of the cement, estimates show a maximum of 96% hydration.

** Value including specified maximum humidity in ballast material.

10.1 Modelling in SR-PSU

This section describes what data are expected from the supplier, and in what SR-PSU modelling activities the data are to be used.

Defining the data requested from the supplier

The supplier should deliver the following data:

- The physical porosity n (–) of the concrete barriers in SFR in their initial condition, i.e. good quality concrete that meets the design requirements of SFR, and in subsequent states as the concrete gradually degrades.
- The hydraulic conductivity K (m/s) of the concrete barriers in SFR in their initial condition, i.e. good quality concrete that meets the design requirements of SFR, and in subsequent states as the concrete gradually degrades.

When considering degradation, the supplier should prioritise mechanical degradation as chemical degradation probably is negligible according to the **Barrier process report**, unless the supplier considers otherwise.

SR-PSU modelling activities in which data will be used

The hydraulic conductivity and porosity of the concrete/cement will be used as input to the hydrogeological calculations. The physical porosity delivered in this section will be input data to the radionuclide transport calculations, where the diffusion available porosity is assessed. All radionuclide transport modelling activities should use the diffusion available porosity.

10.2 Experience from previous safety assessments

This section briefly summarises experience from previous safety assessments, especially the SAFE and SAR-08 safety assessments, which may be of direct consequence for the data qualification in this data report.

Modelling in previous safety assessments

The hydrogeological calculations for SAR-08 were mainly the same as for project SAFE (Holmén and Stigsson 2001a, b). Complementary uncertainty calculations were performed in Holmén (2005, 2007). The used finite difference method and the code, GEOAN, are briefly presented in Holmén (1997).

Conditions for which data were used in previous safety assessments

In the previous safety assessments of the SFR repository; SAFE and SAR-08, some of the concrete barriers' degradation was handled by using a sudden increase in hydraulic conductivity at set points in time during the repository evolution.

In the SAFE safety assessment, a general assumption for the Base Scenario was that the state of barriers at repository closure is in accordance with design criteria (SKB 2001). In the SAFE and SAR-08 safety assessments the structural concrete was given an initial conductivity of $8.3 \cdot 10^{-10}$ m/s, based on the assumption that the concrete may have initial fractures. It was assumed that intact concrete has a hydraulic conductivity of $1 \cdot 10^{-11}$ m/s and that the structures have one fully penetrating fracture per metre of aperture $1 \cdot 10^{-5}$ m. The concrete grout, which has a higher porosity due to the higher water/cement ratio, was assigned an initial conductivity of $8.3 \cdot 10^{-9}$ m/s. After degradation, all the concrete barriers were given a conductivity of $1 \cdot 10^{-8}$ m/s except for the failed barrier sections in the BMA and BTF vaults which were given a conductivity of $1 \cdot 10^{-5}$ m/s.

Sensitivity to assessment results in previous safety assessments

In SAFE and SAR-08, the sudden and large increases in the hydraulic conductivities assumed in the modelling activities resulted in sudden increases in the water flow. It was calculated in Holmén and Stigsson (2001a) and Holmén (2005, 2007) that failed barriers in sections of the vaults would lead to a two to three times higher flow in the BLA and BMA vaults, and a somewhat smaller increase of flow in the BTF vault as result of the changed flow direction in the vaults.

Alternative modelling in previous safety assessments

No alternative modelling was reported in SAFE or SAR-08.

Correlations used in previous safety assessment modelling

Correlations between the barrier degradation, the hydraulic conductivities and the radionuclide migration from the repository parts were used both in SAFE and SAR-08: Increased hydraulic conductivities led to a higher advective flow through the waste packages which increased the release of the radionuclides.

Identified limitations of the data used in previous safety assessment modelling

In its audit of the SAR-08 safety assessment the regulatory (SSM) had the following concerns regarding on how the hydraulic function of the cement and concrete was handled:

- A better reasoning around the argument, presented in the SAR-08 safety assessment, that the engineered barriers in the BMA and Silo repositories would not be affected by the presented degradation processes until after 40,000 years in the main scenario, was requested.
- A better understanding of the freezing processes of the cement barriers in the extreme permafrost scenario was requested.
- An updated understanding of the processes that affect the correlation between the waste materials, the iron present in the repository, and the cement, was also requested. According to the SSM audit this will give better information on if the processes might lead to cracking in the cement matrix.
- SSM also asked for an updated representation of the barrier degradation with regards to risks and hydrogeology. In the SAR-08 safety analysis, as well as in the previous safety analysis SAFE, the barrier degradation was handled with large sudden changes in the hydraulic conductivity of the barriers. In the SSM audit a more smooth transition was requested.

10.3 Supplier input on use of data in SR-PSU and previous safety assessments

When selecting representative data for the hydraulic conductivities of concrete barriers it is essential to consider the anticipated physical status of the actual materials in the SFR repository. In the SAFE safety assessment, a general assumption for the Base Scenario was that the state of barriers at repository closure would be in accordance with design criteria (SKB 2001). High quality concrete is used for construction to supply high mechanical strength; this also means that the hydraulic conductivity may be very low. The mixing proportions used for the concrete will give a low porosity with a low degree of connectivity of the conductive pores. At full hydration of the cement minerals, the major part of the porosity will be gel pores and contraction pores. Neither of these would be expected to contribute significantly to the conduction of water during the early post closure period. The capillary porosity will be low, and the capillary pores are mainly responsible for the conduction of water in the cement phase. Therefore, it would be reasonable to expect that the hydraulic conductivity of a fresh, fully hydrated concrete, produced according to the mixing proportions used for construction concretes in the SFR repository, would be on the order of $1 \cdot 10^{-11}$ m/s or less. However, the occurrence of fractures in the concrete structures may significantly change the expected overall hydraulic conductivity. It has been shown by Höglund and Bengtsson (1991), US DOE (2009) and Höglund (2014) that even a few small fractures may increase the hydraulic conductivity of a concrete structure significantly, even by orders of magnitude.

In concrete constructions, steel reinforcement bars are used to minimise the width and penetration of fractures caused by mechanical loads and volume changes as cement hydrates and dries, as well as in response to any temperature changes. The amount of reinforcement in some of the concrete constructions currently in the SFR repository does not meet present day standards for restricting the width of fractures (cf. Boverket 2004); the Silo bottom and the lower part of the Silo wall contain only about 30% and 70% of the prescribed minimum amount of reinforcement, respectively; for the

1BMA vault, the concrete bottom contains about 50 % of the minimum amount of reinforcement to restrict fracture width (Vattenfall 2011). It therefore seems reasonable to expect that fractures will occur in these structures, although it is difficult to predict the time when this will happen.

Inspection of a 40 m section of the 1BMA vault showed that the concrete barriers are already fractured to an extent that will significantly affect the hydraulic conductivity (SKBdoc 1430853). The fractures have been attributed to early thermal phenomena during the hydration of the concrete and shrinkage as the concrete dries during the early period. The fracturing in the concrete is significantly more extensive than previously known and the fractures observed have also been found to be fully penetrating (SKBdoc 1430853). It should be pointed out that only one quarter of the 1BMA vault has been inspected which means that extrapolation of the results to the entire concrete structure would introduce some uncertainty. Likewise, extrapolation of the observations from the 1BMA concrete barriers to the other parts of the SFR repository would introduce further uncertainty.

The inspection also showed that the steel reinforcement in the concrete has already been affected by corrosion, causing the concrete covering the reinforcement bars to fracture. As a result of this, the surface layer of the concrete has spalled locally. From this, it may be inferred that fracturing may also occur over time as a result of corrosion of the steel form ties that run through the concrete walls in the BMA vault.

The mechanisms leading to fracture formation in concrete are discussed briefly in Höglund (2014) and in more detail in US DOE (2009) and Vattenfall (2011). The types of fractures that form due to shrinkage and heating during early hydration processes are expected to be fully penetrating (US DOE (2009), as observed in the BMA (Vattenfall 2011). In addition to these fractures, which are present from the start and possible to observe, other types of fractures may form at much later stages, and it is highly uncertain when they will occur. Cooling of the concrete structures as a result of groundwater filling the vaults after closure will result in thermal contraction that is likely to cause fractures. Such fractures can be expected to occur within a few years after closure. Further corrosion of reinforcement bars and other steel components, such as form rods, in the concrete barriers may gradually cause additional fractures to form and increase in size as the corrosion progresses. Initially, the alkaline conditions may protect the steel from corrosion by passivation, but the ingress of chloride ions from the saline groundwater will initiate corrosion. Once corrosion has started, the formation of corrosion products, which have larger volume than the corroded steel, will create a mechanical pressure that will eventually initiate fracture formation in the concrete surrounding the steel components. Estimates show that corrosion induced fractures may form within a few decades of the onset of corrosion (Höglund 2014). Other types of fractures, e.g. due to chemical processes leading to the formation of minerals with large molar volumes such as ettringite and thaumasite, may appear at much later stages, although it is highly uncertain when they will occur. Model calculations of such chemical processes are presented in Höglund (2014).

The implications of a more fractured concrete at an early stage are an increased flow of ground water through the barriers (and the waste) after closure and, as a result, a more rapid chemical degradation of the concrete barriers. In turn, as the barriers degrade they will allow an increasing amount of ground water to percolate through the barriers and the waste. The presence of fractures enhances the risk for advective flow through the concrete barriers and also means that the flow will be preferential, hence concentrated to a few locations of the cross-sectional area. Preferential flow means an increased risk that chemical leaching will be preferential, thus over time further increasing the local damage to the concrete barriers. Quantitative estimates of their importance for the barrier integrity have been made and are presented in Höglund (2014). The processes are however complex and the results and interpretation are subject to uncertainty. Since fracturing causes sudden changes of the hydraulic conductivity, the assumption of sudden changes of the hydraulic conductivity of the concrete barriers may be motivated for the safety assessment. The impact of the results has been considered in the radionuclide release calculations (**Radionuclide transport report**). However, further research is necessary to improve the predictions of the temporal evolution of fractures and their consequences.

Calculations presented by Höglund and Bengtsson (1991), Höglund (2014), Vattenfall (2011) and US DOE (2009) have demonstrated that fracture flow will become the dominant hydraulic pathway when one fracture of 1–2 μm aperture width occurs every metre in the concrete. The recent inspections of the 1BMA vault show that the fracturing is already more extensive than this. As this represents a significant deviation from the design requirements of 1BMA, the state of the concrete

structure has recently been investigated in more detail by SKB and a plan has been developed for repairing and reinforcing the barrier extensively, to achieve the desired properties at closure. The Closure Plan for SFR (SKBdoc 1358612) describes the planned measures for closure of 1BMA. Therefore, in the PSU safety assessment, it is reasonable to assume that these concrete barriers will be in a good condition at closure.

A modified barrier system has been designed for the new 2BMA vault to overcome the issues associated with the corrosion of reinforcement. The concrete barriers consist of 14 detached caissons of non-reinforced concrete. The floor and walls are cast in one step to minimise joints in the constructions. During filling, a temporary pre-fabricated concrete cover may be used as a radiation shield over the waste, which will be removed when filling is completed. After filling of the caissons with waste packages, a 0.5 m thick lid will be constructed using cast concrete. The concrete constructions will be supported from the inside by concrete grout embedded waste packages and on the outside by crushed rock/macadam. The grouting will be carried out in steps to minimise the mechanical stress on the non-reinforced concrete walls. The concrete floor rests on a bed of gravel (grain size 6–20 mm) which also acts as part of a hydraulic cage around the caissons.

The concrete walls, floor and lid consist of construction concrete and the composition of this concrete (cement quality, w/c-ratio, ballast quality and content) is assumed to be the same as in 1BMA. The concrete will experience temperature and moisture variations during construction that will cause dimensional changes and may result in mechanical stresses. Such stresses may cause small fractures in the concrete. In the evaluation of 2BMA, it is assumed that thin fractures, with a dimensioning aperture width of 10 µm with an average fracture spacing of 1 m, are present in the concrete at closure. Occasional appearance of fractures with a maximum aperture width of 100 µm is possible. Due to the absence of reinforcement bars and other steel components in the concrete barriers, the impact of steel corrosion on the barrier function does not need to be considered for the 2BMA vault. However, thermal shrinkage of the concrete structures as a result of groundwater filling the vaults after closure is likely to cause fractures within a few years (Höglund 2014). Further, the corrosion of steel components in the waste and the waste packaging may impact the 2BMA concrete barriers.

It is reasonable to expect that fractures are present in the concrete structures of the Silo and the BTF vaults, although the extent of the fractures cannot be deduced unambiguously from the information available. Further inspection of the physical status of the concrete structures in the Silo and the BTF vaults is judged necessary for more precise prediction of their hydraulic properties. However, the impact of initial fractures on groundwater flow may be less significant in the Silo, where flow is likely to be controlled by the surrounding sand/bentonite and bentonite barriers.

Other types of fractures, e.g. due to chemical processes leading to the formation of minerals with large molar volumes such as ettringite and thaumasite, may appear at much later stages, although predictions of when this will occur are uncertain. Model calculations of representative chemical processes are presented in Höglund (2014). It is concluded that the prediction of when fractures would be likely to form is often uncertain and is an area for further study.

Overall, the data selected to represent the hydraulic conductivities of different concrete structures in the SFR repository in the SAFE and SAR-08 studies need to be updated.

Since fracturing causes sudden changes of the hydraulic conductivity, the assumption of sudden changes of the hydraulic conductivity of the concrete barriers may be motivated for the safety assessment.

10.4 Sources of information and documentation of data qualification

Sources of information

In general, specific data for the concrete barriers in the SFR repository are not available, in particular and for obvious reasons, no data exists for concrete in aged and degraded stages. The safety assessments therefore need to be based on judgements of reasonable data sets from typical structural concretes, measurements on other types of concrete structures impacted by fractures and different modelling approaches to estimate the hydraulic properties. In Table 10-2, some data have been compiled from different sources. The sources of information are presented in Table 10-3.

Table 10-2. Some data on hydraulic conductivities of concrete from safety assessments, literature and model estimates. Included are also measurements of the permeability increase factor when comparing fractured and unfractured concretes.

Material	Hydraulic conductivity (m/s)	Permeability increase factor fractured/unfractured	Type of data	Source
Unfractured concrete	$1 \cdot 10^{-11}$	1	Safety assessment	SKB 2001
Concrete with 10 μm fracture aperture width every metre	$8.3 \cdot 10^{-10}$	83	Safety assessment	SKB 2001
Concrete backfill	$8.3 \cdot 10^{-9}$	830	Safety assessment	SKB 2001
Concrete	$10^{-14} - 10^{-10}$	–	Literature review	Luna et al. 2006
Concrete with 1 μm fracture aperture width every metre	$1.1 \cdot 10^{-11}$	1.1	Model estimates	Höglund and Bengtsson 1991
Concrete with 1 μm fracture aperture width every 0.1 metre	$1.6 \cdot 10^{-11}$	1.6	Model estimates	Höglund and Bengtsson 1991
Concrete with 10 μm fracture aperture width every 0.1 metre	$6.3 \cdot 10^{-9}$	630	Model estimates	Höglund and Bengtsson 1991
Concrete with 100 μm fracture aperture width every metre	$6.3 \cdot 10^{-7}$	$6.3 \cdot 10^4$	Model estimates	Höglund and Bengtsson 1991
Concrete with 100 μm fracture aperture width every 0.1 metre	$6.3 \cdot 10^{-6}$	$6.3 \cdot 10^5$	Model estimates	Höglund and Bengtsson 1991
Concrete with 10 μm fracture aperture width every metre penetrating 60% of thickness	$2.5 \cdot 10^{-11}$	2.5	Model estimates	Höglund 2014
Unfractured concrete but chemically degraded to 60% of thickness	$2 \cdot 10^{-11} - 4 \cdot 10^{-11}$	2–4	Model estimates	Höglund 2014
Evaluation of the overall conductivity of the concrete structures considering the observed fractures in the SFR 1BMA vault	$9.7 \cdot 10^{-5} - 4.9 \cdot 10^{-4}$	$9.7 \cdot 10^6 - 4.9 \cdot 10^7$	Model evaluation of observed fractures	Höglund 2014 based on inspection by Vattenfall (SKBdoc 1430853)
30 MPa concrete, compressive stress 70% of ultimate load	–	$10^2 - 10^4$	Measurement	US DOE 2009
Ordinary concrete, 100° C	–	10^2	Measurement	US DOE 2009
Ordinary concrete, bending stress 0.1 mm	–	2.25	Measurement	US DOE 2009
Cement paste, tensile stress 110 μm	–	14	Measurement	US DOE 2009
Cement mortar, tensile stress 130 μm	–	10	Measurement	US DOE 2009
Ordinary concrete, tensile stress 130 μm	–	$2 \cdot 10^3$	Measurement	US DOE 2009
High performance concrete, tensile stress 110 μm	–	10^2	Measurement	US DOE 2009
45 MPa concrete, tensile stress 350 μm	–	10^7	Measurement	US DOE 2009
45 MPa concrete, tensile stress 550 μm under load	–	10^7	Measurement	US DOE 2009
Ordinary concrete, tensile stress 350 μm under load	–	$2.5 \cdot 10^3$	Measurement	US DOE 2009
High performance concrete, tensile stress 300 μm under load	–	35	Measurement	US DOE 2009
Cement mortar, compressive stress 90% of ultimate load	–	16	Measurement	US DOE 2009

Table 10-3. Sources of data on hydraulic conductivities of concrete from safety assessments, model estimates and literature.

Sources of information

Boverket, 2004. Boverkets handbok om betongkonstruktioner: BBK 04. 3rd ed. Karlskrona: Boverket. (In Swedish.)

Höglund L O, 2014. The impact of concrete degradation on the BMA barrier functions. SKB R-13-40, Svensk Kärnbränslehantering AB.

Höglund L O, Bengtsson A, 1991. Some chemical and physical processes related to the long-term performance of the SFR repository. SKB SFR 91-06, Svensk Kärnbränslehantering AB.

Luna M, Arcos D, Duro L, 2006. Effects of grouting, shotcreting and concrete leachates on backfill geochemistry. SKB R-06-107, Svensk Kärnbränslehantering AB.

SKB, 2001. Project SAFE. Compilation of data for radionuclide transport analysis. SKB R-01-14, Svensk Kärnbränslehantering AB.

SKBdoc 1430853. Sprickor i BMA:s betongbarriär – Inspektion och orsak. AE-NCC 12-004, Vattenfall Power Consultant.

US DOE, 2009. Review of mechanistic understanding and modeling and uncertainty analysis methods for predicting cementitious barrier performance. Cementitious Barriers Partnership. CBP-TR-2009-002, Rev.0, U.S. Department of Energy.

Categorising data sets as qualified or supporting data

Qualified data is presented in Höglund (2014) and the other references stated in Table 10-3.

Supporting data is provided in the various references used in the derivation of the data in Höglund (2014) (see reference list of this report).

Excluded data previously considered as important

Data selection has been revised.

10.5 Conditions for which data are supplied

The recent information regarding the status of concrete barriers in SFR suggests that the previous data for safety assessments need reconsideration.

The observations of fractures in 1BMA and the insufficient reinforcement in parts of the 1BMA and Silo discussed in Section 10.3 demonstrate that the data selected for the hydraulic conductivities of the concrete structures in the SFR repository need to be revised. Although the design of 1BMA and 2BMA have been adapted in light of the observed fractures, significant numbers of fractures and other heterogeneities at an early time would change the basis for the assessment of the chemical degradation of the BTF concrete barriers, and this has not been included in previous assessments. It would also enhance the risk for advective flow, and preferential flow, through the concrete barriers, which in turn increases local chemical degradation. Quantitative estimates of the importance of fractures for the barrier integrity have been made and are presented in Höglund (2014).

10.6 Conceptual uncertainty

In general, the conceptual uncertainties related to the hydraulic conductivity of concrete are small. Hydraulic processes are well known and intact concretes are known to be low conductive materials of high durability. However, the status of the concrete barriers in the SFR repository according to recent information (SKBdoc 1430853) introduces significant uncertainty and suggests that the data used previously may not be representative of all vaults. A thorough revision of the basis for hydraulic data for the concrete barriers is therefore necessary.

The progression of physical degradation processes with time, including different processes leading to fracture formation in the concrete, is difficult to predict with present day knowledge (US DOE 2009) and is an area that would require further research.

10.7 Data uncertainty due to precision, bias, and representativity

There is a conceptual uncertainty relating to the effect of chemical degradation on the hydraulic conductivity of the concrete barriers, and vice versa. This needs to be addressed in further investigations. This is furthermore accentuated by the conceptual uncertainties associated with the assessment of how locally enhanced chemical degradation in the vicinity of the fractures will affect hydraulic conductivity.

Fractures may be widespread throughout the concrete structures of the BMA, Silo and BTF, but as yet, only part of the BMA has been inspected. Hence, the lack of knowledge of the current status of these repository parts introduces significant uncertainty. It would therefore be more accurate and defensible to select hydraulic conductivities following a visual inspection of the physical status of these repository parts.

10.8 Spatial and temporal variability

Spatial variability of data

There will be considerable spatial variability in the hydraulic properties of concrete barriers. In particular the occurrence of fractures and other heterogeneities constitute very significant discontinuities in the hydraulic properties of the concrete barriers. Examples of model applications to demonstrate the impact of such defects in concrete barriers are presented in Höglund (2014). For the safety assessment the spatial variability can be averaged by means of calculating equivalent flow resistances. However, it is not currently possible to use a statistical approach to qualify the data. There is more or less a complete lack of site specific data on the hydraulic properties and the presence of fractures for all parts of the SFR repository. Only one part of the 1BMA vault has been inspected and the results show few but large fractures. Fractures less than about 100 μm wide were not recorded. Estimates of the average properties of the barriers based on the fractures documented in the 1BMA vault (SKBdoc 1430853) have been made using simple analytical models (Höglund 2014), as shown in Table 10-2. It is judged inappropriate to attempt any statistical representation based on the available data.

The expected progression of different degradation processes, both chemical and physical, may also cause an evolution over time of the spatial variability. It is also likely that fractures will not be equally distributed in the different concrete structures.

Temporal variability of data

The hydraulic conductivity and porosity of concrete materials in the SFR repository will change over time due to ongoing chemical and physical degradation. The chemical degradation processes are governed by diffusion, the flow of groundwater and the flow resistance in different parts of the repository. The groundwater flow is in turn variable in time due to external factors such as land rise, permafrost periods etc. The flow resistance of different components in the repository will in turn be affected by the different degradation processes, hence creating a coupled system. Despite the inherent difficulties in assessing the properties of such systems over time in detail, the evolution of the processes would be possible to quantify with reasonable accuracy using existing model tools for alternative scenarios. Results of such model exercises are presented for the BMA vaults in Höglund (2014). Available data on the long-term chemical degradation of concrete and the impact of fractures are scarce and would not support a statistical analysis to assess the overall hydraulic conductivity.

The progression of physical degradation processes with time, including different processes leading to fracture formation in the concrete, is difficult to predict with present day knowledge (US DOE 2009) and is an area that would require further research. Further studies would be required for full coverage of the physical degradation processes. Some aspects of the physical degradation in the BMA vaults have been modelled in Höglund (2014). Observations on the physical degradation of the barriers are scarce and would not allow for statistical approaches to study temporal variability.

10.9 Correlations

Correlations exist between fracture formation, overall barrier degradation, hydraulic conductivities and flow, since the processes are coupled. This means that radionuclide migration from the repository parts is also correlated to the degree of fracturing. Correlations need to be considered in the SR-PSU evaluations through the use of relevant models.

The porosity of the concrete also correlates with hydraulic conductivity, flow and therefore radionuclide migration. Fractures also increase the effective porosity of the concrete.

10.10 Result of supplier's data qualification

The results of the inspection of the physical status of the concrete barriers of a part of the 1BMA vault and the insights gained from the models developed to study the impact of fractures on the hydraulic conductivity suggested significant and possibly serious deviations from the desired barrier functions in 1BMA. Investigations also showed that the constructions of the 1BMA and the Silo are not in compliance with present day standards with respect to the amount of reinforcement required to restrict the width of fractures formed due to dry-shrinkage and thermal dimensional changes. This could mean an increased risk for large fractures. Such fractures have also been observed in the inspected part of the 1BMA vault, whereas no information is available for the Silo and the BTF vaults.

For BTF, two different data sets have been proposed: "Briefly fractured" and "Fractured". The purpose has been to provide alternative scenarios that can be applied in different cases in the safety assessment. "Briefly fractured" refers to a concrete barrier which is essentially intact, but with some minor fractures that are difficult to avoid in concrete constructions. "Fractured" refers to concrete where significant fractures are present at an early stage that significantly affects the hydraulic properties of the concrete. After 1,000 years all concrete barriers in BTF are considered fractured.

An extensive investigation of the 1BMA concrete structure has been carried out, which showed that extensive repair and reinforcement measures need to be adopted to achieve the desired properties at closure. The closure plan for SFR (SKBdoc 1358612) describes the planned measures for closure of 1BMA. Therefore, it is reasonable to assume that the 1BMA concrete barriers will be in good condition at closure for the PSU safety assessment.

For the BMA vaults, data have been selected based on the new design of the 2BMA concrete caissons. As in previous assessment (SAR-08), the hydraulic conductivity of intact concrete has been assumed to $1 \cdot 10^{-11}$ m/s, further the concrete was assumed to contain 1 fracture per metre with an aperture width of 10 μm . This equals an overall hydraulic conductivity of the intact but slightly fractured concrete of $8.3 \cdot 10^{-10}$ m/s. This is suggested as an initial value for the concrete barriers of the BMA vaults for the SR-PSU safety assessment.

The anticipated progression of different degradation processes in the 2BMA concrete caissons and in the concrete walls of the Silo is described in Höglund (2014). Values of the hydraulic conductivity and porosity suggested for the safety assessment calculations are presented in Table 10-4 for different periods of time. As far as possible, the suggested values are based on interpretation of the results from modelling the chemical degradation of the 2BMA concrete barriers in combination with estimates generated from simple models that assess different physical degradation processes (Höglund 2014). The time periods considered are indicative and need to be considered uncertain. Where intervals are given for the hydraulic conductivities, all values in the range are equally likely, since the results depend on assumptions regarding the fracture frequency and fracture aperture caused by physical degradation processes. Due to the spatial and temporal variability of fracture formation, frequency and size, the hydraulic conductivity values in the range may be representative for different parts of the barriers.

Table 10-4. Suggested data on hydraulic conductivities and porosities in concrete materials to be used in the SR-PSU for different time periods and for different parts of SFR.

Part of SFR/ Material	Time period (years after closure)	Hydraulic conductivity (m/s)	Total porosity (m ³ /m ³)
Silo			
Construction concrete in bottom, inner and outer walls and lid	0	$8.3 \cdot 10^{-10}$	0.11
Concrete moulds	0	$8.3 \cdot 10^{-10}$	0.11
Concrete grout	0	$8.3 \cdot 10^{-9}$	0.3
Construction concrete in bottom, inner and outer walls and lid	50–500	$4 \cdot 10^{-9} - 7 \cdot 10^{-7}$	0.11
Concrete moulds	50–500	$2 \cdot 10^{-7}$	0.11
Concrete grout	50–500	$4 \cdot 10^{-7}$	0.3
Construction concrete in bottom, inner and outer walls and lid	after 500 –20,000 >20,000	$1 \cdot 10^{-6} - 2 \cdot 10^{-5}$	0.11 0.15–0.17 0.17–0.25
Concrete moulds	after 500	$2 \cdot 10^{-5}$	0.11
Concrete grout	after 500	$4 \cdot 10^{-5}$	0.3
BMA			
Construction concrete in bottom, walls and lid	0	$8.3 \cdot 10^{-10}$	0.11
Concrete moulds	0	$8.3 \cdot 10^{-10}$	0.1
Concrete grout	0	$8.3 \cdot 10^{-9}$	0.3
Construction concrete in bottom, walls and lid	before 100	$5 \cdot 10^{-9} - 5 \cdot 10^{-8}$	0.11
Concrete moulds	before 100	$5 \cdot 10^{-9} - 5 \cdot 10^{-8}$	0.11
Concrete grout	before 100	$5 \cdot 10^{-8} - 5 \cdot 10^{-7}$	0.3
Construction concrete in bottom, walls and lid	100–20,000	$5 \cdot 10^{-8} - 5 \cdot 10^{-7}$	0.11–0.16
Concrete moulds	100–20,000	$5 \cdot 10^{-8} - 5 \cdot 10^{-7}$	0.11–0.16
Concrete grout	100–20,000	$5 \cdot 10^{-7} - 5 \cdot 10^{-6}$	0.4
Construction concrete in bottom, walls and lid	20,000– 50,000	$5 \cdot 10^{-7} - 5 \cdot 10^{-6}$	0.16–0.20
Concrete moulds	20,000– 50,000	$5 \cdot 10^{-7} - 5 \cdot 10^{-6}$	0.16–0.20
Concrete grout	20,000– 50,000	$5 \cdot 10^{-6} - 5 \cdot 10^{-5}$	0.5
Construction concrete in bottom, walls and lid	50,000– 100,000	$5 \cdot 10^{-6} - 5 \cdot 10^{-5}$	0.5
Concrete moulds	50,000– 100,000	$5 \cdot 10^{-6} - 5 \cdot 10^{-5}$	0.5
Concrete grout	50,000– 100,000	$5 \cdot 10^{-5} - 5 \cdot 10^{-4}$	0.5
BTF			
Concrete floor and lid (briefly fractured case)	0–100	$8.3 \cdot 10^{-10}$	0.1
Concrete tanks (briefly fractured case)	0–100	$8.3 \cdot 10^{-10}$	0.1
Concrete grout (briefly fractured case)	0–100	$8.3 \cdot 10^{-9}$	0.2
Concrete floor and lid (briefly fractured case)	100–1,000	$8.3 \cdot 10^{-9}$	0.1
Concrete tanks (briefly fractured case)	100–1,000	$8.3 \cdot 10^{-8}$	0.1
Concrete grout (briefly fractured case)	100–1,000	$8.3 \cdot 10^{-8}$	0.2
Concrete floor and lid (fractured case)	0–100	$1 \cdot 10^{-5}$	0.11
Concrete tanks (fractured case)	0–100	$1 \cdot 10^{-5}$	0.11
Concrete grout (fractured case)	0–100	$1 \cdot 10^{-5}$	0.2
Concrete floor and lid (fractured case)	100–1,000	$1 \cdot 10^{-5}$	0.11
Concrete tanks (fractured case)	100–1,000	$1 \cdot 10^{-5}$	0.11
Concrete grout (fractured case)	100–1,000	$5 \cdot 10^{-5}$	0.3
Concrete floor and lid (fractured case)	1,000–10,000	$1 \cdot 10^{-4}$	0.2
Concrete tanks (fractured case)	1,000–10,000	$1 \cdot 10^{-4}$	0.2
Concrete grout (fractured case)	1,000–10,000	$5 \cdot 10^{-4}$	0.4
Concrete floor and lid (fractured case)	10,000– 100,000	$1 \cdot 10^{-3}$	0.5
Concrete tanks (fractured case)	10,000– 100,000	$1 \cdot 10^{-3}$	0.5
Concrete grout (fractured case)	10,000– 100,000	$1 \cdot 10^{-3}$	0.5

10.11 Judgements by the SR-PSU team

Sources of information

The SR-PSU team agrees with the sources of information used in Section 10.4.

Conditions for which data is supplied

The SR-PSU team finds the conditions given in Section 10.5 valid and reflecting the conditions assumed in the repository.

Conceptual Uncertainty

The SR-PSU team agrees with the statements regarding the need to revisit conceptual uncertainties, given in Section 10.6.

Data uncertainty due to precision, bias, and representativity

The SR-PSU team agrees with the given uncertainties in Section 10.7.

Spatial and temporal variability

The SR-PSU team agrees with the given variabilites given in Section 10.8.

Correlations

The correlations mentioned in Section 10.9 are valid in the SR-PSU safety assessment.

Results of supplier's data qualification

The SR-PSU team agrees with the data given in Table 10-4 and considers it sufficient for usage in the safety assessment.

10.12 Data recommended for use in SR-PSU modelling

As the SR-PSU team agrees with the suppliers the suggested data recommended for use in SR-PSU modelling is given in Table 10-4.

11 Hydraulic pressure field in the SFR local domain

In the SAR-08 safety assessment main report (SKB 2008) it is written that the site of the existing facility, SFR 1, was selected partly because of the low regional hydraulic gradient. The direction and magnitude of the gradient will change over time due to shoreline displacement as well as climate changes: Today, when the repository is below the sea floor, the hydraulic gradient is slightly upward-directed. After about 1,000–2,000 years the gradient is expected to increase and be more horizontal. In this and later phases the gradient is expected to be more controlled by local topography. This is further described in the SR-PSU Hydrogeology report (Odén et al. 2014).

Within the rock vaults (in both SFR 1 and SFR 3) local gradient variations are to be expected. To be able to resolve these variations better a detailed near field groundwater flow modelling activity is performed within SR-PSU. This chapter deals with the input data needed for this detailed near field modelling.

11.1 Modelling in SR-PSU

This section describes what data are expected from the supplier, and in which SR-PSU modelling activities the data are to be used.

Defining the data requested from the supplier

Data are requested for three bedrock cases for the temperate climate domain (three defined time steps; 2000 AD, 3000 AD and 5000 AD, corresponding to the Global warming climate case), and also for the periglacial climate domain with a shallow permafrost depth (–59 m).

The following data are requested as input to the near field modelling:

- The dynamic pressure (Pa).
- Groundwater velocities (m/s).
- Rock permeability field (m²).

It should be noted that it is not the actual data that is delivered. The requested data are delivered in the form of input files for the regional-scale groundwater flow model (DarcyTools input format). The customer then executes DarcyTools, using the delivered files as input, in order to extract the requested data.

SR-PSU modelling activities in which data will be used

The near-field model extracts pressure and flux boundary conditions as well as the rock permeability field from the supplied regional hydrogeological data. A main goal of the near-field model is to provide detailed information regarding the water flow through vaults, barriers, and waste domains of SFR 1 and SFR 3. Modelling is carried out in Comsol Multiphysics and is described in a separate report (Abarca et al. 2014).

11.2 Experience from previous safety assessments

This section briefly summarises experiences from previous safety assessments, especially the SAFE and SAR-08 safety assessments, which may be of direct consequence for the data qualification in this data report.

Modelling in previous safety assessments

In the SAFE safety assessment, the hydro modelling was carried out with GEOAN which uses the Finite Difference Method for calculating groundwater flows (Holmén and Stigsson 2001a). The most detailed model was the last model in a chain of three nested models i.e., each one having a smaller volume but a higher flow resolution than the previous in the chain. At the lowest level of detail the SFR region covered, a total area of 210.8 km² and a depth of 1,000 m, see Figure 11-1.

At the highest level of detail the vaults and the access tunnels except the ramp tunnel were covered; a total area of 0.21 km² and a vertical extension of 108 m, see Figure 11-2. The detailed model results were presented in a separate report (Holmén and Stigsson 2001b).

For SAR-08 two subsequent reports were made, Holmén (2005, 2007), which used an inverse modelling approach to estimate the uncertainties in the SAFE modelling results. Both of the reports generated uncertainty factors which were also used in the SAR-08 safety assessment along with the results from SAFE (Holmén and Stigsson 2001a, b).

Conditions for which data were used in previous safety assessments

In SAFE, the boundary conditions for each model level were supplied by the results from the previous model level in the chain. Therefore the hydraulic pressure gradients used for the detailed model level originated from the boundary conditions and resulting calculations done on the regional level, with a local level between them in the chain.

The regional model used somewhat different boundary conditions on the six sided rectangular domain: For the top side of part which was not covered by the sea an algorithm (further described in Holmén and Stigsson (2001a) was used to calculate a non linear boundary condition reflecting the discharge and recharge areas above land. A specified head boundary condition was used for the top part covered by the sea, governed by the water depth and the time dependent shoreline displacement.

The bottom part, at 900 metres depth, of the regional model domain had had a no flow boundary condition.

As the general topography gradient in the regional model points northeast a no flow boundary condition was set on the southwest and northwest faces of the model domain (see Figure 11-1 for a visual reference). This was also motivated by the fact that the minimum distance between SFR and these two boundaries were about 7 km, and therefore the boundary conditions were expected to have very little, if any, impact on the groundwater flow passing through the repository. The uppermost cells along the southwest face, coincides with actual surface water bodies, which were assumed to be maintained as lakes in the future; consequently, the uppermost cells along the Southeast face was assigned the specified head boundary condition. Below the surface cells a no-flow boundary condition was set. A no-flow boundary condition was also set for the Northeast face because this face is approximately located along the lowest topographic levels in the regional basin. Hence, there will be a groundwater flow from the opposite side of the basin, which prevents further transport towards Northeast.

The chain of running the model simulations was described in Holmén and Stigsson (2001a) in the following way:

1. Simulation with the regional level model with set boundary conditions described above.
2. Simulation with the local level model using specified head boundary conditions from the results from the regional level simulation.
3. Simulation with the repository level model using specified head boundary conditions from the results from the local level simulation.

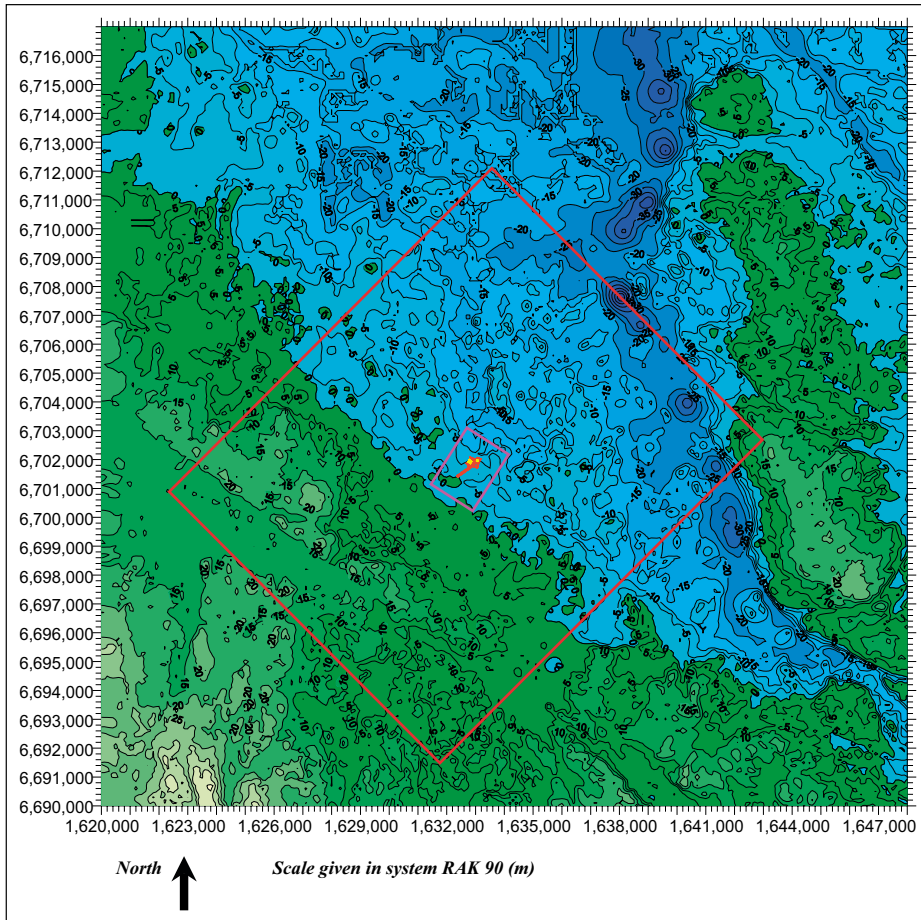


Figure 11-1. Regional (lowest level of detail) model boundary in red and local (intermediate level of detail) model boundary in purple. Reproduced from Holmén and Stigsson (2001b).

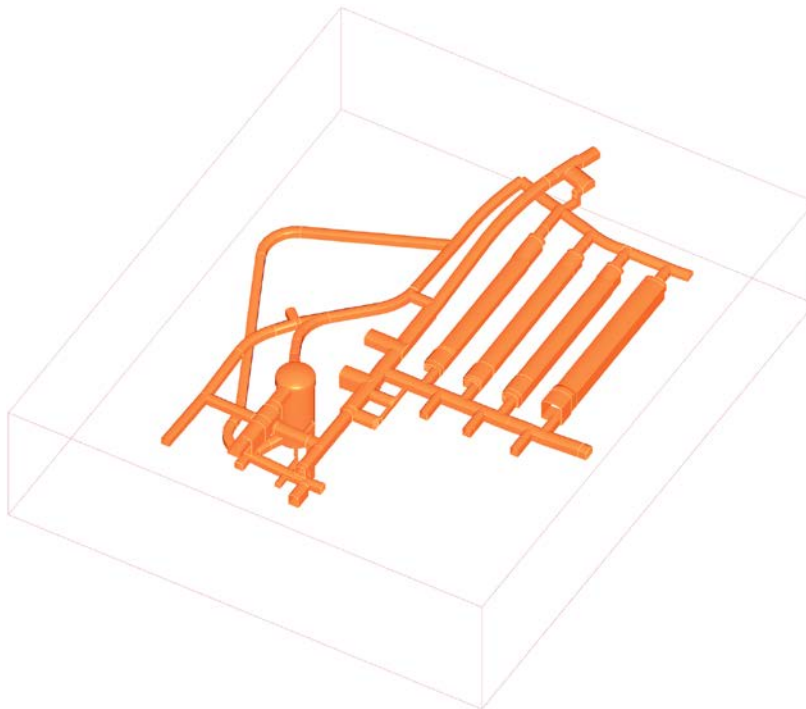


Figure 11-2. Boundaries of the most detailed model in light gray. Reproduced from Holmén and Stigsson (2001a).

Sensitivity to assessment results in previous safety assessments

In the radionuclide transport report for the SAR-08 safety assessment (Thomson et al. 2008) the conclusions state that the SFR facility is sensitive to the regional hydrogeological regime and the assumptions made in it. Regarding the input data to the AMBER model used for the SAR-08 the report states that: “The key changes are in rates of groundwater flow within the repository at 1,000, 2,000 and 3,000 years post-closure (and additionally for those far future at times when environmental changes are considered, such as development of permafrost, submergence of the site etc). The effects in the near-field are propagated to the geosphere, and so in turn effects in the geosphere will be propagated to the biosphere (Thomson et al. 2008).

Alternative modelling in previous safety assessments

For the SAFE safety assessment, analytical approaches were used in conjunction with the GEOAN code, e.g., to the regional models, the groundwater saturation at the repository, and the water flows in the vaults and tunnels. This was to make sure that the latter model results were within reasonable order of magnitudes (Holmén and Stigsson 2001a).

Correlations used in previous safety assessment modelling

No new correlations have been identified in the SR-PSU safety assessment.

Identified limitations of the data used in previous safety assessment modelling

In their review of the SAR-08 safety assessment the regulatory authority SSM asked for better motivations and understanding regarding the groundwater flows both within and outside of the repository. SSM especially pointed out that it was difficult reproducing the results from the regional groundwater flow modelling due to lack of data traceability in SKB’s work. SSM also found that the handling of the interface between the groundwater flow modelling and the radionuclide transport calculations was lacking traceability.

11.3 Supplier input on use of data in SR-PSU and previous safety assessments

The method of selecting and using data for the conditions and model chain used in previous safety assessments was correct.

In SR-PSU a different approach was used, involving two different numerical codes for the far and near-field. The supplied data should be used to extract requested data for different climate domains (temperate and periglacial) and descriptions of the bedrock.

11.4 Sources of information

The underlying data used to produce the delivered files are described in Odén et al. (2014) and its supporting documents, see Table 11-1.

Table 11-1. Sources of information.

Odén M, Follin S, Öhman J, Vidstrand P, 2014. SR-PSU Bedrock hydrogeology. Groundwater flow modelling methodology, setup and results. SKB R-13-25, Svensk Kärnbränslehantering AB.

11.5 Conditions for which data are supplied

The supplied model setups are valid for different shoreline positions and descriptions of the rock mass as described in the delivery.

11.6 Conceptual uncertainty

The delivered data represent different descriptions of the rock mass (Bedrock Cases). These cases cover the uncertainty in the description of the bedrock with one base case and two bounding variants.

11.7 Data uncertainty due to precision, bias, and representativity

Three out of seventeen bedrock cases were delivered. Based on the outcome of the groundwater flow simulations during temperate climate conditions, three bedrock cases were selected to characterise the observed range of heterogeneity and conceptual uncertainty in bedrock parameterisation. The three bedrock cases were selected based on calculated cross flows through the eleven disposal rooms in SFR 1 and SFR 3. They comprised the following.

1. One “low-flow” bedrock case: bedrock parameterisation variant with low disposal-facility cross flows; this case is associated with realisation R01 for the identified (deterministic) deformation zone (HCD) and realisation R18 for the less fractured rock between the deformation zones (HRD).
2. A “base case” bedrock case: a bedrock parameterisation variant with median disposal-facility cross flows; this case is associated with a homogeneous depth trend for the HCD and realisation R85 for the HRD.
3. One “high-flow” bedrock case: a bedrock parameterisation variant with high disposal-facility cross flows; this case is associated with realisation R07 for the HCD and realisation R85 for the HRD.

11.8 Spatial and temporal variability

Spatial variability of data

The spatial variability is captured with the use of three different bedrock cases.

Temporal variability of data

The temporal variability is captured partly by studying two different climate domains and also three different positions of the repository relative the shoreline of the sea for the temperate climate domain:

- Shoreline position 1 (in the global warming and early periglacial climate cases, this position correspond to the situation at 2000 AD): corresponds to a submerged repository
- Shoreline position 2 (in the global warming and early periglacial climate cases, this position would correspond to the situation at 3000 AD): corresponds to an intermediate case in which the shoreline is above the repository and
- Shoreline position 3 (in the global warming and early periglacial climate cases, this position would correspond to the situation after 5000 AD): corresponds to a retreating shoreline position, far away from the repository.

11.9 Correlations

No correlations have been reported.

11.10 Result of supplier's data qualification

The files delivered are presented in Table 11-2.

Table 11-2. Data files delivered.

Delivered files temperate climate domain
Td11_01_BASE_CASE1_DFN_R85_L1BC_RUN_2000AD_COMSOL_2013-01-24.zip
Td11_01_BASE_CASE1_DFN_R85_L1BC_RUN_3000AD_COMSOL_2013-01-24.zip
Td11_01_BASE_CASE1_DFN_R85_L1BC_RUN_5000AD_COMSOL_2013-01-24.zip
Td11_11_nc_DEP_R07_DFN_R85_L1BC_RUN_2000AD_COMSOL_2013-01-24.zip
Td11_11_nc_DEP_R07_DFN_R85_L1BC_RUN_3000AD_COMSOL_2013-01-24.zip
Td11_11_nc_DEP_R07_DFN_R85_L1BC_RUN_5000AD_COMSOL_2013-01-24.zip
Td11_15_nc_NoD_R01_DFN_R18_L1BC_RUN_2000AD_COMSOL_2013-01-24.zip
Td11_15_nc_NoD_R01_DFN_R18_L1BC_RUN_3000AD_COMSOL_2013-01-24.zip
Td11_15_nc_NoD_R01_DFN_R18_L1BC_RUN_5000AD_COMSOL_2013-01-24.zip
DTS_Steady_state_Td11.exe
TD11_Grid_2000AD_2013-01-24.zip
TD11_Grid_3000AD_2013-01-24.zip
TD11_Grid_5000AD_2013-01-24.zip
Td11_Porosity_2013-02.13.zip
Td11_Conductivity_field_01_COMSOL_2013-01-21.zip
Td11_Conductivity_field_11_COMSOL_2013-01-21.zip
Td11_Conductivity_field_15_COMSOL_2013-01-21.zip

Delivered files periglacial climate domain
_18_Permafrost_to_amphos_grid.zip
_18_shallow.zip

11.11 Judgements by the SR-PSU team

Sources of information

The SR-PSU team finds the source given in Section 11.4 sufficient for SR-PSU use.

Conditions for which data is supplied

The SR-PSU team finds the conditions given in section 11.5 are valid for safety assessment use.

Conceptual Uncertainty

The SR-PSU team accepts the handling of conceptual uncertainties provided by the supplier in Section 11.6.

Data uncertainty due to precision, bias, and representativity

The SR-PSU team also accepts the suppliers handling of these uncertainties in Section 11.7.

Spatial and temporal variability

The suppliers handling of spatial and temporal variabilites in Section 11.8 are accepted by the SR-PSU team.

Correlations

The SR-PSU team agrees that there are no correlations with other activities in the SR-PSU safety assessment.

Results of supplier's data qualification

The SR-PSU team accepts the supplied data sets given in Table 11-2.

11.12 Data recommended for use in SR-PSU modelling

The SR-PSU team recommends using the data sets the supplier has given in Table 11-2.

12 Shore-level evolution

The spatial location of the shoreline varies in time due to changes in the relative sea-level. The relative sea-level evolution in Forsmark is determined by the net effect of eustatic changes (i.e. sea-level rise associated with e.g. changes in the volume and spatial distribution of ocean water) and isostatic changes (at the Forsmark site manifested through glacial isostatic rebound). The present-day net effect of the two processes at the Forsmark site is a slow lowering and off-shore migration of the shoreline. In SR-PSU the relative sea-level is also termed *relative shore-level*. The surface above the existing SFR1 and planned SFR3 is submerged at present, with a maximum water depth of 7.2 m over SFR1 and 5.3 m over the planned SFR 3 (Layout L2). Shore-level changes are presently dominated by glacial isostatic rebound in the Forsmark region resulting in an ongoing shore-level lowering. This sea-level lowering results in a continued shoreline regression over the repository, described in the Global warming climate case and Early periglacial climate case (in the **Climate report**, Section 4.1 and Section 4.2). The transformation to fully subaerial conditions above the repository footprint will in these cases take more than one thousand years to complete. In addition, a complementary case with an initial period dominated by a stand-still or possible transgression over the repository is described in the Extended global warming climate case (in the **Climate report**, Section 4.3).

The main question for the safety assessment related to changes in the relative shore-level is related to the surface system and future human actions, including drilling of a well. The salinity in the lake/sea covering the site is also of interest.

12.1 Modelling in SR-PSU

This section describes what data are expected from the supplier, and in what SR-PSU modelling activities the data are to be used.

Defining the data requested from the supplier

The future shore-level evolution at Forsmark has to be provided for each of the SR-PSU climate cases. Relative shore level should be provided in metres, measured as the vertical distance from the present shore-level in Forsmark. It should be provided as a function of time for the period from the time of the Weichselian deglaciation of Forsmark (at 8800 BC) to 100,000 years into the future (102,000 AD) at a minimum time resolution of 500 years.

- *Global warming and early periglacial climate case*
The evolution of relative shore-level for these two climate cases should be identical. It should represent a hypothetical future warm climate with a melting of the Greenland ice sheet. The available evidence indicates that global warming greater than a certain threshold would lead to a near-complete loss of the Greenland ice sheet over a millennium or more, causing a global mean sea-level rise of about 7 m (Church et al. 2013). However, the ice sheet dynamics involved in such a deglaciation process are poorly constrained due to lack of knowledge. In the glacial isostatic adjustment simulations, the Greenland ice sheet therefore should be assumed to melt away at a linear rate over the next 1,000 years, resulting in 7 m of global-average sea-level rise.
- *Extended global warming climate case*
The evolution of relative shore-level for this climate case should be determined based on an assumption of maximum eustatic (sea-level) changes in a future warmer climate. The evolution should thus represent a maximum length of the initial submerged period at Forsmark. The maximum length of the initial submerged period should be determined based on *i)* observed isostatic rebound in Forsmark at present and *ii)* an estimation of the maximum eustatic contribution at Forsmark based on an up-to-date review of the scientific literature. Prior to the present-day, the evolution of relative shore-level should be assumed to be identical to the evolution in the *global warming climate case* for the same period. After the initial submerged period, the evolution of relative shore-level for this climate case should be assumed to be identical to the evolution in the *global warming climate case* as starting from the present.

- *Weichselian glacial climate case*
The evolution of relative shore-level for this climate case should be based on the reconstruction of the last glacial cycle in Forsmark covering the last 120,000 years.

SR-PSU modelling activities in which data will be used

Data on evolution of relative shore-level are used for:

- landscape evolution modelling
- permafrost modelling
- groundwater-flow modelling

12.2 Experience from previous safety assessments

This section briefly summarises experience from previous safety assessments, especially the SAFE and SAR-08 safety assessments, which may be of direct consequence for the data qualification in this data report.

Modelling in previous safety assessments

There is no difference between the SAR-08 and SR-PSU modelling approaches. For SR-PSU, 3D Glacial Isostatic Adjustment (GIA) modelling results (Whitehouse 2009) are used to evaluate the 2D GIA results used from SR-Can. For SR-PSU, the uncertainty in future sea-level changes is re-assessed based on an up-to-date literature review and included in the *extended global warming climate case*.

Conditions for which data were used in previous safety assessments

Conditions have not changed for SR-PSU as compared to SAR-08.

Sensitivity to assessment results in previous safety assessments

The data on shore-level change used in SAR-08 was of consequence for the following safety assessment scenario:

Wells

This safety assessment scenario is based on the assumption that the safety function “No wells” cannot be maintained. The probability of drilling of a well intruding into the SFR repository is dependent on the location of the shoreline. In SAR-08 it was assumed that the probability of intrusion is low during the first thousand years before glacial isostatic rebound has left the ground above the repository elevated and dry.

Alternative modelling in previous safety assessments

No alternative modelling was performed in SAR-08.

Correlations used in previous safety assessment modelling

No correlations with other data were used in SAR-08.

Identified limitations of the data used in previous safety assessment modelling

The uncertainty in the shore-level evolution in SAR-08 was reported to be large (SKB 2008). However, no major limitations in the data have been identified, given the approach taken when using them.

12.3 Supplier input on use of data in SR-PSU and previous safety assessments

The method of selecting and using data practiced in SAR-08 was correct.

12.4 Sources of information and documentation of data qualification

Sources of information

The source of information for the shore-level evolution data set is the **Climate report**. Within the **Climate report**, references to relevant lower-level documents can be found. The full reference is given in Table 12-1.

Table 12-1. Main sources of information used in the data qualification.

Sources of information
Climate report, 2014. Climate and climate-related issues for the safety assessment SR-PSU. SKB TR-13-05, Svensk Kärnbränslehantering AB.

Categorising data sets as qualified or supporting data

The data on shore-level evolution given in the **Climate report** are considered to be qualified, see Table 12-2.

Table 12-2. Qualified and supporting data sets.

Qualified data sets	Supporting data sets
Figure 2-37. Shore-level evolution at Forsmark for the <i>global warming</i> and the <i>Weichselian glacial cycle climate case</i> . The shore-level evolution data are based on Global Isostatic Model simulations and extrapolations of up-to-present Holocene isostatic uplift rates at the Forsmark site. In the Climate report , and lower-level references therein, the modelling strategy, modelling tools, and validity of the modelling are described. It is judged that the modelling approaches are adequate for the purposes of the SR-PSU safety assessment.	None

Excluded data previously considered as important

No data previously considered for qualification were excluded.

12.5 Conditions for which data are supplied

The evolution of relative shore-level is determined by isostatic and eustatic changes which are coupled to climate evolution at different spatial and temporal scales. Current scientific understanding of past and future evolution of climate and climate-related processes is described in the **Climate report**.

12.6 Conceptual uncertainty

As described in the **Climate report**, the processes involved in glacial isostatic adjustment, and their effect upon shore-level evolution, are well understood. There are no major uncertainties in our understanding of the mechanistic processes that cause shoreline migration. There is however uncertainty in the calculated shore-level evolution due to model simplifications and discretisation are significant.

The uncertainties in shore-level evolution are handled in the SR-PSU safety assessment, as in SAR-08, by defining a range of climate cases for Forsmark.

12.7 Data uncertainty due to precision, bias, and representativity

The uncertainty in the future eustatic contribution to shore-level change is large. The SR-PSU climate cases *global warming climate case* and *extended global warming climate case* were defined in order to cover the full uncertainty associated with future sea-level changes. The *global warming climate case* represents the lower end of the uncertainty range, with negligible effects of global sea-level rise, whereas the *extended global warming case* represents the upper end of the uncertainty range. The two cases thus represent a minimum length period of submerged conditions above SFR in the *global warming climate case* as opposed to a maximum length period of submerged conditions above SFR in the *extended global warming climate case*.

12.8 Spatial and temporal variability

Spatial variability of data

Shore-level changes vary spatially, due to spatial variations in the isostatic and eustatic contributions. The spatial scale of such variations however significantly exceeds the size of the Forsmark region considered in the landscape evolution, permafrost and groundwater flow modelling performed. Such variations are therefore judged to be irrelevant for the SR-PSU safety assessment.

Temporal variability of data

The relative shore-level varies on shorter (order of days) to long (inter-annual) time scales. Short-term variations, associate with e.g. storm surges, do not influence the long-term shore-level evolution, which is why such variations are not judged to be of relevance for the landscape, permafrost and groundwater flow evolution.

12.9 Correlations

No correlations are considered relevant, why none were used.

12.10 Result of supplier's data qualification

The requested data are justified in the **Climate report**. A brief summary is given here.

Data on the evolution of relative shore-level for the SR-PSU *global warming, early periglacial* and *extended global warming* climate cases are illustrated in Figure 12-1. The data are based on global isostatic model simulations, extrapolations of up-to-present Holocene isostatic uplift rates at the Forsmark site, and peer-review-published data on future sea-level rise (see details in the **Climate report**, Section 2.2.4, Section 4.1.3 and Section 4.3.3). The figure shows shore-level evolution from the present-day to 100,000 years after present (A), and to 10,000 years after present (B).

Data on the evolution of relative shore-level for the SR-PSU *Weichsleian glacial cycle climate case* are illustrated in Figure 12-2. The data are based on global isostatic model simulations and extrapolations of up-to-present Holocene isostatic uplift rates at the Forsmark site (see details in the **Climate report**, Section 2.2.4 and Section 4.4.3). The figure shows shore-level changes from the time of the Weichselian deglaciation of Forsmark (at 8800 BC/10,800 years before present), through the present time, and until 120,000 years after present.

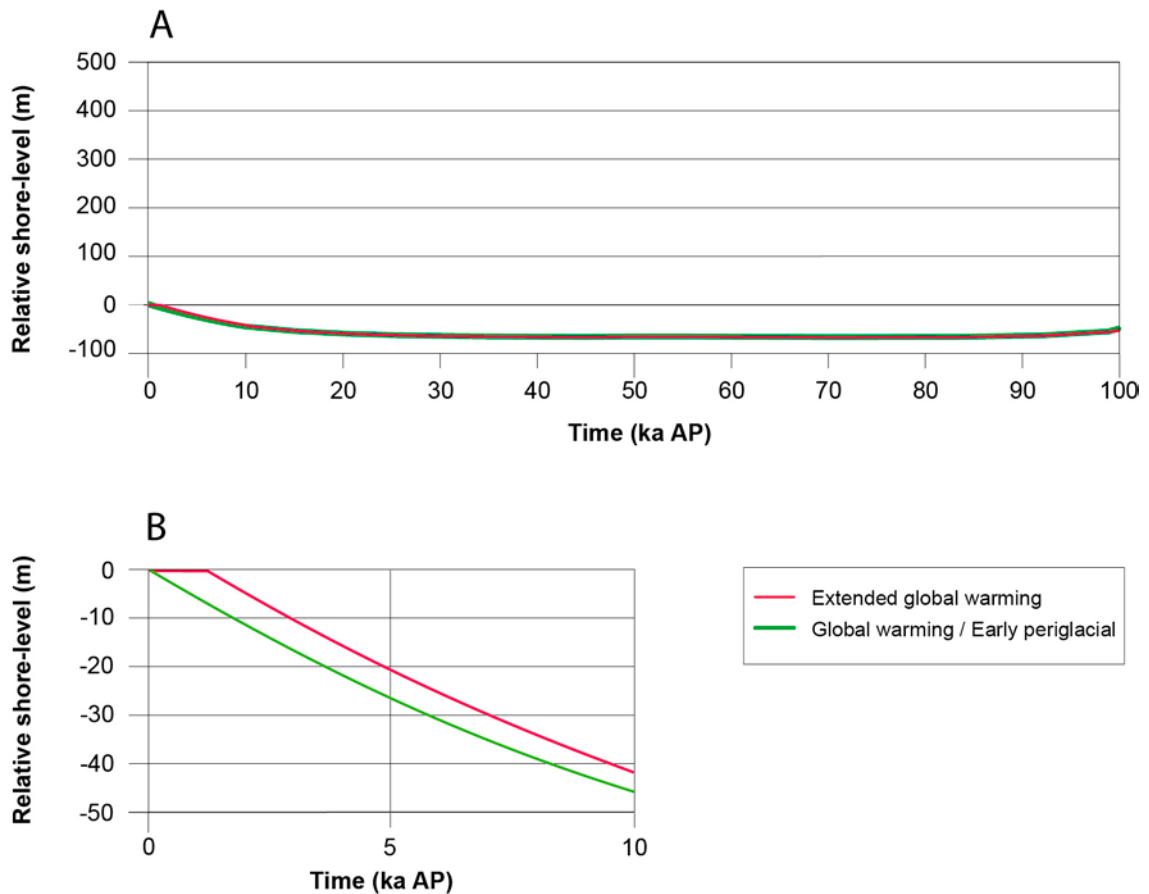


Figure 12-1. Shore-level evolution data from the present (A.) to 100,000 years after present and (B.) to 10,000 years after present for the global warming and early periglacial climate cases (green line) and the extended global warming climate case (red line). Reproduced from the *Climate report* (Figure 4-6).

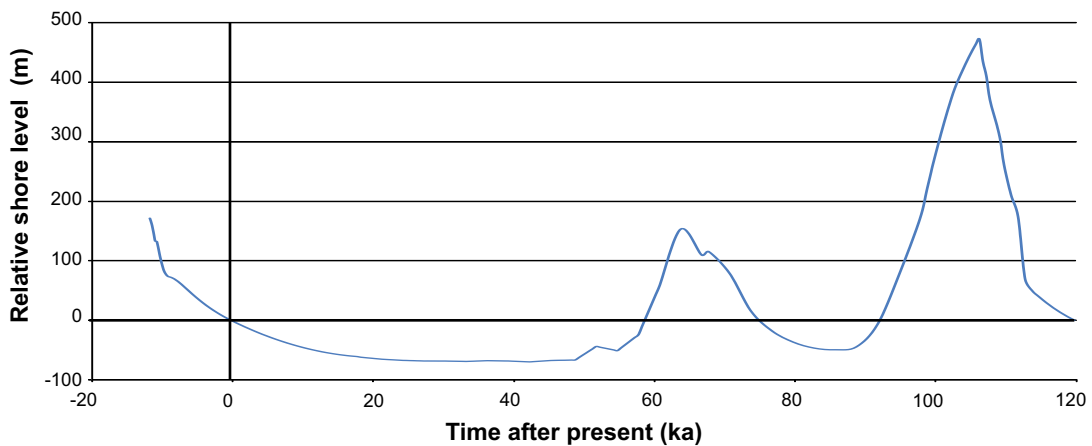


Figure 12-2. Shore-level evolution data for the period 10,800 years before present (8800 BC) to 120,000 years after present for the Weichselian glacial cycle climate case. Reproduced from the *Climate report* (Figure 4-11).

12.11 Judgements by the SR-PSU team

Sources of information

The SR-PSU team considers the source given in Section 12.4 to be sufficient.

Conditions for which data is supplied

The general conditions given in Section 12.5 are deemed sufficient by the SR-PSU team.

Conceptual Uncertainty

The SR-PSU agrees with the suppliers statement that the conceptual uncertainties are well known in Section 12.6.

Data uncertainty due to precision, bias, and representativity

The SR-PSU team also agrees with suppliers the handling of precision, bias and representativity uncertainties in Section 12.7.

Spatial and temporal variability

The handling of spatial and temporal variabilities in Section 12.8 by the supplier is deemed sufficient

Correlations

The SR-PSU team cannot find any correlations regarding this data within the safety assessment.

Results of supplier's data qualification

As all these data have been produced within SR-PSU, no judgement is made, except that all data and descriptions are judged to be adequate.

12.12 Data recommended for use in SR-PSU modelling

The evolution of relative shore-level data presented in Figure 12-1, Figure 12-2 and in the references listed in Table 12-2 are recommended for use in SR-PSU.

References

SKB's (Svensk Kärnbränslehantering AB) publications can be found at www.skb.se/publications. References to SKB's unpublished documents are listed separately at the end of the reference list. Unpublished documents will be submitted upon request to document@skb.se.

References with abbreviated names

Main report, 2014. Safety analysis for SFR. Long-term safety. Main report for the safety assessment SR-PSU. SKB TR-14-01, Svensk Kärnbränslehantering AB.

Barrier process report, 2014. Engineered barrier process report for the safety assessment SR-PSU. SKB TR-14-04, Svensk Kärnbränslehantering AB.

Climate report, 2014. Climate and climate-related issues for the safety assessment SR-PSU. SKB TR-13-05, Svensk Kärnbränslehantering AB.

Initial state report, 2014. Initial state report for the safety assessment SR-PSU. SKB TR-14-02, Svensk Kärnbränslehantering AB.

Input data report, 2014. Input data report for the safety assessment SR-PSU. SKB TR-14-12, Svensk Kärnbränslehantering AB.

Model summary report, 2014. Model summary report for the safety assessment SR-PSU. SKB TR-14-11, Svensk Kärnbränslehantering AB.

Radionuclide transport report, 2014. Radionuclide transport and dose calculations for the safety assessment SR-PSU. SKB TR-14-09, Svensk Kärnbränslehantering AB.

Waste process report, 2014. Waste form and packaging process report for the safety assessment SR-PSU. SKB TR-14-03, Svensk Kärnbränslehantering AB.

Other references

Aalto H, Valkiainen M, 1997. Simulated wetted bituminization product. In Vettyneen bitumointuotteiden jatkokarakterisointi. Työraportti VLJ-6/97. VTT Chemical Technology.

Aalto H, Valkiainen M, 2004. Behaviour of bituminized ion-exchangers under repository conditions. In Long term behaviour of low and intermediate level waste packages under repository conditions. Results of a co-ordinated research project 1997–2002. IAEA-TECDOC-1397, International Atomic Energy Agency, 89–100.

Abarca E, Silva O, Idiart A, Nardi A, Font J, Molinero J, 2014. Flow and transport modelling on the vault scale. Supporting calculations for the safety assessment SR-PSU. SKB R-14-14, Svensk Kärnbränslehantering AB.

Aittola J-P, Kleveland O, 1982. Swelling of bituminized ion exchange resins. NKA AVF (82) 215, Studsvik.

Aittola J-P, Chyssler J, Ringberg H, 1982. Thermal stability of ion-exchange resins. SKBF/KBS TR 81-13, Svensk Kärnbränsleförsörjning AB.

Akafia M M, Reich T J, Koretsky C M, 2011. Assessing Cd, Co, Cu, Ni and Pb sorption on montmorillonite using surface complexation models. Applied Geochemistry 26, S154–S157.

Albinsson Y, 1991. Sorption of radionuclides in granitic rock SKB Arbetsrapport 91-07, Svensk Kärnbränslehantering AB.

Almkvist L, Gordon A, 2007. Low and intermediate level waste in SFR 1. Reference waste inventory 2007. SKB R-07-17, Svensk Kärnbränslehantering AB.

Andra, 2005. Dossier 2005 Argile. Référentiel de comportement des radionucléides et des toxiques chimiques d'un stockage dans le Callovo-Oxfordien jusqu'à l'homme. Site de Meuse/Haute-Marne, Tome 1/2. Rapport C.RP.ASTR.04.0032, Andra, France.

Anunti Å, Larsson H, Edelborg M, 2013. Decommissioning study of Forsmark NPP. SKB R-13-03, Svensk Kärnbränslehantering AB.

- Asea-Atom, 1985.** B1 – Analys av bitumenprodukter: Svällningstester. Rapport KVC 85-204. (In Swedish.)
- Auqué L, Gimeno M, Acero P, Gómez J, 2013.** Proposed composition of groundwater for SFR and its extension, during different climatic cases, SR-PSU. SKB R-13-16, Svensk Kärnbränslehantering AB.
- Baes C F, Mesmer R E, 1976.** The hydrolysis of cations. New York: Wiley-Interscience.
- Baeyens B, Bradbury M H, 1997.** A mechanistic description of Ni and Zn sorption on Na-montmorillonite. Part I: Titration and sorption measurements. *Journal of Contaminant Hydrology* 27, 199–222.
- Bagnall K W, 1962.** The chemistry of polonium. In Emeléus H J, Sharpe A G (eds). *Advances in Inorganic chemistry and radiochemistry*. Vol 4. Academic Press, 197–229.
- Baston G M N, Berry J A, Brownsword M, Heath T G, Ilett D J, McCrohon R, Tweed C J, Yui M, 1998.** The Sorption of Polonium, Actinium and Protactinium Onto Geological Materials. In *Scientific Basis for Nuclear Waste Management XXII*, MRS Proceedings Volume 556, 1107–1114, Boston, Massachusetts.
- Bateman H, 1910.** The solution of a system of differential equations occurring in the theory of radioactive transformations. *Proceedings of the Cambridge Philosophical Society* 15, 423–427.
- Bayliss S, Ewart F T, Howse R M, Smith-Briggs J L, Thomason H P, Willmott H A, 1988.** The solubility and sorption of lead-210 and carbon-14 in a near-field environment. In Apter M J, Westerman R E (eds). *Scientific basis for nuclear waste management XI: symposium held in Boston, Massachusetts, USA, 30 November – 3 December 1987*. Pittsburgh, PA: Materials Research Society. (Materials Research Society Symposium Proceedings 112), 33–42.
- Bergström U, Avila R, Ekström P-A, de la Cruz I, 2008.** Dose assessment for SFR 1. SKB R-08-15, Svensk Kärnbränslehantering AB.
- Berner U, 1990.** A thermodynamic description of the evolution of pore water chemistry and uranium speciation during the degradation of cement. *PSI Bericht 62*, Paul Scherrer Institute, Switzerland.
- Berntsson J, 1992.** Typbeskrivning av avfallskollin (B20) – Bitumensolidifierad jonbytarmassa och filterhjälpmedel i plåtfat förpackade i containrar, Beteckning B.20, PBD-9102-05, Sydkraft Barsebäcksverket. (In Swedish.)
- Bienvenu P, Cassette P, Androletti G, Bé M-M, Comte J, Lépy M-C, 2007.** A new determination of ⁷⁹Se half-life. *Applied Radiation and Isotopes* 65, 355–364.
- Blackwood D J, Gould L J, Naish C C, Porter F M, Rance A P, Sharland S M, Smart N R, Thomas M I, Yates T, 2002.** The localised corrosion of carbon steel and stainless steel in simulated repository environments. Report AEAT/ERRA-0318, AEAT Technology, UK.
- Boverket, 2004.** Boverkets handbok om betongkonstruktioner: BBK 04. 3rd ed. Karlskrona: Boverket. (In Swedish.)
- Bradbury M H, Baeyens B, 1997.** Far-field sorption data bases for performance assessment of a L/ILW repository in a disturbed/altered Palfris marl host rock. Nagra NTB 96-06, Nagra, Switzerland.
- Bradbury M H, Baeyens B, 1999.** Modelling the sorption of Zn and Ni on Ca-montmorillonite. *Geochimica et Cosmochimica Acta* 63, 325–336.
- Bradbury M H, Baeyens B, 2003.** Near-field sorption data bases for compacted MX-80 bentonite for performance assessment of high-level radioactive waste repository in Opalinus Clay host rock. Nagra NTB 02-19, Nagra, Switzerland.
- Bradbury M H, Baeyens B, 2005.** Experimental measurements and modeling of sorption competition on montmorillonite. *Geochimica et Cosmochimica Acta* 69, 4187–4197.
- Bradbury M H, Baeyens B, 2006.** Modelling sorption data for the actinides Am(III), Np(V) and Pa(V) on montmorillonite. *Radiochimica Acta* 94, 619–625.
- Bradbury M H, Baeyens B, 2009.** Sorption modelling on illite. Part I: Titration measurements and the sorption of Ni, Co, Eu and Sn. *Geochimica et Cosmochimica Acta* 73, 990–1003.

- Bradbury M H, Sarott F-A, 1995.** Sorption databases for the cementitious near-field of a L/ILW repository for performance assessment. PSI Bericht 95-06, Paul Scherrer Institute, Switzerland.
- Bradbury M H, Van Loon L R, 1998.** Cementitious near-field sorption data bases for performance assessment of a L/ILW disposal facility in a Palfris Marl Host Rock, CEM-94: Update I, June 1997. PSI Bericht 98-01, Paul Scherrer Institute, Switzerland.
- Brodén K, Wingefors W, 1992.** The effect of temperature on water uptake, swelling and void formation in a bitumen matrix with ion exchange resins. *Waste Management* 12, 23–27.
- Brodersen K, Mose Pedersen B, Vinther A, 1983.** Comparative study of test methods for bituminized and other low- and medium-level solidified waste materials. Final report (1981–1982) for contract WAS 235 DK(G). RISØ-M-2415, Risø National Laboratory, Roskilde, Denmark.
- Brownsword M, Manning M C, Pilkington N J, Williams S J, 2002.** The effect of cellulose degradation products on the solubility and sorption of zirconium and the sorption of lead under cementitious repository conditions. Report AEAT/R/ENV/0549, AEA Technology, UK.
- Choi J-W, Oscarson D W, 1996.** Diffusive transport through compacted Na- and Ca-bentonite. *Journal of Contaminant Hydrology* 22, 189–202.
- Chu S Y F, Ekström L P, Firestone R B, 1999.** Table of Radioactive Isotopes, database version 2/28/99 from URL <http://ie.lbl.gov/toi/index.htm> [november 2011].
- Church J A, Clark P U, Cazenave A, Gregory J M, Jevrejeva S, Levermann A, Merrifield M A, Milne G A, Nerem R S, Nunn P D, Payne A J, Pfeffer W T, Stammer D, Unnikrishnan A S, 2013.** Sea level change. In Working Group I contribution to the IPCC 5th Assessment Report “Climate Change 2013: the physical science basis”. Available at: www.ipcc.org.
- Crawford J, 2010.** Bedrock K_d data and uncertainty assessment for application in SR-Site geosphere transport calculations. SKB R-10-48, Svensk Kärnbränslehantering AB.
- Crawford J, 2013.** Quantification of rock matrix K_d data and uncertainties for SR-PSU. SKB R-13-38, Svensk Kärnbränslehantering AB.
- Cronstrand P, 2005.** Assessment of uncertainty intervals for sorption coefficients. SFR1-1 uppföljning av SAFE. SKB R-05-75, Svensk Kärnbränslehantering AB.
- Cronstrand P, 2007.** Modelling the long-time stability of the engineered barriers of SFR with respect to climate changes. SKB R-07-51, Svensk Kärnbränslehantering AB.
- Dario M, Molera M, Allard B, 2004.** Effect of organic ligands on the sorption of europium on TiO_2 and cement at high pH. SKB TR-04-04, Svensk Kärnbränslehantering AB.
- Daoud W Z, Renken K J, 1999.** Laboratory measurements of the radon gas diffusion coefficient for a fractured concrete sample and radon gas barrier systems. Proceedings of the International Radon Symposium (AARST), Las Vegas, NV, 1999, 14.0–14.12.
- Dverstorp B, Sundström B, 2003.** SSI:s och SKI:s granskning av SKB:s uppdaterade slutlig säkerhetsrapport för SFR 1. Granskningsrapport. SSI Rapport 2003:21, Statens strålskyddsinstitut (Swedish Radiation Protection Authority), SKI Rapport 2003:37, Statens kärnkraftinspektion (Swedish Nuclear Power Inspectorate). (In Swedish).
- Ecke H, Hansson N, 2012.** Determination of carbonate content in concrete from IBMA. Report U 12-82, Vattenfall, 2012.
- Emrén , 1983.** Theoretical calculation of swelling properties of ion-exchange resins. KEFYDA Konsult AB.
- ENDF/B-VI, 2001.T-2 Nuclear information service, database version 12/31/2001.** Available at: <http://t2.lanl.gov/data/decayd.html> [November 2011].
- Ericsson K, Klingstedt G, 1987.** Svällningsegenskaper hos radioaktiva jonbyttarmassor från Forsmarksverket. Rapport 87041, The Swedish Cement and Concrete Research Institute (CBI). (In Swedish.)
- Eriksen T E, Jansson M, 1996.** Diffusion of I^- , Cs^+ and Sr^{2+} in compacted bentonite. Anion exclusion and surface diffusion. SKB TR 96-16, Svensk Kärnbränslehantering AB.

- Eschrich H, 1980.** Properties of long-term behaviour of bitumen and radioactive waste-bitumen mixtures. SKBF/KBS TR 80-14, Svensk Kärnbränslehantering AB.
- Fanger G, Skagius K, Wiborgh M, 2001.** Project SAFE. Complexing agents in SFR. SKB R-01-04, Svensk Kärnbränslehantering AB.
- Figgins P E, 1961.** The radiochemistry of polonium NAS-NS 3037, National Academy of Sciences – National Research Council.
- Firestone R B, Baglin C M (ed), Chu S Y F (ed), 1998.** Table of isotopes: 1998 update. 8th ed. New York: Wiley.
- Forsyth R, 1997.** The SKB fuel corrosion programme. An evaluation of results from the experimental programme performed in the Studsvik Hot Cell Laboratory. SKB TR 97-25, Svensk Kärnbränslehantering AB.
- Gagné R, François R, Masse P, 2001.** Chloride penetration testing of cracked mortar samples. In Banthia N, Sakai K, Gjörv E E (eds). Concrete under severe conditions: environment and loading: proceedings of the Third International Conference on Concrete under Severe Conditions, CONSEC'01, Vancouver, Canada, 18–20 June 2001. Vol 1. Vancouver: University of British Columbia, 198–205.
- Gaucher E, Tournassat C, Nowak C, 2005.** Modelling the geochemical evolution of the multi-barrier system of the Silo of the SFR repository. Final report. SKB R-05-80, Svensk Kärnbränslehantering AB.
- Gerard B, Pijaudier-Cabot G, Laborderie C, 1998.** Coupled diffusion-damage modelling and the implications on failure due to strain localisation. *International Journal of Solids and Structures* 35, 4107–4120.
- Glaus M A, Van Loon L R, 2009.** Chemical reactivity of α -isosaccharinic acid in heterogeneous alkaline systems. PSI Bericht 08-01, Paul Scherrer Institute, Switzerland.
- Glaus M A, Frick S, Rossé R, Van Loon L R, 2010.** Comparative study of tracer diffusion of HTO, $^{22}\text{Na}^+$ and $^{36}\text{Cl}^-$ in compacted kaolinite, illite and montmorillonite. *Geochimica et Cosmochimica Acta* 74, 1999–2010.
- Goldberg S, Glaubig R A, 1988.** Anion sorption on a calcareous, montmorillonitic soil-selenium. *Soil Science Society of America Journal* 52, 954–958.
- Goldberg S, Forster H S, Godfrey C L, 1996.** Molybdenum adsorption on oxides, clay minerals, and soils. *Soil Science Society of America Journal* 60, 425–432.
- Goldberg S, Johnston C T, Suarez D L, Lesch S M, 2007.** Mechanism of molybdenum adsorption on soils and soil minerals evaluated using vibrational spectroscopy and surface complexation modeling. In Barnett M, Kent D (eds). Adsorption of metals by geomedia II: variables, mechanisms, and model applications. Amsterdam: Elsevier. (Developments in Earth & Environmental Sciences 7), 235–266.
- Goutelard F, Charles Y, 2004.** Etude de l'effet de la température et de la viscosité de l'eau sur les paramètres de la diffusion dans les l'argilites du Callovo-Oxfordien et la bentonite. Rapport Andra C.NT.PSTR.04.009; data presented in Andra 2005.
- Gorgeon L, 1994.** Contribution à la modélisation physico-chimique de rétention de radioéléments à vie longue par des matériaux argileux. PhD thesis. Université Paris VI.
- Grambow B, Fattahi M, Montavon G, Moisan C, Giffaut E, 2006.** Sorption of Cs, Ni, Pb, Eu(III), Am(III), Cm, Ac(III), Tc(IV), Th, Zr, and U(IV) on MX 80 bentonite: an experimental approach to assess model uncertainty. *Radiochimica Acta* 94, 627–636.
- Grütter A, von Gunten H R, Rössler E, Keil R, 1994.** Sorption of nickel and cobalt on a size-fraction of unconsolidated glaciofluvial deposits and on clay minerals. *Radiochimica Acta* 65, 181–187.
- He M, Jiang S, Jiang S, Chen Q, Qin J, Wu S, Dong Y, Zhao Z, 2000.** Measurement of ^{79}Se and ^{64}Cu with PXAMS. *Nuclear Instruments and Methods in Physics Research B* 172, 177–181.
- He M, Jiang S, Jiang S, Diao L, Wu S, Li Ch, 2002.** Measurement of the half-life of ^{79}Se with PX-AMS. *Nuclear Instruments and Methods in Physics Research B* 194, 393–398.

- Helmer R G, Browne E, Bé M-M, 2002.** International decay data evaluation project. Journal of Nuclear Science and Technology, Supplement 2, 455–458.
- Holmén J G, 1997.** On the flow of groundwater in closed tunnels. Generic hydrogeological modelling of nuclear waste repository, SFL 3-5. SKB TR 97-10, Svensk Kärnbränslehantering AB.
- Holmén J G, 2005.** SFR-1. Inverse modelling of inflow to tunnels and propagation of estimated uncertainties to predictive stages. SKB R-05-74, Svensk Kärnbränslehantering AB.
- Holmén J, 2007.** SFR inverse modelling Part 2. Uncertainty factors of predicted flow in deposition tunnels and uncertainty in distribution of flow paths from deposition tunnels. SKB R-07-61, Svensk Kärnbränslehantering AB.
- Holmén J G, Stigsson M, 2001a.** Modelling of future hydrogeological conditions at SFR. SKB R-01-02, Svensk Kärnbränslehantering AB.
- Holmén J G, Stigsson M, 2001b.** Details of predicted flow in deposition tunnels at SFR, Forsmark. SKB R-01-21, Svensk Kärnbränslehantering AB.
- Håkansson R, 2000.** Beräkning av nuklidinnehåll, resteffekt, aktivitet samt doshastighet för utbränt kärnbränsle. SKB R-99-74, Svensk Kärnbränslehantering AB. (In Swedish.)
- Höglund L O, 2001.** Project SAFE. Modelling of long-term concrete degradation processes in the Swedish SFR repository. SKB R-01-08, Svensk Kärnbränslehantering AB.
- Höglund L O, 2014.** The impact of concrete degradation on the BMA barrier functions. SKB R-13-40, Svensk Kärnbränslehantering AB.
- Höglund L O, Bengtsson A, 1991.** Some chemical and physical processes related to the long-term performance of the SFR repository. SKB SFR 91-06, Svensk Kärnbränslehantering AB.
- Ikeda T, Amaya T, 1998.** Model development of chemical evolution in repository. Vol.II. Acquisition of nuclide migration data in near-field. Technical Report PNC ZJ 1281 98–03, Power Reactor and Nuclear Development Corporation, Japan.
- Ingemansson T, 2000a.** Osäkerheter vid uppskattning av Sr-90 och aktinidinventariet i SFR 1. SKB R-00-22, Svensk Kärnbränslehantering AB. (In Swedish.)
- Ingemansson T, 2000b.** Aktinidfördelningen i SFR 1. SKB R-00-01, Svensk Kärnbränslehantering AB. (In Swedish.)
- Ismail M, Toumi A, François R, Gagné R, 2004.** Effect of crack opening on the local diffusion of chloride in inert materials. Cement and Concrete Research 34, 711–716.
- Jiang S, Guo J, Jiang S, Li Ch, Cui A, He M, Wu S, Li S, 1997.** Determination of the half-life of ⁷⁹Se with the accelerator mass spectrometry technique. Nuclear Instruments and Methods in Physics Research B 123, 405–409.
- Jiang S, He M, Diao L, Guo J, Wu S, 2001.** Remeasurement of the half-life of ⁷⁹Se with the projectile x-ray detection method. Chinese Physics Letters 18, 746–749.
- Jörg G, Bühnemann R, Hollas S, Kivel N, Kossert K, Van Winckel S, Gostomski C L, 2010.** Preparation of radiochemically pure ⁷⁹Se and highly precise determination of its half-life. Applied Radiation and Isotopes 68, 2339–2351.
- Kaplan D, Robers K, Coates J, Siegfried M, Serkitz S, 2008.** Saltstone and concrete interactions with radionuclides: sorption (K_d), desorption, and reduction capacity measurements. Report SRNS-STI-2008-00045, Savannah River National Laboratory, Aiken, South Carolina.
- Keith-Roach M, Lindgren M, Källström K, 2014.** Assessment of complexing agent concentrations in SFR. SKB R-14-03, Svensk Kärnbränslehantering AB.
- Khan S A, Rehman R, Khan M A, 1995.** Adsorption of chromium (III), chromium (VI) and silver (I) on bentonite. Waste Management 15, 271–282.
- Kritsky V G, Morozov V V, Nechaev A F, Khitrov Y A, Petrik N G, Kalyazin N N, Makarchuk T F, 1987.** Material corrosion under spent nuclear nuclear fuel storage conditions. In Materials reliability in the back end of the nuclear fuel cycle. IAEA-TECDOC-421, International Atomic Energy Agency, 51–62.

- Kulmala S, Hakanen M, 1993.** The solubility of Zr, Nb and Ni in groundwater and concrete water, and sorption on crushed rock and cement. YJT-93-21, Nuclear Waste Commission of Finnish Power Companies.
- Kuron D, Gräfen H, Batroff H-P, Fäßler K, Münster R, 1985.** Einfluß des Chloridgehaltes in Trinkwasser auf die Korrosion von unlegiertem Stahl (Influence of chloride content in tap water on the corrosion of unalloyed steel). *Werkstoffe und Korrosion* 36, 68–79.
- Kursten B, Smalios E, Azkarate I, Werme L, Smart N R, Santarini G, 2003.** COBECOMA State-of-the-art document on the CORrosion BEhaviour of CONtainer Materials. Contract FIKW-CT-20014-20138, Final report, European Commission.
- Laaksoharju M, Gurban I, Skårman, 1998.** Summary of hydrochemical conditions at Aberg, Beberg and Ceberg. SKB TR-98-03, Svensk Kärnbränslehantering AB.
- Larsson H, Anunti Å, Edelborg M, 2013.** Decommissioning study of Oskarshamn NPP. SKB R-13-04, Svensk Kärnbränslehantering AB.
- Lindgren M, Petterson M, Karlsson S, Moreno L, 2001.** Project SAFE. Radionuclide release and dose from the SFR repository. SKB R-01-18, Svensk Kärnbränslehantering AB.
- Lindgren M, Petterson M, Wiborgh M, 2007.** Correlation factors for C-14, Cl-36, Ni-59, Ni-63, Mo-93, Tc-99, I-129 and Cs-135. In operational waste for SFR 1. SKB R-07-05, Svensk Kärnbränslehantering AB.
- Lu Y, Garboczi E, Bentz D, Davis J, 2012.** Modeling chloride transport in cracked concrete: a 3-D image-based microstructure simulation. In Proceedings of COMSOL Conference 2012, Boston, MA, 3–5 October 2012. Available at: http://www.nist.gov/customcf/get_pdf.cfm?pub_id=912153.
- Luna M, Arcos D, Duro L, 2006.** Effects of grouting, shotcreting and concrete leachates on backfill geochemistry. SKB R-06-107, Svensk Kärnbränslehantering AB.
- Magnusson Å, Stenström K, Aronsson P-O, 2007.** Characterization of ^{14}C in process water systems, spent resins and off-gas of Swedish LWRs. Report 01-07, Lund University, Department of Physics.
- Mariën A, Mokni N, Valcke E, Olivella S, Smets S, Li X, 2013.** Osmosis-induced water uptake by Eurobitum bituminized radioactive waste and pressure development in constant volume conditions. *Journal of Nuclear Materials* 432, 348–365.
- Marques Fernandes M, Baeyens B, Bradbury M H, 2008.** The influence of carbonate complexation on lanthanide/actinide sorption on montmorillonite. *Radiochimica Acta* 96, 691–697.
- Matsuda M, Nishi T, Chino K, Kikuchi M, 1992.** Solidification of spent ion exchange resin using new cementitious material, (I). Swelling pressure of ion exchange resin. *Journal of Nuclear Science and Technology* 29, 883–889.
- Mattigod S V, Bovaird C C, Wellman D M, Skinner D J, Cordova E A, Wood M I, 2009.** Effect of concrete waste form properties on radionuclide migration. PNNL-18745, Pacific Northwest National Laboratory, Richland, Washington.
- Mihara M, Honda A, Nishimura T, Wada R, 2002.** Estimation on gas generation and corrosion rates of carbon steel, stainless steel and zircaloy in alkaline solutions under low oxygen condition, *Saikuru Kiko Giho* 15, 91–101. (In Japanese.)
- Missana T, Alonso U, García-Gutiérrez M, 2009.** Experimental study and modeling of selenite sorption onto illite and smectite clays. *Journal of Colloid and Interface Science* 334, 132–138.
- Mokni N, Olivella S, Valcke E, Mariën A, Smets S, Li X, 2011.** Deformation and flow driven by osmotic processes in porous materials: application to bituminised waste materials. *Transport in Porous Media* 86, 635–662.
- Molera M, Eriksen T, 2002.** Diffusion of $^{22}\text{Na}^+$, $^{85}\text{Sr}^{2+}$, $^{134}\text{Cs}^+$ and $^{57}\text{Co}^{2+}$ in bentonite clay compacted to different densities: experiments and modeling. *Radiochimica Acta* 90, 753–760.
- Montavon G, Guo Z, Lützenkirchen J, Alhajji E, Kedziorek M A M, Bourg A C M, Grambow B, 2009.** Interaction of selenite with MX-80 bentonite: effect of minor phases, pH, selenite loading, solution composition and compaction. *Colloids and Surfaces A: Physicochemical and Engineering Aspects* 332, 71–77.

- Moreno L, Skagius K, Södergren S, Wiborgh M, 2001.** Project SAFE. Gas related processes in SFR. SKB R-01-11, Svensk Kärnbränslehantering AB.
- Motta M M, Miranda C F, 1989.** Molybdate adsorption on kaolinite, montmorillonite and illite: constant capacitance modelling. *Soil Science Society of America Journal* 53, 380–385.
- Mu S, De Schutter G, Ma B-G, 2013.** Non-steady state chloride diffusion in concrete with different crack densities. *Materials and Structures* 46, 123–133.
- Muurinen A, Penttilä-Hiltunen P, Rantanen J, 1987.** Diffusion mechanisms of strontium and caesium in compacted sodium bentonite. In Bates J K, Seefeldt W B (eds). *Scientific basis for nuclear waste management X: symposium held in Boston, Massachusetts, USA, 1–4 December 1986.* (Materials Research Society Symposium Proceedings 84), 803–812.
- Naish C C, Blackwood D J, Thomas M I, Rance A P, 2001.** The anaerobic corrosion of carbon steel and stainless steel. Report AEAT/ENV/0224, AEAT Technology, UK.
- NEA, 2005.** NEA Sorption Project. Phase II: Interpretation and prediction of radionuclide sorption onto substrates relevant for radioactive waste disposal using thermodynamic sorption models. Paris: OECD/NEA.
- NEA, 2012.** NEA Sorption Project. Phase III: Thermodynamic sorption modelling in support of radioactive waste disposal safety cases. a guideline document. Paris: OECD/NEA.
- Nilsson A-C, Högfeldt E, Muhammed M, Wingefors S, 1988.** On the swelling of ion exchange resins used in the Swedish nuclear power plants. SKI TR 1988:1, Statens kärnkraftinspektion (Swedish Nuclear Power Inspectorate).
- Noshita N, Nishi T, Yoshida T, Fujihara H, Saito N, Tanaka S, 2001.** Categorization of cement hydrates by radionuclide sorption mechanism. In Hart K P, Lumpkin G R (eds). *Scientific basis for nuclear waste management XXIV: symposium held in Sydney, Australia, 27–31 August 2000.* Warrendale, PA: Materials Research Society. (Materials Research Society Symposium Proceedings 663), 115–121.
- Ochs M, Talerico C, 2004.** SR-Can. Data and uncertainty assessment. Migration parameters for the bentonite buffer in the KBS-3 concept. SKB TR-04-18, Svensk Kärnbränslehantering AB.
- Ochs M, Talerico C, Lothenbach B, Giffaut E, 2003.** Systematic trends and empirical modelling of lead uptake by cements and cement minerals. In Finch R J, Bullen D B (eds). *Scientific basis for nuclear waste management XXVI.* Warrendale, PA: Materials Research Society. (Materials Research Society Symposium Proceedings 757), 693–698.
- Ochs M, Vielle-Petit L, Wang L, Mallants D, Leterme B, 2011.** Additional sorption parameters for the cementitious barriers of a near-surface repository. NIRONDR-TR 2010–06 E, ONDRAF/NIRAS, Belgium.
- Oda C, Ikeda T, Shibata M, 1999.** Experimental studies for sorption behavior of tin on bentonite and rocks, and diffusion behavior of tin in compacted bentonite. JNC TN8400 99-073, Japan Nuclear Cycle Development Institute.
- Odén M, Follin S, Öhman J, Vidstrand P, 2014.** SR-PSU Bedrock hydrogeology. Groundwater flow modelling methodology, setup and results. SKB R-13-25, Svensk Kärnbränslehantering AB.
- Pabalan R T, Turner D R, 1997.** Uranium(6+) sorption on montmorillonite: experimental and surface complexation modeling study. *Aquatic Geochemistry* 2, 203–226.
- Pettersson M, Elert M, 2001.** Characterisation of bituminised waste in SFR 1. SKB R-01-26, Svensk Kärnbränslehantering AB.
- Pointeau I, 2000.** Étude mécanistique et modélisation de la rétention de radionucléides par les silicates de calcium hydrates (CSH) des ciments. PhD thesis. University of Reims, France.
- Pointeau I, Coreau N, Reiller P, 2002.** Étude expérimentale et modélisation de la rétention de $^{14}\text{CO}_3$ par les matériaux constituant le béton dans le cadre d'un entreposage de barres graphite UNGG. Note Technique CEA. NT DPC/SCPA 02-046, CEA.

- Pointeau I, Reiller P, Macé N, Landesman C, Coreau N, 2006.** Measurement and modelling of the surface potential evolution of hydrated cement pastes as a function of degradation. *Journal of Colloid and Interface Science* 300, 33–44.
- Pointeau I, Coreau N, Reiller P E, 2008.** Uptake of anionic radionuclides onto degraded cement pastes and competing effect of organic ligands. *Radiochimica Acta* 96, 367–374.
- Polettini A, Pomi R, Sirini P, 2002.** Fractional factorial design to investigate the influence of heavy metals and anions on acid neutralization behavior of cement-based products. *Environmental Science & Technology* 36, 1584–1591.
- Pomiès M-P, Lequeux N, Boch P, 2001.** Speciation of cadmium in cement: Part I. Cd²⁺ uptake by C-S-H. *Cement and Concrete Research*, 31, 563–569.
- Puranen A, 2010.** Near field immobilization of selenium oxyanions. PhD thesis. School of Chemical Science and Engineering, Royal Institute of Technology, Stockholm.
- Pusch R, Cederström M, 1987.** Material- och byggnadskontroll av bentonitbarriärer i SFR, Forsmark. SKB SFR 87-08, Svensk Kärnbränslehantering AB. (In Swedish.)
- Rabung T, Pierret M C, Bauer A, Geckeis H, Bradbury M H, Baeyens B, 2005.** Sorption of Eu(III)/Cm(III) on Ca-montmorillonite and Na-illite. Part 1: Batch sorption and time-resolved laser fluorescence spectroscopy experiments. *Geochimica et Cosmochimica Acta* 69, 5393–5402.
- Riggare P, Johansson C, 2001.** Project SAFE. Low and intermediate level waste in SFR-1. Reference Waste Inventory. SKB R-01-03, Svensk Kärnbränslehantering AB.
- Sato H, 1998.** Data setting for effective diffusion coefficients (De) of nuclides in the buffer for reference case in performance assessments of the geological disposal of high-level radioactive waste (I). PNC Technical Report TN8410 98–097, Power Reactor and Nuclear Fuel Development Corporation, Japan.
- Savage D, Stenhouse, M, 2002.** SFR 1 vault database. SKI Report 02:53, Statens kärnkraftinspektion (Swedish Nuclear Power Inspectorate).
- Schenk R, 1988.** Untersuchungen über die Wasserstoffbildung durch Eisenkorrosion unter Endlagerbedingungen. Nagra NTB 86-24, Nagra, Switzerland.
- Schrader H, 2004.** Half-life measurements with ionization chambers – a study of systematic effects and results. *Applied Radiation and Isotopes* 60, 317–323.
- Shibutani T, Yui M, Yoshikawa H, 1994.** Sorption mechanism of Pu, Am and Se on sodium bentonite. In Barkatt A, Van Konynenburg R A (eds). *Scientific basis for nuclear waste management XVII: symposium held in Boston, Massachusetts, USA, 29 November – 3 December*. Pittsburgh, PA: Materials Research Society. (Materials Research Society Symposium Proceedings 333), 725–730.
- Simpson J P, Weber J, 1988.** Hydrogen evolution from corrosion in nuclear waste repositories. In *Proceedings of UK Corrosion '88 with EUROCORR*, Brighton, 3–5 October 1988. Birmingham: Institution of Corrosion Science and Technology, 33.
- Simpson J P, Schenk R, Knecht B, 1985.** Corrosion rate of unalloyed steels and cast irons in reducing granitic groundwaters and chloride solutions. In Werme L O (ed). *Scientific basis for nuclear waste management IX: symposium held in Stockholm, Sweden, 9–11 September 1985*. Pittsburgh, PA: Materials Research Society. (Materials Research Society Symposium Proceedings 50), 429–436.
- SKB, 2001.** Project SAFE. Compilation of data for radionuclide transport analysis. SKB R-01-14, Svensk Kärnbränslehantering AB.
- SKB, 2006.** Data report for the safety assessment SR-Can. SKB TR-06-25, Svensk Kärnbränslehantering AB.
- SKB, 2008.** Safety analysis SFR 1. Long-term safety. SKB R-08-130, Svensk Kärnbränslehantering AB.
- SKB, 2010a.** Data report for the safety assessment SR-Site. SKB TR-10-52, Svensk Kärnbränslehantering AB.

- SKB, 2010b.** Buffer, backfill and closure process report for the safety assessment SR-Site. SKB TR-10-47, Svensk Kärnbränslehantering AB.
- SKB, 2013.** Låg- och medelaktivt avfall i SFR. Referensinventarium för avfall 2013. SKB R-13-37, Svensk Kärnbränslehantering AB.
- Smart N R, Hoch A R, 2010.** A survey of steel and zircaloy corrosion data for use in the SMOGG gas generation model. Report to the NDA RWMD. SA/ENV-0841, Issue 3, Serco, UK.
- Smart N R, Blackwood D J, Marsh G P, Naish C C, O'Brien T M, Rance A P, Thomas M I, 2004.** The anaerobic corrosion of carbon and stainless steels in simulated cementitious repository environments: a summary review of Nirex research. AEAT/ERRA-0313, AEAT Technology, UK.
- Snellman M, Valkiainen M (eds), 1985.** Long-term properties of bitumenised waste products. Nordic Liaison Committee for Atomic Energy (NKA).
- Snellman M, Valkiainen M, Airola C, Bonnevie-Svendsen M, Brodersen K, Forsström H, Wingefors S, 1986.** Long-term behavior of bituminized waste, Waste Management '86 Proceedings of the Symposium on Waste Management at Tuscon, Arizona, March 2–6, 1986. American Nuclear Society. Vol 3, 501–507.
- Suzuki S, Sato H, Ishidera T, Fujii N, 2004.** Study on anisotropy of effective diffusion coefficient and activation energy for deuterated water in compacted sodium bentonite. *Journal of Contaminant Hydrology* 68, 23–37.
- Tachi Y, Shibutani T, Nishikawa Y, Shinozaki T, 1999.** Sorption behavior of selenium on bentonite and granodiorite under reducing conditions. JNC TN8410 94-395, Japan Nuclear Cycle Development Institute.
- Taylor H F W, 1990.** Cement chemistry. New York: Academic Press.
- Tertre E, Berger G, Castet S, Loubet M, Giffaut E, 2005.** Experimental sorption of Ni²⁺, Cs⁺ and Ln³⁺ onto a montmorillonite up to 150°C. *Geochimica et Cosmochimica Acta* 69, 4937–4948.
- Thomson G, Miller A, Smith G, Jackson D, 2008.** Radionuclide release calculations for SAR-08. SKB R-08-14, Svensk Kärnbränslehantering AB.
- Tiller K G, Hodgson J F, 1960.** The specific sorption of cobalt and zinc by layer silicates. *Clays and Clay Minerals* 9, 393–403.
- Tits J, Wieland E, Dobler J-P, Kunz D, 2004.** The uptake of strontium by calcium silicate hydrates under high pH conditions: an experimental approach to distinguish adsorption from co-precipitation processes. In Oversby V M, Werme L O (eds). Scientific basis for nuclear waste management XXVII: symposium held in Kalmar, Sweden, 15–19 June 2003. Warrendale, PA: Materials Research Society. (Materials Research Society Symposium Proceedings 807), 689–694.
- Treadaway K W J, Cox R N, Brown B L, 1989.** Durability of corrosion resting steels in concrete. Proceedings – Institution of Civil Engineers, Part 1, 86, 305–331.
- Turner D R, Pabalan R T, Bertetti F P, 1998.** Neptunium(V) sorption on montmorillonite: an experimental and surface complexation modeling study. *Clays and Clay Minerals* 46, 259–269.
- Ulrich H J, Degueldre C, 1993.** The sorption of ²¹⁰Pb, ²¹⁰Bi and ²¹⁰Po on montmorillonite: a study with emphasis on reversibility aspects and on the radioactive decay of adsorbed nuclides. *Radiochimica Acta* 62, 81–90.
- US DOE, 2009.** Review of mechanistic understanding and modeling and uncertainty analysis methods for predicting cementitious barrier performance. Cementitious Barriers Partnership. CBP-TR-2009-002, Rev.0, U.S. Department of Energy.
- Valcke E, Mariën A, Smets S, Li X, Mokni N, Olivella S, Sillen X, 2010.** Osmosis-induced swelling by Eurobitum bituminized radioactive waste in constant total stress conditions. *Journal of Nuclear Materials* 406, 304–316.
- Valkiainen M, Vuorinen U, 1985.** Properties of bituminization product from Olkiluoto power plant. Report YJT-85-24, Nuclear Waste Commission of Finnish Power Companies.

- Valkiainen M, Vuorinen U, 1989.** Long-term properties of TVO's bituminized resins. Report YJT-89-06, Nuclear Waste Commission of Finnish Power Companies.
- Van Loon L R, Glaus M A, 1998.** Experimental and theoretical studies on alkaline degradation of cellulose and its impact on the sorption of radionuclides. Nagra NTB 97-04, Nagra, Switzerland.
- Vattenfall, 2011.** Metodik för bedömning av långsiktig funktion hos betongbarriärer. SFR. AE-NCC 11-013, Vattenfall Power Consultant. (In Swedish.)
- Volchek K, Miah M Y, Kuang W, DeMaleki Z, Tezel F H, 2011.** Adsorption of cesium on cement mortar from aqueous solutions. *Journal of Hazardous Materials* 194, 331–337.
- von Schenck H, Bultmark F, 2014.** Effekt av bitumensvällning i silo och BMA. SKB R-13-12, Svensk Kärnbränslehantering AB. (In Swedish.)
- Wang L, Martens E, Jacques D, de Cannière P, Berry J, Mallants D, 2009.** Review of sorption values for the cementitious near field of a near surface radioactive waste disposal facility. NIROND TR 2008-23E, ONDRAF/NIRAS, Belgium.
- Weast R C, 1985.** CRC Handbook of chemistry and physics: a ready-reference book of chemical and physical data. 65th ed. Cleveland, OH: CRC Press.
- Whitehouse P, 2009.** Glacial isostatic adjustment and sea-level change. State of the art report. SKB TR-09-11, Svensk Kärnbränslehantering AB.
- Wieland E, Van Loon L R, 2002.** Cementitious near-field sorption data base for performance assessment of an ILW repository in Opalinus Clay. Nagra NTB 02-20, Nagra, Switzerland.
- Wieland E, Tits J, Ulrich A, Bradbury M H, 2006.** Experimental evidence for solubility limitation of the aqueous Ni(II) concentration and isotopic exchange of ^{63}Ni in cementitious systems. *Radiochimica Acta* 94, 29–36.
- Wieland E, Tits J, Kunz D, Dähn R, 2008.** Strontium uptake by cementitious materials. *Environmental Science and Technology* 42, 403–409.
- Yoon I-S, 2012.** Chloride penetration through cracks in high performance concrete and surface treatment system for crack healing. *Advances in Materials Science and Engineering* 2012, 294571. doi:10.1155/2012/294571
- Yu J-W, Neretnieks I, 1997.** Diffusion and sorption properties of radionuclides in compacted bentonite. SKB TR 97-12, Svensk Kärnbränslehantering AB.
- Yu R, Guo J, Cui A, Tang P, Li D, Liu D, 1995.** Measurement of the half-life of ^{79}Se using a radiochemical method. *Journal of Radioanalytical and Nuclear Chemistry* 196, 165–170.
- Yui M, Azuma J, Shibata M, 1999.** JNC thermodynamic database for performance assessment of high-level radioactive waste disposal system. JNC Technical Report TN8400 99-070, Japan Nuclear Cycle Development Institute.
- Zhang J, Lounis Z, 2006.** Sensitivity analysis of simplified diffusion-based corrosion initiation model of concrete structures exposed to chlorides. *Cement and Concrete Research* 36, 1312–1323.
- Zhou W, Kozak M W, Xu S, Stenhouse M, 2009.** Review and Assessment of SFR 1 long-term safety analyses. Report MSCI-2818-3 Rev 3.1.

Unpublished documents

SKBdoc id, version	Title	Issuer, year
1339709 ver 1.0	C-14 accumulated in ion exchange resins in Swedish nuclear power plants	SKB, 2012
1341356 ver 1.0	Uppskattning av Mo-93, Tc-99, I-129 och Cs-135 i driftavfall – Uppdatering till och med 2011 (In Swedish.)	ALARA Engineering, 2012
1358612 ver 1.0	SFR förslutningsplan. (In Swedish.)	SKB, 2014
1393443 ver 1.0	Assessing uncertainty to correlation factors for ¹⁴ C, ³⁶ Cl, ⁵⁹ Ni, ⁶³ Ni, ⁹³ Mo, ⁹⁹ Tc, ¹²⁹ I and ¹³⁵ Cs in operational waste for SFR 1.	Vattenfall Power Consultant, 2007
1393449 ver 1.0	Klor-36 – Uppskattning av aktivitet i driftavfall från svenska LWR. (In Swedish.)	ALARA Engineering, 2006
1400742 ver 2.0	Kontroll av SFR-avfall. Delprojekt mätteknik. (In Swedish.)	Gammadata mätteknik AB, 1990
1416968 ver 1.0	Low and Intermediate Level Waste in SFL 3-5: Reference Inventory	SKB, 1998
1427105 ver 4.0	Radionuclide inventory for application of extension of the SFR repository – Treatment of uncertainties.	SKB, 2014
1430853 ver 1.0	Sprickor i BMA:s betongbarriär – Inspektion och orsak. (In Swedish.)	Vattenfall, 2012
1434594 ver 1.0	Svar på föreläggande om redovisning rörande betydelsen av jordströmmar vid SFR. (In Swedish.)	SKB, 2014
1481419 ver 1.0	Ny beräkning av Mo-93 i normkolli till PSU 2015-05 (In Swedish.)	SKB, 2015